



Molecular tectonics : functionalized dipyrrens for the construction of metallo-organic architectures

Fan Zhang

► To cite this version:

Fan Zhang. Molecular tectonics : functionalized dipyrrens for the construction of metallo-organic architectures. Other. Université de Strasbourg, 2017. English. NNT : 2017STRAF054 . tel-01737721

HAL Id: tel-01737721

<https://theses.hal.science/tel-01737721>

Submitted on 19 Mar 2018

HAL is a multi-disciplinary open access archive for the deposit and dissemination of scientific research documents, whether they are published or not. The documents may come from teaching and research institutions in France or abroad, or from public or private research centers.

L'archive ouverte pluridisciplinaire **HAL**, est destinée au dépôt et à la diffusion de documents scientifiques de niveau recherche, publiés ou non, émanant des établissements d'enseignement et de recherche français ou étrangers, des laboratoires publics ou privés.

ÉCOLE DOCTORALE ED222 Sciences Chimiques

UMR 7140

THÈSE

présentée par :

Fan ZHANG

soutenue le : **05 Octobre 2017**

pour obtenir le grade de : **Docteur de l'Université de Strasbourg**

Discipline/ Spécialité : Sciences Chimiques / chimie

Molecular tectonics: Functionalized dipyrrins for the construction of metallo-organic architectures

Titre en français : ***Tectonique moléculaire : Dipyrrines fonctionnalisées pour la
construction d'architectures métallo-organiques***

THÈSE dirigée par :

Dr. Stéphane Baudron

Pr. Mir Wais Hosseini

Chargé de recherches au CNRS, Université de Strasbourg

Professeur, Université de Strasbourg

RAPPORTEURS :

Pr. Bruno Andrioletti

Pr. Jean-Bernard Regnouf de Vains

Professeur, Université Claude Bernard Lyon 1

Professeur, Université de Lorraine

AUTRES MEMBRES DU JURY :

Pr. Bernold Hasenknopf

Dr. Jean Weiss

Professeur, Université Pierre et Marie Curie

Directeur de recherches au CNRS, Université de Strasbourg

To my family

Acknowledgements

First of all, I would like to thank the members of my jury: Pr. Bruno Andrioletti, Pr. Jean-Bernard Regnouf de Vains, Pr. Bernold Hasenknopf and Dr. Jean Weiss for accepting to evaluate my PhD thesis work.

My following thanks go to my thesis supervisor: Pr. Mir Wais Hosseini. I would like to thank him for having welcomed me in his laboratory, for his trust and for the motivation that he brought me during all these years. My dear Prof, thank you for teaching the knowledge in the classroom, which let me deeply understand the charm of science.

I would like to give a huge thank to my co-supervisor, Dr. Stéphane Baudron. Thank you for the patient guidance in science, the expertise in chemistry during those three years. Thank you for keeping your door open for discussion at any time. And also, thanks to your support for my administrative documents, the help to deal with some paper works, which made my work and my living in Strasbourg easier.

To all my present and past lab colleagues, Pr. Sylvie Ferlay-Charitat, thanks for her scientific guidance and patient help during my Master internships. Thanks to our excellent crystallographer Nathalie Kyritsakas, for her help in X-ray diffraction analysis. Thanks to Dr. Aurélie Guenet and Dr. Matteo Mauro, for their help in fluorescent measurements. Thanks to our secretary Valérie Rey, for her help to deal with all the administrative issues. And also thanks to Pr. Jean-Marc Planeix, Pr. Véronique Bulach, Dr. Abdelaziz Jouaiti, Audrey, Cyril, Damien, Romain, Bérangère, Maxime, Ekataryna, Elsa, Nicolas M, Nicolas Z, Patrick, Chaojie, Bowen, Elena for your help, your kindness, as well as the nice atmosphere in the laboratory.

A lot of thanks to the Service NMR, Service spectrométrie de masse and Service d'analyses, de mesures physiques et de spectroscopie optique.

And I also would like to thank the Labex Chemistry of complex systems and the foundation icFRC for the financial support.

All my friends who help and support me during the five years in Strasbourg. Thank you for your support, your help, your companionship and every happy moment we shared together.

At the end, I also thank my family for your support, your understanding and your encouragement.

Table of Contents

RESUME en français	1
Introduction	13
1. Supramolecular Chemistry.....	15
1.1 Molecular recognition.....	15
1.2 Molecular self-assembly.....	16
2. Molecular Tectonics.....	17
2.1 The design of the molecular tectons.....	18
2.2 Intermolecular interactions.....	20
2.2.1 Van der Waals interaction.....	20
2.2.2 π - π interaction.....	21
2.2.3 Ag- π interaction.....	22
2.2.4 Hydrogen bonding interaction.....	23
2.2.5 Coordination bonding interaction.....	23
2.2.5.1 One dimensional networks.....	24
2.2.5.2 Two dimensional networks.....	25
2.2.5.3 Three dimensional networks.....	27
3. The Chemistry of dipyrins.....	28
3.1 Structures and nomenclature of dipyrin.....	28
3.2 Synthesis and properties of dipyrins.....	29
3.3 Coordination chemistry of dipyrin.....	32
3.4 Properties and applications of dipyrinato complexes.....	36
3.4.1 Dipyrinato complexes as catalysts.....	36
3.4.2 Luminescent properties and applications of dipyrinato complexes.....	38
3.5 Coordination networks.....	42
3.5.1 Homometallic networks.....	42
3.5.2 Heterometallic networks.....	44
4. Objectives of the research project.....	49

Chapter I: Coordination polymers based on 1,9-divinyldipyrrin derivatives	57
I.1 Introduction	57
I.2 Synthesis and characterization of 1,9-divinyldipyrrin ligands	61
I.3 Preparation of BODIPYs complexes	68
I.4 Formation of coordination polymers with BODIPYs	71
I.4.1 Formation of coordination networks with tecton 10	71
I.4.2 Characterization of crystalline compounds in the solid state	77
I.4.3 Formation of coordination networks with tectons 11, 14 and 15	79
I.4.4 Formation of coordination networks with tecton 13	80
I.5 Preparation of Zn(dipyrrinato) ₂ complexes	82
I.6 Formation of heterometallic coordination polymers with Zn(II) complexes	85
I.7 Conclusion and perspectives	86
Chapter II: Functionalized 2,2'-bisdipyrrin derivatives for the formation of complex architectures	95
II.1 Introduction	95
II.2 Formation of a strapped helicate based on a benzaldehyde-appended 2,2'-bis-dipyrrin	101
II.2.1 Preliminary investigation for the synthesis of imine functionalized dipyrin derivatives	102
II.2.2 Synthesis of a strapped helical complex	104
II.3 Amide functionalized 2,2'-bisdipyrrin derivatives	110
II.3.1 Symmetrical 5,5'-diamide-2,2'-bisdipyrrin derivatives	110
II.3.2 Dissymmetrical 5-amide-2,2'-bisdipyrrin derivatives	113
II.4 Conclusion and perspectives	116
Conclusion and Perspectives	125
Experimental section	133

Abbreviations

Å	Ångström
ACN	acetonitrile
AcOEt	ethyl acetate
acac	acetylacetonate
aq.	aqueous
bodipy	boron dipyrromethene
Boc	tert-butyloxycarbonyl
calcd.	calculated
CN	cyano
<i>conc.</i>	concentrated
DABCO	1,4-diazabicyclo[2.2.2]octane
DCM	dichloromethane
DDQ	2,3-dichloro-5,6-dicyano-1,4-benzoquinone
DMF	dimethylformamide
DMS	dimethyl succinate
DMSO	dimethyl sulfoxide
DNA	deoxyribonucleic acid
dpm	dipyrromethene
DOSY	Diffusion ordered spectroscopy
equiv.	equivalent
ESI	electrospray ionization
Et ₂ O	Diethyl ether
EDCi	1-ethyl-3-(3-dimethylaminopropyl)carbodiimide
Fmoc-OSuc	9-Fluorenylmethyl N-succinimidyl carbonate
h	hour
HRMS	high resolution mass spectrometry
Hz	Hertz
hfac	hexafluoroacetylacetonate
HOBt	1-Hydroxybenzotriazole
IR	infrared spectroscopy
IRMOFs	isorecticular metal-organic frameworks
<i>J</i>	coupling constant
LiOH	lithium hydroxide
MS	mass spectrometry
MOFs	Metal-organic Frameworks
NMR	nuclear magnetic resonance
NIR	near infrared
OAc	Acetate
Ph	phenyl

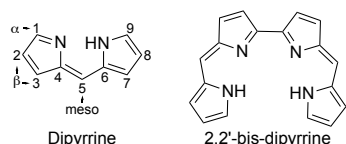
pH	potential of hydrogen
pK _a	acidity constant
<i>P</i> -TSA	<i>p</i> -toluenesulfonic acid
py	pyridine
PeT	photoinduced electron transfer
PXRD	powder X-ray diffraction
ROS	reactive oxygen species
rt	room temperature
TFA	trifluoroacetic acid
THF	tetrahydrofuran
TLC	thin layer chromatography
UV	ultraviolet
vdw	van der Waals
Φ_f	quantum yield
λ	wavelength
ϵ	molar absorption coefficient

Résumé de la thèse en français

Tectonique moléculaire : Dipyrroles fonctionnalisées pour la construction d'architectures métallo-organiques

1) Introduction

Parmi les nombreux défis en sciences des matériaux moléculaires, la conception et la fabrication de nouveaux matériaux fonctionnels complexes sont d'une grande importance. La confection de ce type de matériaux peut être réalisée par une approche « bottom-up » en utilisant des processus spontanés d'auto-assemblage et d'auto-organisation entre composants moléculaires préprogrammés. Alors qu'il y a eu beaucoup de progrès concernant le contrôle de l'organisation moléculaire à l'échelle nanométrique, le contrôle de l'organisation au niveau micro- ou milli-métrique menant à des architectures étendues est un véritable défi pour les chimistes : ceci est crucial pour obtenir de nouveaux matériaux possédant des propriétés ciblées pour de nombreuses applications. La *tectonique moléculaire*,¹ une branche de la chimie supramoléculaire, traite de la conception et de la formation de réseaux moléculaires à l'état solide.² Cette approche manipule des interactions réversibles telles que la liaison de coordination, la liaison hydrogène ou les forces de van der Waals pour la construction d'architectures cristallines. Ainsi, les polymères ou réseaux de coordination métallo-organiques, dont les Metal-Organic Frameworks MOFs constituent une classe particulière, résultent de l'auto-assemblage par liaison de coordination entre des ligands organiques, appelés tectons,³ et un ou plusieurs centres métalliques.⁴ Ce type de matériaux présente un intérêt particulier pour des applications dans des domaines aussi variés que le stockage de gaz, la catalyse hétérogène, la capture de dioxyde de carbone et les matériaux luminescents.⁵



Connue depuis les années 1920, la dipyrrole ou dipyrrométhène⁶ possède des propriétés intéressantes telle que la facilité de synthèse et une fonctionnalisation aisée, (formation de dipyrrométhane par réaction de condensation entre un aldéhyde fonctionnalisé et du pyrrole en excès puis son oxydation en dipyrrométhène) et sa capacité à complexer de nombreux centres métalliques.^{6a} La dipyrrole est constituée de deux cycles pyrroliques conjugués, coplanaires et structuralement équivalents liés par un pont méthylène fonctionnalisé. En milieu basique, elle peut être déprotonée menant à la formation d'un chélate mono-anionique. Ces caractéristiques en font un ligand de choix pour la formation de complexes luminescents ou présentant une activité catalytique ainsi

qu'un excellent tecton pour la construction de polymères de coordination homo- et/ou hétéro-métalliques.⁷ L'introduction d'unités coordinantes secondaires en position 5 a été particulièrement étudiée pour la préparation de tels réseaux.⁸

L'objectif de mes travaux de thèse a été de développer de nouvelles approches pour la fonctionnalisation de la dipyrroline par des groupements coordinants à la périphérie du squelette bispyrrolique sur d'autres positions afin de former de nouveaux tectons pouvant être ensuite utilisés pour la construction d'architectures discrètes et infinies, homo- et hétéro-métalliques.

Dans la première partie de la thèse, la fonctionnalisation par des groupements coordinants en positions 1 et 9 par des réactions du type Knoevenagel⁹ combinée à l'introduction d'une autre unité coordinante ou solubilisante en position 5 a été explorée menant à une série de nouveaux dérivés à base de dipyrroline. Les complexes de zinc et de bore (BODIPY) de ces dérivés ont été préparés et leurs propriétés photophysiques ont été explorées. En outre, ces complexes luminescents ont été utilisés comme métallatectons⁴ pour la construction de polymères de coordination hétérométalliques émissifs dans le proche-IR.

La deuxième partie de ce travail a porté sur la fonctionnalisation de polydipyrrolines. Ce type de dérivés comprenant plusieurs unités dipyrrolines connectées avec ou sans pont permet la formation d'architectures supramoléculaires métallo-organiques.¹⁰ La 2,2'-bisdipyrroline a été particulièrement étudiée pour son assemblage avec le cation Zn(II) menant à des hélicates linéaires. Récemment, notre groupe s'est intéressé à la coordination et à la chimie supramoléculaire de ce ligand; l'association d'hélicates linéaires avec le cation Ag(I) a pu être étudiée et la formation d'hélicates circulaires tri- et tétra-nucléaires démontrée.¹¹ Au cours de cette thèse, une unité réactive telle qu'un aldéhyde ou un acide carboxylique a été introduite à la périphérie de 2,2'-bisdipyrroline permettant la synthèse d'une variété d'espèces par formation d'imine ou d'amide.

2) Résultats et discussions

2.1) Formation de polymères de coordination (hétéro)-métalliques à base de 1,9-divinyldipyrrolines

Récemment, des dérivés de 1,9-divinyldipyrroline et leurs complexes de Zn(II) ou B(III) ont été étudiés pour leur émission dans le proche-IR due au système conjugué étendu du ligand.¹² De façon intéressante, cette fonctionnalisation en positions 1 et 9 n'a pas été mise à profit pour l'introduction de groupements coordinants conduisant aux réseaux de coordination. Ainsi, le but a

été ici la conception et la synthèse d'un nouveau ligand permettant d'introduire de telles unités, pouvant mener à la formation de tectons luminescents (Zn/B) et par la suite à des architectures émissives en suivant les principes de la tectonique moléculaire (Schéma 1).

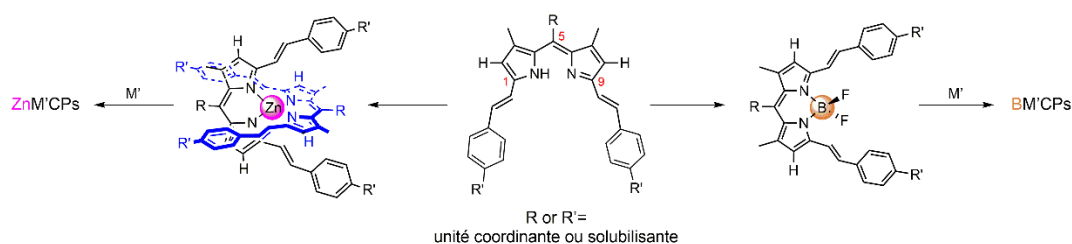


Schéma 1 : Stratégies pour la préparation des réseaux de coordination basés sur des dérivés de la 1,9-divinyldipyrrine.

En tirant parti de l'acidité des atomes d'hydrogène des groupements méthyles en position 1 et 9 de la 1,3,7,9-tétraméthylidipyrrine pour réaliser une condensation de type Knoevenagel⁹ avec des aldéhydes, une famille de cinq nouveaux ligands a été préparée et caractérisée. Ces composés comprennent le chélate dipyrroline, les unités vinyliques en positions 1 et 9 et une fonction coordinante ou solubilisante (mésityle) en position 5. Les tétraméthylidipyrrolines **1**, **5**, **6**¹³ ont ainsi été mises à réagir avec le 4-cyanobenzaldéhyde, le 4-pyridinecarboxaldéhyde ou le 4-formylbenzoate de méthyle, en présence de piperidine et d'une quantité catalytique d'acide *p*-toluènesulfonique. Les dérivés **2-4**, **7-9** ont été obtenus avec des rendements de 50 à 63 %. Avec ces ligands, de nouveaux BODIPY **10-15** et des complexes homoleptiques de Zn(II) **21-25** ont été synthétisés (Schéma. 2) selon des méthodes décrites dans la littérature.¹⁴ Tous les composés ont été caractérisés par RMN ¹H et ¹³C, HRMS (ESI) et spectroscopie UV-Visible en solution.

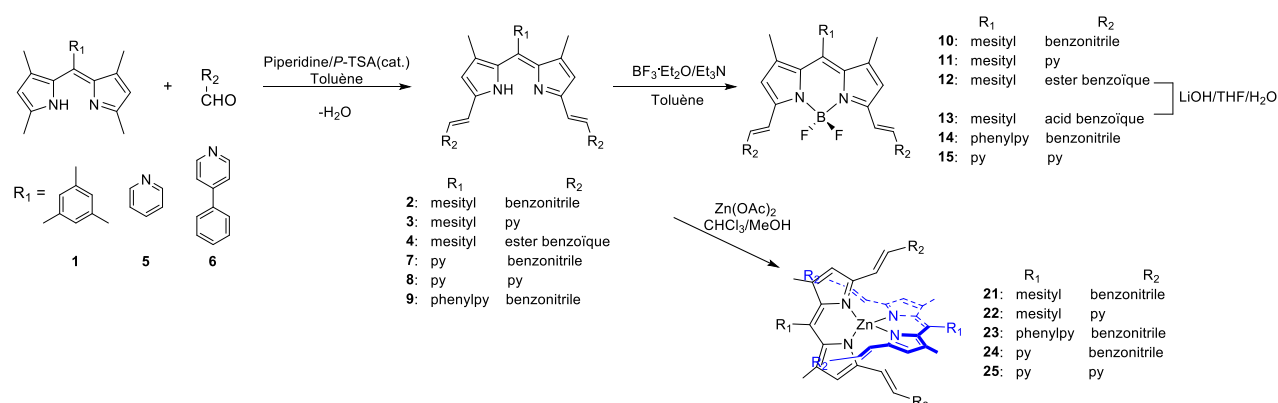


Schéma. 2 : Schéma de synthèse des ligands dipyrrolines dérivés **2-4**, **7-9** et des complexes **10-15**, **21-25**.

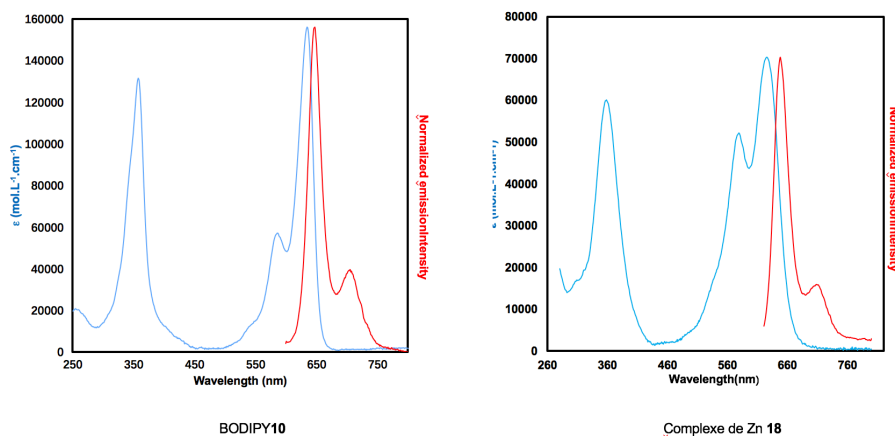


Figure 1: Spectres d'absorption et d'émission ($\lambda_{\text{ex}} = 570 \text{ nm}$) du BODIPY **10** et du complexe de Zn **23** en solution dans le DMF respectivement.

Une étude photophysique des complexes en solution a confirmé leur luminescence. Sous une excitation à 570 nm, deux bandes d'émission sont observées à 626-648 et 684-711 nm pour les BODIPY **10-15**. Cette fluorescence est centrée sur le ligand bipyrrrolique du BODIPY. Pour les complexes de Zn(II), une première bande intense d'émission est observée à 620-649 nm, une deuxième bande dans la région 674-710 nm est également présente. Ces résultats sont similaires à ceux décrits pour des BODIPYs ou complexes de zinc analogues dans la littérature.^{12d,15} Deux exemples représentatifs sont décrits sur la Figure 1.

Ces composés ont été utilisés comme (métalla)tectons pour la construction de réseaux (hétéro)-métalliques par assemblage avec différents sels métalliques. Les résultats obtenus avec le BODIPY **10** et les sels d'AgX ($X^- = \text{AsF}_6^-, \text{BF}_4^-, \text{ClO}_4^-$) dans différents solvants sont présentés ici (Figure 2). Quatre réseaux de coordination différents **16-19** ont été caractérisés par diffraction des rayons X sur monocristal. Ils contiennent un motif métalla-macrocyclique [2+2] du type $[(\text{BODIPY})\text{Ag}]_2^{2+}$. L'arrangement de ce motif cyclique à l'état cristallin est dépendant de la nature de l'anion X^- et des solvants utilisés. Les macrocycles s'organisent en un dimère ou en réseau infini en raison de l'interaction avec l'anion ou de solvant agissant comme des ponts, ainsi que, dans certains cas, des interactions Ag- π avec le système pyrrolique du BODIPY. Pour toutes les structures, les anions sont situés à l'intérieur de la cavité du métalla-macrocycle et liés par liaison hydrogène aux CH internes des fragments de type benzonitrile.

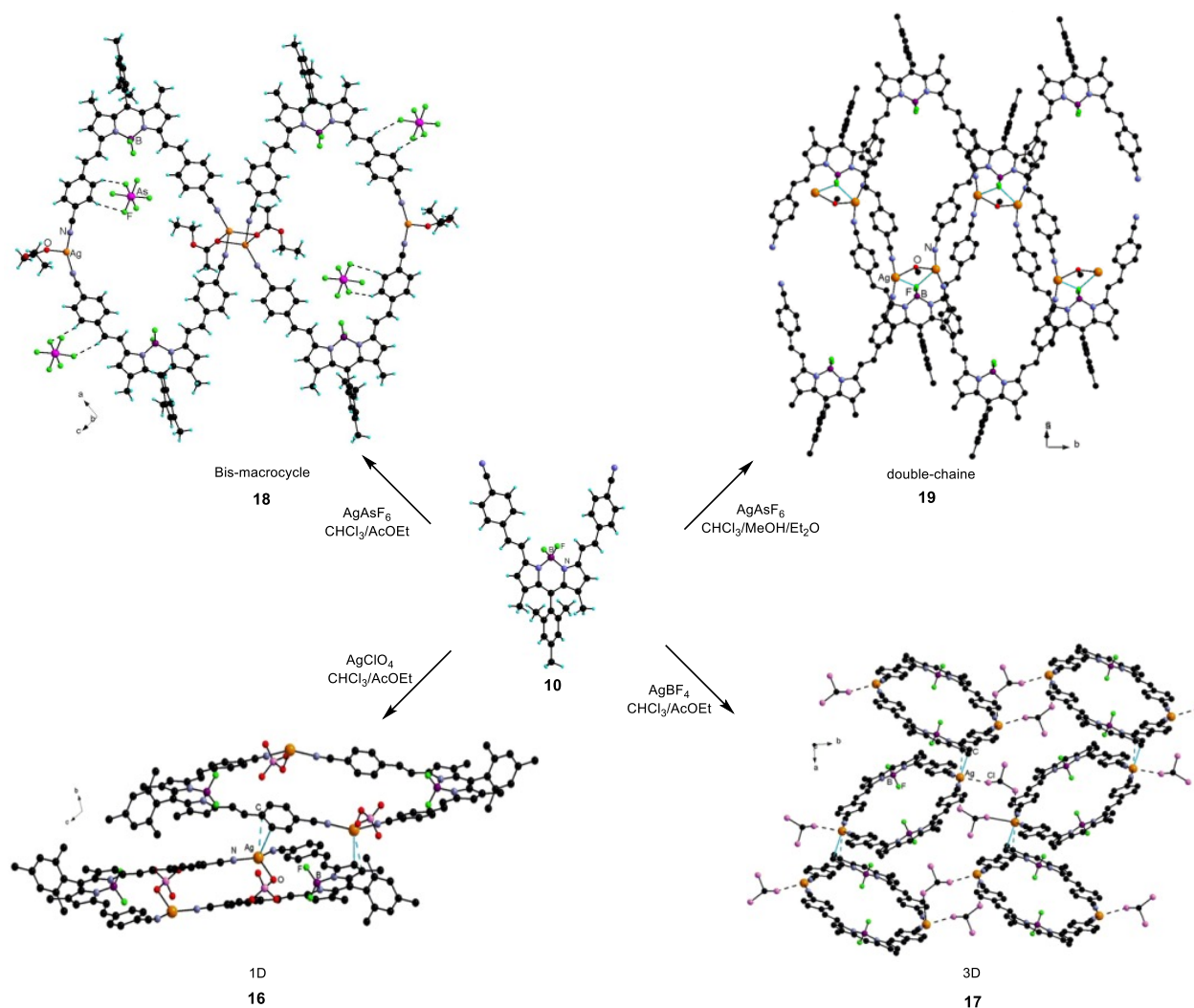


Figure 2: Structures cristallines du BODIPY **10** et des métalla-macrocycles [2+2] **16-19**.

La luminescence des composés **16-19** a été étudiée à l'état cristallin. Sous une excitation à 530 nm, deux bandes d'émission centrées sur 750 et 790 nm sont observées. Un décalage vers le rouge des bandes est observé par rapport au BODIPY **10** en solution. Ce changement peut résulter de la coordination des cations Ag(I) et / ou d'effet d'empilement à l'état solide. Un tel comportement a été observé dans les cas de MOFs basés sur des BODIPYs récemment décrits dans la littérature.¹⁶

Un nouveau réseau hétéro-métallique bidimensionnel **26** (Figure 3) construit par assemblage du complexe de zinc **23** et d'AgAsF₆ a été obtenu par diffusion de vapeur d'Et₂O dans un mélange DMF/CH₃CN (1/1). Dans ce cas, le groupe pyridine périphérique du complexe de zinc coordonne le cation Ag⁺ pour former une chaîne monodimensionnelle. Ces chaînes sont reliées par liaisons de coordination entre le cation Ag⁺ et le groupement benzonitrile d'un complexe de zinc voisin conduisant à une double chaîne hétérométallique. Par ailleurs, des cations argent supplémentaires sont coordonnés aux mêmes unités nitriles, occupant les cavités du réseau. Au sein du cristal, ces chaînes sont séparées par des molécules de solvant et les anions AsF₆⁻.

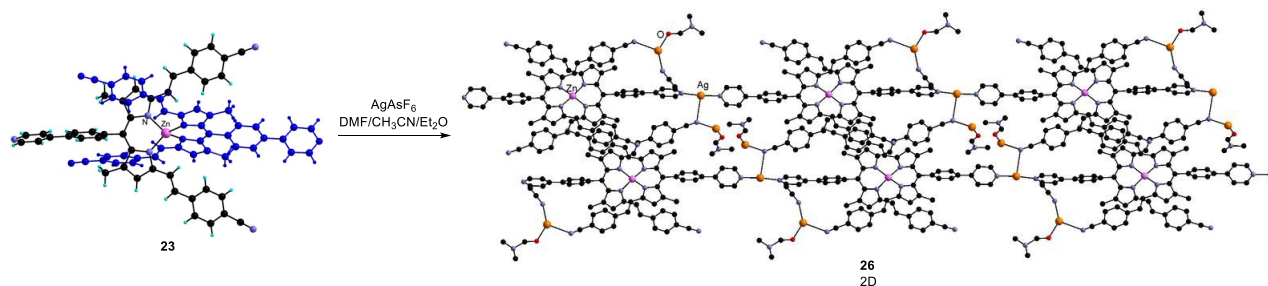


Figure 3: Structures cristallines du complexe **23** et du réseau de coordination hétérométallique **26**.

2.2) Dérivés bisdipyrines fonctionnalisés

La deuxième partie du travail a porté sur le développement de nouveaux dérivés du type bisdipyrine, d'une part pour la préparation de macrocycles par effet de matrice et, d'autre part, pour la construction de réseaux de coordination.

2.2.a) Synthèse de macrocycle à partir d'un hélicate comme template

Il a tout d'abord été envisagé d'utiliser les hélicates linéaires formés par l'assemblage de cations Zn(II) et de ligands 2,2'-bisdipyrines portant des groupements réactifs périphériques comme matrices (templates) pour la synthèse de macrocycles par formation de liaisons imines. La réaction de formation d'imine étant réversible, une étude préliminaire sur la réactivité des monodipyrines a été menée. Ainsi, une voie de synthèse optimisée pour la préparation de deux monodipyrines portant des groupes aniline ou benzaldéhyde périphériques en position 5 a été établie. Les amino- et aldéhyde-dipyrrométhane ont été générés par réduction de nitro- et cyanophenyl-dipyrrométhanes, obtenus pour leur part par réaction de l'aldéhyde correspondant dans du pyrrole pur avec une quantité catalytique d'acide trifluoroacétique avec un rendement de 85%. L'oxydation du squelette pyrrolique par le DDQ a donné les dérivés dipyrines **33-35** (Schéma 3).¹⁷

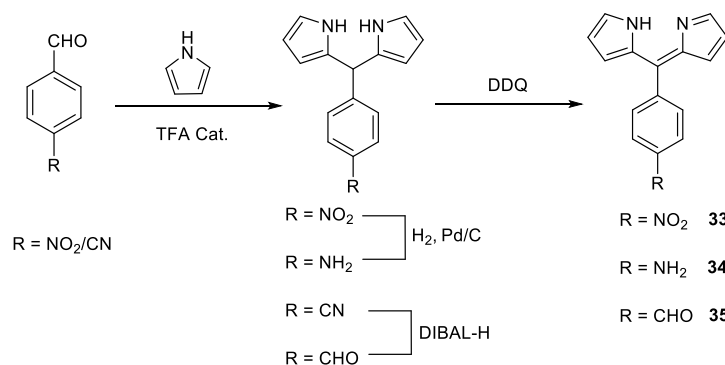


Schéma 3 : Stratégies de synthèse des monodipyrines **33-35**.

Au regard de la plus grande solubilité du dérivé **35** par rapport à la dipyrrole **34**, le premier a été utilisé pour mettre au point les conditions de la synthèse d'imine. Ainsi, le nouveau ligand bis-dipyrrole **37** a été préparé avec 96% de rendement par condensation de **35** et de la *m*-xylylènediamine en présence d'une quantité catalytique d'acide trifluoroacétique (Schéma 4).¹⁸ Fondé sur ce résultat, la formation d'un macrocycle par réaction analogue avec un hélicate linéaire portant le même type de groupements benzaldéhydes a été envisagée.

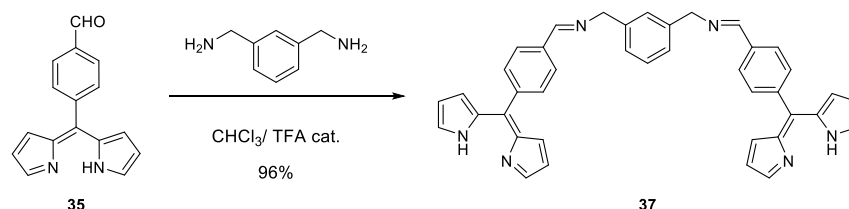


Schéma 4 : Stratégie de synthèse de la bis-dipyrrole **37**.

La voie de synthèse de l'hélicate linéaire **42** est présentée sur le Schéma 5 et suit la méthode basée sur un complexe de Ni(II) comme « template » décrite par Scott.¹⁹

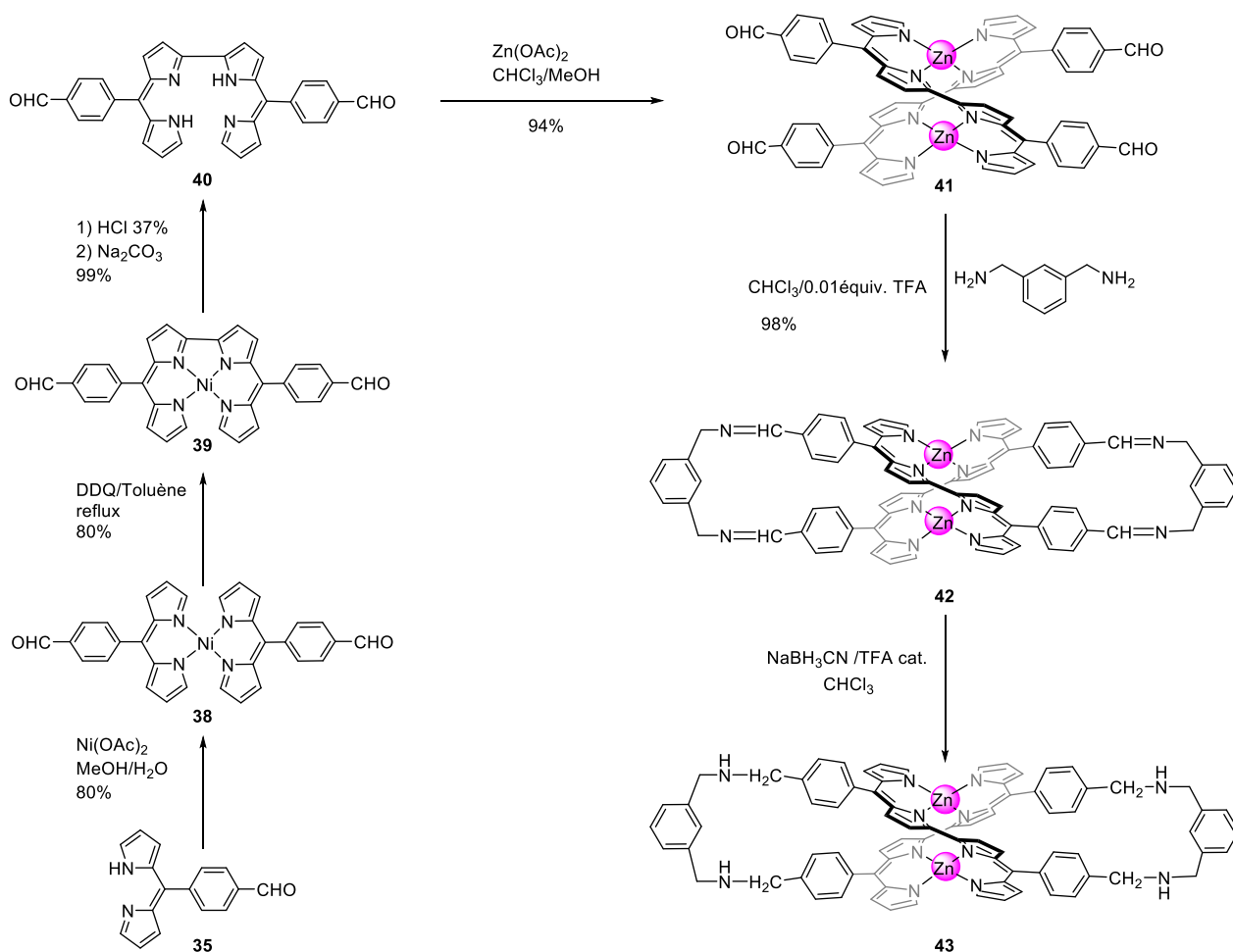


Schéma 5 : Stratégie de synthèse des macrocycles métalliques **42** et **43**.

Ainsi, le complexe **38** a été obtenu avec 80 % de rendement par réaction de la dipyrroline **35** avec $\text{Ni}(\text{OAc})_2$. L'oxydation au DDQ suivie d'une démétallation à l'aide de HCl a conduit à la formation du complexe **39** et de la bis-dipyrroline **40** avec 80 et 99% de rendements respectivement. L'hélicate **41** a été obtenu par réaction de **40** avec $\text{Zn}(\text{OAc})_2$ avec 94% de rendement.¹¹ En présence de 0.01 équiv. de TFA, la réaction de condensation entre l'hélicate **41** et *m*-xylylènediamine mène à la formation de l'hélicate fermé **42** avec 98% de rendement. Il est également intéressant d'étudier la réduction de la fonction imine en amine au niveau de ce macrocycle métallique. Le réactif de réduction NaBH_3CN utilisé mène à la formation de l'hélicate **43**.²⁰ Tous les composés ont été caractérisés par RMN ^1H , ^{13}C et HRMS (ESI).

2.2.b) Synthèse de 2,2'-bisdipyrroles symétriques

L'introduction de fonctions acides carboxylique a ensuite été envisagée pour la formation de différents ligands 2,2'-bisdipyrroles par réaction avec des amines. Ainsi, deux nouveaux composés 2,2'-bisdipyrroles symétriques fonctionnalisés **45** et **46** ont été obtenus à partir du dérivé **44** portant deux groupes acides benzoïque. **44** est obtenu par saponification de la 5,5'-diester-2,2'-bisdipyrroline avec 10 équivalents de LiOH dans un mélange THF/ H_2O (1/1). La réaction de **44** avec la 4-aminométhylpyridine, le chlorhydrate de EDC et HOBt dans le méthanol sec mène au nouveau ligand **46** avec 43 % de rendement.²¹ Malheureusement, le ligand **45** n'a pu être formé dans les mêmes conditions réactionnelles. En effet, c'est la 2,2'-bisdipyrroline dissymétrique portant une fonction ester et une fonction amide qui a été isolée. Ceci résulte de la compétition entre l'aniline et le solvant MeOH. Considérant l'effet du solvant et la solubilité du réactif de départ, la formation du nouveau ligand 2,2'-bisdipyrroline **45** a été réalisée dans le DMF sec avec 18 % de rendement (Schéma 6). Ces deux nouveaux composés ont été caractérisés et leur assemblage avec des cations $\text{Zn}(\text{II})$ est actuellement exploré par diffusion liquide-liquide des ligands 2,2'-bisdipyrroles **45** et **46** et de sels de zinc. Les deux hélicates correspondants ont pu être isolés.

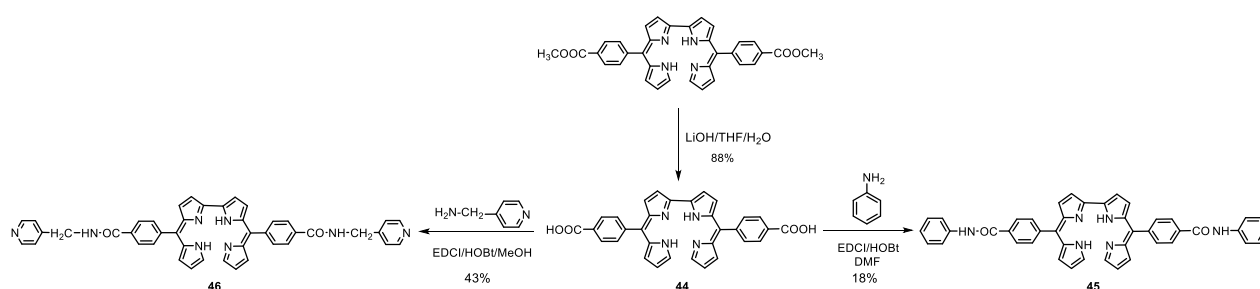


Schéma. 6 : Stratégie de synthèse des deux 2,2'-bisdipyrroles symétriques **45** et **46**.

2.2.c) Synthèse de 2,2'-bisdipyrroles dissymétriques

Enfin, de nouveaux ligands 2,2'-bisdipyrroles dissymétriques **54-57** ont été préparés (Schéma 7). Ils sont construits à partir du dérivé **50** comprenant d'une part une unité tolyle, pour améliorer la solubilité des composés, et d'autre part une fonction acide benzoïque pour la formation de liaisons amides. Le complexe dissymétrique **51** est formé à partir des deux monodipyrroles avec 43% de rendement. Après démétallation et saponification, la bisdipyrrole dissymétrique **53** est isolée. Par réaction avec des amines en présence de chlorhydrate de EDCi et HOBt dans le CH₂Cl₂ sec, les quatre nouveaux ligands **54-57** ont pu être obtenus avec 17 à 98 % de rendement.

Ces quatre nouveaux ligands ont été caractérisés par RMN ¹H, ¹³C, HRMS (ESI). Leur combinaison avec des cations Zn(II) a également été explorée. A ce jour, seule la formation d'hélicates linéaires a été observée. Dans le cas du ligand bis-bisdipyrrole **57**, un complexe bis-hélicate tétranucléaire a été caractérisé par spectrométrie de masse.

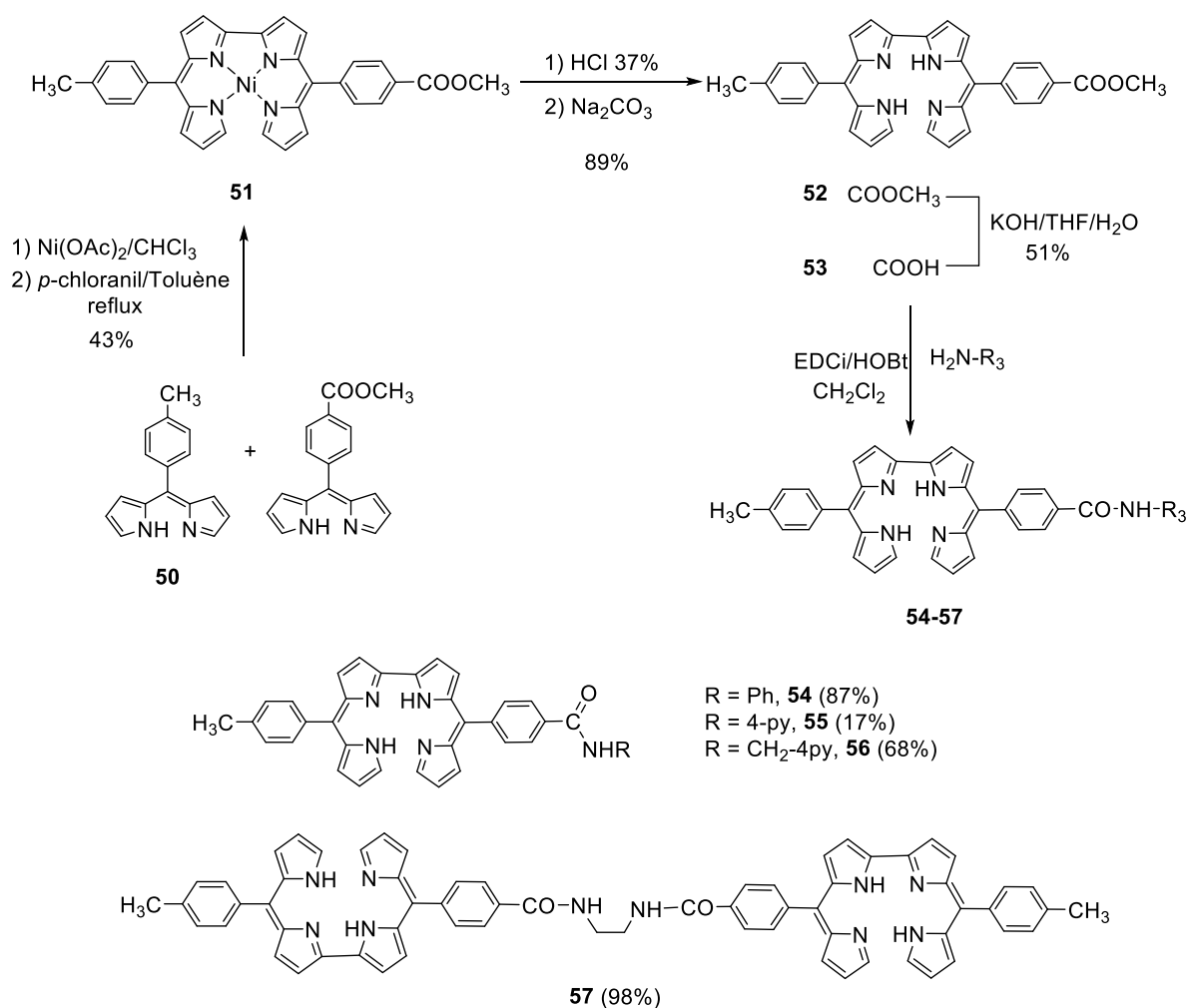


Schéma. 7 : Stratégie de synthèse des 2,2'-bisdipyrroles dissymétriques **54-57**.

3) Conclusion générale

En résumé, au cours de ce travail de thèse, la synthèse de nouveaux dérivés du type 1,9-divinyldipyrriine et de leurs complexes (B/Zn) a été étudiée. Tous les composés ont été caractérisés en solution, avec un accent mis sur leurs propriétés photophysiques qui a montré leur émission dans le proche-IR sous une excitation dans le visible. La formation de réseaux de coordination (hétéro)-métalliques à l'aide de ces complexes a été explorée avec différents systèmes de solvant et sels métalliques et étudiée par diffraction des rayons X. La dimensionnalité des réseaux est déterminée par l'interaction avec des anions et/ou les molécules de solvant, ainsi que des interactions Ag- π . D'autre part, la synthèse d'un macrocycle métallique portant des liaisons imines périphériques ou amines à partir d'un hélicate binucléaire comme « template » a été explorée avec succès. Enfin, de nouveaux ligands 2,2'-bisdipyrriines symétriques et dissymétriques ont été obtenus par condensation de bis-dipyrriines portant un ou deux groupements réactifs périphériques et leur assemblage avec des sels de Zn(II) a été étudiée.

4) Références

-
- ¹ M. W. Hosseini, *L'actualité chimique*, **2005**, 290-291, 51.
² M. W. Hosseini, *Coord. Chem. Rev.*, **2003**, 240, 157.
³ (a) M. Simard, D. Su, J. D. Wuest, *J. Am. Chem. Soc.*, **1991**, 113, 4696. (b) M. W. Hosseini, *CrystEngComm.*, **2004**, 318.
⁴ M. W. Hosseini, *Acc. Chem. Res.*, **2005**, 38, 313-323.
⁵ (a) S. R. Batten, R. Robson, *Angew. Chem., Int. Ed.*, **1998**, 37, 1460. (b) M. Eddaoudi, D. B. Moler, H. Li, B. Chen, T. M. Reineke, M. O'Keeffe, O. M. Yaghi, *Acc. Chem. Res.*, **2001**, 34, 319. (c) S. Kitagawa, R. Kitaura, S. I. Noro, *Angew. Chem. Int. Ed.*, **2004**, 43, 2334. (d) J. R. Long, O. M. Yaghi, *Chem. Soc. Rev.*, **2009**, 38, 1213-1214. (e) *Chem. Soc. Rev.*, **2009**, 38 (5), themed issue on metal-organic frameworks. (f) C. Janiak, J. K. Vieth, *New J. Chem.*, **2010**, 34, 2366. (g) *Chem. Rev.*, **2012**, 112 (2), 2012 Metal–Organic Frameworks special issue. (h) C. Wang, W. Lin, *J. Am. Chem. Soc.*, **2013**, 135, 13222.
⁶ (a) T. E. Wood and A. Thompson, *Chem. Rev.*, **2007**, 107, 1831. (b) H. Maeda, *Eur. J. Org. Chem.*, **2007**, 5313. (c) S. A. Baudron, *Dalton Trans.*, **2013**, 42, 7498. (d) T. Nabeshima, M. Yamamura, G. J. Richards, T. Nakamura, J. Synth. Org. Chem. Jpn., **2015**, 73, 1111. (e) R. Sakamoto, T. Iwashima, M. Tsuchiya, R. Toyoda, R. Matsuoka, J. F. K. gel, S. Kusaka, K. Hoshiko, T. Yagi, T. Nagayama and H. Nishihara, *J. Mater. Chem. A.*, **2015**, 3, 15357.
⁷ (a) S. A. Baudron, *CrystEngComm.*, **2010**, 12, 2288. (b) S. A. Baudron, *CrystEngComm.*, **2016**, 18, 4671.
⁸ (a) S. R. Halper, L. Do, J. R. Stork, S. M. Cohen, *J. Am. Chem. Soc.*, **2006**, 128, 15255. (b) A. Béziau, S. A. Baudron, A. Guenet, M. W. Hosseini, *Chem. Eur. J.*, **2013**, 19, 3215. (c) A. Béziau, S. A. Baudron, A. Fluck, M. W. Hosseini, *Inorg. Chem.*, **2013**, 52, 14439. (d) A. Béziau, S. A. Baudron, G. Rogez, M. W. Hosseini, *Inorg. Chem.*, **2015**, 54, 2032.
⁹ (a) E. Knoevenagel, *Ber. Dtsch. Chem. Ges.*, **1898**, 31, 2596. (b) R. Ziessel, T. Bura, J. H. Olivier, *Synlett.*, **2010**, 15, 2304.
¹⁰ (a) M. Bröring, Beyond dipyrriins: Coordination interaction and templated macrocyclizations of open-chain oligopyrroles, in *Handbook of Porphyrin Science*, 2010, vol. 8, p. 343. (b) Y. Zhang, A. Thompson, S. J. Rettig and D. Dolphin, *J. Am. Chem. Soc.*, **1998**, 120, 13537. (c) H. Maeda, T. Nishimura, R. Akuta, K. Takaishi, M. Uchiyama and A. Muranaka, *Chem. Sci.*, **2013**, 4, 1204.
¹¹ (a) H. Ruffin, S. A. Baudron, D. Salazar-Mendoza and M. W. Hosseini, *Chem. Eur. J.*, **2014**, 20, 2449. (b) S. A. Baudron, H. Ruffin, M. W. Hosseini, *Chem. Commun.*, **2015**, 51, 5906. (c) S. A. Baudron and M. W. Hosseini, *Chem. Commun.*, **2016**, 52, 13000.
¹² (a) R. Ziessel, G. Ulrich, A. Harriman, M. A. H. Alamiry, B. Stewart and P. Retailleau, *Chem. Eur. J.*, **2009**, 15, 1359. (b) K. Rurack, M. Kollmannsberger and J. Daub., *New J. Chem.*, **2001**, 25, 289. (c) J. Bartelmeß and W. W.

-
- Weare, *Dyes and Pigments.*, **2013**, 97, 1. (d) R. Sakamoto, T. Iwashima, J. F. Kögel, S. Kusaka, M. Tsuchiya, Y. Kitagawa and H. Nishihara, *J. Am. Chem. Soc.*, **2016**, 138, 5666.
- ¹³ (a) L. Fu, F.-L. Jiang, D. Fortin, P. D. Harvey and Y. Liu, *Chem. Commun.*, **2011**, 47, 5503.
- ¹⁴ (a) G. Ulrich, R. Ziessel and A. Harriman, *Angew. Chem. Int. Ed.*, **2008**, 47, 1184. (b) S. Kusaka, R. Sakamoto, Y. Kitagawa, M. Okumura and H. Nishihara, *Chem. Asian. J.*, **2012**, 7, 907.
- ¹⁵ C. O. Obondi, G. N. Lim, P. A. Karr, V. Nesterov and F. D'Souza, *Phys. Chem. Chem. Phys.*, **2016**, 18, 18187.
- ¹⁶ (a) C. Y. Lee, O. K. Farha, B. J. Hong, A. A. Sarjeant, S. B. T. Nguyen and J. T. Hupp, *J. Am. Chem. Soc.*, **2011**, 133, 15858. (b) L. Zhou, Y. S. Xue, J. Zhang and H. B. Du, *CrystEngComm.*, **2013**, 15, 7315. (c) M. Li, Y. Yao, J. Ding, L. Liu, J. Qin, Y. Zhao, H. Hou and Y. Fan, *Inorg. Chem.*, **2015**, 54, 1346.
- ¹⁷ (a) C. Brückner, Y. Zhang, S. J. Rettig, D. Dolphin, *Inorganica. Chimica. Acta.*, **1997**, 263, 279. (b) B. J. Littler, M. A. Miller, C. H. Hung, R. W. Wagner, D. F. O'Shea, P. D. Boyle and J. S. Lindsey, *J. Org. Chem.*, **1999**, 64, 1391. (c) P. D. Rao, S. Dhanalekshmi, B. J. Littler and J. S. Lindsey, *J. Org. Chem.*, **2000**, 65, 7323.
- ¹⁸ S. Hong, M. R. Rohman, J. Jia, Y. Kim, D. Moon, Y. Kim, Y. H. Ko, E. Lee and K. Kim, *Angew. Chem. Int. Ed.*, **2015**, 54, 13241.
- ¹⁹ H. S. Gill, I. Finger, I. Bozidarević, F. Szydło and M. J. Scott, *New. J. Chem.*, **2005**, 29, 68.
- ²⁰ J. S. Lindsey and D. C. Mauzerall, *J. Am. Chem. Soc.*, **1982**, 104, 4499.
- ²¹ L. C. Chan and B. G. Cox, *J. Org. Chem.*, **2007**, 72, 8863.
-

LISTE DES PRESENTATIONS

1. Fan Zhang, Stéphane Baudron, Mir Wais Hosseini, Journée des Doctorants de l'Ecole Doctorale des Sciences Chimiques, 02/11/2016, Strasbourg, Présentation Orale.
2. Fan Zhang, Stéphane Baudron, Mir Wais Hosseini, Journée de Réunion d'UMR 7140, 06/01/2017, Strasbourg, Présentation Orale.
3. Fan Zhang, Stéphane Baudron, Mir Wais Hosseini, International Symposium on Macrocyclic and Supramolecular Chemistry (ISMSC), 02-06/07/2017, Cambridge (UK), Présentation Poster.
"2,2'-Bis-dipyrrin ligands for the construction of supramolecular metallo-organic architectures"
4. Fan Zhang, Stéphane Baudron, Mir Wais Hosseini, The 28th International Conference on Photochemistry (ICP 2017), 16-21/07/2017, Strasbourg, Présentation Poster.
"Solvent and anion effects on the organization of a luminescent BODIPY/Ag(I) metallamacrocyle in the crystalline state"

PUBLICATION

1. *Solvent and anion effects on the organization of a luminescent [2+2] BODIPY/Ag(I) metallamacrocyle in the crystalline state*
 Fan Zhang, Stéphane Baudron, Mir Wais Hosseini, *CrystEngComm*, **2017**, 19, 4393-4400.

Introduction

Introduction

1 Supramolecular Chemistry

In 1978, Pr. Jean-Marie Lehn, 1987 Nobel Prize winner in Chemistry, introduced the notion of supramolecular chemistry. This new concept is described as “*the chemistry beyond the molecule*” and explained as follows: “*If molecular chemistry deals with the design and synthesis of individual units based on covalent bond, their assay by weak interactions is according to the concepts of supramolecular chemistry*”.¹ The association of molecular entities by intermolecular reversible interactions such as van der Waals forces, hydrogen bonding, coordination bonding, electrostatic or π - π interaction, which are less energetic than the covalent bond is thus concerned by the frame of this concept.² Supramolecular chemistry, as a discipline involving inorganic and organic chemistry, coordination chemistry, polymer chemistry, biochemistry has already developed as an independent branch of chemistry. It constitutes today an important part of nanotechnology, materials and life sciences. Finally, the use of weak intermolecular interactions provides the possibility to deeply understand some of the physical, biological and chemical properties of natural systems and to mimic them.

Along with the emergence of supramolecular chemistry, other new concepts have been introduced such as molecular recognition, self-assembly and self-organization which play an important role in the understanding and development of supramolecular materials.

1.1 Molecular recognition

The assembly between a guest molecule and a complementary (including electronic properties and shape) host molecule is called molecular recognition. It does not refer only to simple intermolecular binding, but includes selection of a target substrate through molecular recognition processes. The energy and information involved in this process are used to generate an assembly

¹ (a) J. M. Lehn, *Pure Appl. Chem.*, **1978**, 50, 871. (b) J. M. Lehn, *Angew. Chem. Int. Ed. Engl.*, **1988**, 28, 89. (c) J. M. Lehn, *Angew. Chem. Int. Ed. Engl.*, **1990**, 29, 1304.

² (a) J. M. Lehn, *Supramolecular chemistry: Concepts and Perspectives*, Wiley-VCH, **1995**. (b) J. M. Lehn, *Proceedings of the national Academy of Sciences.*, **2002**, 99, 4763. (c) J. M. Lehn, *Chem. Soc. Rev.*, **2007**, 36, 151. (d) J. W. Steed, D. R. Turner and K. Wallace, *Core concepts in Supramolecular Chemistry and Nanochemistry.*, **2007**.

(host - guest complex), a programmed supramolecular entity. Therefore, supramolecular chemistry can be also considered as a chemical information science or as molecular informatics.^{2a}

1.2 Molecular self-assembly

Molecular self-assembly is based on the assembly of pre-organized individual molecules leading to aggregates *via* weak non-covalent intermolecular interactions. At first, the self-assembly approach, as a spontaneous process, follows the rules of thermodynamics. In other words, the self-assembled species are thermodynamically more stable than the single, unassembled units. In theory, the one with the lowest Gibbs free energy tends to be formed during the self-assembly process. (Figure 1b) However, most of the self-assembly processes cannot be perfectly designed. In general, several thermodynamically stable states may be generated. As shown in Figure 1, depending on the difference of energy barrier between these final states, they can convert into each other or not. For example, in case c, the barrier between the two different final states is rather low and they can easily convert into one another whereas, in case d, the barrier is too high and they can both coexist. This explains the formation of polymorphs and supramolecular structural isomers. On the other hand, the molecular self-assembly allows self-healing processes due to the use of reversible interactions. Thus, the self-assembly is governed by equilibrium processes, and the low activation energy barrier of the non-covalent interactions leads to the reversible events. It allows the system to repair potential construction mistakes by itself during the assembling process and leads ultimately to the thermodynamically stable state.³ (Figure 1e)

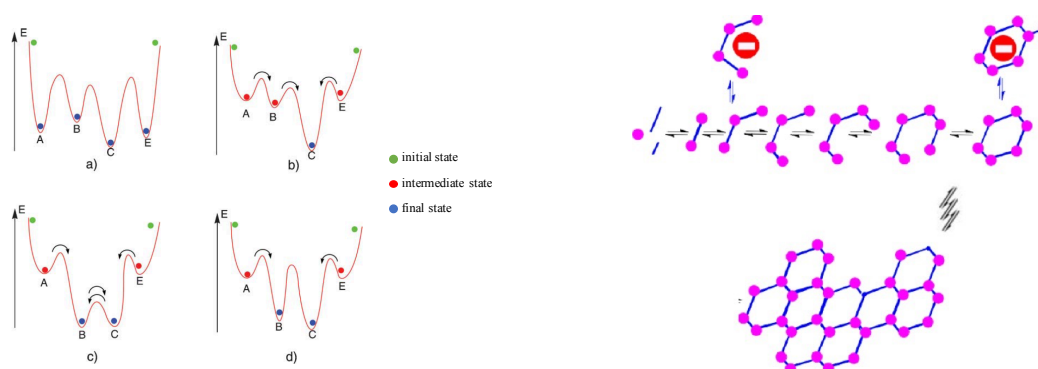


Figure 1: Schematic representations of the activation energy barrier (left) and self-healing events (right) for molecular self-assembly process.³

³ M. W. Hosseini, *CrystEngComm.*, **2004**, 6, 318.

Compared with synthesis based on covalent bond, the self-assembly approach appears more difficult to be controlled, in particular the final structure of the materials and more specifically their arrangement in space for crystalline architectures. Through a rigorous programming of the building units, some control such as connectivity pattern can be envisioned. The molecular tectonics approach, a sub-branch of supramolecular chemistry, deals with this issue.

2 Molecular Tectonics

The term “molecular tectonics” was first introduced by Pr. Stephan Mann in 1993.⁴ This approach is defined as: “*the use of designed building blocks (called tectons), which have at least two complementary interaction sites and are able to recognize each other via non-covalent interactions, to construct periodic architectures through self-assembly processes*”. Molecular recognition, involved in the context of molecular tectonics, is a selective association behaviour between two complementary interactions sites. The nature and the number of the recognition sites determine not only the strength of the attractive interactions, but also their directionality.^{3,5} Furthermore, the repeating behaviour leads to the translation of recognition pattern and to the construction of molecular networks. This means that the dimensionality of the periodic infinite architectures (mono-, bi-, or tri-dimensional) is defined by translation of the recognition patterns in one, two or three directions of space.

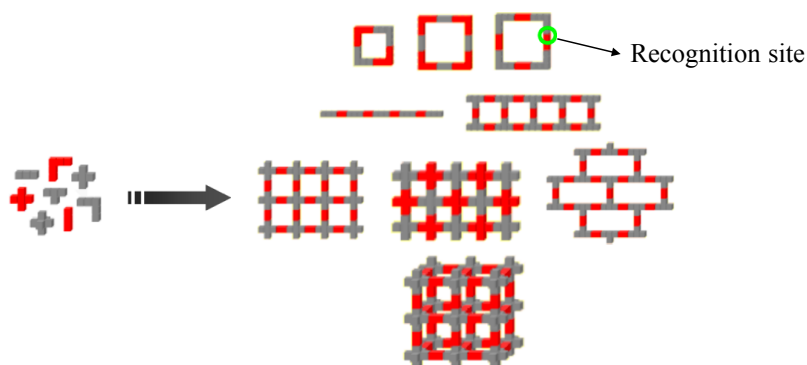


Figure 2: Schematic illustration of supramolecular structures obtained by recognition processes based on different geometrical complementary tectons.

Thus, for the molecular tectonics approach, the nature of the molecular tectons and parameters such as energy and directionality of intermolecular interactions play key roles for the formation of molecular networks.

⁴ S. Mann, *Nature.*, **1993**, 365, 499.

⁵ (a) M. W. Hosseini, *Coord. Chem. Rev.*, **2003**, 240, 157. (b) M. W. Hosseini, *Chem. Commun.*, **2005**, 5825.

2.1 The design of the molecular tectons

The design of molecular tectons is essential for the formation of molecular networks. In principle, two features should be taken account. Firstly, for the self-assembly process, molecular networks are generated through either the self-complementarity of a molecular tecton or the complementarity of at least two different molecular tectons (Figure 3). The single-component strategy appears advantageous owing to its simplicity, however, an inherent drawback sometimes resides in the low solubility of the tectons, as a result of its tendency to self-assemble leading thus to amorphous powders. In contrast, a system composed of several complementary tectons is more viable, because the formation of the product in the crystalline state provides the possibility of structural characterization and investigation.

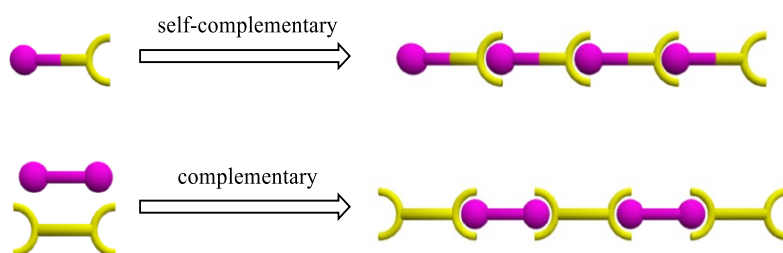


Figure 3: Schematic representations of the assembly of either a single self-complementary or two complementary tectons.

The geometry of molecular tectons is also a key feature for iterative recognition processes. Depending on the relative positions of the recognition sites, molecular tectons can be classified into two categories: *endo*-receptor and *exo*-receptor. In the case of the *endo*-receptors, only discrete complexes can be formed because its recognition sites are positioned in a convergent fashion (Figure 4). However, *exo*-receptors, based on divergently oriented recognition units, may generate either discrete complexes or infinite periodic molecular entities. Thus, *exo*-receptors are adequate tectons for the construction of molecular networks.



Figure 4: Schematic representation of the formation of discrete complex based on an *endo*-receptor.

In the case of *exo*-receptors, the formation of either discrete species or infinite architectures depends on the nature (*c.a.* geometry, number, localization and orientation of interaction sites) of the tectons and the associated substrates or connectors. If the iterative process is interrupted, for example by using blocking units, a discrete entity will be obtained as shown in Figure 5(a). In contrast, using appropriate connectors, 1D-, 2D- or 3D-infinite molecular networks can be constructed (Figure 5b, c, d). Moreover, P. J. Stang and coworkers has reported a “molecular library” for the classification of discrete molecular species.⁶ According to the schematic illustration shown in Figure 5(b), it has been demonstrated that tectons with predetermined angles may be assembled into 2D planar entities, as well as 3D non-planar entities with different morphologies.

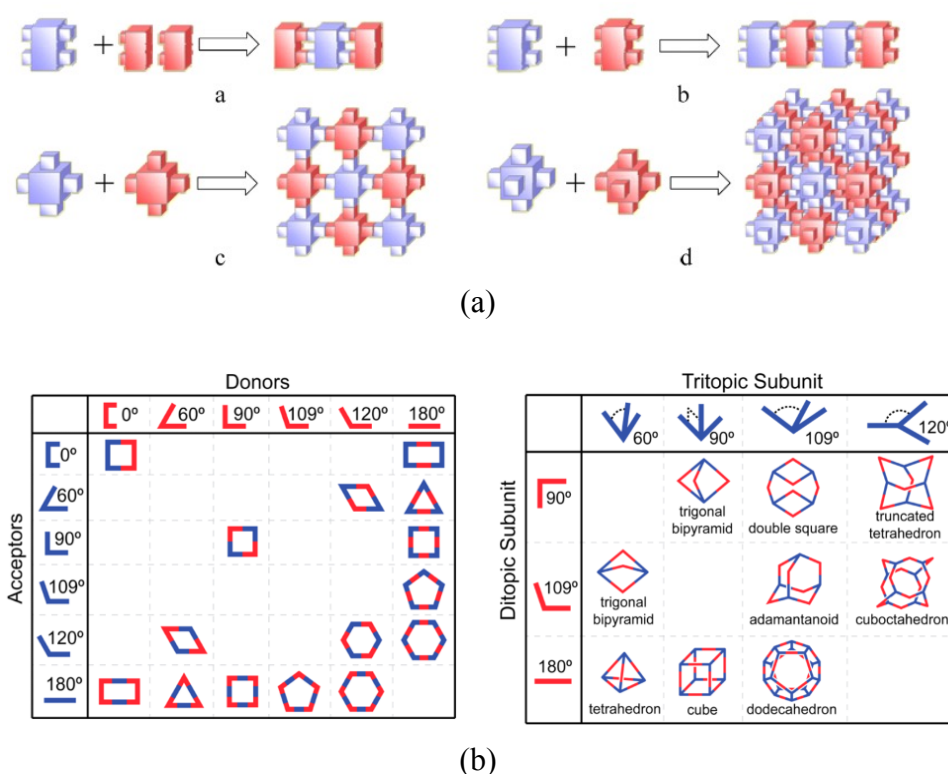


Figure 5: (a) Schematic representations of the formation of discrete complex or infinite molecular networks upon combination of an *exo*-receptor and substrates or connectors.³ (b) “Molecular library” of discrete 2D (left) or 3D (right) molecular entities.⁶

⁶ T. R. Cook, R. Y. Zheng and J. P. Stang, *Chem. Rev.*, **2013**, *113*, 743.

2.2 Intermolecular interactions

As mentioned above, the formation of molecular networks is based on the repetition of molecular recognition events resulting from a variety of reversible interactions between molecular tectons. According to their energy (range 0 to *c.a.* 100 kcal/mol), they can be divided into several categories: van der Waals interactions, charge assisted electrostatic interactions, π - π interactions, metal-metal interactions, hydrogen, coordination bonds etc. (Figure 6). All these interactions can be used to generate infinite molecular networks. The formation of the latter and their packing in the crystalline state may involve a single or several types of interactions. Depending on the nature of the binding mode used, molecular networks can be named as coordination, H-bonded or hybrid network. Some typical intermolecular interactions and their corresponding networks will be discussed in the following section.

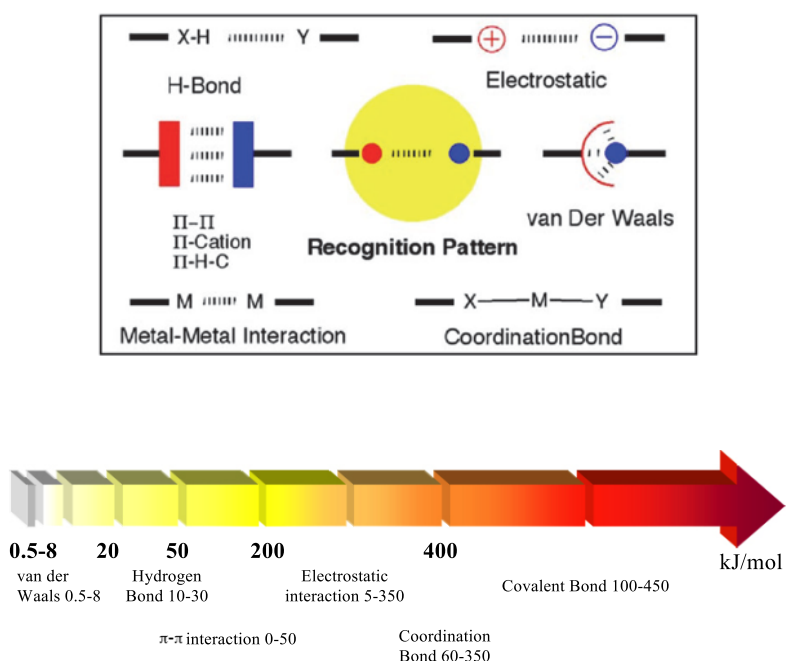


Figure 6: Schematic representations of the toolbox of intermolecular interactions (top)³ and the energy of intermolecular and intramolecular interactions (bottom).

2.2.1 Van der Waals interaction

Van der Waals interactions (vdW) (0.5-8 kJ/mol), being the weakest of weak intermolecular interactions, have some features such as a lack of directionality and selectivity and the difficulty to be controlled. Although van der Waals interactions are weaker than the other chemical forces, it

is nonetheless possible to exploit them for the preparation of molecular networks in the solid state. Indeed, inclusion networks between concave and convex tectons have been described using such interaction.⁷ For example, the functionalized calix[4]arene **i-1** presented in Figure 7 acts as a receptor for *p*-xylene behaving as a connector and their self-assembly leads to the formation of a one-dimensional network, **i-2**, by a self-inclusion process (Figure 7).⁸ For the sake of clarity, compounds presented in the introduction section will be numbered **i-1**, **i-2**, ..., while those prepared in the frame of this PhD. work will be numbered simply as **1**, **2**, ... throughout of the document.

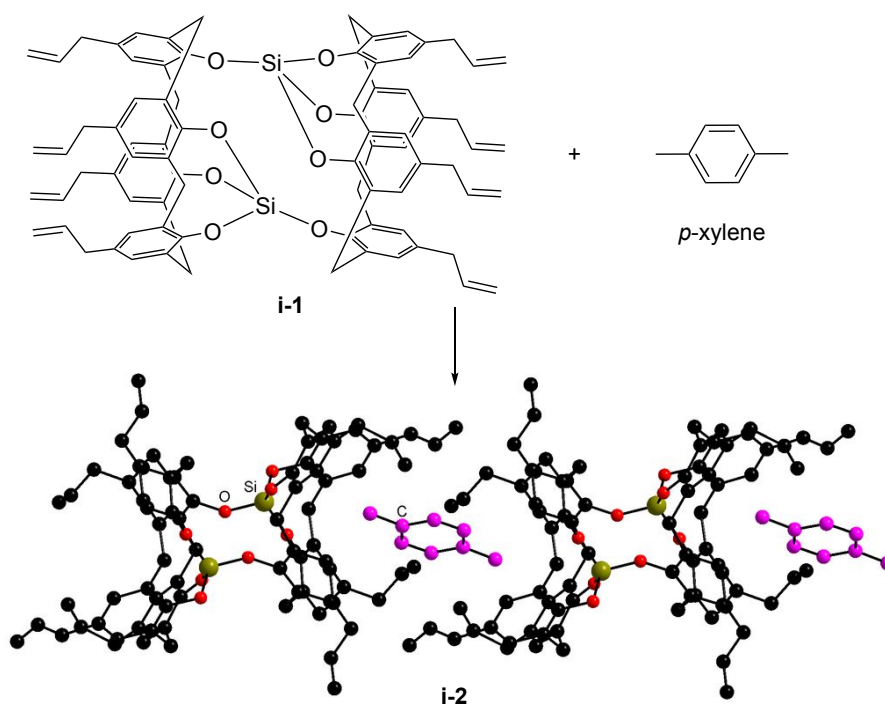


Figure 7: Formation of self-inclusion network **i-2** by assembly of bis-calixarene **i-1** with *p*-xylene.

2.2.2 π - π interaction

π - π interactions also called π - π stacking with an energy range of 0-50 kJ/mol is an important non-covalent interaction in molecular recognition and impacts the packing of supramolecular architectures as well as of coordination networks in the crystalline state. Not only they do have structural effects but they may also influence the solid-state properties such as the photophysical ones for example. Recently, a 3D coordination network **i-6** consisting of 1,4-bis(4-pyridyl)-2,3-diaza-1,3-butadiene (4-bpdb) **i-4**, pimelic acid **i-5** and cadmium cation has

⁷ (a) X. Delaigue, M. W. Hosseini, A. De Cian, J. Fischer, E. Leize, S. Kieffer and A. Van Dorsselaer, *Tetrahedron Lett.*, **1993**, 34, 3285. (b) X. Delaigue, M. W. Hosseini, R. Graff, J.-P. Kintzinger and J. Raya, *Tetrahedron Lett.*, **1994**, 35, 1711.

⁸ M. W. Hosseini and A. De Cian, *Chem. Commun.*, **1998**, 727.

been described.⁹ The π - π stacking interactions patterns were established between pyridyl rings of neighbouring 4-bpdb ligands, as shown in the Figure 8. The arrangement of two neighbouring pyridyl rings has been proposed to cause a blue shift of the emission band of the network due to the destabilization of the π - π stacking interactions with respect to other networks.

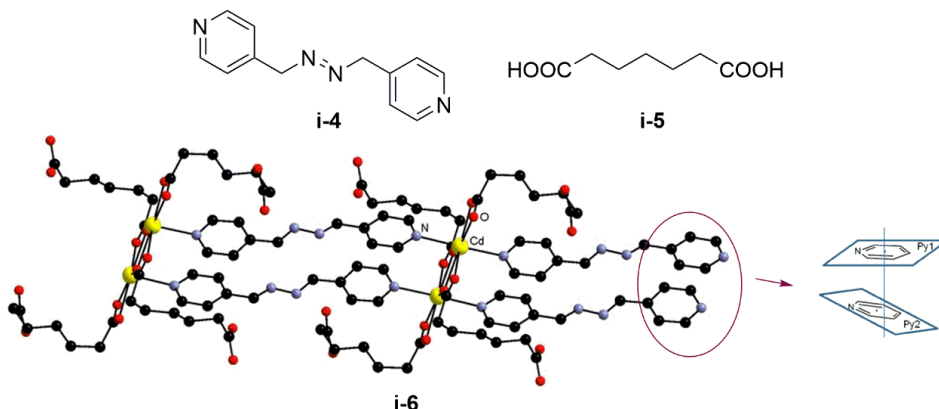


Figure 8: A fragment of the crystal structure of the three-dimensional network **i-6** based on the assembly of **i-4** and **i-5** with Cd(II) cations and schematic representation of the π - π interaction configuration of two pyridyl moieties.

2.2.3 Ag- π interaction

Metal- π interactions have been described for numerous metal cations¹⁰ and play an important role in natural and synthetic systems. In particular, Ag(I) cation, used in this work, has been shown to be prone to complexation by electron-rich π -systems. Compared with other non-covalent interactions, Ag- π interactions are comparatively weaker, but represent an important force in the formation of molecular networks and play a non-negligible role in the construction of the supramolecular architectures in the solid state. For example, the group of Munakata and co-workers has showed that the assembly of hexaphenylbenzene **i-7** with Ag(I) triflate leads to a 1D network **i-8** formed by Ag- π interaction of the binuclear $[\text{Ag}(\text{TfO})_2]$ (Figure 9).¹¹

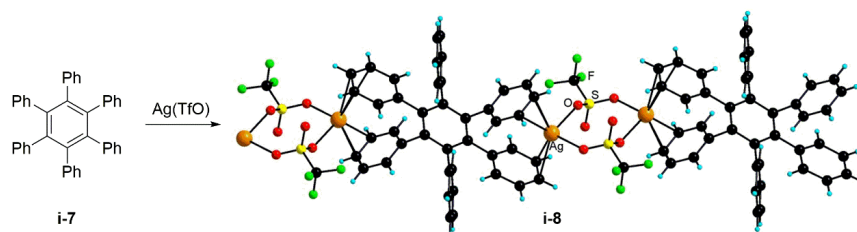


Figure 9: Formation of 1D network **i-8** based on Ag- π interactions.

⁹ A. J. Calahorra, E. S. Sebastián, A. Salinas-Castillo, J. M. Seco, C. Mendicute-Fierro, B. Fernández and A. Rodríguez-Diéguez, *CrystEngComm.*, **2015**, 17, 3659.

¹⁰ (a) J. C. Ma and D. A. Dougherty, *Chem. Rev.*, **1997**, 97, 1303. (b) A. S. Mahadevi and G. N. Sastry, *Chem. Rev.*, **2013**, 113, 2100.

¹¹ G. L. Ning, M. Munakata, L. P. Wu, M. Maekawa, Y. Suenaga, T. Kuroda-Sowa and K. Sugimoto, *Inorg. Chem.*, **1999**, 38, 5668.

For this compound, the Ag-C distances range from 2.58(1) to 2.82(1) Å. These distances are in line with what has been reported in a CSD analysis of compounds featuring such interactions.¹²

2.2.4 Hydrogen bonding interaction

Neutral and charge assisted hydrogen bonding is one of the most widely exploited interactions for the formation of supramolecular architectures and networks. The energy of this directional dipole-dipole interaction is different from the van de Waals one, and can range from weak to rather strong interactions (10-30 kJ/mol).¹³ A large variety of molecular networks based on hydrogen bonding and/or charge assisted hydrogen bonding has been developed.¹⁴ The case of assembly of amidinium and carboxylate derivatives, particularly investigated in our laboratory, leading to a broad range of molecular networks is relevant.¹⁵ For example, the bis-amidine **i-9** has been shown to interact with biphenyl-4,4'-dicarboxylic acid to form the amidinium/carboxylic acid pair that self-assembles in the crystalline state into one-dimensional polymer **i-10** by charge-assisted hydrogen bonding *via* a bis-dihapto mode of interaction as shown in Figure 10.¹⁶

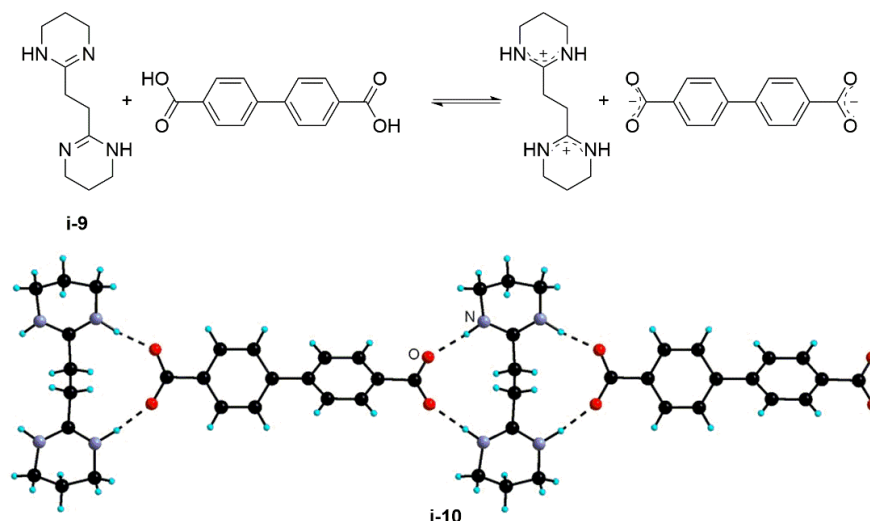


Figure 10: A portion of the 1D network **i-10** based on the dihapto mode of charge assisted H-bonding.

2.2.5 Coordination bonding interaction

Coordination bonding, with an energy ranging from medium to strong (60-350 kJ/mol), is, with hydrogen bonding, one of the most commonly used interactions for the construction of

¹² S. V. Lindeman, R. Rathore and J. K. Kochi, *Inorg. Chem.*, **2000**, 39, 5707.

¹³ T. Steiner, *Angew. Chem. Int. Ed.*, **2002**, 41, 48.

¹⁴ (a) A. M. Beatty, *Coord. Chem. Rev.*, **2003**, 246, 131. (b) Michael D. Ward, *Chem. Commun.*, **2005**, 0, 5838.

¹⁵ S. Ferlay and M. W. Hosseini, *Actualité Chimique*, **2015**, 399, 16

¹⁶ O. Félix, M. W. Hosseini, A. de Cian and J. Fischer, *Tetrahedron Lett.*, **1997**, 38, 1755.

supramolecular architectures.¹⁷ The infinite periodic assemblies obtained by combining organic ligands with metal centres or metallic complexes are named coordination networks or coordination polymers. It is worth noting that some 2D or 3D networks showing potential porosity are also called Metal-Organic Frameworks (MOFs).¹⁸ Compared with other non-covalent interactions, the relatively strong coordination bonding can produce more stable and robust supramolecular architectures. In addition, the advantages of coordination networks are shown in the two following features: 1) the nature of both the ligand and metal center can govern the geometry and dimensionality of the molecular networks. 2) the properties of the metal center may introduce interesting additional properties such as luminescence, magnetism into the networks.

In the following section, the topology and geometry (size, shape etc.) of the coordination networks depending on the nature of the organic tectons and metal center will be discussed. In particular, some examples of 1D, 2D and 3D coordination networks reported in the literature will be described.

2.2.5.1 One dimensional networks

If the translational symmetry or the repetition of recognition events takes place along only one direction, a 1D molecular network is obtained. These architectures may be constructed either by a self-complementary tecton or by combination of several complementary tectons. In addition, these networks may be organized by only one recognition pattern or several different assembling nodes. For the geometry of one dimensional networks, there are several types: linear, stair, helical and zig-zag.¹⁹ Some different shapes of 1D networks such as cylinder, ladder or tubular types have also been reported (Figure 11).²⁰

¹⁷ (a) R. Robson, *Dalton Trans.*, **2008**, 5113. (b) S. L. James, *Chem. Soc. Rev.*, **2003**, 32, 276. (c) S. M. Cohen, *Chem. Sci.*, **2010**, 1, 32. (d) M. D. Allendorf, C. A. Bhakta and R. J. Houk, *Chem. Soc. Rev.*, **2009**, 38, 1330. (e) S. R. Batten, N. R. Champness, X. M. Chen, J. Garcia-Martinez, S. Kitagawa, L. Ohrstrom, M. O'Keeffe, M. Paik Suh and J. Reedijk, *CrystEngComm.*, **2012**, 14, 3001. (f) M. Fujita, M. Tominaga, A. Hori and B. Therrien, *Acc. Chem. Res.*, **2005**, 38, 369. (g) T. R. Cook and P. J. Stang, *Chem. Rev.*, **2015**, 115, 701.

¹⁸ (a) J. R. Long and O. M. Yaghi, *Chem. Soc. Rev.*, **2009**, 38, 1213. (b) S. R. Batten, N. R. Champness, X.-M. Chen, J. Garcia-Martinez, S. Kitagawa, L. Öhrström, M. O'Keeffe, M. P. Suh and J. Reedijk, *Pure Appl. Chem.*, **2013**, 85, 1715.

¹⁹ (a) S. Ferlay, A. Jouaiti, M. Loi, M. W. Hosseini, A. De Cian and P. Turek, *New. J. Chem.*, **2003**, 27, 1801. (b) P. Larpen, A. Jouaiti, N. Kyrissakas and M. W. Hosseini, *Dalton. Trans.*, **2007**, 5126. (c) M. J. Lin, A. Jouaiti, N. Kyrissakas and M. W. Hosseini, *Chem. Commun.*, **2010**, 46, 115. (d) P. Larpen, A. Jouaiti, N. Kyrissakas and M. W. Hosseini, *Dalton Trans.*, **2014**, 43, 166.

²⁰ W. Leong and J. J. Vittal, *Chem. Rev.*, **2011**, 111, 688.

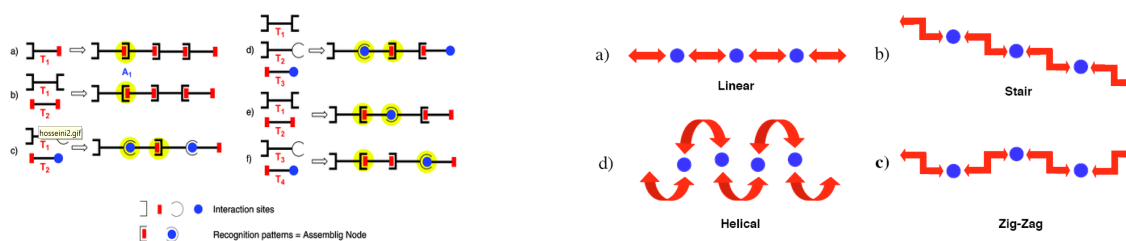


Figure 11: Schematic representations of the formation of 1D networks by self-assembly (left).³ Four geometries of 1D networks (right).

Recently, an example of 1D zig-zag type bimetallic coordination networks has been reported by our group; this investigation was part of my master's thesis.²¹ The organometallic Pt(II) complex bearing peripheral 3-pyridyl units **i-11** has been prepared and used as a metallatecton²² for the formation of 1D zig-zag infinite chain **i-12** upon assembly with Zn(II) cations (Figure 12).

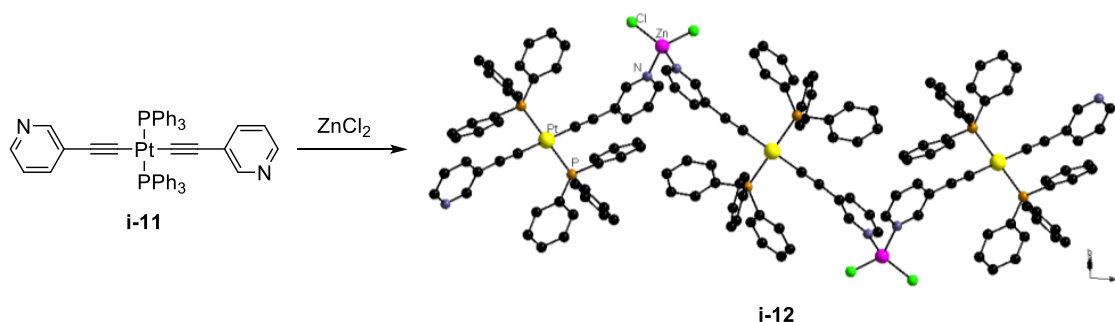


Figure 12: Portion of the crystal structure of a 1D zig-zag type coordination network.

2.2.5.2 Two dimensional networks

To form 2-D networks, the tectons should have at least three divergently oriented recognition sites. Similarly to the case of 1-D networks, these molecular networks may be constructed either by self-complementary tectons or by combinations of several complementary tectons. However, in the case of 2-D networks, the repetition of the assembling nodes will extend into two different directions. (Figure 13)

To form 2-D networks, the tectons should have at least three divergently oriented recognition sites. Similarly to the case of 1-D networks, these molecular networks may be constructed either by self-complementary tectons or by combinations of several complementary tectons. However,

²¹ F. Zhang, C. R. R. Adolf, N. Zigon, S. Ferlay, N. Kyritsakas and M. W. Hosseini, *Chem. Commun.*, **2017**, 53, 3587.

²² M. W. Hosseini, *Acc. Chem. Res.*, **2005**, 38, 313.

in the case of 2-D networks, the repetition of the assembling nodes will extend into two different directions. (Figure 13)

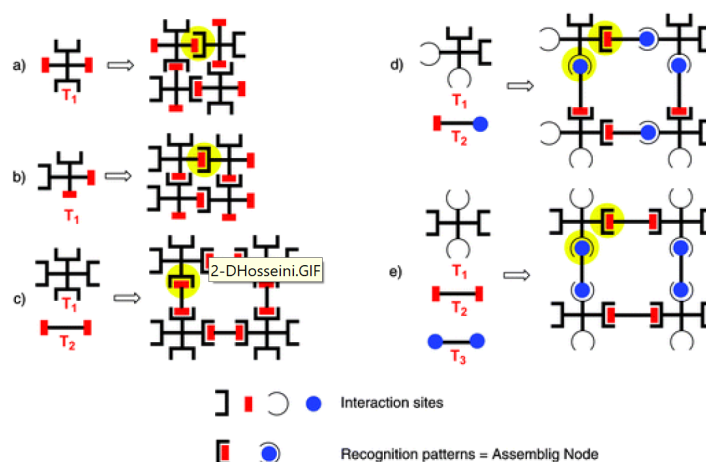


Figure 13: Schematic representations of the formation of 2-D networks by self-assembly.³

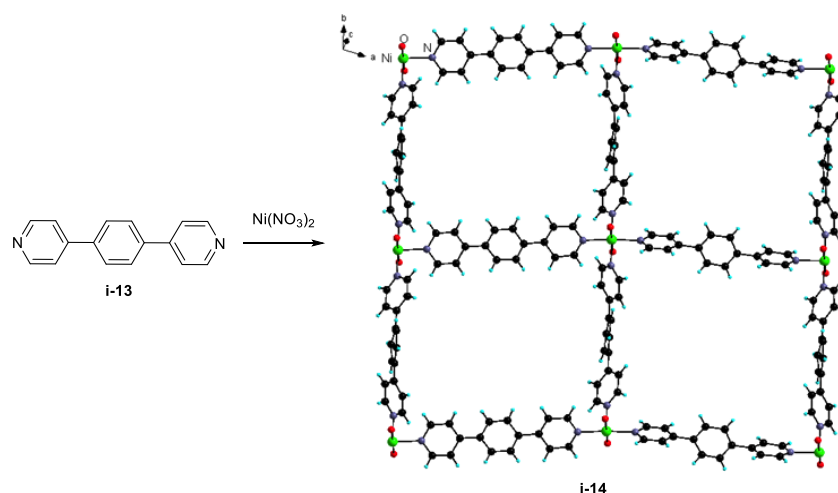


Figure 14: Crystal structure of the 2D grid-type coordination network **i-14** $\{[\text{Ni}(\text{1,4}-(4\text{-py})\text{benzene})_2(\text{H}_2\text{O})_2](\text{Benzene})(\text{MeOH})_5(\text{NO}_3)_2\}_n$. Anions and solvent molecules are not shown for clarity.

2D coordination network can exhibit different shapes such as planar, corrugated, slot or wavy.²³ The grid arrangement is one of the most common type. Depending on the angle of the grid, square, rectangle, honeycomb or chevron type grids may be generated. Here, the example of a 2-D square grid coordination network is described.²⁴ Combination of 1,4-bis(4-pyridyl)benzene **i-13** possessing two divergent coordinating sites with Ni(II) cation leads to the formation of structure

²³ (a) T. Ohmura, A. Usuki, K. Fukumori, T. Ohta, M. Ito and K. Tatsumi, *Inorg. Chem.*, **2006**, 45, 7988. (b) G. Zhang, E. C. Constable, C. E. Housecroft and J. A. Zampese, *Inorg. Chem. Commun.*, **2014**, 43, 51.

²⁴ K. Biradha and M. Fujita, *J. Chem. Soc., Dalton Trans.*, **2000**, 3805.

i-14 shown in Figure 14. The Ni center adopts an octahedral coordination environment with four N atoms belonging to four different organic tectons in equatorial positions and two water molecules in the apical positions. The structure and dimensionality of this coordination network are thus determined by the coordination geometry of Ni(II) metal center and the orientation of the binding sites on the bridging ligand.

2.2.5.3 Three dimensional networks

When one type or different recognition patterns translate in three directions of space, three-dimensional coordination networks are obtained. In this case, the tectons having at least four non-planar and divergently oriented recognition sites are required. As shown in Figure 15, the positioning of coordinating sites oriented towards all three directions of space is imposed. Thus, the formation of the 3-D networks requires a precise design of the tectons. Concerning the arrangement of 3-D networks, three types can be generated: tetrahedral, cuboid or octahedral and giroid. For example, the prototypical examples of 3D cubic MOFs resulting from the assembly of dicarboxylic acid with Zn(II) cations known as MOF-5 and IRMOFs are presented in Figure 16.²⁵ In these structures, the edges of the tetranuclear Zn_4O nodes are bridged by the carboxylates leading to the 3D arrangement. The properties (stability, porosity, size of the pores) of these 3-D MOFs render them attractive materials with excellent performance in the fields of gas adsorption, separation and catalysis.²⁶

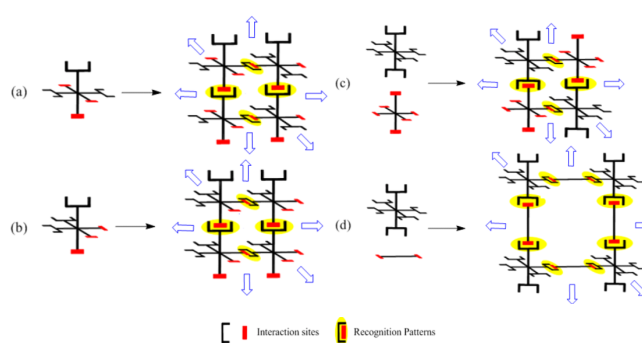


Figure 15: Schematic representations of the formation of 3-D networks by self-assembly.

²⁵ (a) H. Li, M. Eddaoudi, M. O’Keeffe and O. M. Yaghi, *Nature.*, **1999**, 402, 276. (b) M. Eddaoudi, J. Kim, N. Rosi, D. Vodak, J. Wachter, M. O’Keeffe and O. M. Yaghi, *Science.*, **2002**, 295, 469.

²⁶ (a) J. Lee, O. K. Farha, J. Roberts, K. A. Scheidt, S. T. Nguyen, J. T. Hupp, *Chem. Soc. Rev.*, **2009**, 38, 1450. (b) C. Janiak, J. K. Vieth, *New. J. Chem.*, **2010**, 34, 319. (c) J.-R. Li, J. Sculley, H. -C. Zhou, *Chem. Rev.*, **2012**, 112, 869. (d) Y. Pemh, V. Krunglreviciute, I. Eryazici, J. T. Hupp, O. K. Farha, T. Yildirim, *J. Am. Chem. Soc.*, **2013**, 135, 11887. (e) H. Furukawa, M. O’Keeffe, O. M. Yaghi, *Science.*, **2013**, 341, 974.

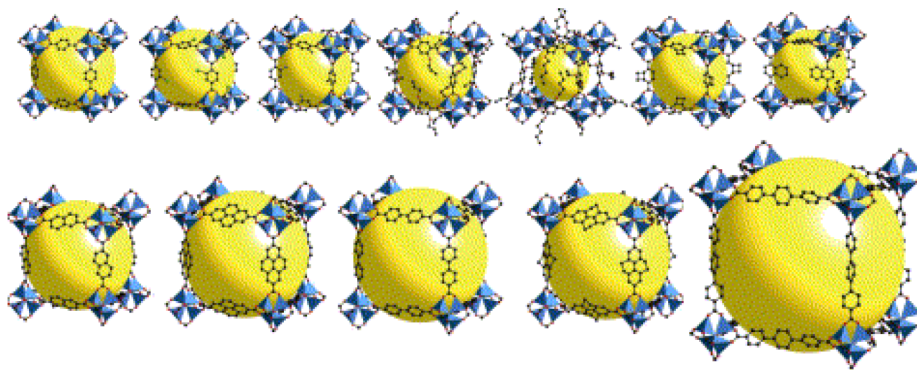


Figure 16: Family of different pore sized 3-D MOFs reported by Yaghi and coworkers based on dicarboxylate derivatives and Zn(II) cations.^{25b}

This PhD. research project mainly focused on the design and formation of supramolecular entities employing coordination bonds as the dominant interaction using organic ligands based on the dipyrin backbone. The chemistry of these derivatives will be briefly highlighted in the following section.

3 The chemistry of dipyrins

3.1 Structures and nomenclature of dipyrins

The dipyrin, also known as dipyrromethene, consists of two conjugated coplanar and structurally equivalent pyrrole rings linked by a methylene bridge and is the oxidized form of dipyrromethane. The general structure of a dipyrin and its numbering system (IUPAC) are shown in Figure 17(a). Paralleling the nomenclature of porphyrins, (Figure 17(b)) the positions 1,9 of dipyrins are regarded as α -positions, positions 2,3,7,8 of dipyrins as β -positions and position 5 of dipyrins as the *meso*-position.

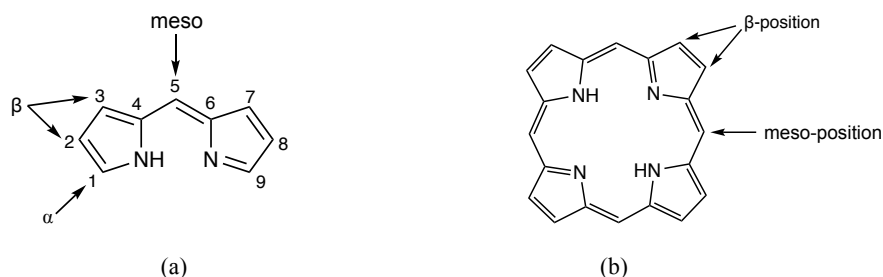
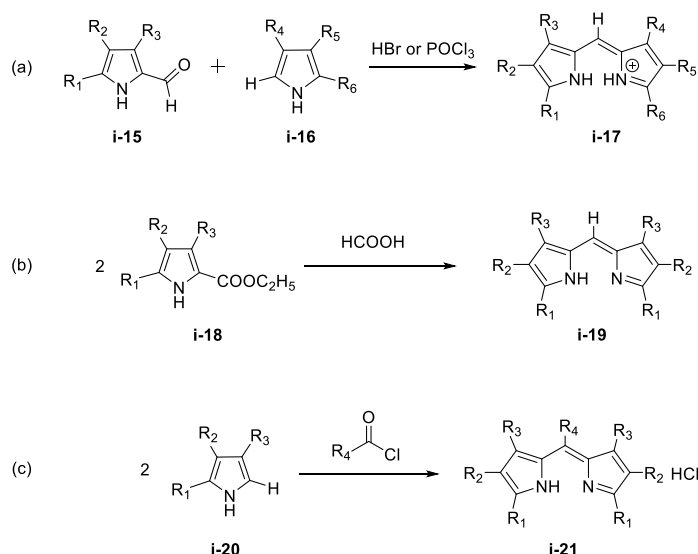


Figure 17: Structure and numbering system of dipyrin and comparison with a porphyrin molecule.

Research on dipyrins was at first highly motivated by their role as intermediates in porphyrin chemistry. The synthesis of dipyrins has been first developed by Hans Fischer as early as 1937.²⁷ However, over the last two decades, this class of molecules became the subject of investigations for their own properties and complexation ability.²⁸

3.2 Synthesis and properties of dipyrins

In 1960, MacDonald reported a synthetic strategy named as the MacDonald coupling for the preparation of dipyrins in analogy with the reaction used in porphyrin chemistry.²⁹ This approach affords 5-unsubstituted dipyrin **i-17** by condensation of a 2-formyl pyrrole **i-15** with an α -unsubstituted pyrrole **i-16** in the presence of an acid such as hydrobromic acid³⁰ or phosphorus oxychloride (Scheme 1a).³¹ The products isolated are dipyrin salts that are usually more stable than free dipyrins. It is worth noting that the MacDonald coupling is often employed for the synthesis of asymmetrical dipyrins, since functionalized pyrrolic species are used as starting materials in the reaction.



Scheme 1: Strategies for the synthesis of asymmetrical or symmetrical dipyrin derivatives.

²⁷ H. Fischer and H. Orth, *Die Chemie des Pyrrols.*, Akademische Verlagsgesellschaft, Leipzig, **1937**.

²⁸ T. E. Wood and A. Thompson, *Chem. Rev.*, **2007**, *107*, 1831.

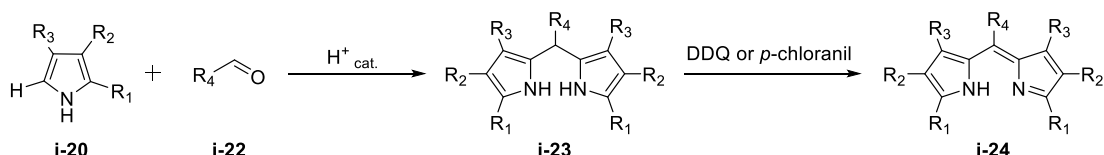
²⁹ G. P. Arsenault, E. Bullock and S. F. MacDonald, *J. Am. Chem. Soc.*, **1960**, *82*, 4384.

³⁰ A. Al-Sheikh-Ali, K. S. Cameron, T. S. Cameron, K. N. Robertson and A. Thompson, *Org. Lett.*, **2005**, *7*, 4773.

³¹ C. W. Wan, A. Burghart, J. Chen, F. Bergstroem, L. B. A. Johansson, M. F. Wolford, T. G. Kim, M. R. Topp, R. M. Hochstrasser and K. Burgess, *Chem. Eur. J.*, **2003**, *9*, 4430.

In a paper published in 1996, Brückner, Dolphin *et al.* have highlighted different synthetic strategies for the preparation of dipyrin derivatives.³² The symmetrical 5-unsubstituted dipyrin **i-19** can be synthesized by combination of two equivalents of pyrrolylester **i-18** in the presence of formic acid. During this reaction, formic acid is not only involved in the release of the group in α -position of pyrrole **i-18**, but can also be used as a carbonyl synthon affording 5-unsubstituted dipyrin **i-19** (Scheme 1b). Other reported synthetic procedures focus on the formation of symmetrical 5-substituted dipyrin derivatives. One strategy consists in the reaction between two equivalents of α -unsubstituted pyrroles **i-20** and acid halide yielding dipyrin derivatives of the type **i-21**. (Scheme 1c)

J. S. Lindsey reported a reliable synthetic method allowing the synthesis of α -, β -, (un)substituted and *meso*-substituted dipyrin derivatives in large scale.³³ An aromatic aldehyde **i-22** reacts with α -unsubstituted pyrrole **i-20** in the presence of a mild acid catalyst such as trifluoroacetic acid (TFA) or InCl_3 ³⁴ under argon at room temperature to produce the precursor, dipyrromethane **i-23**. This latter intermediate is a species sensitive to light, thus its synthesis requires to be carried out under protection to ensure a higher yield. The isolation of dipyrromethane can be achieved by column chromatography or recrystallization. The corresponding dipyrin **i-24** can be obtained by oxidation of the dipyrromethane with 2,3-dichloro-5,6-dicyano-1,4-benzoquinone (DDQ) or *p*-chloranil as oxidant. (Scheme 2)



Scheme 2: Synthesis of dipyrins via dipyrromethane intermediates.

The rotation of the pyrrolyl units around the methylene linkage leads to three different configurations *E*-syn, *E*-anti and *Z*-syn shown in Figure 18a. In addition, the dipyrin is an amphoteric molecule due to the coexistence of conjugated imine and amine functionalities. Under

³² C. Bruckner, V. Karunaratne, S. J. Rettig and D. Dolphin, *Can. J. Chem.*, **1996**, 74, 2182.

³³ C. H. Lee and J. S. Lindsey, *Tetrahedron.*, **1994**, 50, 11427.

³⁴ (a) B. J. Littler, M. A. Miller, C.-H. Hung, R. W. Wagner, D. F. O'Shea, P. D. Boyle and J. S. Lindsey, *J. Org. Chem.*, **1999**, 64, 1391. (b) J. K. Laha, S. Dhanalekshmi, M. Taniguchi, A. Ambroise and J.S. Lindsey, *Org. Proc. Res. Dev.*, **2003**, 7, 799.

either acidic or basic conditions, the dipyrin molecule can thus exist in three different states: cationic, neutral or anionic (Figure 18b).³⁵

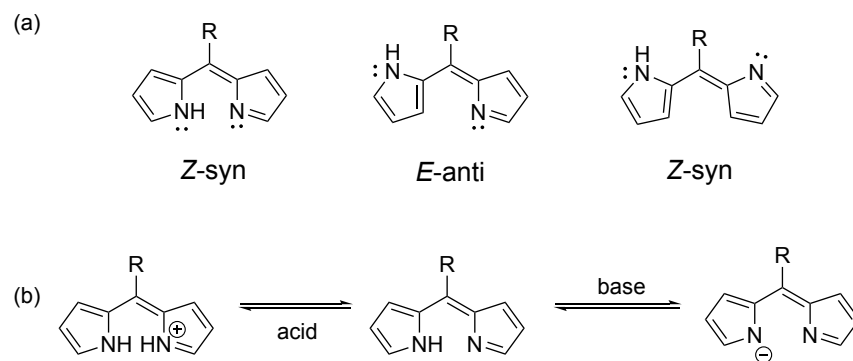
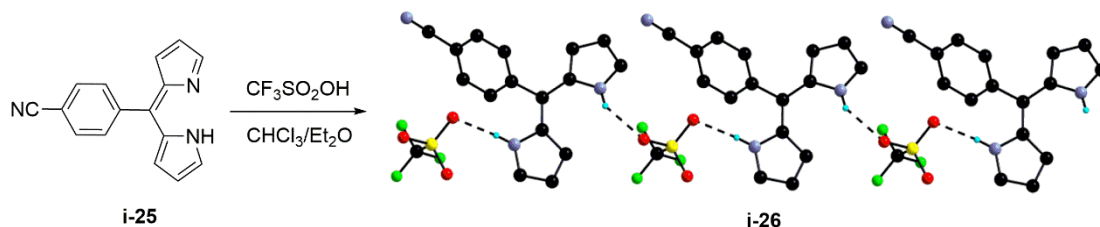


Figure 18: (a) Three configurations of the dipyrin molecule. (b) Dipyrin acid-base equilibria reaction.

The organization of dipyrins in the crystalline state has been studied. In 2008, our group reported the one-dimensional hydrogen bonded network obtained upon reaction of 5-benzonitriledipyrin **i-25** with trifluoromethanesulfonic acid.³⁶ Compound **i-26** organized by hydrogen bonding between the two N-H groups of the bipyrrolic core **i-25-H⁺** and the oxygen atoms of the CF₃SO₃⁻ anions (Scheme 3).



Scheme 3: 1-D network **i-26** obtained upon protonation of dipyrin **i-25** by trifluoromethanesulfonic acid.

1-D hydrogen bond chain can also be formed with neutral dipyrin depending on the nature of substituent at the *meso* position, like in the case of 5-pyridyldipyrin. The N atom of the 5-pyridyl group is hydrogen bonded to the NH of a neighbouring pyrrolic unit leading to an infinite network **i-27** (Figure 19).³⁷

³⁵ J.-Y. Shin, D. Dolphin and B. O. Patrick, *Cryst. Growth. Des.*, **2004**, 4, 659.

³⁶ D. Salazar-Mendoza, S. A. Baudron and M. W. Hosseini, *Inorg. Chem.*, **2008**, 47, 766.

³⁷ J. R. Stork, V. S. Thoi and S. M. Cohen, *Inorg. Chem.*, **2007**, 46, 11213.

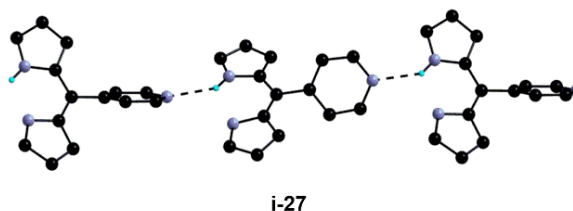
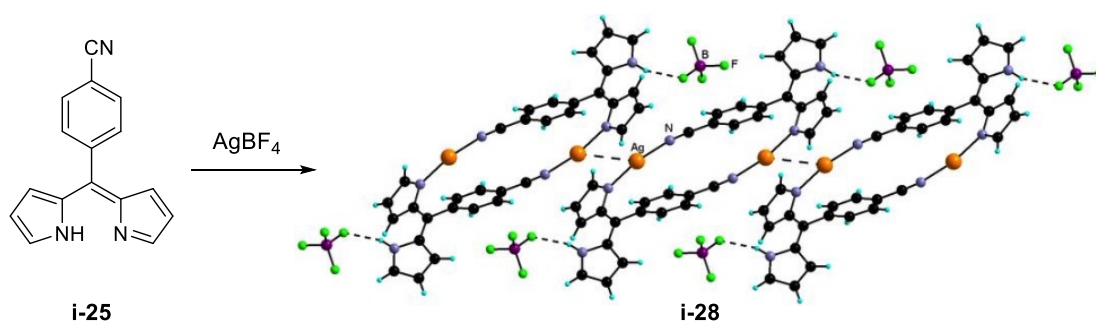


Figure 19: Hydrogen bonded 1-D chain in the structure of 5-pyridyldipyrin **i-27**.

3.3 Coordination chemistry of dipyrin

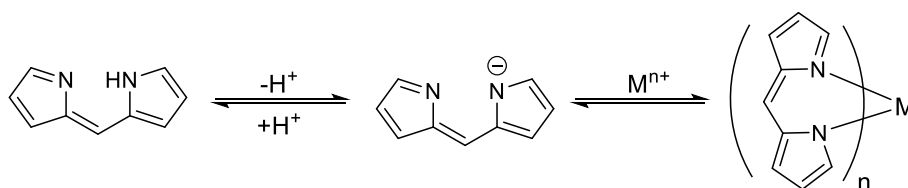
Dipyrins possess a rather rich coordination chemistry. The neutral dipyrin molecule can be regarded as a monodentate ligand *via* its imine nitrogen atom. However, only few examples of complexes with neutral dipyrins have been described. One such reported complex is shown in Scheme 4.³⁶ As observed in the structure of compound **i-28** in the crystalline state, two neutral ligands **i-25** form upon assembly with two silver(I) cations a dicationic [2+2] metallamacrocycle. In this case, the metal centres are linearly coordinated to one nitrile group and the N atom belonging to the un-protonated pyrrolic unit of a second dipyrin ligand. Interestingly, a d^{10} - d^{10} interaction between silver cations with a distance of 3.396(4) Å leads to a 1-D network. This tendency to form [2+2] metallamacrocycles has been observed with other dipyrins bearing a *meso* coordinating group in *para* position such as pyridine, phenylpyridine or phenyl-imidazolyl.³⁸



Scheme 4: Synthesis of [2+2] metallamacrocycle compound **i-28**.

Dipyrins can also be deprotonated under basic conditions to form mono-anionic chelates. This character makes it a ligand of choice for the formation of complexes with various metal centres including transition metals and semimetals (Scheme 5).²⁸

³⁸ D. Pogozhev, S. A. Baudron and M. W. Hosseini, *Dalton Trans.*, **2011**, 40, 437.



Scheme 5: An approach for the formation of complexes based on dipyrinato chelates.

Depending on the degree of oxidation of the metal center, homoleptic neutral complexes of the $M(\text{dpm})_2$ or $M(\text{dpm})_3$ type can be formed (dpm = dipyrinato ligand). The synthesis of $M(\text{dpm})_2$ complexes is usually achieved by reaction of a dipyrrole ligand and a metal acetate in methanol with satisfactory yield. Methanol is generally used as the solvent during the complexation reaction because complexes are often insoluble in methanol and can be isolated by direct precipitation/filtration. It is also worth noting that the acetate here also acts as a base. The coordination geometry is influenced by the preference of the metal center as well as by steric effects between the substituents at the α -positions of the pyrrolic system. Even with α -H atoms, the formation of complexes with square planar geometry can be disfavoured. Thus, in the case of dipyrinato complexes of $M(\text{dpm})_2$ type, the metal center such as Ni(II),³⁹ Cu(II),⁴⁰ Pd(II)⁴¹ and, less surprisingly, Zn(II)⁴² usually adopts a distorted tetrahedral coordination geometry (Figure 20).

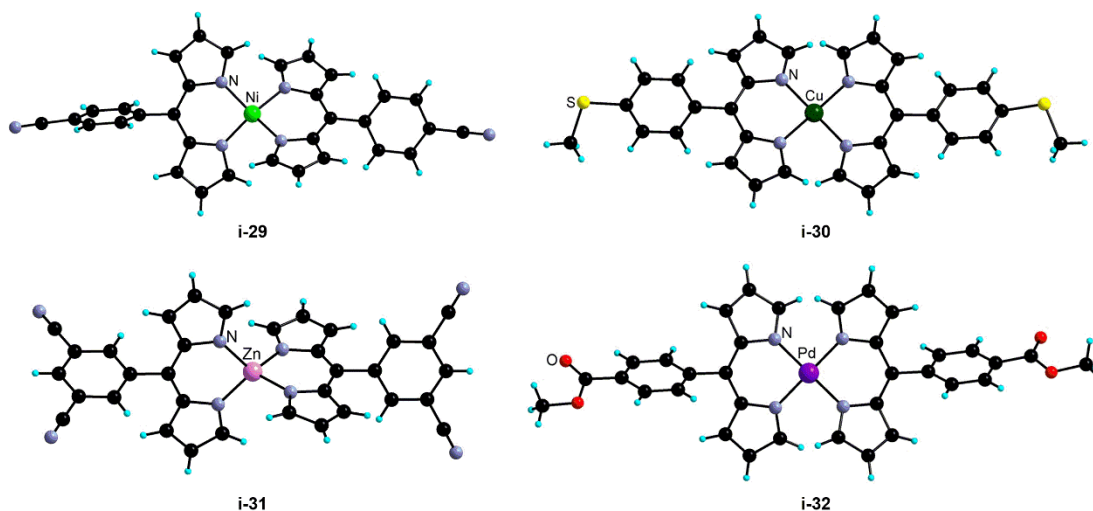


Figure 20: Crystalline structures of homoleptic discrete complexes with Nickel(II) **i-29**, Copper(II) **i-30**, Zinc(II) **i-31** and Palladium(II) **i-32**.

³⁹ H. Ruffin, S. A. Baudron, D. Salazar-Mendoza and M. W. Hosseini, *Chem. Eur. J.*, **2014**, 20, 2449.

⁴⁰ L. Do, S. R. Halper, S. M. Cohen, *Chem. Commun.*, **2004**, 2662.

⁴¹ J. D. Hall, T. M. McLean, S. J. Smalley, M. R. Waterland and S. G. Telfer, *Dalton Trans.*, **2010**, 39, 437.

⁴² D. Salazar-Mendoza, S. A. Baudron and M. W. Hosseini, *Chem. Commun.*, **2007**, 2252.

As expected, complexation reaction of dipyrin ligand with metal in the +3 oxidation state leads to the formation of $M(dpm)_3$ type complexes. In recent years, a family of homoleptic tris(dipyrinato) $M(III)$ complexes with cobalt,⁴³ iron,⁴⁴ indium and gallium⁴⁵ has been described. According to the crystalline structures of these $M(dpm)_3$ complexes shown in Figure 21, the metal cations are in an octahedral coordination environment and the three *meso* groups are in a pseudo-3-fold symmetric environment about the metal center. However, the coordination sphere of the indium(III) ion is distorted from a perfect octahedron, since two of the ligands are canted from their associated N-In-N coordination planes. The synthesis of complexes involves the reaction of pure dipyrin and metal salt, often chlorides, at room temperature or under refluxing conditions. The desired product can be purified by column chromatography. It is worth noting that cobalt(II) and iron(II) species may be obtained and separated during the reaction, but they are air-sensitive and easily convert into the tris(dipyrinato) complexes in the presence of excess of ligands and oxygen.⁴³ However, with ligands bearing methyl groups at the 1 and 9 positions, divalent Co(II) complexes have been isolated.⁴⁶ These compounds are stable in air, and cannot be transformed into the tris-chelate complexes because the oxidation process and tris-chelation are inhibited by the steric effect due to the presence of methyl substituents.

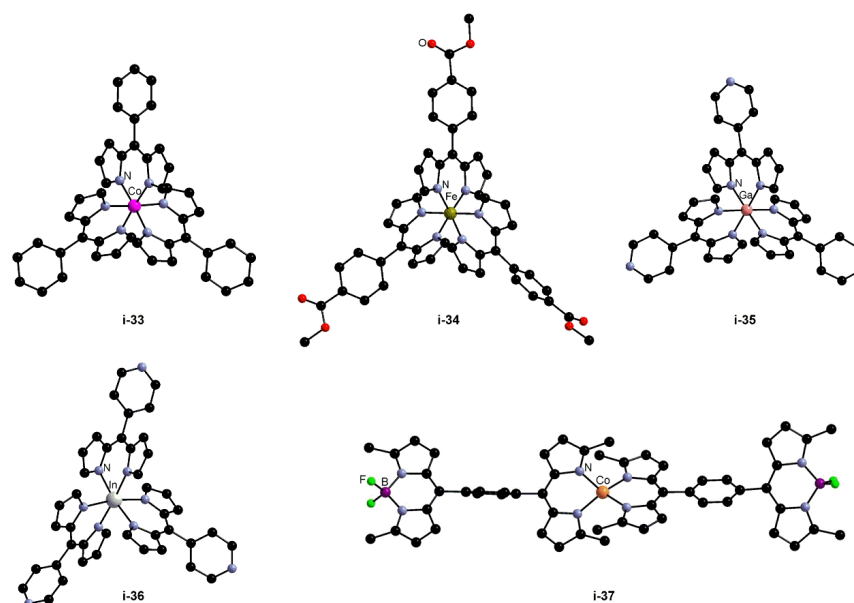


Figure 21: Crystalline structures of $M(dpm)_3$ type dipyrinato complexes with Co(III) **i-33**, Fe(III) **i-34**, Ga(III) **i-35** and In(III) **i-36** and an example of structure of bis(dipyrinato)cobalt(II) **i-37**. Hydrogen atoms have been omitted for clarity

⁴³ C. Brückner, Y. Zhang, S. J. Rettig and D. Dolphin, *Inorg. Chim. Acta.*, **1997**, 263, 279.

⁴⁴ S. M. Cohen and S. R. Halper, *Inorg. Chim. Acta.*, **2002**, 341, 12.

⁴⁵ J. R. Stork, V. S. Thoi and S. M. Cohen, *Inorg. Chem.*, **2007**, 46, 11213.

⁴⁶ Q. Miao, J. -Y. Shin, B. O. Patrick and D. Dolphin, *Chem. Commun.*, **2009**, 2541.

Heteroleptic complexes incorporating at least two different types of ligands on a metal center have been also obtained. Here, selected examples of heteroleptic copper dipyrin complexes reported by Cohen and coworkers in 2004 are presented.⁴⁷ The reaction of the *meso*-substituted dipyrin derivatives and ~1 molar equivalent of Cu(acac)₂ was employed for the formation of heteroleptic [Cu(dpm)(acac)] complexes. Only 0.4 equiv. of Cu(acac)₂ was required for the synthesis of the corresponding homoleptic Cu(dpm)₂ analogues. Interestingly, when comparing the structure of homoleptic Cu(dpm)₂ and heteroleptic Cu(dpm)(acac) complexes in the solid state, for example compounds **i-38** and **i-39**, difference in coordination environment is observed. The metal center adopts the square planar coordination geometry in the latter species due to the absence of steric hindrance between α -H of the dipyrinato ligand and the acetylacetonate derivative. An interesting point should be noted here, (acac)Cu(*p*-PhCNDpm) **i-39** and (acac)Cu(*o*-pydpm) **i-40** complexes crystallize as discrete mononuclear entities in the solid state, whereas (acac)Cu(*m*-pydpm) **i-41** and (acac)Cu(*p*-pydpm) **i-42** self-assemble into 1D coordination polymers with different geometry owing to the binding of the nitrogen atom belonging to the *meso* pyridine unit of a neighbouring complex.

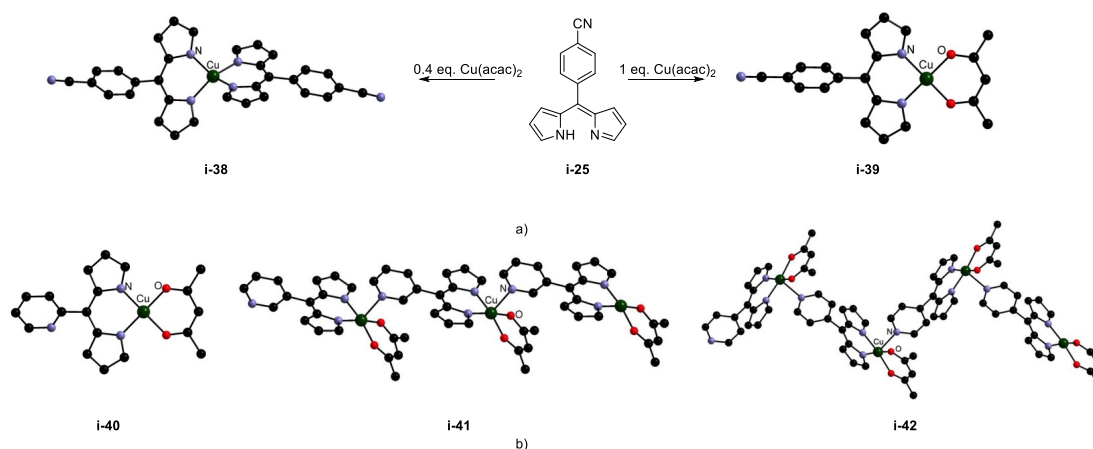


Figure 22: (a): Synthesis and crystal structures of homo- and heteroleptic complexes with 5-PhCNDipyrin **i-38** and **i-39**. (b): Structures of (acac)Cu(*o*-pydpm) **i-40**, 1D chain of (acac)Cu(*m*-pydpm) **i-41** and (acac)Cu(*p*-pydpm) **i-42**. Hydrogen atoms have been omitted for clarity.

Several other heteroleptic complexes such as (hfac)Cu(dpm), (acacCN)Cu(dpm) and (acacCN)Co(dpm)₂ (hfac = hexafluoroacetylacetonate; acacCN = 3-cyanoacetylacetonate.) have also been prepared and characterized by our laboratory.⁴⁸ These heteroleptic dipyrinato complexes were designed as metallatectons for the formation of extended networks and

⁴⁷ S. R. Halper, M. R. Malachowski, H. M. Delaney and S. M. Cohen, *Inorg. Chem.*, **2004**, *43*, 1242.

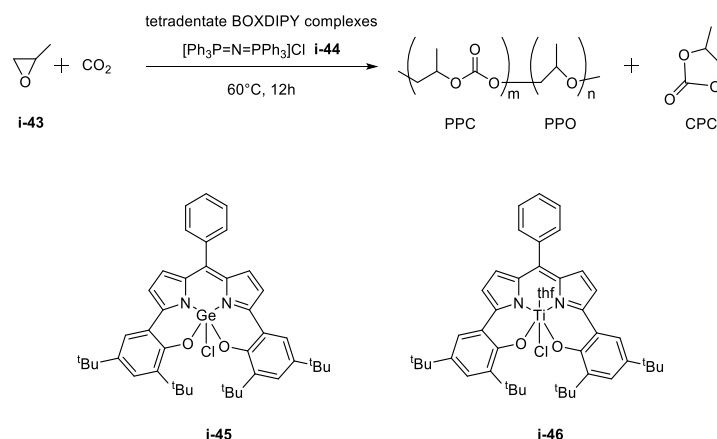
⁴⁸ B. Kilduff, D. Pogozev, S. A. Baudron and M. W. Hosseini, *Inorg. Chem.*, **2010**, *49*, 11231.

coordination polymers following a strategy described below (see Section 3.5). Finally, other heteroleptic complexes incorporating Cu(I), Re(I), Sn(II), Ru(II), Pd(II), Pt(II) and Ir(III) have also been reported but mostly for their photophysical properties.⁴⁹

3.4 Properties and applications of dipyrinato complexes

3.4.1 Dipyrinato complexes as catalysts

In recent years, Nozaki and co-workers have designed a series of complexes with metal centres such as Ti^{4+} , Zr^{4+} , Ge^{4+} , Sn^{4+} and a 1,9-bis(2-oxido-phenyl)dipyrinate (BOXDIPY) ligand.⁵⁰ Similarly to the structure of the salen ligand, the BOXDIPY derivative has a {ONNO}-tetradentate coordination unit which allows to stabilize metal centres with a high oxidation degree leading to the formation of rigid complexes. These tetravalent metal complexes can be used as catalysts in the epoxide/ CO_2 copolymerization.



Scheme 6: Copolymerization of propylene oxide with CO_2 using Ge(IV) or Ti(IV) BOXDIPY complexes as catalysts.

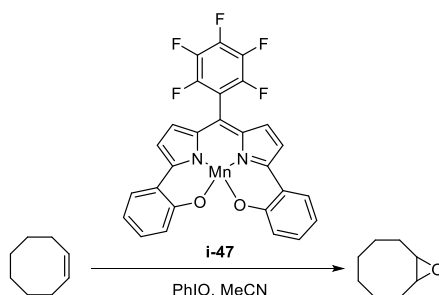
For example, the copolymerization between propylene oxide **i-43** and CO_2 at 2.0 MPa pressure proceeds in the presence of a catalytic amount of ammonium salts **i-44** at 60°C for 12 hours in the presence of BOXDIPY complexes catalyst. The reaction produces an alternating copolymer poly(propylene carbonate) (PPC) / poly(propylene oxide) (PPO), along with the cyclic carbonate (CPC) (Scheme 6). In particular, the germanium complex **i-45** and titanium complex **i-46** can

⁴⁹ (a) X. Liu, H. Nan, W. Sun, Q. Zhang, M. Zhan, L. Zou, Z. Xie, X. Li, C. Lu and Y. Cheng, *Dalton Trans.*, **2012**, 41, 10199. (b) J. Kobayashi, T. Kushida and T. Kawashima, *J. Am. Chem. Soc.*, **2009**, 131, 10836. (c) T. M. McLean, J. L. Moody, M. R. Waterland and S. G. Telfer, *Inorg. Chem.* **2012**, 51, 446. (d) C. Bronner, S. A. Baudron, M. W. Hosseini, C. A. Strassert, A. Guenet and L. De Cola, *Dalton Trans.*, **2010**, 39, 180. (e) S. J. Smalley, M. R. Waterland and S. G. Telfer, *Inorg. Chem.*, **2009**, 48, 13. (f) K. Hanson, A. Tamayo, V. V. Diev, M. T. Whited, P. I. Djurovich and M. E. Thompson, *Inorg. Chem.*, **2010**, 49, 6077

⁵⁰ K. Nakano, K. Kobayashi and K. Nozaki, *J. Am. Chem. Soc.*, **2011**, 133, 10720.

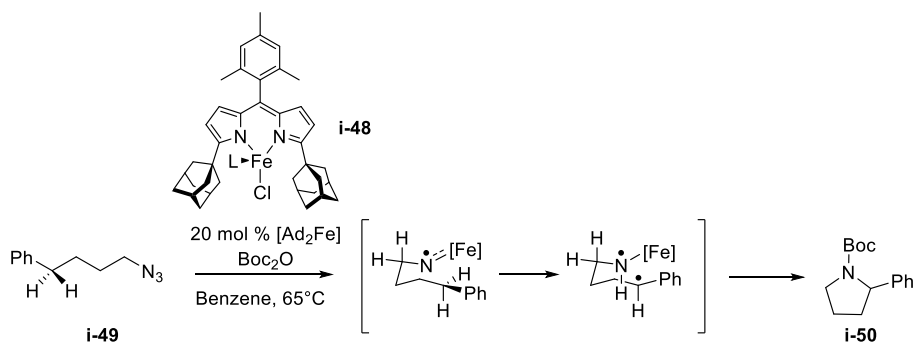
produce alternating copolymer PPC selectively. However, when the selectivity for the polymer is maximum, the yield of copolymerization became lower and the yield of formation of PC can be improved by temperature increase.⁵¹

Based on a similar ligand, the group of Andrioletti and Aukauloo have developed the Mn complex **i-47** for the epoxidation of alkenes (Scheme 7).⁵²



Scheme 7: Epoxidation of alkene based on Mn(III) complex **i-47**.

Another interesting example concerns the iron (II) dipyrinato complex [Ad₂Fe] **i-48** bearing additional adamantyl groups (Ad) at positions 1,9. The latter has been used as a catalyst for C-H bond activation.⁵³ A variety of alkyl azides such as compound **i-49** can be transformed into cyclic amines **i-50** by using this iron-dipyrinato complex. During the reaction, a high-spin iron imido intermediate is formed facilitating a stepwise C–H bond amination through hydrogen atom abstraction followed by radical recombination. One equivalent of a protecting reagent (such as Boc₂O or Fmoc-OSuc) was added to prevent product inhibition of the electrophilic Ad₂Fe. (Scheme)



Scheme 8: Cyclization of alkyl azide with [Ad₂Fe] catalyst **i-48**.

⁵¹ T. Ohkawara, K. Suzuki, K. Nakano, S. Mori and K. Nozaki, *J. Am. Chem. Soc.*, **2014**, 136, 10728.

⁵² S. El Ghachtouli, K. Wojcik, L. Copey, F. Szydlo, E. Framery, C. Goux-Henry, L. Billon, M.-F. Charlot, R. Guillot, B. Andrioletti and A. Aukauloo, *Dalton Trans.*, **2011**, 40, 9090.

⁵³ (a) E. R. King, E. T. Hennessy and T. A. Betley, *J. Am. Chem. Soc.*, **2011**, 133, 4917. (b) E. T. Hennessy and T. A. Betley, *Science*, **2013**, 340, 591.

3.4.2 Luminescent properties and applications of dipyrinato complexes

When it comes to the luminescence of dipyrin compounds, the first species that should be mentioned are BODIPY derivatives (4,4-difluoro-4-bora-3a,4a-diaza-sindacene, boron dipyrromethene). This type of BF₂ complexes were first reported in 1968, and their intense fluorescence was found and described by these authors.⁵⁴ Focusing on the chemical structure of BODIPY, it is formally a zwitterion (B⁻ and N⁺) and its numbering system differs from the one of dipyrins. Similarly to the dipyrin and porphyrin cases, the α , β and meso nomenclature has been also preferred for BODIPY complexes. (Figure 23)

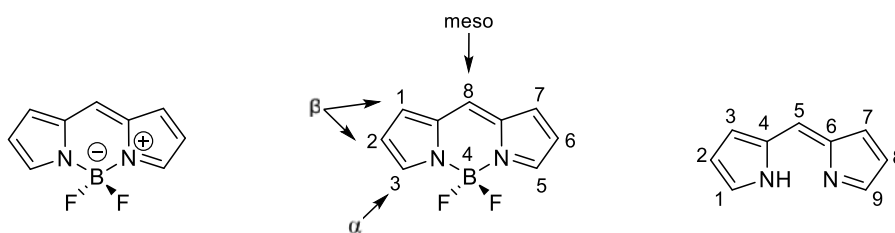


Figure 23: Structure and nomenclature of BODIPY compared with the one of dipyrin.

In the early 1980s, the fluorescence of BODIPYs complexes was employed in experiments for the study of gas chromatographic processes.⁵⁵ Since the 1990s, more and more BODIPYs derivatives have been designed, prepared and studied as tuneable dyes with applications in the domain of biological labelling.⁵⁶ As research on BODIPYs developed, a broad range of properties have been discovered and taken advantage of such as photochemical and chemical stability in solution and the solid state, easy functionalization, intense absorption and fluorescence, high fluorescence quantum yield and negligible triplet-state formation. This has made them interesting derivatives for novel materials in various fields.⁵⁷

One of the features of BODIPY dyes is that it is rather straightforward to introduce additional groups on their backbone to modulate their optical properties or to provide recognition sites for a variety of analytes. Thus, based on this property, BODIPY derivatives bearing different peripheral substituents can be used as pH sensors,⁵⁸ for trapping iron⁵⁹ and for the recognition of transition

⁵⁴ A. Treibs and F. H. Kreuzer, *Justus Liebigs Ann. Chem.*, **1968**, 718, 208.

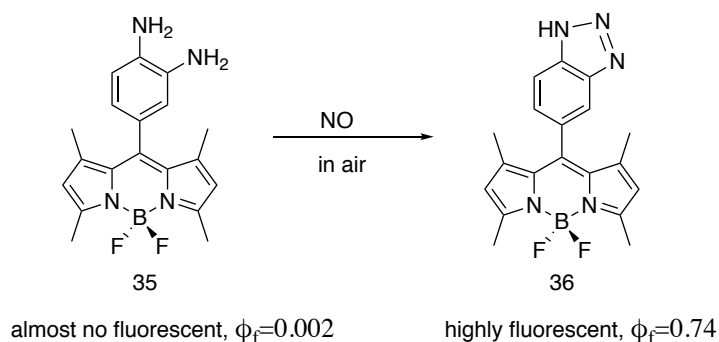
⁵⁵ (a) O. Driessen and J. Lugtenberg, *J. High Resolut. Chromatogr. Chromatogr. Commun.*, **1980**, 3, 405. (b) A. Emonds, J. Bonnet, J. Lugtenburg and O. Driessen, *J. Chromatogr.*, **1983**, 279, 477.

⁵⁶ M. Shah, K. Thangraj, M. L. Soong, L. Wolford, J. H. Boyer, I. R. Politzer and T. G. Pavlopoulos, *Heteroat. Chem.*, **1990**, 1, 389.

⁵⁷ G. Ulrich, R. Ziessel and A. Harriman, *Angew. Chem. Int. Ed.*, **2008**, 47, 1184.

⁵⁸ (a) M. Kollmannsberger, T. Gareis, S. Heinl, J. Breu and J. Daub, *Angew. Chem. Int. Ed. Engl.*, **1997**, 36, 1333. (b) T. Gareis, C. Huber, O. S. Wolfbeis and J. Daub, *Chem. Commun.*, **1997**, 1717. (c) K. Rurack, M. Kollmannsberger and J. Daub, *New J. Chem.*,

metals.⁶⁰ The most common mechanism for chemical sensing with these species is that the trapping of an analyte at a pre-designed site of the BODIPY dye causes an observable change in its fluorescence properties. A selected example presented here has been published by Nagano *et al.* in 2004.⁶¹ The anilino-based BODIPY **i-51** showing a very weak luminescence with a low quantum yield of 0.002, reacts with nitric oxide (NO) giving the triazole derivative **i-52**, that fluoresces strongly ($\Phi_f = 0.74$) (Scheme The change in the fluorescence intensity is caused by an intramolecular photoinduced electron transfer (PeT)).



Scheme 9: Reaction of anilino-based BODIPY **i-51** and nitric oxide yielding the luminescent adduct **i-52**.

BODIPY derivatives can be used as building blocks for the development of synthetic artificial light harvesting systems. This field of research is very active because such systems can mimic natural photosynthesis aiming at an understanding of the process of bioenergetics and at the realization of solar energy conversion. In this system, BODIPY acts usually as an antenna which can absorb light energy and transport energy to a photosynthetic reaction center. For example, F. D'Souza and O. Ito's groups have reported a model of the photosynthetic antenna-reaction center complex.⁶² This supramolecular triad, **i-53**, is constructed by axially coordinating imidazole-fulleropyrrolidine to the zinc center of a linked zinc porphyrin-boron dipyrin dye *via* a self-assembled supramolecular approach. In this case, the excited state of the BODIPY unit of the pyrrole based dyad allows to realize an efficient energy transfer leading to the formation of a

2001, 25, 289. (d) C. N. Baki, E. U. Akkaya, *J. Org. Chem.*, **2001**, 66, 1512. (e) M. Baruah, W. Qin, N. Basaric, W. M. De Borggraeve and N. Boens, *J. Org. Chem.*, **2005**, 70, 4152. (f) W. Qin, M. Baruah, W. M. De Borggraeve and N. Boens, *J. Photochem. Photobiol. A*, **2006**, 183, 190.

⁵⁹ (a) V. V. Matin, A. Rothe, Z. Diwu and K. R. Gee, *Bioorg. Med. Chem. Lett.*, **2004**, 14, 5313. (b) M. Baruah, W. Qin, R. A. L. VallQe, D. Beljonne, T. Rohand, W. Dehaen and N. Boens, *Org. Lett.*, **2005**, 7, 4377. (c) K. Yamada, Y. Nomura, D. Citterio, N. Iwasawa and K. Suzuki, *J. Am. Chem. Soc.*, **2005**, 127, 6956.

⁶⁰ (a) K. Rurack, M. Kollmannsberger, U. Resch-Genger and J. Daub, *J. Am. Chem. Soc.*, **2000**, 122, 968. (b) J. L. Bricks, A. Kovalchuk, C. Trieflinger, M. Nofz, M. BJsche, A. I. Tolmachev, J. Daub and K. Rurack, *J. Am. Chem. Soc.*, **2005**, 127, 13522. (c) X. Qi, E. J. Jun, L. Xu, S.-J. Kim, J. S. J. Hong, Y. J. Yoon and J. Yoon, *J. Org. Chem.*, **2006**, 71, 2881.

⁶¹ Y. Gabe, Y. Urano, K. Kikuchi, H. Kojima and T. Nagano, *J. Am. Chem. Soc.*, **2004**, 126, 3357.

⁶² F. D'Souza, P. M. Smith, M. E. Zandler, A. L. McCarty, M. Itou, Y. Araki and O. Ito, *J. Am. Chem. Soc.*, **2004**, 126, 7898.

singlet excited zinc porphyrin. The latter gives rise to a charge-separated state to the coordinated fullerene through an efficient electron transfer process (Figure 24).

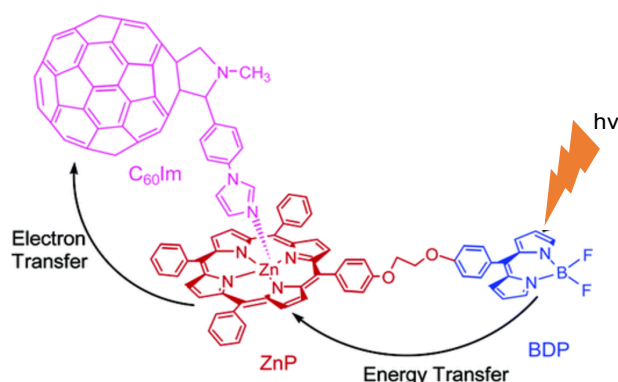


Figure 24: A combined antenna-reaction center model system, **i-53**⁶².

As mentioned above, one of the features of BODIPY-based dyes is a weak triplet yield. However, this problem can be overcome by introducing heavy atoms such as iodine⁶³ on the BODIPY backbone. This type of modified derivatives favours intersystem crossing leading to the triplet state. Thanks to this property, BODIPYs can be used as photosensitizers to efficiently generate singlet oxygen $^1\text{O}_2$, one type of reactive oxygen species (ROS) with great capacity to selectively damage cancer cells, from the triplet excited state $^3\text{O}_2$. Recently, a bifunctional platinated BODIPY molecule **i-54** was synthesized by *H. Chen et al.* and self-assembled to Bodiplatine nanoparticles (BODIPYplatine-NPs) with ultralow radiative transition.⁶⁴ In the cell, BODIPYplatine-NPs can produce efficiently $^1\text{O}_2$ under light irradiation, leading to the ablation of tumor cells. (Figure 25)

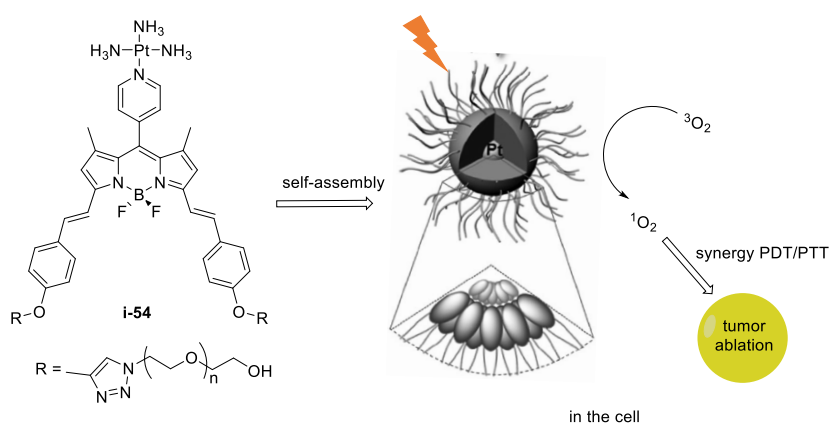


Figure 25: Schematic illustration of tumor cell ablation by BODIPYplatine-NPs.

⁶³ T. Yogo, Y. Urano, Y. Ishitsuka, F. Maniwa and T. Nagano, *J. Am. Chem. Soc.*, **2005**, 127, 12162.

⁶⁴ Z. Guo, Y. Zou, H. He, J. Rao, S. Ji, X. Cui, H. Ke, Y. Deng, H. Yang, C. Chen, Y. Zhao and H. Chen, *Adv. Mater.*, **2016**, 28, 10155.

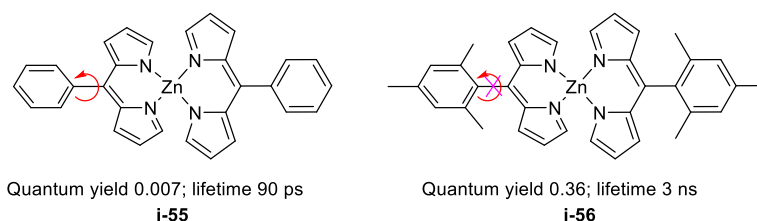


Figure 26: Schematic representation of bis(5-phenyldipyrinato)Zn(II) complex (left) and bis(5-mesityldipyrinato)Zn(II) complex (right) and their corresponding quantum yields and lifetimes in toluene solution.

In addition to BODIPYs, metal dipyrinato complexes have also been investigated for their photophysical properties albeit more recently.⁶⁵ Indeed, Fischer reported first in 1924 a series of bis(dipyrinato)metal complexes lacking acceptable luminescence properties.⁶⁶ Owing to the negligible or weak luminescence properties, in particular when compared with BODIPYs, such metal based compounds did not attract much attention from researchers working in the field of photochemistry/physics until 15 years ago. Since then several luminescent metal complexes have been described such as the heteroleptic ones already briefly mentioned above.⁴⁹ The larger family of emissive dipyrinato complexes are based on the Zn(II) cation. Playing with the nature of the backbone or the coordination sphere of the metal center have been efficient strategies to reach performance sometimes comparable with the boron analogues. The example described by Lindsey, Bocian and Holten is worth mentioning. They found that the fluorescence of bis(dipyrinato)zinc(II) complexes was enhanced by introducing bulky aryl groups at the *meso* position. The rotation of this peripheral group has been demonstrated to be a favourable non-radiative deactivation pathway leading to a decrease in quantum yield.⁶⁷ Therefore, groups such as mesityl and/or introduction of methyl groups on the dipyrrolic backbone at positions 3 and 7 limit this rotation, hence improving the emission. More recently, the group of Nishihara and Sakamoto developed heteroleptic bis(dipyrinato)Zn(II) complexes functionalized not only at the *meso* position but also on the pyrrolic ring by groups such as π -extended moieties.⁶⁸ These compounds have shown intense absorption and fluorescence.

⁶⁵ S. A. Baudron, *Dalton Trans.*, **2013**, 42, 7498.

⁶⁶ H. Fischer and M. Schubert, *Ber. Dtsch. Chem. Ges.*, **1924**, 57, 610.

⁶⁷ I. V. Sazanovich, C. Kirmaier, E. Hindin, L.-H. Yu, D. F. Bocian, J. S. Lindsey and D. Holten, *J. Am. Chem. Soc.*, **2004**, 126, 266.

⁶⁸ (a) M. A. Filatov, A. Y. Lebedev, S. N. Mukhin, S. A. Vinogradov, A. V. Cheprakov, *J. Am. Chem. Soc.*, **2010**, 132, 9552. (b) M. Tsuchiya, R. Sakamoto, S. Kusaka, Y. Kitagawa, M. Okumura and H. Nishihara, *Chem. Commun.*, **2014**, 50, 5881. (c) R. Sakamoto, T. Iwashima, J. F. Kögel, S. Kusaka, M. Tsuchiya, Y. Kitagawa and H. Nishihara, *J. Am. Chem. Soc.*, **2016**, 138, 5666.

As will be detailed below and in Chapter I, such BODIPY and Zn(dpm)₂ complexes have been employed for the preparation of emissive coordination networks.

3.5 Coordination networks

As shown above, homo- or heteroleptic dipyrinato complexes can crystallize as discrete species or organize into infinite architectures. Indeed, dipyrinato complexes incorporating secondary peripheral coordinating groups can either afford homometallic coordination networks by self-assembly, or react with a second metal center leading to the formation of heterometallic coordination networks. The introduction of secondary coordinating units at position 5 has been particularly studied for the preparation of such networks. A brief overview of the different approaches for preparing homo- or heterometallic coordination networks is given here.

3.5.1 Homometallic networks

For the formation of homometallic networks, the dipyrin ligand needs to bear additional coordinating or interacting sites such as a hydrogen bond donor/acceptor group. In the case of a coordinating group, the second moiety may be another dipyrin or a different binding moiety. Both approaches have been described in the literature. Nishihara, Sakamoto and co-workers have described ligand **i-57** based on two dipyrin groups oriented in a divergent fashion and have shown that it leads to a 1D coordination network **i-58** upon assembly with Zn(II) cations.⁶⁹

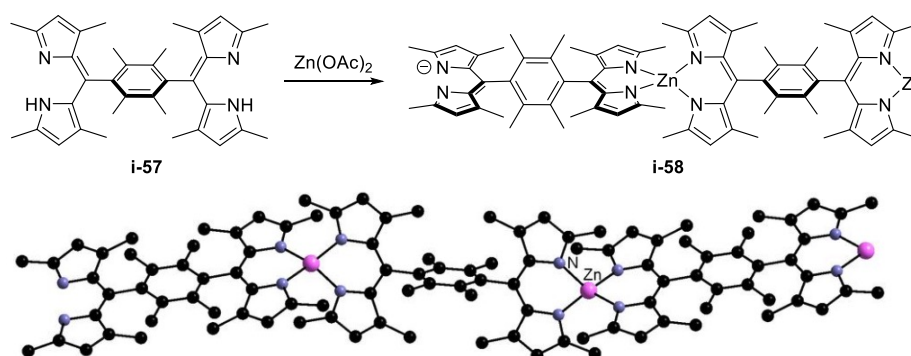


Figure 27: Formation of a crystalline 1D coordination network by reaction of bis-dipyrin ligand **i-57** with Zn(II) cations.

This is a rare example of a crystalline polymer obtained with such type of divergent

⁶⁹ R. Matsuoka, R. Toyoda, R. Sakamoto, M. Tsuchiya, K. Hoshiko, T. Nagayama, Y. Nonoguchi, K. Sugimoto, E. Nishibori, T. Kawai and H. Nishihara, *Chem. Sci.*, **2015**, 6, 2853.

bis-dipyrin ligands since these derivatives have a tendency to form non-crystalline materials upon coordination.⁷⁰

The other strategy, relying on the introduction of another different binding group at the periphery of the dipyrin backbone, has been shown to be more successful for the preparation of homometallic coordination networks. As presented in the previous section, a series of infinite architectures based on heteroleptic dipyrinato complexes with acac or hfac ligand have been reported by Cohen *et al.*⁴⁷ and our laboratory⁴⁸ (see compounds **i-41** and **i-42**).

Networks based on homoleptic dipyrinato complexes have also been described. Indeed, the reaction of the dipyrin ligand functionalized with a pyridyl or imidazolyl group with Ni(II) cation affords the homonuclear coordination networks for which the metal center is in an octahedral environment.⁷¹ It is coordinated to two dipyrinato chelates and two neutral monodentate moieties belonging to neighbouring complexes. The arrangement and dimensionality of infinite architectures are dependent on the nature of the secondary peripheral coordinating unit. For example, in the case of network **i-59** based on the pyridyl appended ligand shown in Figure 28a, a 2D network is obtained with only the Δ enantiomer of the complex as revealed by the structural analysis. With the Ph-imidazolyl dipyrin, a 3D coordination network, **i-60**, comprising both Δ and Λ enantiomers in the solid state is obtained. (Figure 28b)

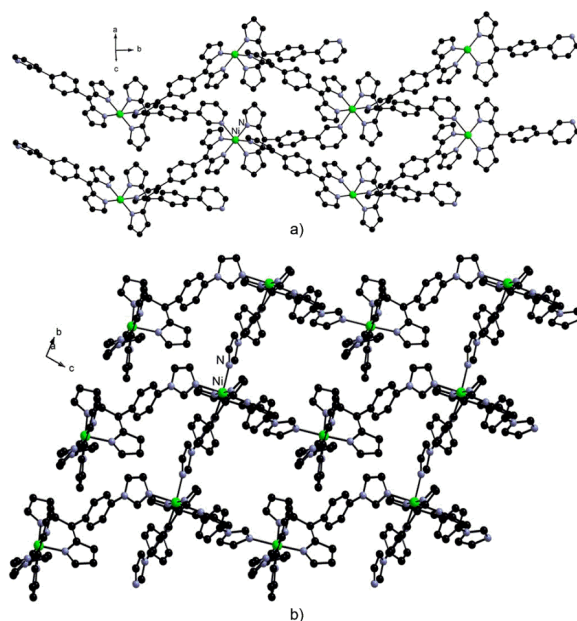


Figure 28: Crystal structures of Ni(Ph-4pydpm)₂ **i-59** (a) and Ni(Ph-imiddpm)₂ **i-60** (b) via self-assembly. Hydrogen atoms and solvent molecules have been omitted for clarity.

⁷⁰ (a) H. Maeda, M. Hasegawa, T. Hashimoto, T. Kakimoto, S. Nishio and T. Nakanishi, *J. Am. Chem. Soc.*, **2006**, *128*, 10024. (b) R. Sakamoto, K. Hoshiko, Q. Liu, T. Yagi, T. Nagayama, S. Kusaka, M. Tsuchiya, Y. Kitagawa, W.-Y. Wong and H. Nishihara, *Nat. Commun.*, **2015**, *6*, 6713. (c) H. Maeda, H. Kobayashi and R. Akuta, *J. Porphyrins Phthalocyanines*, **2013**, *17*, 86.

⁷¹ A. Béziau, S. A. Baudron, G. Roger and M. W. Hosseini, *CrystEngComm.*, **2013**, *15*, 5980.

Another strategy to obtain homometallic network requires a tecton bearing on one hand a dipyrin and on the other hand a hydrogen bond donor/acceptor group such as 5-(benzamide)dipyrin **i-61**.⁷² This ligand is thus prone to chelation of metal and the resulting complexes may self-assemble *via* hydrogen bonding interaction. The example of the 2D network obtained with the Cu complex **i-62** is presented in Figure 29.

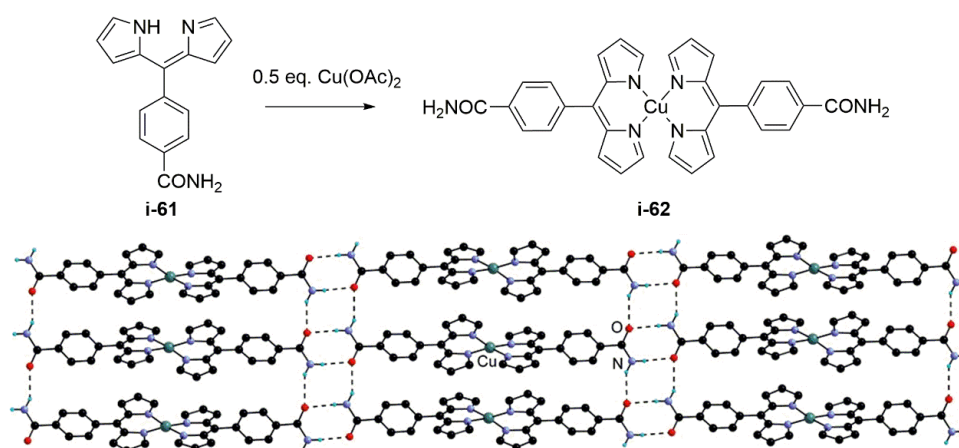


Figure 29: Strategy for the formation of homometallic networks with ligand **i-61** upon both coordination and hydrogen bonding.

3.5.2 Heterometallic networks

Heterometallic networks involve an inherently higher degree of complexity, since these infinite architectures combine at least one organic ligand with several different metal cations. The latter can influence the arrangements and the geometry of the materials obtained as well as their physical properties. An effective synthetic method for the preparation of heteronuclear networks has recently been developed. This sequential strategy shown in Figure 30 and illustrating the formation of a 1D network consists in the reaction of the organic ligand, possessing two divergently coordination sites, with a first metal center M1 to produce a discrete complex. The following step for the construction of heterometallic M1M2-network is then completed by combination of the discrete complex, as metallatecton, and the second metal center by coordination interaction. The arrangement and dimensionality of the final network is controlled by the nature of the peripheral coordinating site, the geometry of the metal center as well as the nature of the anion and solvent molecules.

⁷² S. A. Baudron, D. Salazar-Mendoza and M. W. Hosseini, *CrystEngComm.*, **2009**, *11*, 1245.

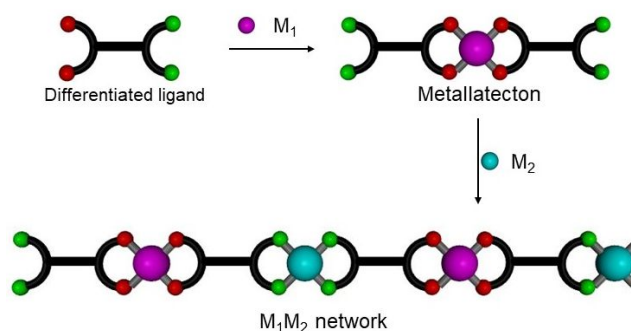


Figure 30: Schematic illustration of synthesis of heterometallic coordination networks.

While this strategy can be applied using a large diversity of differentiated ligands,⁷³ functionalized dipyrin ligands can be particularly interesting because they can be easily functionalized with additional coordinating units at their peripheral positions. Furthermore, introduction of a neutral monodentate unit at the *meso* position of the dipyrinato monoanionic chelate leads to a ligand differentiated in terms of charge and denticity allowing the sequential process to take place. In our laboratory, crystalline heterometallic coordination polymers using dipyrin derivatives bearing additional pyridine, benzonitrile or phenyl-imidazolyl moieties at the *meso*-position have been developed.⁷⁴ For example, using the pyridyl appended dipyrin **i-27**, the metallatectons based on Zn(II), Cu(II) or Pd(II) have been prepared as illustrated in Figure 31 top. Subsequent assembly with CdCl₂ afforded a series of heterometallic 2D grid-type networks. Interestingly, it has also been demonstrated that direct combinations of **i-27** with CdCl₂ and M(OAc)₂ (M = Cu(II), Zn(II), Pd(II)) also produced the same 2D grid-type heterometallic MOFs directly (Figure 31 bottom). The recognition of the Cd(II) cation by the pyridyl unit and the bonding of Zn(II), Cu(II), or Pd(II) by the dipyrin chelate can be explained by the difference of affinity between the metal centres and the coordinating sites. The identity of compounds synthesized by the one-pot approach with those prepared by the sequential strategy was ascertained by X-Ray diffraction. Compared with the sequential strategy, the one-pot method has some advantages such as no need for isolation and solubility problem for metallatecton and less volume of solvent required.

⁷³ (a) S. Kitagawa, S. Noro and T. Nakamura, *Chem. Commun.*, **2006**, 701. (b) M. Andruh, *Chem. Commun.*, **2007**, 2565. (c) S. J. Garibay, J. R. Stork and S. M. Cohen, *Prog. Inorg. Chem.* **2009**, *56*, 335. (d) A. D. Burrows, *CrystEngComm.*, **2011**, *13*, 3623. (e) M. C. Das, S. Xiang, Z. Zhang and B. Chen, *Angew. Chem. Int. Ed.*, **2011**, *50*, 10510. (f) G. Kumar and R. Gupta, *Chem. Soc. Rev.*, **2013**, *42*, 9403.

⁷⁴ A. Béziau, S. A. Baudron, A. Fluck and M. W. Hosseini, *Inorg. Chem.*, **2013**, *52*, 14439.

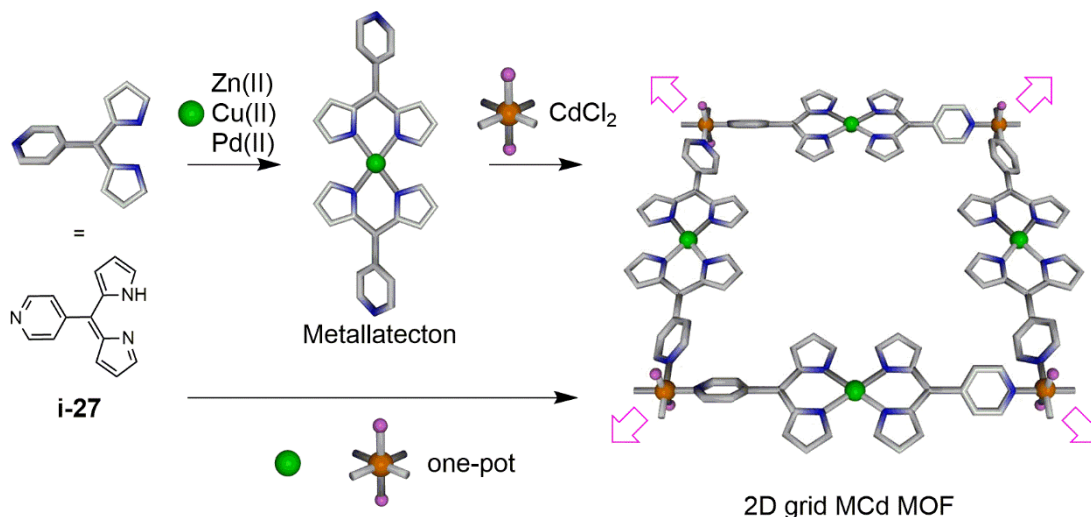


Figure 31: Schematic illustration of two kinds of synthetic strategies for the formation of heterometallic coordination networks as used in ⁷⁴.

Another synthetic approach developed recently in the group involves the conversion of homonuclear coordination network into heterometallic coordination network MM'MOF. It is based on an assembly-disassembly-reassembly process (Figure 32).⁷⁵

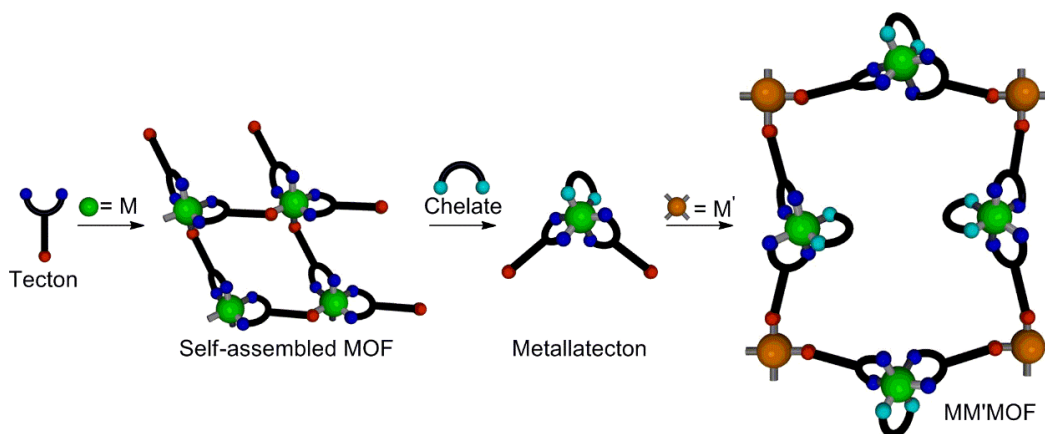


Figure 32: Schematic illustration of the assembly-disassembly-reassembly process.

This approach was applied to the self-assembled Ni(II) networks described above (Figure 28). Indeed, these architectures rely on the coordination of two monodentate peripheral binding units such as a pyridyl or a phenyl-imidazolyl moiety. Taking advantage of the chelate effect, these compounds can be disassembled by reaction with a diamine ligand such as 1,10-phenanthroline (phen) or 2,2'-bipyrimidine (bpm) (Figure 33). This leads to soluble heteroleptic metallatectons that can be subsequently reassembled with a second metal center such as CdCl₂ to produce 2D grid-type networks with two- or three-fold interpenetration, and also a 3D MM'MOF with a triple

⁷⁵ A. Béziau, S. A. Baudron, G. Rogez and M.W. Hosseini, *Inorg. Chem.*, **2015**, 54, 2032.

interpenetration and large cavities (Figure 33).

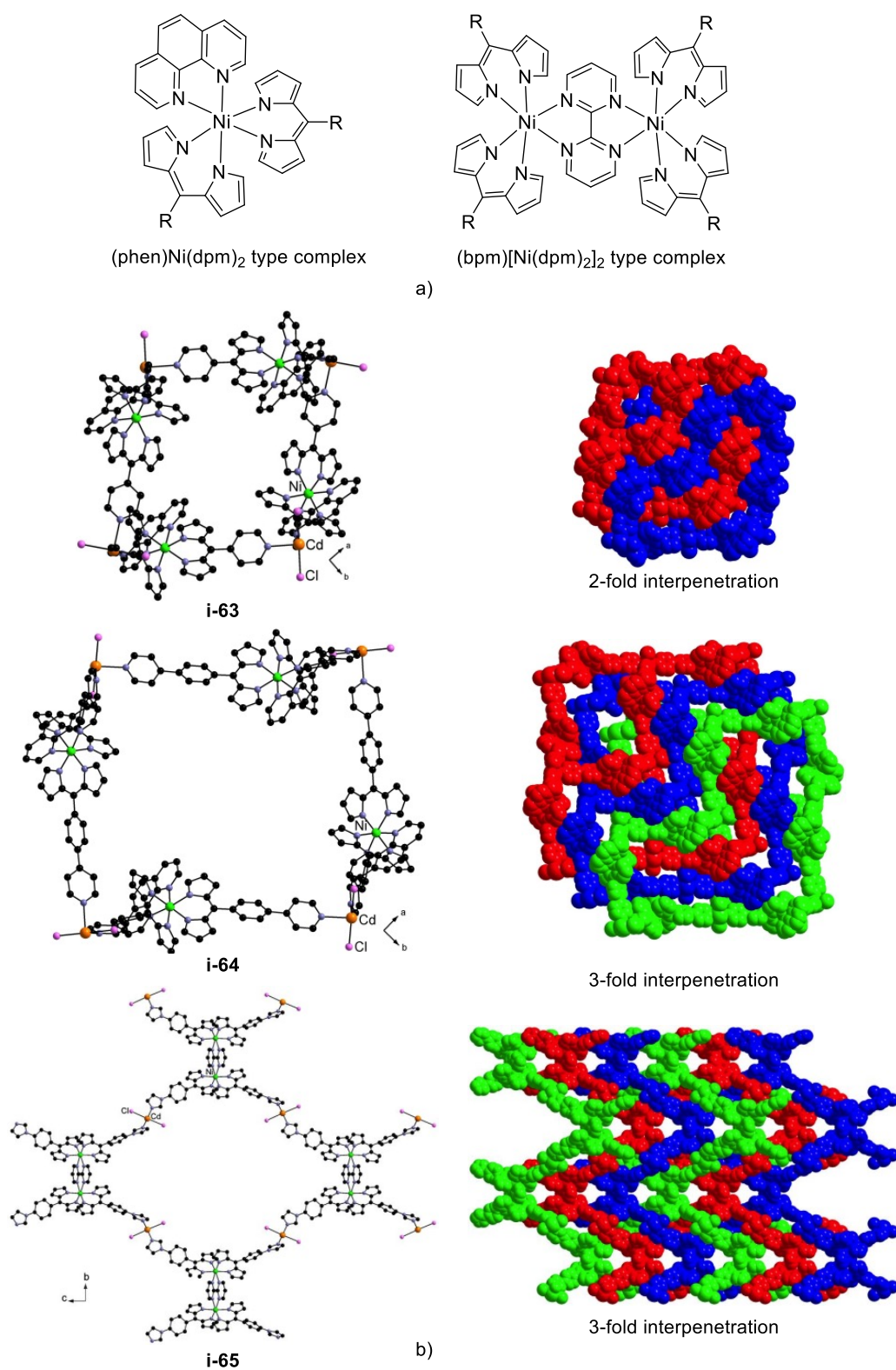


Figure 33: (a) Chemical structures of (phen)Ni(dpm)₂ or (bpm)[Ni(dpm)₂]₂ type complex. (b) 2D grid-type heterometallic network with (phen)Ni(5-pyridyldpm)₂ (top), 2D grid-type heterometallic network with (phen)Ni(5-phenylpydpm)₂ (medium), 3D heterometallic network with (bpm)Ni(5-phenylimidazoyldpm)₂ (bottom).

The different construction strategies presented above rely on the use of CdCl_2 as connecting unit and secondary metal center. Other metal salts can be and have been used. In particular, Ag(I) salts have been exploited. The strategy presented in Figure 30 has been successfully applied with such salts by the group of Cohen and our laboratory.⁷⁶ However, it is worth noting that, in some cases, in addition to the expected coordination of the Ag(I) cation to the peripheral coordinating unit, silver(I)- π interactions with a $\text{C}=\text{C}$ double bond of the pyrrolic units have been also observed.⁷⁷ In the example shown in Figure 34, the Cu(dpm)_2 metallatecton **i-66** bearing peripheral benzonitrile groups assembles with AgOTf in benzene affording a 1D network **i-67**. Based on the crystal structure determination, one can observe that the silver cations are connected with the nitrile units, triflate anions (not shown here for clarity) and pyrrolic $\text{C}=\text{C}$ bonds with $d_{\text{Ag}\cdots\text{C}}$ ranging from 2.394 to 2.465 Å. This is in agreement with what is observed with carbon based aromatic compounds as described in Figure 9 above. This interaction has been observed with several bis-pyrrolic systems by us and others.⁷⁸ As will be detailed in Chapter II, 2,2'-bisdipyririn Zn(II) helicates have been particularly investigated for the promotion of this interaction.

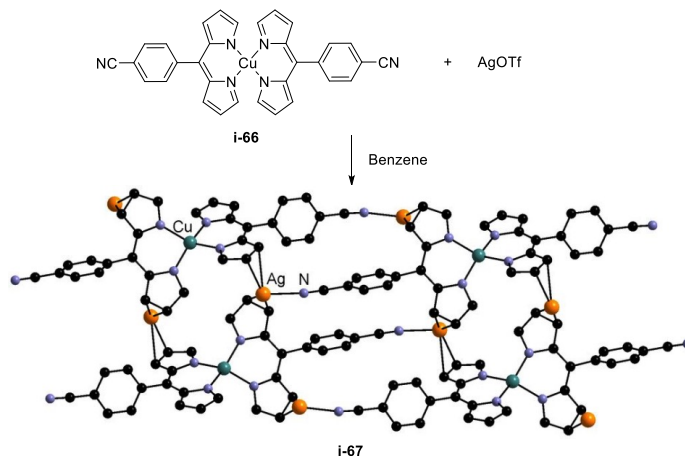


Figure 34: Assembly of Cu(II) metallatecton **i-66** with AgOTf in benzene affording network **i-67** built on the combination of coordination and $\text{Ag}-\pi$ interactions. The hydrogen atoms and the anions have been omitted from the presentation of the crystal structure.

⁷⁶ (a) S. R. Halper, L. Do, J. R. Stork and S. M. Cohen, *J. Am. Chem. Soc.* **2006**, *128*, 15255. (b) D. Pogozhev, S. A. Baudron and M. W. Hosseini, *Inorg. Chem.* **2010**, *49*, 331.

⁷⁷ D. Salazar-Mendoza, S. A. Baudron and M. W. Hosseini, *Chem. Commun.*, **2007**, 2252.

⁷⁸ ((a) A. Béziau, S. A. Baudron and M. W. Hosseini, *Dalton Trans.*, **2012**, *41*, 7227. (b) S. A. Baudron and M. W. Hosseini, *Chem. Commun.*, **2016**, *52*, 13000. (c) A. Mazel, S. A. Baudron and M. W. Hosseini, *CrystEngComm*, **2017**, *19*, 897. (d) J. Wojaczyński, J. Maciołek and P. J. Chmielewski, *Chem. Asian J.*, **2017**, *12*, 643.

4 Objectives of the research project

In light of the state of the art presented above, it appears that dipyrin based derivatives are excellent ligands for the elaboration of coordination networks. However, the scope of functionalization explored so far appears rather limited. The aim of the research develop during this PhD has thus been focused on new approaches for the introduction of coordinating groups on the dipyrin backbone periphery in order to form new tectons which can then be used for the construction of discrete and infinite, homo- or hetero-metallic architectures, with a special attention on their luminescence.

In the first part of the manuscript (chapter I), the functionalization by coordinating groups in positions 1 and 9 using the Knoevenagel type reactions, as well as the introduction of another coordinating or solubilizing unit in position 5 has been explored leading to a series of new dipyrin derivatives. The zinc and boron complexes (BODIPY) of these derivatives were prepared and their photophysical properties were studied. In addition, these luminescent compounds have been used as (metalla)tectons for the construction of (hetero)metallic emissive coordination polymers in the near-IR.

The second part of the thesis (chapter II) is focused on the functionalization of polydipyrins. This type of derivatives comprising several dipyrin moieties, connected with or without a bridge, are interesting for the formation of metallo-organic supramolecular architectures. The 2,2'-bisdipyrin backbone has been particularly studied for its assembly with Zn (II) cations leading to linear helicates. Finally, reactive units such as aldehyde or carboxylic acid have been introduced at the periphery of the 2,2'-bisdipyrin allowing the synthesis of a variety of species by formation of imine or amide groups.

- ¹ (a) J. M. Lehn, *Pure Appl. Chem.*, **1978**, 50, 871. (b) J. M. Lehn, *Angew. Chem. Int. Ed. Engl.*, **1988**, 28, 89. (c) J. M. Lehn, *Angew. Chem. Int. Ed. Engl.*, **1990**, 29, 1304.
- ² (a) J. M. Lehn, *Supramolecular chemistry: Concepts and Perspectives*, Wiley-VCH, **1995**. (b) J. M. Lehn, *Proceedings of the national Academy of Sciences.*, **2002**, 99, 4763. (c) J. M. Lehn, *Chem. Soc. Rev.*, **2007**, 36, 151. (d) J. W. Steed, D. R. Turner and K. Wallace, *Core concepts in Supramolecular Chemistry and Nanochemistry.*, **2007**.
- ³ M. W. Hosseini, *CrystEngComm.*, **2004**, 6, 318.
- ⁴ S. Mann, *Nature.*, **1993**, 365, 499.
- ⁵ (a) M. W. Hosseini, *Coord. Chem. Rev.*, **2003**, 240, 157. (b) M. W. Hosseini, *Chem. Commun.*, **2005**, 5825.
- ⁶ T. R. Cook, R. Y. Zheng and J. P. Stang, *Chem. Rev.*, **2013**, 113, 743.
- ⁷ (a) X. Delaigue, M. W. Hosseini, A. De Cian, J. Fischer, E. Leize, S. Kieffer and A. Van Dorsselaer, *Tetrahedron Lett.*, **1993**, 34, 3285. (b) X. Delaigue, M. W. Hosseini, R. Graff, J.-P. Kintzinger and J. Raya, *Tetrahedron Lett.*, **1994**, 35, 1711.
- ⁸ M. W. Hosseini and A. DeCian, *Chem. Commun.*, **1998**, 727.
- ⁹ A. J. Calahorra, E. S. Sebastián, A. Salinas-Castillo, J. M. Seco, C. Mendicute-Fierro, B. Fernández and A. Rodríguez-Diéguez, *CrystEngComm.*, **2015**, 17, 3659.
- ¹⁰ (a) J. C. Ma and D. A. Dougherty, *Chem. Rev.*, **1997**, 97, 1303. (b) A. S. Mahadevi and G. N. Sastry, *Chem. Rev.*, **2013**, 113, 2100.
- ¹¹ G. L. Ning, M. Munakata, L. P. Wu, M. Maekawa, Y. Suenaga, T. Kuroda-Sowa and K. Sugimoto, *Inorg. Chem.*, **1999**, 38, 5668.
- ¹² S. V. Lindeman, R. Rathore and J. K. Kochi, *Inorg. Chem.*, **2000**, 39, 5707.
- ¹³ T. Steiner, *Angew. Chem. Int. Ed.*, **2002**, 41, 48.
- ¹⁴ (a) A. M. Beatty, *Coord. Chem. Rev.*, **2003**, 246, 131. (b) Michael D. Ward, *Chem. Commun.*, **2005**, 0, 5838.
- ¹⁵ S. Ferlay and M. W. Hosseini, *Actualité Chimique*, **2015**, 399, 16.
- ¹⁶ O. Félix, M. W. Hosseini, A. de Cian and J. Fischer, *Tetrahedron Lett.*, **1997**, 38, 1755.
- ¹⁷ (a) R. Robson, *Dalton Trans.*, **2008**, 5113. (b) S. L. James, *Chem. Soc. Rev.*, **2003**, 32, 276. (c) S. M. Cohen, *Chem. Sci.*, **2010**, 1, 32. (d) M. D. Allendorf, C. A. Bhakta and R. J. Houk, *Chem. Soc. Rev.*, **2009**, 38, 1330. (e) S. R. Batten, N. R. Champness, X. M. Chen, J. Garcia-Martinez, S. Kitagawa, L. Ohrstrom, M. O’Keeffe, M. Paik Suh and J. Reedijk, *CrystEngComm.*, **2012**, 14, 3001. (f) M. Fujita, M. Tominaga, A. Hori and B. Therrien, *Acc. Chem. Res.*, **2005**, 38, 369. (g) T. R. Cook and P. J. Stang, *Chem. Rev.*, **2015**, 115, 701.
- ¹⁸ (a) J. R. Long and O. M. Yaghi, *Chem. Soc. Rev.*, **2009**, 38, 1213. (b) S. R. Batten, N. R. Champness, X.-M. Chen, J. Garcia-Martinez, S. Kitagawa, L. Öhrström, M. O’Keeffe, M. P. Suh and J. Reedijk, *Pure Appl. Chem.*, **2013**, 85, 1715.
- ¹⁹ (a) S. Ferlay, A. Jouaiti, M. Loi, M. W. Hosseini, A. De Cian and P. Turek, *New. J. Chem.*, **2003**, 27, 1801. (b) P. Larpent, A. Jouaiti, N. Kyrisakas and M. W. Hosseini, *Dalton. Trans.*, **2007**, 5126. (c) M. J. Lin, A. Jouaiti, N. Kyrisakas and M. W. Hosseini, *Chem. Commun.*, **2010**, 46, 115. (d) P. Larpent, A. Jouaiti, N. Kyrisakas and M. W. Hosseini, *Dalton Trans.*, **2014**, 43, 166.
- ²⁰ W. Leong and J. J. Vittal, *Chem. Rev.*, **2011**, 111, 688.
- ²¹ F. Zhang, C. R. R. Adolf, N. Zigon, S. Ferlay, N. Kyritsakas and M. W. Hosseini, *Chem. Commun.*, **2017**, 53, 3587.
- ²² M. W. Hosseini, *Acc. Chem. Res.*, **2005**, 38, 313.
- ²³ (a) T. Ohmura, A. Usuki, K. Fukumori, T. Ohta, M. Ito and K. Tatsumi, *Inorg. Chem.*, **2006**, 45, 7988. (b) G. Zhang, E. C. Constable, C. E. Housecroft and J. A. Zampese, *Inorg. Chem. Commun.*, **2014**, 43, 51.
- ²⁴ K. Biradha and M. Fujita, *J. Chem. Soc., Dalton Trans.*, **2000**, 3805.
- ²⁵ (a) H. Li, M. Eddaoudi, M. O’Keeffe and O. M. Yaghi, *Nature.*, **1999**, 402, 276. (b) M. Eddaoudi, J. Kim, N. Rosi, D. Vodak, J. Wachter, M. O’Keeffe and O. M. Yaghi, *Science.*, **2002**, 295, 469.

- ²⁶ (a) J. Lee, O. K. Farha, J. Roberts, K. A. Scheidt, S. T. Nguyen, J. T. Hupp, *Chem. Soc. Rev.*, **2009**, 38, 1450. (b) C. Janiak, J. K. Vieth, *New. J. Chem.*, **2010**, 34, 319. (c) J.-R. Li, J. Sculley, H. -C. Zhou, *Chem. Rev.*, **2012**, 112, 869. (d) Y. Pemh, V. Krunglreviciute, I. Eryazici, J. T. Hupp, O. K. Farha, T. Yildirim, *J. Am. Chem. Soc.*, **2013**, 135, 11887. (e) H. Furukawa, M. O'Keeffe, O. M. Yaghi, *Science.*, **2013**, 341, 974.
- ²⁷ H. Fischer and H. Orth, *Die Chemie des Pyrrols.*, Akademische Verlagsgesellschaft, Leipzig, **1937**.
- ²⁸ T. E. Wood and A. Thompson, *Chem. Rev.*, **2007**, 107, 1831.
- ²⁹ G. P. Arsenault, E. Bullock and S. F. MacDonald, *J. Am. Chem. Soc.*, **1960**, 82, 4384.
- ³⁰ A. Al-Sheikh-Ali, K. S. Cameron, T. S. Cameron, K. N. Robertson and A. Thompson, *Org. Lett.*, **2005**, 7, 4773.
- ³¹ C. W. Wan, A. Burghart, J. Chen, F. Bergstroem, L. B. A. Johansson, M. F. Wolford, T. G. Kim, M. R. Topp, R. M. Hochstrasser and K. Burgess, *Chem. Eur. J.*, **2003**, 9, 4430.
- ³² C. Bruckner, V. Karunaratne, S. J. Rettig and D. Dolphin, *Can. J. Chem.*, **1996**, 74, 2182.
- ³³ C. H. Lee and J. S. Lindsey, *Tetrahedron.*, **1994**, 50, 11427.
- ³⁴ (a) B. J. Littler, M. A. Miller, C.-H. Hung, R. W. Wagner, D. F. O'Shea, P. D. Boyle and J. S. Lindsey, *J. Org. Chem.*, **1999**, 64, 1391. (b) J. K. Laha, S. Dhanalekshmi, M. Taniguchi, A. Ambroise and J.S. Lindsey, *Org. Proc. Res. Dev.*, **2003**, 7, 799.
- ³⁵ J.-Y. Shin, D. Dolphin and B. O. Patrick, *Cryst. Growth. Des.*, **2004**, 4, 659.
- ³⁶ D. Salazar-Mendoza, S. A. Baudron and M. W. Hosseini, *Inorg. Chem.*, **2008**, 47, 766.
- ³⁷ J. R. Stork, V. S. Thoi and S. M. Cohen, *Inorg. Chem.*, **2007**, 46, 11213.
- ³⁸ D. Pogozhev, S. A. Baudron and M. W. Hosseini, *Dalton Trans.*, **2011**, 40, 437.
- ³⁹ H. Ruffin, S. A. Baudron, D. Salazar-Mendoza and M. W. Hosseini, *Chem. Eur. J.*, **2014**, 20, 2449.
- ⁴⁰ L. Do, S. R. Halper, S. M. Cohen, *Chem. Commun.*, **2004**, 2662.
- ⁴¹ J. D. Hall, T. M. McLean, S. J. Smalley, M. R. Waterland and S. G. Telfer, *Dalton Trans.*, **2010**, 39, 437.
- ⁴² D. Salazar-Mendoza, S. A. Baudron and M. W. Hosseini, *Chem. Commun.*, **2007**, 2252.
- ⁴³ C. Brückner, Y. Zhang, S. J. Rettig and D. Dolphin, *Inorg. Chim. Acta.*, **1997**, 263, 279.
- ⁴⁴ S. M. Cohen and S. R. Halper, *Inorg. Chim. Acta.*, **2002**, 341, 12.
- ⁴⁵ J. R. Stork, V. S. Thoi and S. M. Cohen, *Inorg. Chem.*, **2007**, 46, 11213.
- ⁴⁶ Q. Miao, J. -Y. Shin, B. O. Patrick and D. Dolphin, *Chem. Commun.*, **2009**, 2541.
- ⁴⁷ S. R. Halper, M. R. Malachowski, H. M. Delaney and S. M. Cohen, *Inorg. Chem.*, **2004**, 43, 1242.
- ⁴⁸ B. Kilduff, D. Pogozhev, S. A. Baudron and M. W. Hosseini, *Inorg. Chem.*, **2010**, 49, 11231.
- ⁴⁹ (a) X. Liu, H. Nan, W. Sun, Q. Zhang, M. Zhan, L. Zou, Z. Xie, X. Li, C. Lu and Y. Cheng, *Dalton Trans.*, **2012**, 41, 10199. (b) J. Kobayashi, T. Kushida and T. Kawashima, *J. Am. Chem. Soc.*, **2009**, 131, 10836. (c) T. M. McLean, J. L. Moody, M. R. Waterland and S. G. Telfer, *Inorg. Chem.* **2012**, 51, 446. (d) C. Bronner, S. A. Baudron, M. W. Hosseini, C. A. Strassert, A. Guenet and L. De Cola, *Dalton Trans.*, **2010**, 39, 180. (e) S. J. Smalley, M. R. Waterland and S. G. Telfer, *Inorg. Chem.*, **2009**, 48, 13. (f) K. Hanson, A. Tamayo, V. V. Diev, M. T. Whited, P. I. Djurovich and M. E. Thompson, *Inorg. Chem.*, **2010**, 49, 6077.
- ⁵⁰ K. Nakano, K. Kobayashi and K. Nozaki, *J. Am. Chem. Soc.*, **2011**, 133, 10720.
- ⁵¹ T. Ohkawara, K. Suzuki, K. Nakano, S. Mori and K. Nozaki, *J. Am. Chem. Soc.*, **2014**, 136, 10728.
- ⁵² S. El Ghachtouli, K. Wojcik, L. Copey, F. Szydlo, E. Framery, C. Goux-Henry, L. Billon, M.-F. Charlot, R. Guillot, B. Andrioletti and A. Aukauloo, *Dalton Trans.*, **2011**, 40, 9090.
- ⁵³ (a) E. R. King, E. T. Hennessy and T. A. Betley, *J. Am. Chem. Soc.*, **2011**, 133, 4917. (b) E. T. Hennessy and T. A. Betley, *Science.*, **2013**, 340, 591.
- ⁵⁴ A. Treibs and F. H. Kreuzer, *Justus Liebigs Ann. Chem.*, **1968**, 718, 208.

- ⁵⁵ (a) O. Driessen and J. Lugtenberg, *J. High Resolut. Chromatogr. Chromatogr. Commun.*, **1980**, 3, 405. (b) A. Emonds, J. Bonnet, J. Lugtenburg and O. Driessen, *J. Chromatogr.*, **1983**, 279, 477.
- ⁵⁶ M. Shah, K. Thangraj, M. L. Soong, L. Wolford, J. H. Boyer, I. R. Politzer and T. G. Pavlopoulos, *Heteroat. Chem.*, **1990**, 1, 389.
- ⁵⁷ G. Ulrich, R. Ziessel and A. Harriman, *Angew. Chem. Int. Ed.*, **2008**, 47, 1184.
- ⁵⁸ (a) M. Kollmannsberger, T. Gareis, S. Heinl, J. Breu and J. Daub, *Angew. Chem. Int. Ed. Engl.*, **1997**, 36, 1333. (b) T. Gareis, C. Huber, O. S. Wolfbeis and J. Daub, *Chem. Commun.*, **1997**, 1717. (c) K. Rurack, M. Kollmannsberger and J. Daub, *New J. Chem.*, **2001**, 25, 289. (d) C. N. Baki, E. U. Akkaya, *J. Org. Chem.*, **2001**, 66, 1512. (e) M. Baruah, W. Qin, N. Basaric, W. M. De Borggraeve and N. Boens, *J. Org. Chem.*, **2005**, 70, 4152. (f) W. Qin, M. Baruah, W. M. De Borggraeve and N. Boens, *J. Photochem. Photobiol. A.*, **2006**, 183, 190.
- ⁵⁹ (a) V. V. Matin, A. Rothe, Z. Diwu and K. R. Gee, *Bioorg. Med. Chem. Lett.*, **2004**, 14, 5313. (b) M. Baruah, W. Qin, R. A. L. VallQe, D. Beljonne, T. Rohand, W. Dehaen and N. Boens, *Org. Lett.*, **2005**, 7, 4377. (c) K. Yamada, Y. Nomura, D. Citterio, N. Iwasawa and K. Suzuki, *J. Am. Chem. Soc.*, **2005**, 127, 6956.
- ⁶⁰ (a) K. Rurack, M. Kollmannsberger, U. Resch-Genger and J. Daub, *J. Am. Chem. Soc.*, **2000**, 122, 968. (b) J. L. Bricks, A. Kovalchuk, C. Trieflinger, M. Nofz, M. BJsche, A. I. Tolmachev, J. Daub and K. Rurack, *J. Am. Chem. Soc.*, **2005**, 127, 13522. (c) X. Qi, E. J. Jun, L. Xu, S.-J. Kim, J. S. J. Hong, Y. J. Yoon and J. Yoon, *J. Org. Chem.*, **2006**, 71, 2881.
- ⁶¹ Y. Gabe, Y. Urano, K. Kikuchi, H. Kojima and T. Nagano, *J. Am. Chem. Soc.*, **2004**, 126, 3357.
- ⁶² F. D'Souza, P. M. Smith, M. E. Zandler, A. L. McCarty, M. Itou, Y. Araki and O. Ito, *J. Am. Chem. Soc.*, **2004**, 126, 7898.
- ⁶³ T. Yogo, Y. Urano, Y. Ishitsuka, F. Maniwa and T. Nagano, *J. Am. Chem. Soc.*, **2005**, 127, 12162.
- ⁶⁴ Z. Guo, Y. Zou, H. He, J. Rao, S. Ji, X. Cui, H. Ke, Y. Deng, H. Yang, C. Chen, Y. Zhao and H. Chen, *Adv. Mater.*, **2016**, 28, 10155.
- ⁶⁵ S. A. Baudron, *Dalton Trans.*, **2013**, 42, 7498.
- ⁶⁶ H. Fischer and M. Schubert, *Ber. Dtsch. Chem. Ges.*, **1924**, 57, 610.
- ⁶⁷ I. V. Sazanovich, C. Kirmaier, E. Hindin, L.-H. Yu, D. F. Bocian, J. S. Lindsey and D. Holten, *J. Am. Chem. Soc.*, **2004**, 126, 266.
- ⁶⁸ (a) M. A. Filatov, A. Y. Lebedev, S. N. Mukhin, S. A. Vinogradov, A. V. Cheprakov, *J. Am. Chem. Soc.*, **2010**, 132, 9552. (b) M. Tsuchiya, R. Sakamoto, S. Kusaka, Y. Kitagawa, M. Okumura and H. Nishihara, *Chem. Commun.*, **2014**, 50, 5881. (c) R. Sakamoto, T. Iwashima, J. F. Kögel, S. Kusaka, M. Tsuchiya, Y. Kitagawa and H. Nishihara, *J. Am. Chem. Soc.*, **2016**, 138, 5666.
- ⁶⁹ R. Matsuoka, R. Toyoda, R. Sakamoto, M. Tsuchiya, K. Hoshiko, T. Nagayama, Y. Nonoguchi, K. Sugimoto, E. Nishibori, T. Kawai and H. Nishihara, *Chem. Sci.*, **2015**, 6, 2853.
- ⁷⁰ (a) H. Maeda, M. Hasegawa, T. Hashimoto, T. Kakimoto, S. Nishio and T. Nakanishi, *J. Am. Chem. Soc.*, **2006**, 128, 10024. (b) R. Sakamoto, K. Hoshiko, Q. Liu, T. Yagi, T. Nagayama, S. Kusaka, M. Tsuchiya, Y. Kitagawa, W.-Y. Wong and H. Nishihara, *Nat. Commun.*, **2015**, 6, 6713. (c) H. Maeda, H. Kobayashi and R. Akuta, *J. Porphyrins Phthalocyanines*, **2013**, 17, 86.
- ⁷¹ A. Béziau, S. A. Baudron, G. Rogezb and M. W. Hosseini, *CrystEngComm.*, **2013**, 15, 5980.
- ⁷² S. A. Baudron, D. Salazar-Mendoza and M. W. Hosseini, *CrystEngComm.*, **2009**, 11, 1245.
- ⁷³ (a) S. Kitagawa, S. Noro and T. Nakamura, *Chem. Commun.* **2006**, 701. (b) M. Andruh, *Chem. Commun.* **2007**, 2565. (c) S. J. Garibay, J. R. Stork and S. M. Cohen, *Prog. Inorg. Chem.* **2009**, 56, 335. (d) A. D. Burrows, *CrystEngComm.* **2011**, 13, 3623. (e) M. C. Das, S. Xiang, Z. Zhang and B. Chen, *Angew. Chem. Int. Ed.* **2011**, 50, 10510. (f) G. Kumar and R. Gupta, *Chem. Soc. Rev.* **2013**, 42, 9403.
- ⁷⁴ A. Béziau, S. A. Baudron, A. Fluck and M. W. Hosseini, *Inorg. Chem.*, **2013**, 52, 14439.
- ⁷⁵ A. Béziau, S. A. Baudron, G. Rogez and M. W. Hosseini, *Inorg. Chem.*, **2015**, 54, 2032.

- ⁷⁶ (a) S. R. Halper, L. Do, J. R. Stork and S. M. Cohen, *J. Am. Chem. Soc.* **2006**, *128*, 15255. (b) D. Pogozhev, S. A. Baudron and M. W. Hosseini, *Inorg. Chem.* **2010**, *49*, 331.
- ⁷⁷ D. Salazar-Mendoza, S. A. Baudron and M. W. Hosseini, *Chem. Commun.*, **2007**, 2252.
- ⁷⁸ (a) A. Béziau, S. A. Baudron and M. W. Hosseini, *Dalton Trans.*, **2012**, *41*, 7227. (b) S. A. Baudron and M. W. Hosseini, *Chem. Commun.*, **2016**, *52*, 13000. (c) A. Mazel, S. A. Baudron and M. W. Hosseini, *CrystEngComm*, **2017**, *19*, 897. (d) J. Wojaczyński, J. Maciołek and P. J. Chmielewski, *Chem. Asian J.*, **2017**, *12*, 643.

Chapter I

Chapter I: Coordination polymers based on 1,9-divinyldipyrin derivatives

In the first part of this work, a series of novel functionalized dipyrins bearing coordinating units at different positions (1, 5, 9) has been developed. Indeed, using Knoevenagel type reaction, different functional groups such as pyridine, benzonitrile or carboxylic acid moieties could be introduced, thus leading to ligands incorporating the dipyrin chelate and coordinating groups at positions 1 and 9. Furthermore, either a binding unit or a more solubilizing group has been also introduced at position 5. Using these ligands, the synthesis of the corresponding BODIPYs and homoleptic Zn(II) complexes has been developed and the photophysical properties of these species have been investigated. Furthermore, these luminescent dipyrinato complexes, regarded as (metalla)tectons, have been employed for the construction of (hetero)metallic coordination polymers which emit in the NIR region, upon assembly with different metal salts, in particular silver(I) ones.

I.1 Introduction

Over the past two decades, coordination polymers and porous metallo-organic crystalline architectures (also named Metal-Organic Frameworks, MOFs) have emerged as an active class of materials owing to their wide applications in the domain of gas storage, separation and catalysis for example.¹ In addition to these above-mentioned applications, this type of polymers has also been considered as luminescent materials with excellent performance in the field of detection and sensing.² Dipyrin, a π -conjugated planar molecule, can absorb visible light efficiently by π - π^* transition process. As mentioned in the introduction of this dissertation, some discrete dipyrinato complexes such as BODIPY and Zn(dipyrinato)₂ have been developed for their interesting

¹ (a) S. R. Batten, R. Robson, *Angew. Chem., Int. Ed.*, **1998**, 37, 1460. (b) M. Eddaoudi, D. B. Moler, H. Li, B. Chen, T. M. Reineke, M. O’Keeffe, O. M. Yaghi, *Acc. Chem. Res.*, **2001**, 34, 319. (c) S. Kitagawa, R. Kitaura, S. I. Noro, *Angew. Chem. Int. Ed.*, **2004**, 43, 2334. (d) J. R. Long, O. M. Yaghi, *Chem. Soc. Rev.*, **2009**, 38, 1213. (e) *Chem. Soc. Rev.*, **2009**, 38 (5), themed issue on metalorganic frameworks. (f) C. Janiak, J. K. Vieth, *New J. Chem.*, **2010**, 34, 2366. (g) *Chem. Rev.*, **2012**, 112 (2), 2012 Metal–Organic Frameworks special issue. (h) C. Wang, W. Lin, *J. Am. Chem. Soc.*, **2013**, 135, 13222.

² (a) M. D. Allendorf, C. A. Bauer, R. K. Bhakta and R. J. T. Houk, *Chem Soc Rev.*, **2009**, 38, 1330. (b) J. Rocha, L. D. Carlos, F. A. Almeida Paz and D. Ananias, *Chem. Soc. Rev.*, **2011**, 40, 926. (c) Y. Cui, Y. Yue, G. Qiang and B. Chen, *Chem. Rev.*, **2012**, 112, 1126. (d) J. Heine and K. Müller-Buschbaum, *Chem. Soc. Rev.*, **2013**, 42, 9232. (e) Z. Hu, B. J. Deibert and J. Li, *Chem Soc Rev.*, **2014**, 43, 5815. (f) M. C. So, G. P. Wiederrecht, J. E. Mondloch, J. T. Hupp and O. K. Farha, *Chem. Commun.*, **2015**, 51, 3501. (g) D. E. Williams and N. B. Shustova, *Chem. Eur. J.*, **2015**, 21, 15474. (h) L. Zhang, Z. Kang, X. Xin and D. Sun, *CrystEngComm.*, **2016**, 18, 193.

photophysical properties. Furthermore, these dipyrin based complexes bearing a peripheral coordinating group can either self-assemble or act as luminescent metallatectons for the elaboration of emissive homo- or hetero-metallic coordination polymers.³

In 2011, J. T. Hupp and co-workers reported two MOFs called BOB and BOP consisting of three components: a 2,6-bipyridyl-BODIPY, zinc(II) cations and either 2,3,5,6-tetracarboxyphenylbenzene or tetracarboxylic acid-porphyrin respectively (Figure 1). For these two compounds, the tetra-carboxylic derivative forms two dimensional layers upon formation of the paddle-wheel motif with the Zn(II) cations, while the BODIPY acts as a pillar connecting these sheets. In addition to this structural role, the BODIPY also acts as either an emitter or a sensitizer. Indeed, in the case of the MOF BOB, upon excitation at 520 nm, an emission band was observed at 596 nm. This band corresponds to the typical luminescence of BODIPYs. Interestingly, in the case of the MOF BOP, an emission band was detected at 667 nm instead of 596 nm, upon excitation at 520 nm. This observation demonstrates the existence of an efficient energy transfer process from the BODIPY struts to the porphyrin ones (Figure 1).⁴

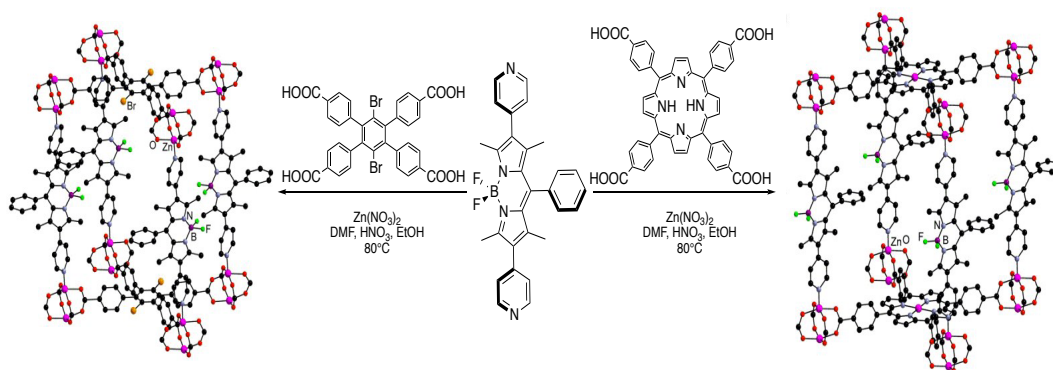


Figure 1: Strategies for the formation of two luminescent MOFs with 2,6-bipyridyl-BODIPY.

Another strategy for the preparation of emissive coordination networks with different dimensionalities using a BODIPY bearing carboxylic acid moieties at positions 2 and 6 (BODIPY-COOH) has been employed by Ding, Zhao, Hou and coworkers (Figure 2).⁵ BODIPY-COOH was assembled with a Zn(II) or Cd(II) nitrate salt in the presence of either 1,2-bi(4-pyridyl)ethane (bpe) or 1,3-bi(4-pyridyl)propane (bpp) as a linker to form five different luminescent MOFs. Upon excitation at 450 nm, all of these MOFs are emissive around 524-539

³ S. A. Baudron, *CrystEngComm.*, **2016**, 18, 4671.

⁴ C. Y. Lee, O. K. Farha, B. J. Hong, A. A. Sarjeant, S. T. Nguyen and J. T. Hupp, *J. Am. Chem. Soc.*, **2011**, 133, 15858.

⁵ M. Li, Y. Yao, J. Ding, L. Liu, J. Qin, Y. Zhao, H. Hou and Y. Fan, *Inorg. Chem.*, **2015**, 54, 1346.

nm and their quantum yields (Φ_f) are low and in the range of 0.0067 to 0.017. It is worth noting that one of the networks (Figure 2) shows a higher quantum yield than the others due to the absence of BODIPYs dimers and of aggregation of the fluorescent dyes as demonstrated by the long distance between the BODIPY-planes ($d_{\text{BODIPY}\cdots\text{BODIPY}} = 13.984 \text{ \AA}$, $\alpha_{\text{BODIPY}\cdots\text{BODIPY}} = 84^\circ$), in the crystalline state.

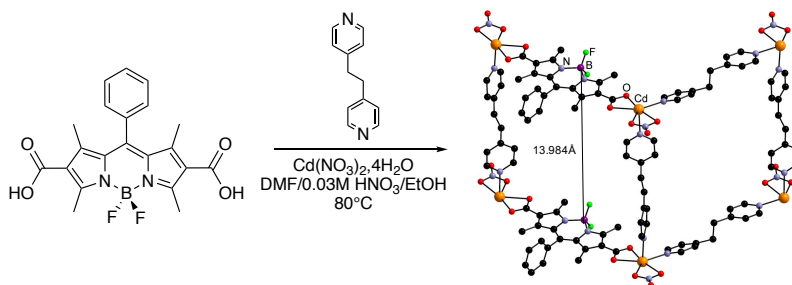


Figure 2: Strategy for the formation of a bidimensional network using a carboxylic acid functionalized BODIPY, Cd(II) cations and the bpe linker.

In our laboratory, some homo- and heterometallic luminescent networks have been prepared using 5-pyridyl (R_1) or 5-phenylimidazolyl (R_2) appended dipyrinato Cd(II) or Zn(II) complexes.⁶ The earlier complexes incorporating Cd(II) cations have been shown to self-assemble into networks owing to the increase in the coordination number of the metal centers (Figure 3), as described in the introduction chapter for the Ni analogues.⁷ For these Cd-R networks, two emission bands were observed upon excitation at 430 nm (Cd- R_1 : 563 nm and 602 nm; Cd- R_2 : 577 nm and 616 nm). The luminescent properties of these networks are ligand centered and result the π - π^* transition of the dipyrin chromophore (Figure 3). Interestingly, heterometallic networks ZnCdMOFs can be obtained by two different strategies: (a) synthesis of 5-substituted dipyrinato (pyridyl or phenylimidazolyl) Zn(II) complexes, not prone to self-assembly into a homometallic architecture in a first step, and then assembly with Cd(II) cation leading to the corresponding 2D networks; (b) organization of ZnCdMOFs (Zn- R_1 or Zn- R_2) by combining 5-substituted dipyrins and the two types of metal centers in a one-pot reaction. Investigation of the luminescent properties of these crystalline materials have shown emission bands at 577-646 nm due to the luminescence of the zinc complexes.

⁶ (a) A. Béziau, S. A. Baudron, A. Guenet and M. W. Hosseini., *Chem. Eur. J.*, **2013**, *19*, 3215. (b) A. Béziau, S. A. Baudron, A. Fluck and M. W. Hosseini, *Inorg. Chem.*, **2013**, *52*, 14439.

⁷ A. Béziau, S.A. Baudron, G. Rogez and M. W. Hosseini, *CrystEngComm.*, **2013**, *15*, 5980.

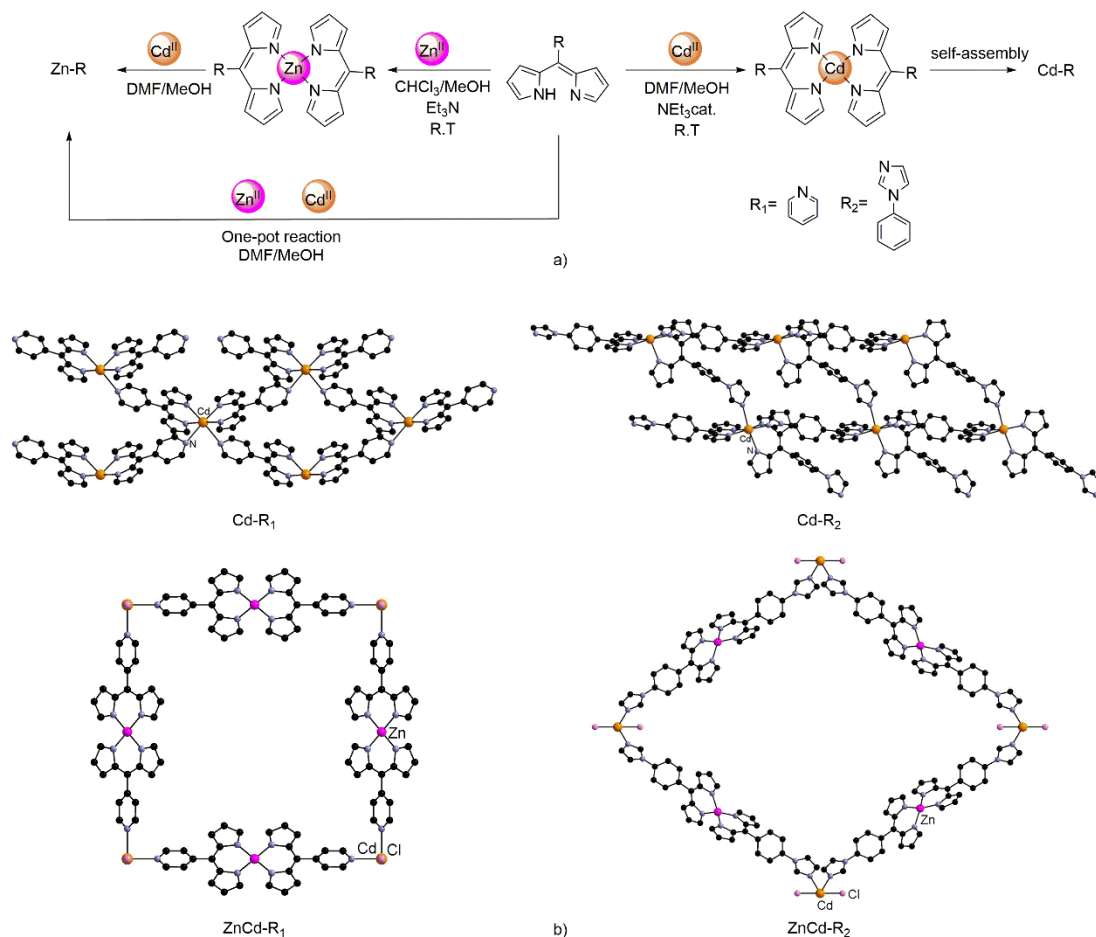


Figure 3: (a) Synthetic strategies for the preparation of homo- or heterometallic networks with 5-substituted dipyrins. (b) crystallographic structures of networks Cd-R₁/R₂ and ZnCd-R₁/R₂.

Recently, 1,9-divinyldipyrin derivatives equipped with long π -extended conjugated system have been used for complexation with Zn(II) or B(III) centers affording a series of dyes with intense absorption and fluorescence bands, even emitting in the near infrared (NIR) region.⁸ For example, Ziessel *et al.* have reported an interesting mixed 1,9-distyrylBodipy derivative which is sensitive to pH.⁹ The tuning of its optical properties allows this species to be used as a pH sensor (Figure 4). The maximum absorption band of the neutral mixed distyrylBodipy compound appears at 676 nm. The protonation of its dimethylamino group induces a blue-shifted band due to the loss of the lone pair delocalization. In contrast, the deprotonation of the phenol group causes a strong bathochromic shift, with an absorption band at 718 nm due to the delocalization of the phenolate charge over the entire conjugated pathway.

⁸ (a) K. Rurack, M. Kollmannsberger and J. Daub., *New J. Chem.*, **2001**, 25, 289. (b) R. Ziessel, G. Ulrich, A. Harriman, M. A. H. Alamiry, B. Stewart and P. Retailleau., *Chem. Eur. J.*, **2009**, 15, 1359 – 1369. (c) J. Bartelmess and W. W. Weare, *Dyes and Pigments.*, **2013**, 97, 1. (d) R. Sakamoto, T. Iwashima, J. F. Kögel, S. Kusaka, M. Tsuchiya, Y. Kitagawa and H. Nishihara, *J. Am. Chem. Soc.*, **2016**, 138, 5666.

⁹ T. Bura, P. Retailleau, G. Ulrich and R. Ziessel, *J. Org. Chem.*, **2011**, 76, 1109.

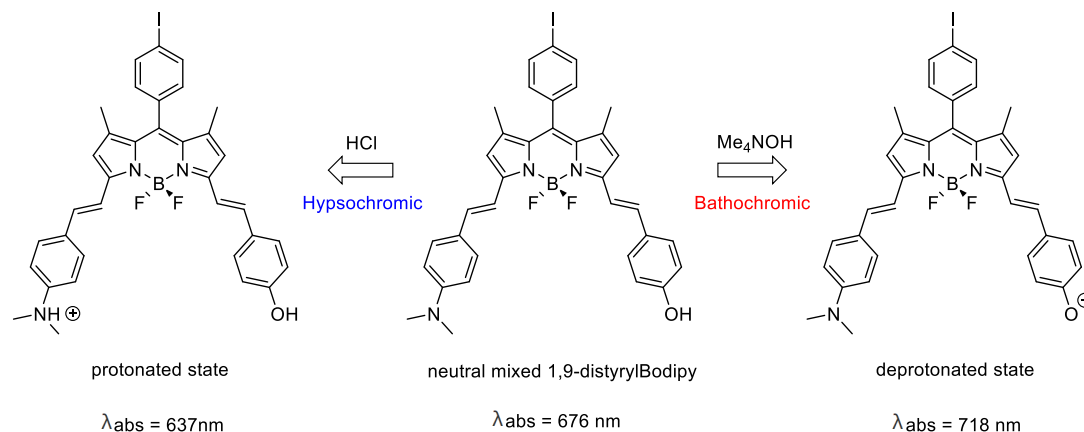


Figure 4: Schematic representation of the change of absorption bands of mixed 1,9-distyrylBodipy by controlling the pH value.

Surprisingly, to the best of our knowledge, to date, no coordination polymers with this type of functionalized tunable dipyrin ligands have been reported. Thus, the aim of the research described in this chapter has been to design such new derivatives bearing additional coordinating units on the 1,9-divinyldipyrin backbone for the formation of luminescent complexes (Zn/B), and subsequently of emissive coordination polymers following the molecular tectonics approach (Figure 5).¹⁰

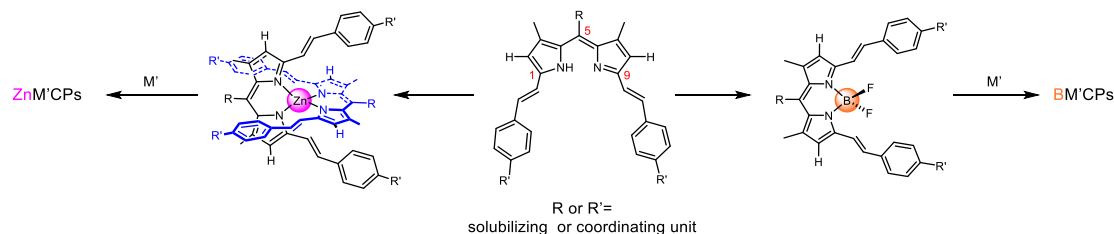


Figure 5: Strategies for the preparation of coordination polymers based on 1,9-divinyldipyrin derivatives.

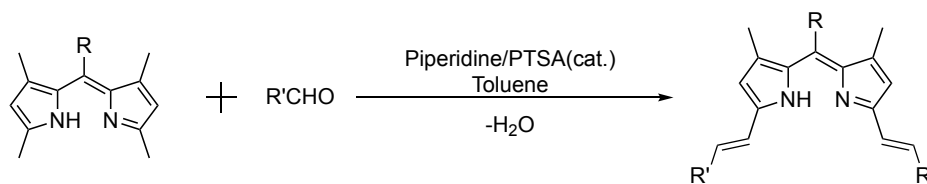
1.2 Synthesis and characterization of 1,9-divinyldipyrin ligands

In order to access the new ligands, a synthetic strategy has been developed (Scheme 1) that takes advantage of the reactivity of the acidic hydrogen atoms of 1,9-dimethyl-dipyrins towards aldehyde using a Knoevenagel type condensation.¹¹ This approach allows to easily introduce coordinating units at positions 1 and 9 of the dipyrin skeleton. Furthermore, a 1,3,7,9-tetramethyl dipyrin has been chosen, since the presence of the additional Me groups at positions 3 and 7 may

¹⁰ M. W. Hosseini, *CrystEngComm.*, **2004**, *6*, 318.

¹¹ (a) E. Knoevenagel, *Ber. Dtsch. Chem. Ges.*, **1898**, *31*, 2596. (b) R. Ziessel, T. Bura, J. H. Olivier, *Synlett.*, **2010**, *15*, 2304.

hinder the rotation of the functional group present at position 5 (*meso*) thus disfavoring a non-radiative deactivation pathway and hence enhancing the emission properties of these compounds.¹²



Scheme 1: Synthesis of 1,9-divinyldipyrins ligands.

Following this strategy, two series of ligands bearing different functional groups at the *meso* position have been prepared. For the first one, dipyrin **1**, obtained as described,¹³ was reacted with 4-cyanobenzaldehyde, 4-pyridinecarboxaldehyde or methyl 4-formylbenzoate, in the presence of piperidine and a catalytic amount of *p*-toluenesulfonic acid to produce ligands **2-4** in 50-63% yield (Figure 6). The identity and purity of these products have been demonstrated by ¹H-NMR, ¹³C-NMR, HRMS(ESI) analysis. In particular, for all compounds, the two hydrogen atoms of the vinyl groups are in *trans* position as shown by the coupling constant, J_{H-H} =16.3-16.6 Hz, in the ¹H-NMR spectrum (see Experimental section). This first family of 1,9-divinyldipyrins ligands have two different coordinating sites, the dipyrin chelate (blue part) and two vinyl arms (red part). The ester appended derivative has been envisioned as a precursor of the carboxylic acid functionalized ligand. This intermediate appeared indeed easier to prepare and purify than the acid one. At the *meso* position, a mesityl moiety has been introduced in order to increase the solubility of these compounds.

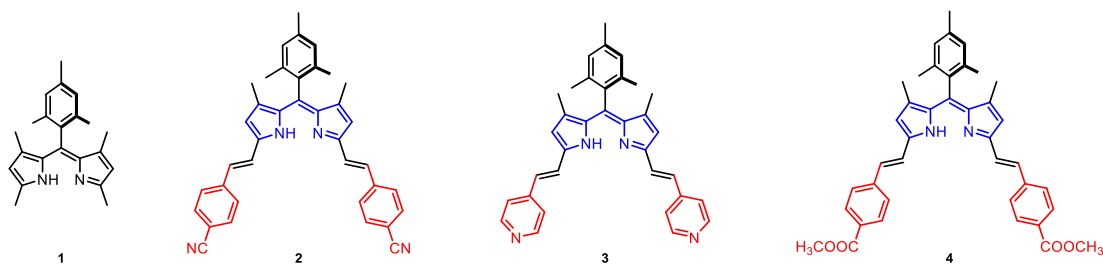


Figure 6: Chemical structures of dipyrins **1-4**.

¹² (a) H. L. Kee, C. Kirmaier, L. Yu, P. Thamyonkit, W. J. Youngblood, M. E. Calder, L. Ramos, B. C. Noll, D. F. Bocian, W. R. Scheidt, R. R. Birge, J. S. Lindsey, D. Holtz, *J. Phys. Chem. B*, **2005**, *109*, 20433. (b) V. S. Thoi, J. R. Stork, D. Magde, S. M. Cohen, *Inorg. Chem.*, **2006**, *45*, 10688. (c) J. Kobayashi, T. Kushida, T. Kawashima, *J. Am. Chem. Soc.*, **2009**, *131*, 10836. (d) C. Bronner, S. A. Baudron, M. W. Hosseini, C. A. Strassert, A. Guenet, L. De Cola, *Dalton Trans.*, **2010**, *39*, 180. (e) K. Hanson, A. Tamayo, V. V. Diev, M. T. Whited, P. I. Djurovich, M. E. Thompson, *Inorg. Chem.*, **2010**, *49*, 6077. (f) T. M. McLean, J. L. Moody, M. R. Waterland, S. G. Telfer, *Inorg. Chem.*, **2012**, *51*, 446. (g) C. Bronner, M. Veiga, A. Guenet, L. De Cola, M. W. Hosseini, C. A. Strassert, S. A. Baudron, *Chem. Eur. J.*, **2012**, *18*, 4041.

¹³ L. Fu, F.-L. Jiang, D. Fortin, P. D. Harvey and Y. Liu, *Chem. Commun.*, **2011**, *47*, 5503.

In addition to the above-mentioned characterization, the crystal structure of these compounds has been determined by single-crystal X-Ray diffraction. Crystallization of **2** upon slow evaporation of a toluene solution of the compound afforded single crystals (monoclinic, $P2_1/n$) (see Experimental part). Single crystals of **3** and **4** were obtained upon pentane vapor diffusion into a CHCl_3 solution of the ligands (orthorhombic $Pbcn$ and monoclinic Pc for **3** and **4** respectively). The three compounds show similar features. Owing to the π -conjugation and an intramolecular hydrogen bond ($d_{\text{N}\cdots\text{N}} = 2.628(2) \text{ \AA}$, $\alpha_{\text{NH}\cdots\text{N}} = 124.75^\circ$), the pyrrolic rings are almost coplanar (3.34°) in **2**. As expected, the mesityl group at the *meso* position is perpendicular to the chelate plane ($\alpha_{\text{meso}\cdots\text{chelate plane}}: 86.36^\circ$ for **2**; 83.31° for **3**; 89.30° for **4**) (Figure 7a). The two pyrrolic units of **3** are also almost coplanar with an angle of 4.33° as a result of the intramolecular hydrogen bond ($d_{\text{N}\cdots\text{N}} = 2.649(2) \text{ \AA}$, $\alpha_{\text{NH}\cdots\text{N}} = 125.20^\circ$), while this angle for ligand **4** is 1.57° with an analogous intramolecular hydrogen bond ($d_{\text{N}\cdots\text{N}} = 2.623(3) \text{ \AA}$, $\alpha_{\text{NH}\cdots\text{N}} = 126.30^\circ$) (Figure 7 b/c).

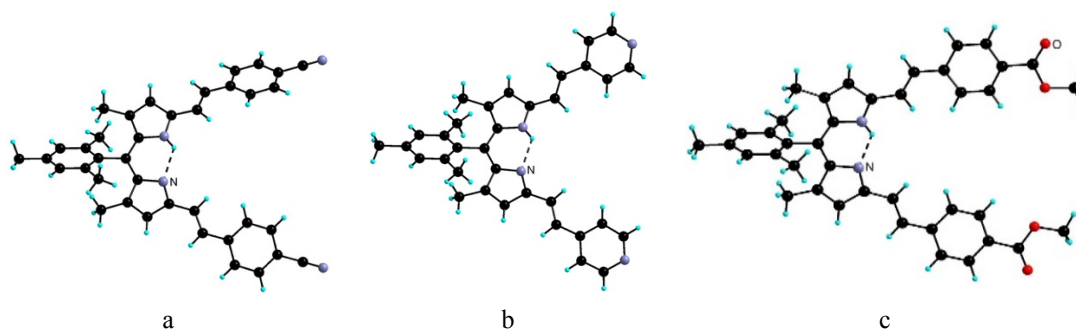


Figure 7: Crystallographic structure of compounds **2** (a), **3** (b) and **4** (c).

In the second series of ligands, the coordinating moieties have been introduced not only at the 1, 9-positions of the dipyrin backbone but also at the *meso* position, in order to afford ligands featuring more binding sites. Reactions of 5-py or 5-phenylpy tetramethyldipyrrins **5** and **6**, prepared in our laboratory by Audrey Fluck, with either 4-cyanobenzaldehyde or 4-pyridinecarboxaldehyde produced ligands **7-9** in 62-81% yield (Figure 8). All five compounds have been characterized by $^1\text{H-NMR}$, $^{13}\text{C-NMR}$ in solution and by HRMS(ESI).

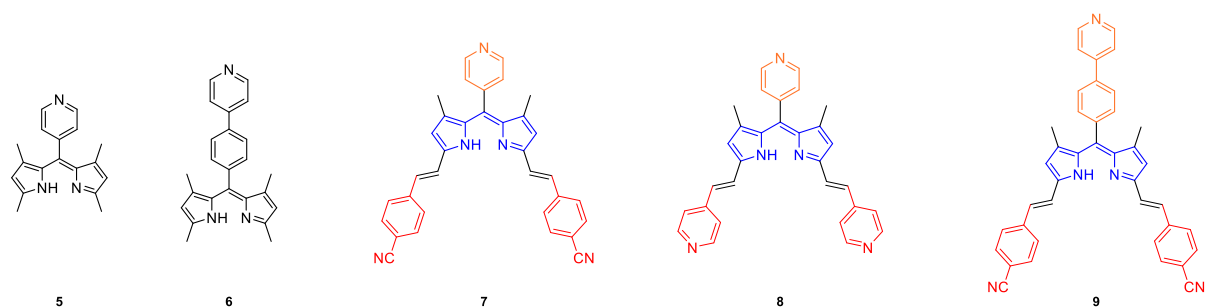


Figure 8: Chemical structures of dipyrrens **5-9**.

Crystals of ligands **7** and **9** suitable for X-Ray diffraction analysis were obtained upon pentane vapour diffusion into a concentrated CHCl_3 or THF solution containing the respective compounds. Unfortunately, for ligand **8**, the crystal quality was not sufficient for X-ray diffraction analysis. Both ligands, shown in Figure 8, crystallize in the triclinic space group $P-1$. For both dipyrrens, an intramolecular hydrogen bond is present with similar distance and angle ($d_{\text{N}\cdots\text{N}} = 2.660(4)$ Å and $\alpha_{\text{NH}\cdots\text{N}} = 124.88^\circ$ for **7**; $2.668(2)$ Å and 125.49° for **9**). Differences between the compounds can be observed. Whereas in the structure of **9**, the two pyrrolic units within the chelate are almost coplanar (8.18°), a slight distortion is present for **7** (16.33°). The angle between the substituent at the *meso* position and the chelate plane is 69.53° for compound **7** and 83.24° for **9**. Furthermore, while the two vinylic groups point outward for **7** as well as for **2-4**, one of them points inward for **9**. The vinyl groups are nonetheless in a *trans* arrangement for all compounds.

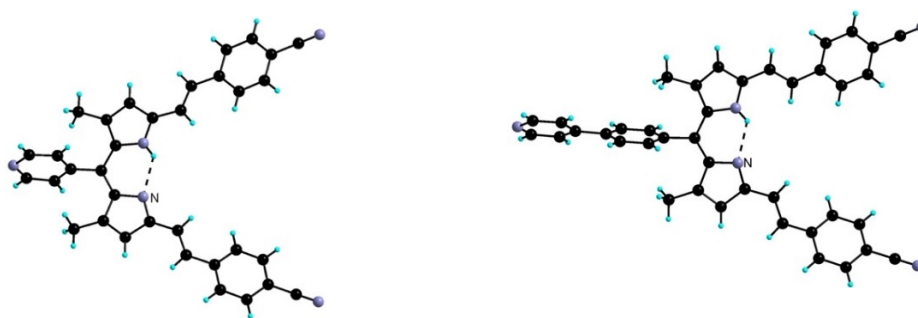


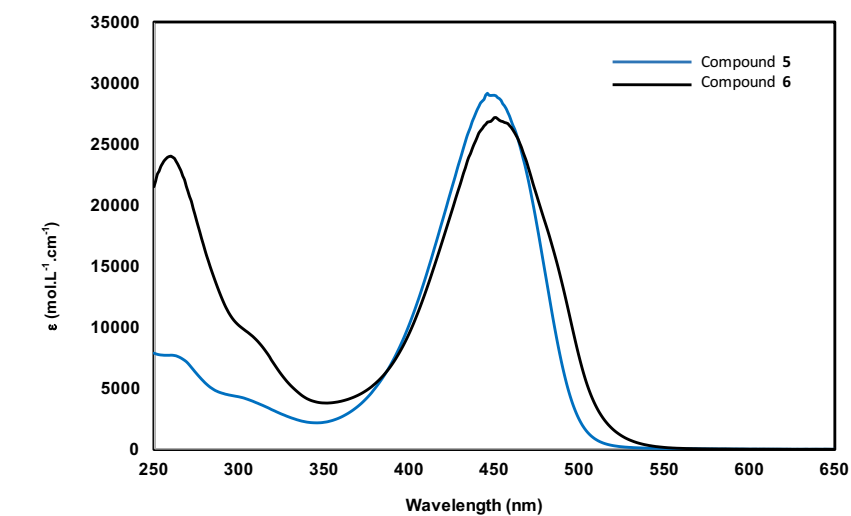
Figure 9: Crystallographic structure of compound **7** (left) and compound **9** (right).

Table 1: Selected bond distances (Å) and angles (°) for structures of compounds **2-9**.

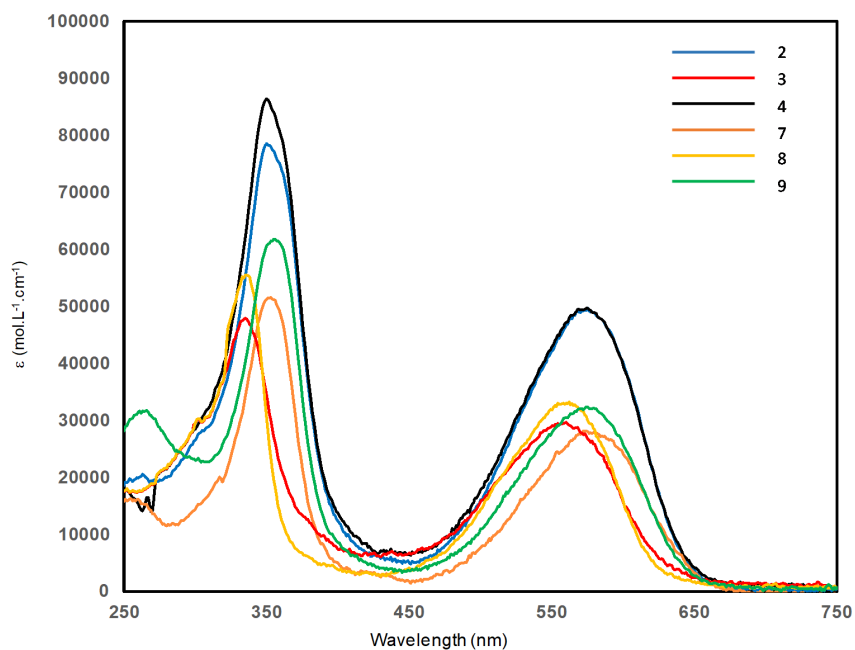
1,9-divinyldipyrin	$d_{N...N}$ (Å)	$\alpha_{NH...N}$ (°)	$\alpha_{pyrrolic}$ plane 1...pyrrolic plane 2 (°)	α_{meso} group...pyrrolic plane (°)
2	2.628(2)	124.75	3.34	86.36
3	2.649(2)	125.20	4.33	83.31
4	2.623(3)	126.30	1.57	89.30
7	2.660(4)	124.88	16.33	69.53
9	2.668(2)	125.49°	8.18	83.24

As mentioned in the introduction of this chapter, this series of ligands should have the capacity to absorb light efficiently. The photophysical properties of these π -extended 1,9-divinyldipyrins as well as the ones of intermediates **5** and **6** have thus been investigated in CH₂Cl₂ solution (Table 2 and Figure 10). For the 1, 9-unsubstituted dipyrin **5** and **6** (Figure 10a), an intense absorption band at around 450 nm (446 nm for **5**; 451 nm for **6**) resulting from π - π^* transition of the dipyrinato chromophore is observed along with a high energy peak at 266 nm for dipyrin **6** corresponding to π - π^* transition of the peripheral *meso* group. For the vinyl appended derivatives, the impact of the functionalization is apparent first with the presence of an absorption band assigned to the π - π^* transition of the vinyl group itself in the 333-355 nm region and, secondly, by a bathochromic shift of the absorption associated with the dipyrin centered around 550-580 nm. This shift results from the increased conjugation of the system owing to the introduction of the vinyl moieties at positions 1 and 9. Ligands **3** and **8** exhibit blue shifted absorption bands (*ca.*14-25 nm), as a result of the electron-withdrawing nature of 1, 9-pyridyl groups on the vinylic part, when compared with the other benzonitrile appended derivatives. The nature of the group at the *meso* position does not seem to have a strong influence on the absorption spectrum of these ligands probably owing to the fact that it is almost perpendicular to the conjugated dipyrin system as observed in the crystalline structures discussed above. Finally, in the case of ligand **9**,

the third absorption band is observed at 266 nm due to π - π^* transition of the *mesophenyl*-pyridine group.¹⁴



(a)



(b)

Figure 10: (a) Absorption spectrum of dipyrins **5** and **6** in CH_2Cl_2 at R.T (10^{-4} mol/L). (b) Absorption spectrum of ligand **2-9** in CH_2Cl_2 at room temperature (10^{-6} mol/L).

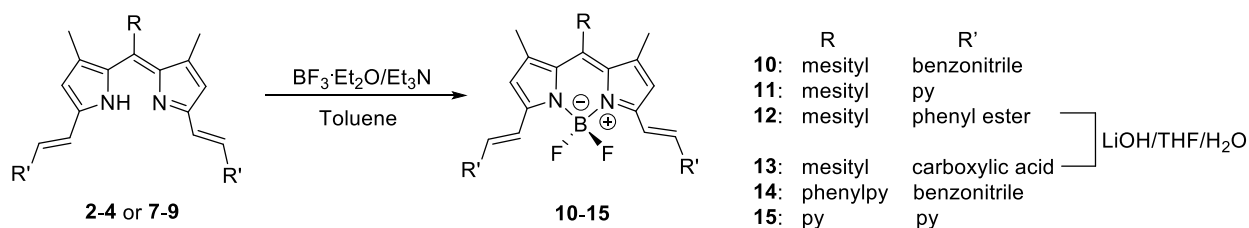
¹⁴ (a) C. Bruckner, V. Karunaratne, S. J. Rettig and D. Dolphin, *Can. J. Chem.*, **1996**, 74, 2182. (b) C. Bruckner, Y. J. Zhang, S. J. Rettig and D. Dolphin, *Inorg. Chim. Acta.*, **1997**, 263, 279.

Table 2: Absorption and molar extinction coefficient (ϵ) of 1,9-divinyldipyrin derivatives in CH_2Cl_2 solution at room temperature.

Compound	$\lambda_{\text{ab}}/\text{nm}$ ($\epsilon \cdot 10^3 \text{ M}^{-1}\text{cm}^{-1}$)
2	350 (78.6)
	575 (49.7)
3	336 (47.9)
	560 (29.7)
4	350 (86.4)
	574 (49.7)
7	353 (51.6)
	580 (28)
8	333 (55.1)
	562 (33.1)
9	266 (31.7)
	355 (61.8)
	574 (32.3)

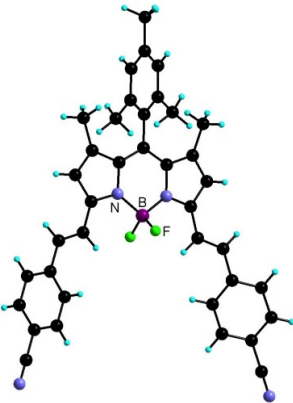
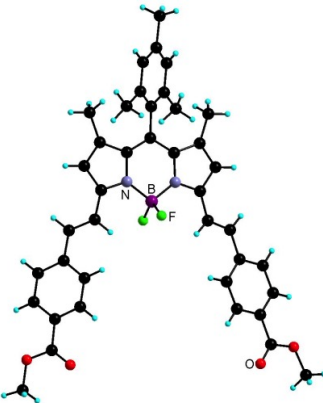
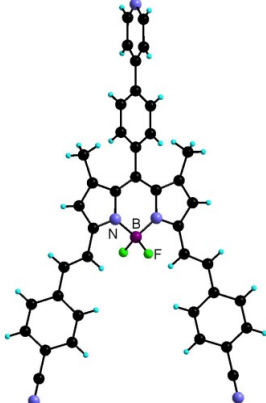
I.3 Preparation of BODIPYs complexes

As described in the literature, BODIPYs (4,4-difluoro-4-bora-3a,4a-diaza-indacene) can be prepared by reaction between a free dipyrin ligand and $\text{BF}_3 \cdot \text{Et}_2\text{O}$ under basic conditions.¹⁵ Following this strategy, in the presence of triethylamine, a toluene solution of ligands **2-4** or **7-9** was reacted with $\text{BF}_3 \cdot \text{Et}_2\text{O}$ and brought to reflux under argon for 4 hours. Cold ethanol and methanol were used for quenching the reaction and removing the impurities thus producing BODIPYs **10-15** in 92-96% yield (Scheme 2). All BODIPYs were characterized in solution by ^1H -NMR, ^{13}C -NMR and UV-visible spectroscopy and by HRMS(ESI). Furthermore, BODIPY **13** bearing carboxylic acid groups has been obtained in 84% yield by saponification of the methyl benzoate-BODIPY **12** with 10 equivalents of LiOH in a THF/ H_2O mixture (1/1).



Scheme 2: Synthesis of BODIPY derivatives **10-15**.

Table 3: Structures and selected bond lengths (Å) for BODIPYs **10,12** and **14**.

	BODIPY 10	BODIPY 12	BODIPY 14
			
dB-N	1.544(2)	1.544(3) 1.548(3)	1.5375(17)
dB-F	1.384(4) 1.393(4)	1.382(3) 1.394(2)	1.3843(17)

¹⁵ G. Ulrich, R. Ziessel and A. Harriman, *Angew. Chem. Int. Ed.*, **2008**, 47, 1184.

The crystal structures of BODIPYs **10**, **12** and **14** have been determined by X-ray diffraction (table 3). All three BODIPYs crystallize in the monoclinic system, but with different space groups (**10**: $P2_1/m$, **12**: $P2_1/n$, **14**: $C2/c$). The boron center adopts a tetrahedral coordination environment with the two nitrogen atoms of the dipyrinato chelate ($d_{B-N} = 1.5375\text{-}1.548\text{ \AA}$) and two fluoride anions. ($d_{B-F} = 1.382\text{-}1.394\text{ \AA}$)

A photophysical study of BODIPYs **10-15** has been performed in DMF solution (10^{-6} mol/L). The data are listed in Table 3. The absorption and emission spectra for BODIPY **10** are presented in Figure 11 as a representative example of this series of compounds. Three types of absorptions bands were observed in DMF solution. The two low energy bands correspond to the absorption of the BODIPY core and the high energy one at 340-361 nm arises from the absorption of the vinyl moieties. Upon excitation at 570 nm, two emission bands at 626-648 and 684-711 nm are observed for BODIPYs **10-15**. Comparing with the absorption spectrum, we can observe that these emission bands are exactly the mirror image of the $S_0 \rightarrow S_1$ absorption band. Thus, the fluorescence of compounds **10-15** derives from the $\pi\text{-}\pi^*$ excited state of the corresponding BODIPY units. These results are similar to those reported for other analogous derivatives.¹⁶ As for the corresponding dipyrin, the absorption bands of BODIPY **11** and **15** are also blue shifted owing to the presence of 3,5-pyridyl groups on the vinylic part (numbering follows the rules for Bodipy). The quantum yields of these compounds in solution have been also determined and shown in Table 4. The relative method is used for determining the quantum yields of the unknown compounds (Q_f).¹⁷ Cresyl Violet perchlorate has been chosen as the standard, because it emits in the same region with a similar quantum yield.¹⁸ It is worth noting that, the pyridyl-appended compounds **11** and **15** stand out with a higher quantum yield ($\Phi_f = 0.87$ and 0.77 respectively) compared with the other ones. This observation can be explained by increasing of the coupling of $S_1 \rightarrow S_0$ due to the presence of the pyridyl group as an electron-withdrawing unit. In contrast, introduction of carboxylic acid groups as for BODIPY-COOH **13** results in a less emissive species ($\Phi_f = 0.43$). Furthermore, comparing **11**

¹⁶ C. O. Obondi, G. N. Lim, P. A. Karr, V. Nesterov and F. D'Souza, *Phys. Chem. Chem. Phys.*, **2016**, *18*, 18187.

¹⁷ (a) A. T. Rhys Williams and S. A. Winfield, *Analyst.*, **1983**, *108*, 1067.

¹⁸ D. Magde, J. H. Brannon, T. L. Cremers and J. Olmsted, *J. Phys. Chem.*, **1976**, *83*, 696.

with **15** highlights the role of the peripheral group at the *meso* position, since the ones bearing a mesityl unit with a hindered rotation show a higher fluorescence quantum yield.^{12,19}

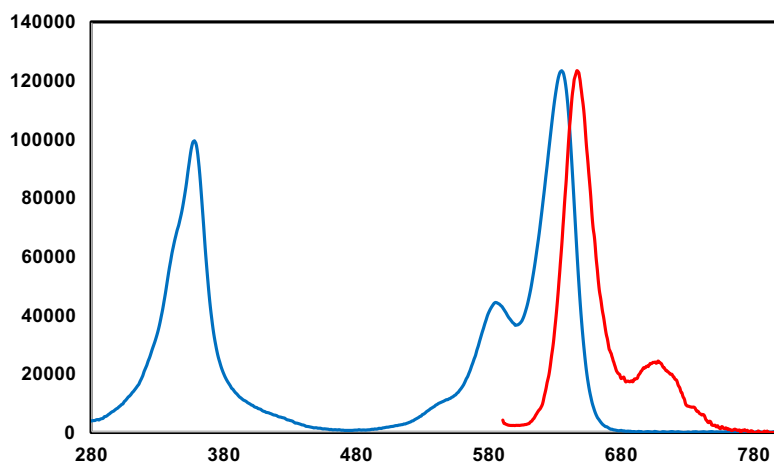


Figure 11: Absorption and emission spectra of BODIPY **10** in DMF as a representative example.

Table 4: Absorption and fluorescence data in DMF solution of BODIPYs **10-15** at room temperature.

Sample	λ_{ab}/nm ($\epsilon \cdot 10^3 \text{ M}^{-1}\text{cm}^{-1}$)	λ_{em}/nm^a	Φ_f^b
10	358 (99.7)	646	0.61
	585 (44.4)	708	
	635 (123.6)		
11	340 (38.6)	626	0.87
	568 (23.1)	684	
	616 (70.3)		
12	359 (87)	647	0.71
	586 (38.2)	711	
	635 (118.3)		
13	359 (67.9)	646	0.43
	585 (32.8)	707	
	628 (64.2)		
14	361 (94.4)	648	0.59
	586 (41.6)	709	
	636 (112.8)		
15	341 (51.7)	630	0.77
	572 (22.1)	684	
	620 (69.2)		

(a) excited at 570 nm. (b) using Cresyl Violet perchlorate as reference ($\Phi_s = 0.54$ in MeOH, aerated solution)¹⁸. $\Phi_f = \Phi_s \cdot (A_s/A_f) \cdot (E_f/E_s) \cdot (n_f^2/n_s^2)$, Φ_s is the quantum yield of the standard, A is the absorbance of the solution, E is the corrected emission intensity, and n is the average refractive index of the solution.

¹⁹ (a) G. J. Hedley, A. Ruseckas, A. Harriman, I. D. W. Samuel, *Angew. Chem., Int. Ed.*, **2011**, 50, 6634. (b) M. Buyuktemiz, S. Duman and Y. Dede, *J. Phys. Chem. A.*, **2013**, 117, 1665.

I.4 Formation of coordination polymers with BODIPYs

The generation of coordination polymers with these new BODIPYs has then been investigated. These compounds bearing the peripheral coordinating groups have been used as tectons for the construction of molecular networks by assembly with various metal salts. All suitable single crystals have been prepared by two crystallization methods: (a) liquid-liquid diffusion or (b) vapor diffusion. The silver cation has been particularly employed as the second metal center because of the adaptability of the d^{10} Ag(I) that should allow a large range of possible coordination modes and should bind even weak terminal units, such as benzonitrile. Moreover, it has been demonstrated that the silver cation can also assemble with polypyrrolic derivatives *via* Ag- π interactions leading to networks.²⁰

I.4.1 Formation of coordination networks with tecton 10

In order to investigate the assembly of BODIPY **10** with Ag(I) cations, CHCl₃ solutions of **10** were layered with either AcOEt or MeOH solution of a AgX salt ($X^- = ClO_4^-, BF_4^-, AsF_6^-$). In the case of AcOEt, single crystals were obtained directly by the liquid-liquid diffusion method after few days. In contrast, no crystalline material was directly obtained upon diffusion of MeOH. However, upon subsequent Et₂O vapor diffusion into the resulting clear CHCl₃/MeOH mixtures, single crystals have been obtained after few days. Four different materials (**16-19**) have been prepared and characterized by single-crystal X-Ray diffraction. This work has recently been published in *CrystEngComm*.²¹

In the CHCl₃/AcOEt crystallization mixture, two types of crystalline morphologies (large plates and small needles) were observed by using a AgClO₄ salt. Unfortunately, only the single crystals with the plate form could be characterized by single-crystal X-ray diffraction and the latter were not of sufficient quality for structure determination. The large plate type crystals corresponding to compound **16**, formulated as (**10**)₂Ag₂(ClO₄)₂(CHCl₃)₂ crystallize in the triclinic space group *P*-1.

²⁰ (a) D. Salazar-Mendoza, S. A. Baudron and M. W. Hosseini, *Chem. Commun.*, **2007**, 2252. (b) D. Salazar-Mendoza, S. A. Baudron and M. W. Hosseini, *Inorg. Chem.*, **2008**, *47*, 766. (c) D. Pogozhev, S. A. Baudron and M. W. Hosseini, *Inorg. Chem.*, **2010**, *49*, 331. (d) B. Kilduff, D. Pogozhev, S. A. Baudron and M. W. Hosseini, *Inorg. Chem.*, **2010**, *49*, 11231. (e) A. Béziau, S. A. Baudron and M. W. Hosseini, *Dalton Trans.*, **2012**, *41*, 7227.

²¹ F. Zhang, S. A. Baudron and M. W. Hosseini, *CrystEngComm.*, **2017**, *19*, 4393.

Two different molecules of BODIPY **10** and two AgClO₄ pairs (one perchlorate anion being disordered over two positions) form a [2+2] metallamacrocyclic motif of the [(**10**)Ag]₂²⁺ type. The metal center coordinates to two nitrile groups of two metallatectons **10** and one oxygen atom of ClO₄[−] in a T-shape geometry. Within the cyclic motif, the distance between the silver(I) centers Ag(1)-Ag(2) is *ca.* 13.4 Å. Interestingly, the Ag- π interactions are observed between these metallamacrocyclic motif due to two crystallographically independent Ag(I) cations interacting with C atoms of either the pyrrolic cycle of the dipyrin backbone or of a benzonitrile moiety. In particular, the resulting Ag-C distance is longer with the C-CH₃ fragment than with the C-H fragment (Table 5). This type of interaction²² has been also observed with other dipyrin or azadipyrin ligands, as detailed in the Introduction.^{16(a-b)(e),23} This combination of interactions leads to a two-dimensional network (Figure 12). Weak hydrogen bonding can be also observed between the perchlorate anions and the inner C-H of the benzonitrile units of **10** (*d*_{C...O} = 3.270(3) Å-3.428(3) Å, $\alpha_{\text{CH}\cdots\text{O}}$ = 134.84-136.36°; Figure 12). This type of weak hydrogen bonding has been reported in the literature with numerous derivatives.²⁴

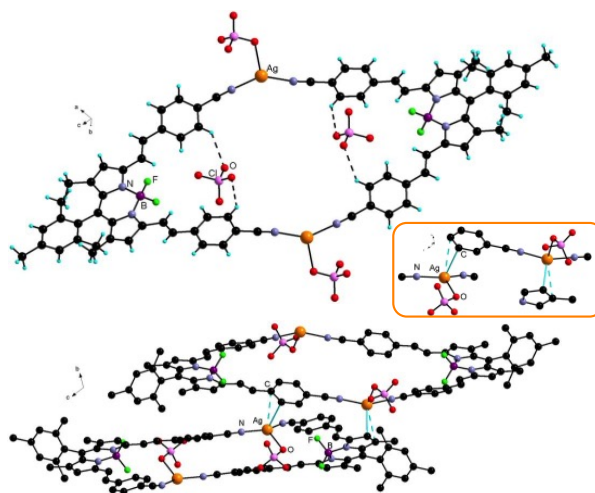


Figure 12: [2+2] (**10**)₂Ag₂(ClO₄)₂ macrocycle motif **16** in the crystal structure (top) and view along the *a* axis highlighting the Ag- π interactions shown in cyan (bottom). Hydrogen atoms and CHCl₃ molecules have been omitted for clarity; only one of the two positions of the disordered ClO₄[−] anion is presented. (bottom)

²² (a) E. A. Hall Griffith and E. L. Amma, *J. Am. Chem. Soc.*, **1974**, *96*, 743. (b) K. Shelly, D. C. Finster, Y. J. Lee, R. Scheidt and C. A. Reed, *J. Am. Chem. Soc.*, **1985**, *107*, 5955. (c) M. Munakata, L. P. Wu and G. L. Ning, *Coord. Chem. Rev.*, **2000**, *198*, 171. (d) S. V. Lindeman, R. Rathore and J. K. Kochi, *Inorg. Chem.*, **2000**, *39*, 5707. (e) A. N. Khlobystov, A. J. Blake, N. R. Champness, D. A. Lemenovskii, A. G. Majouga, N. V. Zyk and M. R. Schröder, *Coord. Chem. Rev.*, **2001**, *222*, 155. (f) T. C. W. Mak and L. Zhao, *Chem. Asian J.*, **2007**, *2*, 456. (g) J. Burgess and P. J. Steel, *Coord. Chem. Rev.*, **2011**, *255*, 2094.

²³ (a) H. Ruffin, S. A. Baudron, D. Salazar-Mendoza and M. W. Hosseini, *Chem. Eur. J.*, **2014**, *20*, 2449. (e) S. A. Baudron and M. W. Hosseini, *Chem. Commun.*, **2016**, *52*, 13000. (f) A. Mazel, S. A. Baudron and M. W. Hosseini, *CrystEngComm*, **2017**, *19*, 897. (g) J. Wojaczyński, J. Maciolek and P. J. Chmielewski, *Chem. Asian J.*, **2017**, *12*, 643.

²⁴ G. R. Desiraju, *Chem. Commun.*, **2005**, 2995.

When metallatecton **10** was assembled with AgBF_4 , instead of AgClO_4 under the same conditions (solvent and temperature), the formation of single crystals of **17** with the chemical formula $[\text{Ag}_2(\mathbf{10})_2(\text{CHCl}_3)_2](\text{BF}_4)_2$ was observed. The latter crystallizes in the monoclinic $P2_1/n$ space group. In this compound, again a [2+2] type metallamacrocycle is formed with the silver cations coordinated to the nitrile groups of two BODIPY metallatectons. In this case, the Ag(I) center is also interacting with CHCl_3 solvent molecules instead of the ClO_4^- as observed in **16**. Two observed Ag-Cl distances (2.850(3) Å / 3.193(3) Å) are indeed below the sum of the van der Waals radii. Considering these interactions between the Ag(I) cations and solvent molecules, the metallamacrocycles organize into one-dimensional chains with two CHCl_3 molecules as bridging units (Figure 13right). In addition, Ag- π interactions are observed with one pyrrolic ring of a neighboring dipyrin producing a three-dimensional network (Figure 13left). Similarly to the case of compound **16**, the Ag-CCH₃ distance here is also longer than the Ag-CH distance (Table 5). In the crystals, disordered tetrafluoroborate anions are occupying the center of the macrocycles. In particular, hydrogen bonding to the inner CH of the benzonitrile units can be observed ($d_{\text{C}\cdots\text{F}} = 2.981(5)$ Å - $3.289(5)$ Å, $\alpha_{\text{CH}\cdots\text{F}} = 128.64$ - 159.28° , shown in Figure 13left).

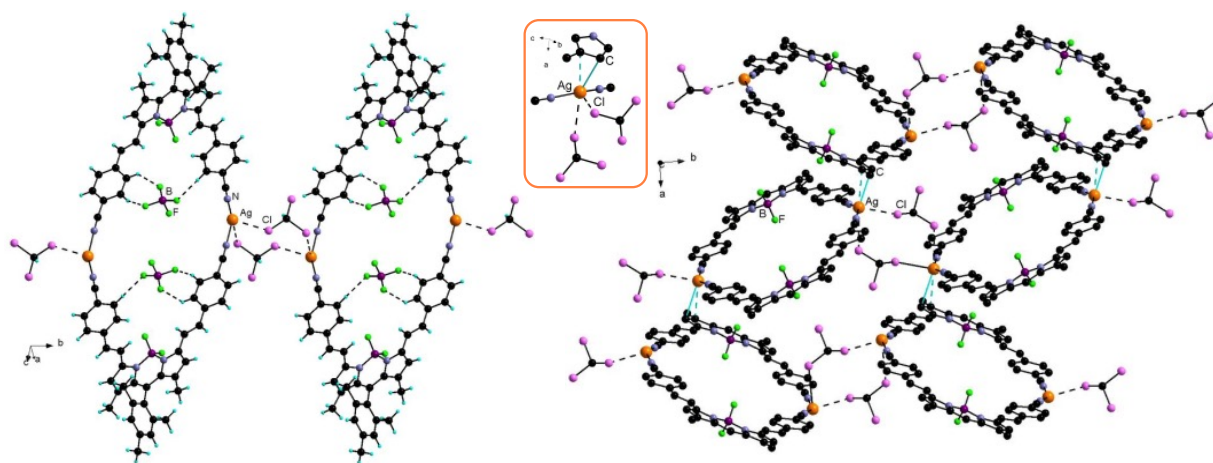
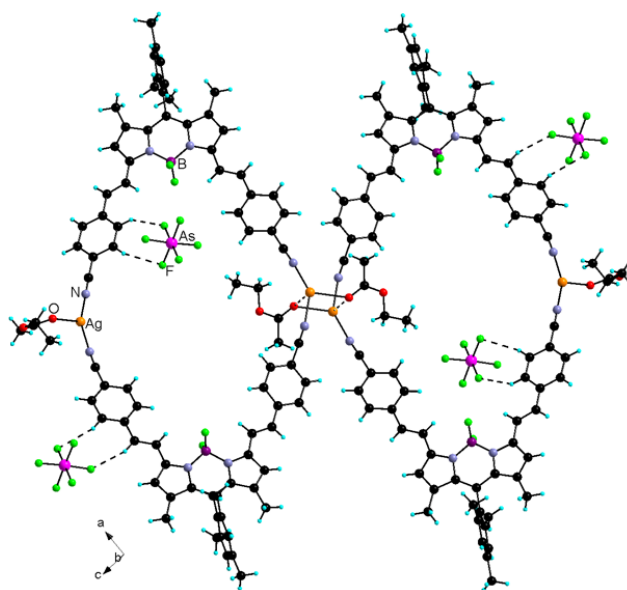


Figure 13: Portion of 1D chain of [2+2] $[(\mathbf{10})\text{Ag}(\text{CHCl}_3)]_2(\text{BF}_4)_2$ **17** (left) and the 3D network with Ag- π interactions shown in cyan (right). Hydrogen atoms, BF_4^- anions and mesityl units have been omitted for clarity.

In the $\text{CHCl}_3/\text{AcOEt}$ solvent system, combination of BODIPY **10** with AgAsF_6 produced crystalline compound **18** (Triclinic, $P-1$) that can be formulated as $[\text{Ag}_2(\mathbf{10})_2(\text{AcOEt})_2]_2(\text{AsF}_6)_4(\text{CHCl}_3)_2$ as determined by X-Ray diffraction. In this case, additional

solvent molecules present within the crystal could not be properly refined because of high disorder. Therefore, the SQUEEZE command was employed to account for the corresponding electron density.²⁵ In the structure, a discrete tetranuclear bis-metallamacrocycle combining two [2+2] [(**10**)₂Ag₂] type motives was formed by coordination interaction between the nitrile groups of **10** to Ag(I) cations and interaction between Ag(I) cations and solvent molecules (Figure 14). Regarding the two crystallographically independent metal centers, one is coordinated to only a single solvent molecule of ethyl acetate whereas the other is linked to the carbonyl oxygen atom of two AcOEt molecules acting as bridges with Ag-O distances differing in their length (Table 5) but in line with other reported AcOEt /Ag⁺ complexes.²⁶ Furthermore, a short inter-metallamacrocycle Ag-Ag distance of 3.521(3) Å and a slightly longer intra-macrocycle Ag-Ag distance of 14.012(17) Å were observed (Table 5). Unlike the other two previous compounds, no Ag- π interactions have been identified in the structure of **18**. Concerning the AsF₆⁻ anions, one is connected to the inner CH of the benzonitrile unit by hydrogen bond and, the other one is bound to one outer CH and to a vinylic C=CH. ($d_{C\cdots F}$ = 3.148(4) Å-3.437(4) Å, $\alpha_{CH\cdots F}$ = 140.78-160.41°; Figure 14 left).²⁷ Furthermore, a weak hydrogen bond was identified between the carbonyl oxygen atom bound to the outer Ag(I) cations of one bis-macrocycle and the metal cation of a neighboring tetranuclear motif leading to the construction of a one-dimensional polymer ($d_{C\cdots O}$ = 3.383(4) Å, $\alpha_{CH\cdots O}$ = 126.90°; Figure 14bottom).



²⁵ A. L. Spek, PLATON, The University of Utrecht, Utrecht, The Netherlands, 1999.

²⁶ K. Škoch, F. Uhlík, I. Cisařová and P. Štěpnička, *Dalton Trans.*, **2016**, 45, 10665.

²⁷ F. Grepioni, G. Cojazzi, S. M. Draper, N. Scully and D. Braga, *Organometallics*, **1998**, 17, 296.

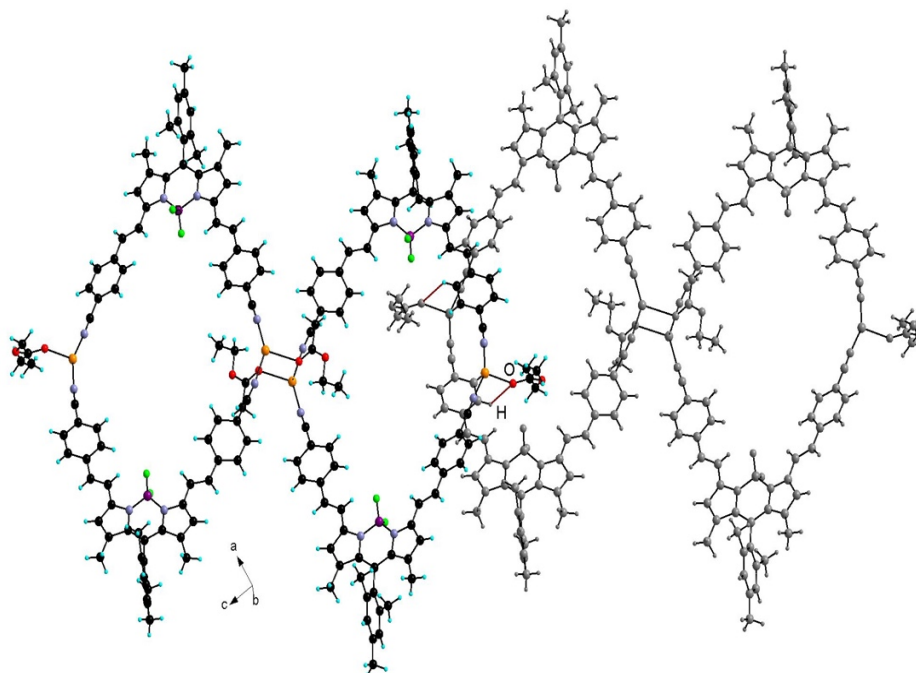


Figure 14: Structure of bis-macrocycle $[\text{Ag}_2(\mathbf{10})_2(\text{AcOEt})_2]_2(\text{AsF}_6)_4(\text{CHCl}_3)_2$ **18** (top) and a 1D network by H-bonding shown in red (bottom).

Upon vapour diffusion of Et_2O into a $\text{CHCl}_3/\text{MeOH}$ mixture of BODIPY **10** and AgAsF_6 , single crystals of **19** (Monoclinic, $P2_1$), $[\text{Ag}_2(\mathbf{10})_2(\text{MeOH})](\text{AsF}_6)_2(\text{Et}_2\text{O})$, were obtained. In the asymmetric unit, two BODIPY derivatives, two $\text{Ag}(\text{I})$ cations, two AsF_6^- anions, one MeOH molecule and one Et_2O solvent molecules are present. As for compounds **16-18**, the same $[2+2]$ metallamacrocyclic motif is formed with similar bond distances (Table 5). In this case, a one-dimensional chain is formed by interaction between a bridging methanol molecule and silver (I) cations of the $[2+2]$ motif (Figure 15 left) similarly to the one observed with AcOEt in **18** (Figure 14) and to other reported $\text{Ag}(\text{I})$ complexes.²⁸ Interestingly, an additional interaction between the metal centers and one of the fluorine atoms of **10** belonging to a neighboring chain ($d_{\text{F}\cdots\text{Ag}} = 2.697(4) \text{ \AA} - 2.723(4) \text{ \AA}$) is present (Figure 15 right). Whereas in the other crystalline compounds, the two B-F bond distances are similar, in agreement with the free tecton **10**, they differ in compound **19**. The distance between the boron center and the fluorine atom coordinated to the Ag cations ($1.412(6) \text{ \AA}$) is longer than with the other uncoordinated one ($1.383(6) \text{ \AA}$). In addition, the AsF_6^- anions located inside the cavity are bound to the inner CH of the benzonitrile

²⁸ (a) A. P. Côté, M. J. Ferguson, K. A. Khan, G. D. Enright, A. D. Kulynych, S. A. Dalrymple and G. K. H. Shimizu, *Inorg. Chem.*, **2002**, 41, 287. (b) Y.-M. Lin, Z.-J. Guan, K.-G. Liu, Z.-G. Jiang and Q.-M. Wang, *Dalton Trans.*, **2015**, 44, 2439.

units by hydrogen bonding. ($d_{C\cdots F} = 3.2371(5) \text{ \AA}$ - $3.408(5) \text{ \AA}$, $\alpha_{CH\cdots F} = 117.64^\circ$ - 158.38° ; Figure 15 left). Here, as for **18**, no Ag- π interactions were observed in the crystal of **19**.

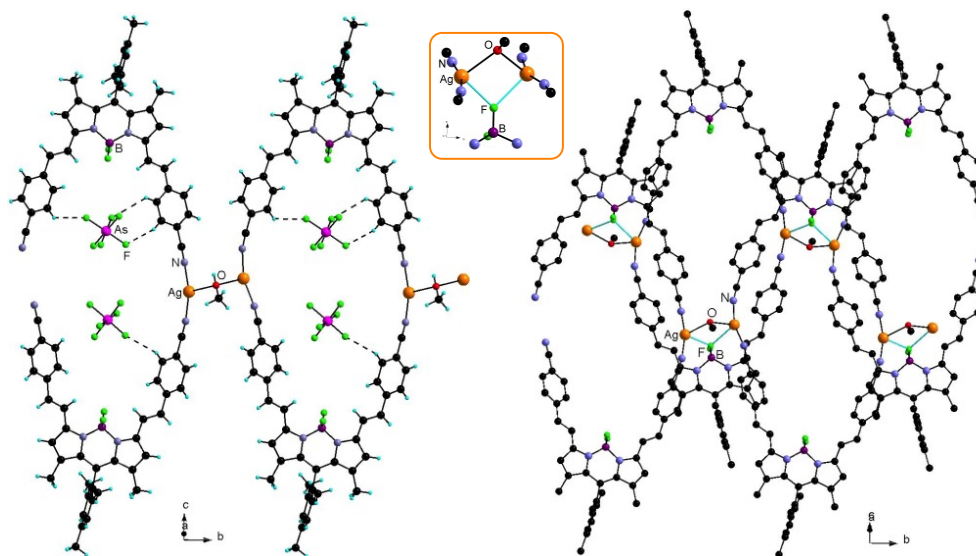
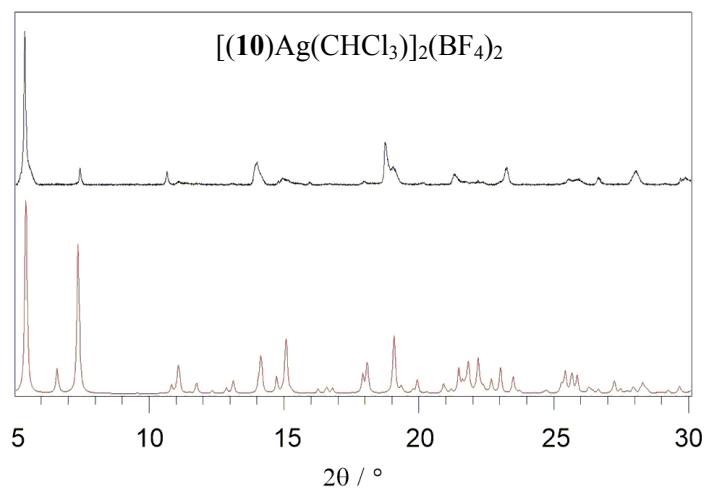


Figure 15: Portion of the 1D chain of metallamacrocycle in **19** (left). Organization of a double-chain owing to B-F \cdots Ag interactions in cyan. The Et₂O solvent molecules are not shown and the hydrogen atoms and the anions have been omitted for clarity. (right)

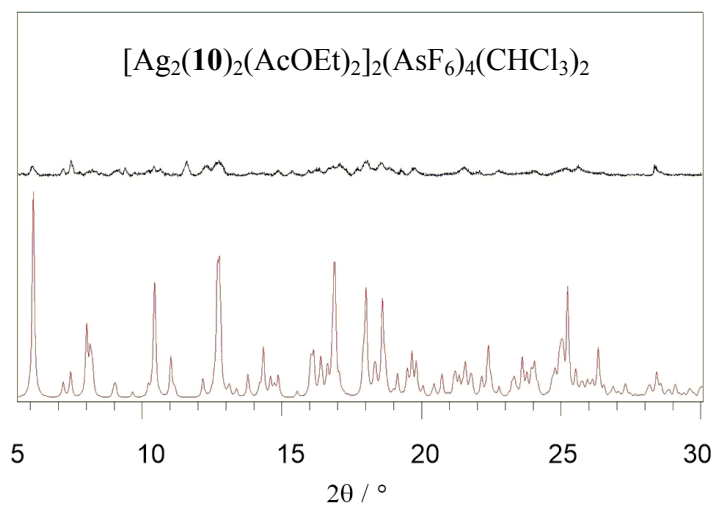
Table 5: Selected bond distances (Å) and angles (°) for the structures of **16-19**.

	Compound 16	Compound 17	Compound 18	Compound 19
Ag-N	2.138(4)	2.111(6)	2.100(6)	2.113(4)
	2.159(4)	2.130(7)	2.155(5)	2.114(4)
	2.179(4)		2.132(6)	2.119(4)
	2.180(4)		2.194(5)	2.148(5)
N-Ag-N	145.82(16)	151.0(3)	143.1(2)	164.6(2)
	136.29(16)		154.7(3)	159.4(2)
Ag-S_{solvent}	-	2.850(3)	2.320(7)	2.532(4)
		3.193(3)	2.444(5)	2.592(4)
			2.812(5)	
Ag-X	2.431(4)	-	-	-
	2.38(2)			
	2.48(2)			
Ag-C_{pyrrole}	2.605(4)	2.871(4)	-	-
	2.916(4)	2.983(4)		
Ag-C_{Ph}	2.837(5)	-	-	-
	3.050(5)			
Ag-Ag	13.426(15)	12.718(5)	14.012(17)	11.803(10)
	13.443(13)		3.521(3)	3.983(5)

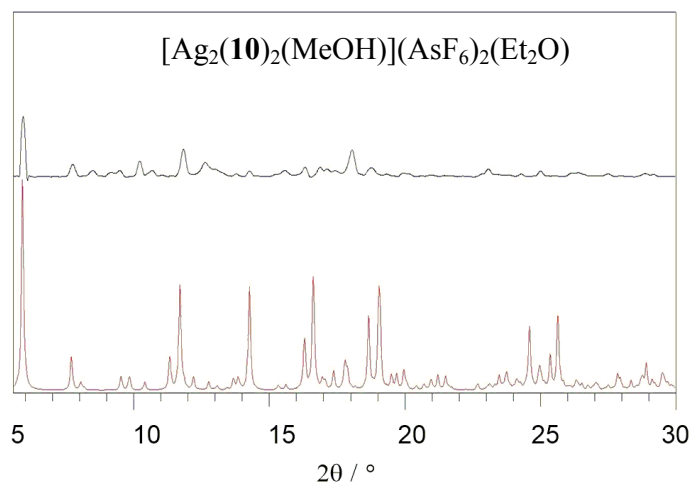
I.4.2 Characterization of crystalline compounds in the solid state



(a)



(b)



(c)

Figure 16: Simulated (red) and experimental (black) powder patterns for crystalline materials **17** (a), **18** (b) and **19** (c).

Compounds **16-19** have been characterized by X-ray powder diffraction to assess the homogeneity of the crystalline phase as well as its behavior out of the mother liquor. The experimental diffractograms (black lines) obtained for batches of compounds **17-19** and their comparison with the simulated powder pattern obtained from single-crystal data (red lines) are presented in (Figure 16). For **17**, a loss of crystallinity of a single phase can be observed owing to solvent loss upon exposure to air. For compounds **18** and **19**, a single phase is observed albeit with difference in intensities, resulting from preferential orientations. For compound **16**, as mentioned above, the powder pattern showed the presence of different crystalline phases that could not be identified because, at least, two different types of crystalline morphologies were obtained during the crystallization process.

The optical properties of compounds **17-19** have been investigated in the crystalline state. Three absorption bands were observed for these three species. The two low energy bands are centered around 602-604 nm and 661-663 nm, the high energy one is observed at 368 nm. All three metallamacrocyclic based architectures feature similar solid-state absorption spectra (Figure 17 left) in agreement with the UV-Visible spectrum in solution of BODIPY **10**. Upon excitation at 530 nm, two emission bands centered at 750 nm and 790 nm for all three materials are shown in Table 6. The bands observed (Figure 17 right) are shifted bathochromically compared with the free BODIPY **10** in solution. Such a red-shift can be explained by the coordination to silver(I) cation and/or packing effects in the solid state. The behavior observed is similar to the cases which have been described in the introduction part of this chapter and recently reported in the literature.^{4,5,29} It is worth noting that the slight difference in emission may also be due to solid state packing effect affecting the relative arrangement of the chromophore in the crystal. Quantum yield and lifetimes in these cases have not been determined due to the detection limit of the instrument available in our laboratory.

Table 6: Absorption and fluorescence data of **17-19** in the solid state at room temperature.

Compound	λ_{ab}/nm	λ_{em}/nm^a
17	368, 602, 662	790
18	368, 604, 661	750
19	368, 602, 663	750

(a) excited at 530 nm at room temperature

²⁹ L. Zhou, Y. S. Xue, J. Zhang and H. B. Du, *CrystEngComm.*, **2013**, *15*, 7315.

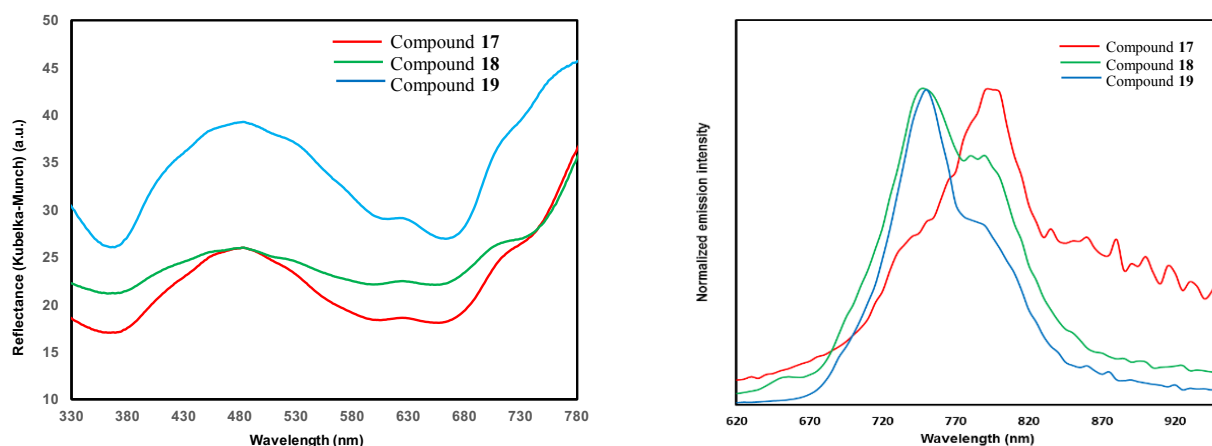


Figure 17: The UV-visible spectrum of compounds **17-19** in the solid-state (left). Kubelka-Munch Function $F(R) = (1-R)^2/2R$. Normalized solid state emission spectra for compounds **17-19** upon excitation at 530 nm (right).

1.4.3 Formation of coordination networks with tectons **11**, **14** and **15**

The investigation of the assembly of the four other synthesized BODIPYs **11**, **14**- and **15** bearing neutral peripheral binding units with a variety of metal centers such as Ag(I), Cd(II), Cu(II), Co(II) and Hg (II) has been also performed. It is worth noting that, owing to the poor solubility of these tectons, the choice of solvent for crystallization has been limited to DMF. In the DMF/MeOH solvent system, precipitation or some crystalline needle-shape species were observed for silver cation probably due to the speed of coordination between the pyridyl unit and metal center. However, some single crystals were obtained upon combination of compound **14** with one equivalent of AgOTf in the DMF/MeOH mixture. The crystals were of poor quality but a preliminary investigation by X-Ray diffraction afforded a first characterization of the mononuclear complex **20**, that can be formulated as $[(\mathbf{14})_2\text{Ag}(\text{TfO})](\text{DMF})_4$. The latter crystallizes in the triclinic *P*-1 space group with one independent Ag(TfO), one BODIPY and two DMF molecules. The metal cation, lying on an inversion center, is coordinated to two molecules of **14** through the pyridyl group ($d_{\text{Ag-N}} = 2.165(1) \text{ \AA}$) and two TfO⁻ anions with a 0.5 occupancy ($d_{\text{Ag-O}} = 2.603(2) \text{ \AA}$). It is interesting to note that, for this compound, the benzonitrile groups are not involved in the coordination and no polymer is obtained. Attempts at using an excess of silver salts in the crystallization led only to the formation of **20**. The use of Ag(ClO₄)

as an alternative source of Ag(I) also affords crystalline material. Optimization of the crystallization conditions and subsequent X-Ray analysis are currently under way.

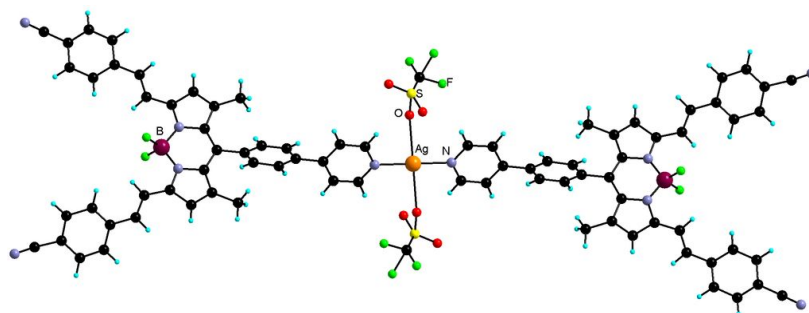


Figure 18: Preliminary structure of the mononuclear complex **20**.

In order to reduce the speed of crystal formation, counter ligands such as pyridine have been used to slow down the complexation process between the tectons and metal cation during the liquid-liquid diffusion. Following this method, some crystals were formed in the case of CdCl₂ and HgCl₂. Unfortunately, once again, they could not be successfully characterized by X-ray diffraction.

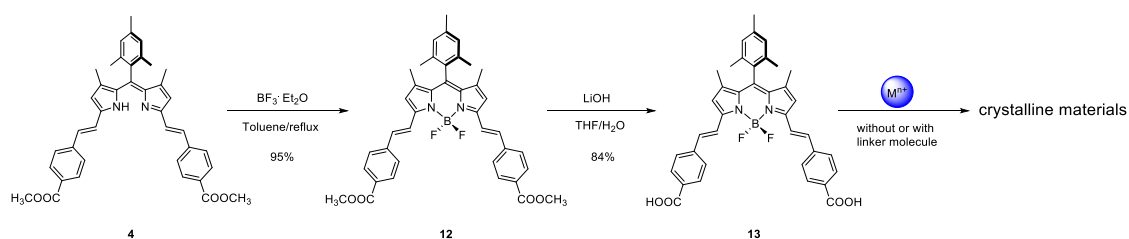
I.4.4 Formation of coordination networks with tecton **13**

Over the last two decades, a significant number of coordination polymers have been reported in the literature. These materials have been widely investigated because of their stability and interesting properties such as porosity.³⁰ In particular, the carboxylic acid group has been exploited as a coordinating unit, since it can react with various metal centers and forming rather stable bonds. It was thus believed that the introduction of the carboxylic acid function at the peripheral 1 and 9 positions of 1,9-divinyldipyrrin would be interesting and their complexes could be used as tectons for the synthesis of infinite coordination networks with different topology and geometry. In this context, BODIPY **13** with two additional carboxylic acid unit was regarded as a potential tecton capable of assembling with a series of transition metal cations for the construction of coordination polymers. Besides, the preparation of porous 3D networks can also be envisioned by the addition of a third component such as a tecton bearing neutral

³⁰ (a) D. Zhao, D. J. Timmons, D. Yuan, H.-C. Zhou, *Acc. Chem. Res.*, **2011**, *44*, 123. (b) W. Lu, Z. Wei, Z.-Y. Gu, T.-F. Liu, J. Park, J. Tian, M. Zhang, Q. Zhang, T. Gentle III, M. Bosch, H.-C. Zhou, *Chem. Soc. Rev.*, **2014**, *43*, 5561. (c) Y.-B. He, B. Li, M. O’Keeffe and B.-L. Chen, *Chem. Soc. Rev.*, **2014**, *43*, 5618.

coordinating sites such as DABCO or 4,4'-bipyridine for example.³¹ These materials are commonly called pillared-layer MOFs.

As already mentioned above, a synthetic strategy for preparing the target carboxylic acid appended BODIPY **13** has been developed (Scheme 3). The ester-1,9-divinyldipyrin **4** was produced by the Knoevenagel reaction. In the presence of triethylamine, the reaction between ligand **4** and boron trifluoride was performed in toluene affording the corresponding BODIPY complex in 95% yield. Subsequently, the ester BODIPY **12** was treated with lithium hydroxide in a THF/H₂O mixture affording the desired compound **13** with satisfactory yield (84%).



Scheme 3: Synthetic route for the preparation of carboxylic acid-BODIPY **13** and corresponding CPs.

The first attempts at obtaining coordination networks were centered on the assembly of tecton **13** with Cu(II), Zn(II) or Ni(II) nitrate salts with or without the additional 4,4'-bipyridine linker molecule in the DMF/methanol solvent system by using either the solvothermal method or liquid-liquid diffusion. However, only under the latter condition, the combination of BODIPY **13** and $\text{Cu}(\text{NO}_3)_2$ with/without 4,4'-bipyridine has afforded crystalline materials. Unfortunately, the crystals obtained were of small size and too difficult to manipulate for analysis by X-ray diffraction. An alternative synthesis based on acetate salts has been investigated. In the DMF/MeOH solvent system, combination of BODIPY **13** and $\text{Cu}(\text{OAc})_2$ with or without 4,4'-bipyridine indeed produced crystals of suitable size for diffraction analysis. However, the diffracting power of these crystals appeared too low for a complete structure determination, even under long exposure time. Consequently, the synthetic approach has been reconsidered. Modifying the solvent system to increase the crystal size was attempted. Substituting EtOH or *i*-PrOH for MeOH in the solvent system yielding larger crystals, albeit still with poor diffracting

³¹ (a) D. N. Dybtsev, H. Chun, K. Kim, *Angew. Chem. Int. Ed.*, **2004**, 43, 5033. (b) D. H. Hong, M. P. Suh, *Chem. Commun.*, **2012**, 48, 9168.

power. In order to obtain the structure of this material, analysis at the synchrotron will be done. A shift has been obtained at the SOLEIL facility under the common BAG program and data should be collected next Fall.

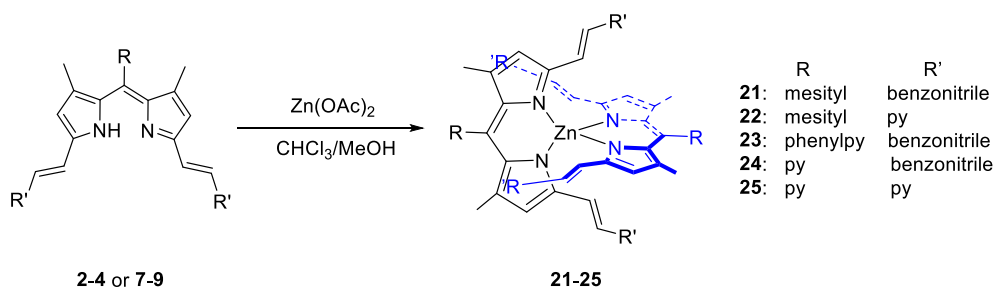
I.5 Preparation of Zn(dipyrrinato)₂ complexes

Following the investigation of BODIPYs as tectons for the formation of coordination polymers, homoleptic Zn(II) dipyrrinato complexes were considered as metallatectons. Indeed, these species feature more peripheral coordinating units, yet maintaining luminescent properties, although the emission quantum yields of such compounds is notably lower than the boron based ones. Their synthesis shown in Scheme 4 has been achieved following the synthetic method developed in the literature for other dipyrrin ligands.³² The free 1,9-divinyldipyrrins derivatives **2-4** or **7-9** dissolved in CHCl₃ were reacted with a MeOH solution of zinc acetate affording the corresponding complexes **21-25** in of 79-90% yield. These complexes were characterized in solution by ¹H-NMR, ¹³C-NMR and UV-visible spectroscopy and by HRMS (ESI).

Furthermore, complexes **21** and **23** were also characterized by X-Ray diffraction. Deep blue single crystals of complex **21** were obtained by vapor diffusion of diethyl ether into a THF solution of the compound, while deep blue crystals of **23** were obtained in the CHCl₃/MeOH solvent system by liquid-liquid diffusion. These two species crystallize in the triclinic *P*-1 space group. For both compounds, the central zinc cation is in a distorted tetrahedral coordination environment with four nitrogen atoms belonging to two dipyrrinato ligands. (*d*_{Zn-N} = 1.9645(18) Å-1.9785(18) Å; $\alpha_{N\cdots Zn\cdots N}$ = 93.16(7)°-115.97(8)° for **21**, 1.967(3) Å-1.976(3) Å; $\alpha_{N\cdots Zn\cdots N}$ = 93.38(11)°-110.73(12)° for **23** (Table 7). Moreover, the two dipyrrin ligands are almost perpendicular (89.31°) in the case of complex **21**, but they are in a more distorted arrangement in complex **23** with an angle of 72.56°. This may result from packing effects since no specific interaction is observed that could explain this organization in a straightforward manner. Deep blue crystals of complex **24** were also obtained in the CHCl₃/MeOH solvent system by liquid-liquid diffusion, but were found to be too fragile to be manipulated for analysis by X-ray

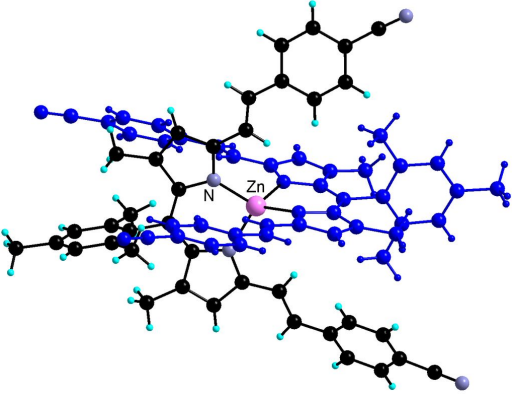
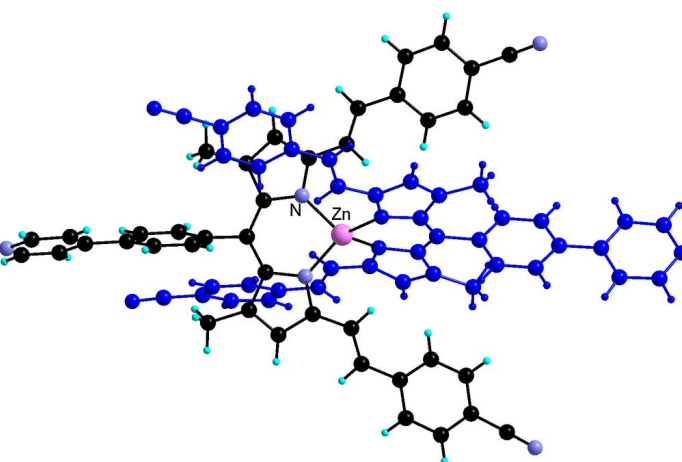
³² (a) Y. Li and D. Dolphin, *Can. J. Chem.*, **2011**, *89*, 481. (b) R. Toyoda, M. Tsuchiya, R. Sakamoto, R. Matsuoka, K. -H. Wu, Y. Hattori and H. Nishihara, *Dalton Trans.*, **2015**, *44*, 15103.

diffraction. Unfortunately, no crystals of complexes **22** and **25** could be obtained under the same conditions.



Scheme 4: Synthesis of compounds **21-25**.

Table 7: Structures and selected bond lengths (Å) and angle (°) for Zn type complexes **21** and **23**.

Complex 21		Complex 23	
			
dZn-N	1.9645(18) 1.9684(18) 1.9775(18) 1.9785(18)		1.967(3) 1.969(3) 1.974(3) 1.976(3)
αN-Zn-N	93.16(7) 93.86(7) 114.99(7) 115.97(7)		94.19(11) 93.38(11) 109.76(11) 110.73(11)

The photophysical properties of the zinc type complexes **21-25** in DMF solution (10^{-6} mol/L) were studied and are shown in Table 8. For these compounds, DMF was chosen as the solvent because of their otherwise poor solubility. As for the absorption spectra of compound **21-25**, all of these complexes exhibit three intense absorption bands between 329 nm and 626 nm. Two low energy bands centered at 557 - 626 nm are consistent with π - π^* transition of the dipyrinato

ligands and the high energy one at 329 - 358 nm corresponds to the absorption of the vinyl moieties.

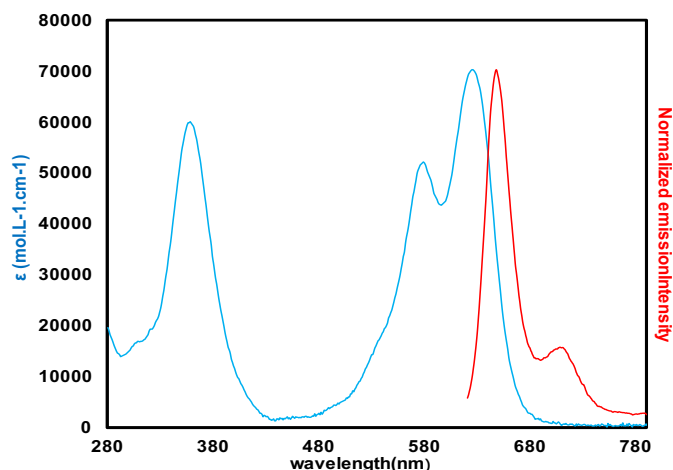


Figure 19: Absorption and emission spectra of complex **23** in DMF as a representative example.

Table 8: Absorption and fluorescence in DMF solution of compounds **21-25** at room temperature

Sample	λ_{ab}/nm ($\epsilon \cdot 10^3 M^{-1}cm^{-1}$)	λ_{em}/nm ^a	Φ_f ^b
21	355 (68.6)	648	0.03
	580 (74.1)	701	
	623 (109.6)		
22	339 (32.6)	620	0.14
	560 (40.6)	674	
	606 (58.1)		
23	358 (81.3)	647	<i>n.d.</i>
	579 (68.9)	710	
	626 (92.3)		
24	353 (47.1)	649	<i>n.d.</i>
	581 (37.7)	705	
	622 (47.1)		
25	329 (33.5)	626	0.003
	557(26.1)	677	
	607(35.5)		

(a) excited at 580 nm. (b) using Cresyl Violet as reference ($\Phi_f = 0.54$ in MeOH, aerated solution)¹⁸; *n.d.* = not determined; $\Phi_f = \Phi_s \cdot (A_s/A_f) \cdot (E_f/E_s) \cdot (n_f^2/n_s^2)$, Φ_s is the quantum yield of the standard, A is the absorbance of the solution, E is the corrected emission intensity, and n is the average refractive index of the solution.

Two emission bands stemming from π - π^* transition of the dipyrinato ligands are observed at 620 - 649 nm and 674 - 710 nm, upon excitation at 580 nm. Similar to the case of the BODIPYs, the

absorption bands of Zn complexes **22** and **25** are blue-shifted due to the presence of 1,9-divinylpyridyl groups. The quantum yields of the Zn dipyrinato complexes in DMF solution were also determined at room temperature. The low quantum yields of these Zn complexes can be explained by the deexcitation phenomenon in polar solution known for such type of homoleptic species.^{8d,33} Similarly to the cases of Bodipys, the relatively higher quantum yield of complex **22** ($\Phi_f = 0.14$) can be explained by both the presence of the mesityl group at the *meso* position with a hindered rotation and the presence of pyridine group as electron-withdrawing unit.

1.6 Formation of heterometallic coordination polymers with Zn(II) complexes

Compared with the V-shape BODIPY tecton **10** or the triangle-shape tecton **14**, complexes **21-25** bearing at least four divergently oriented interaction sites are potentially able to construct heterometallic coordination networks with different dimensionality and geometry by coordination of a second metal center. The strategy for the synthesis of crystalline materials with the novel zinc complexes **21-25** is similar to the one developed previously with the BODIPYs.

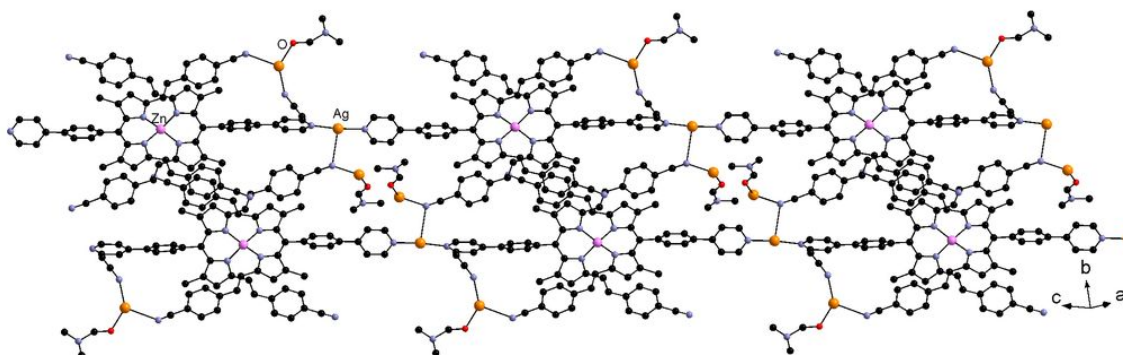


Figure 20: Double chains in the structure of **26**. Hydrogen atoms and hexafluoroarsenate have been omitted for clarity.

Many attempts at preparing heterometallic architectures have been done using a variety of metal cations. However, owing to the limited solubility of the metallatectons, obtaining

³³ M. Asaoka, Y. Kitagawa, R. Teramoto, K. Miyagi, Y. Natori, R. Sakamoto, H. Nishihara, M. Nakano, *Polyhedron*, **2017**, doi: 10.1016/j.poly.2017.01.058.

crystalline material proved to be difficult. The new heterometallic network **26** has nonetheless been constructed by assembling the zinc complex **23** with AgAsF₆ in a DMF / CH₃CN (1/1) mixture and by subsequent diffusion of Et₂O vapor. It crystallizes in the triclinic space group *P*-1 with one complex, three Ag(I) cations (two having a 0.5 occupancy), two AsF₆[−] anions and two DMF molecules. In this case, the peripheral pyridine groups of the zinc complex coordinate the Ag(I) cation to form monodimensional chains ($d_{\text{Ag-N}} = 2.116(2) - 2.127(2) \text{ \AA}$). The latter can be regarded as the symmetrization of what is observed with the BODIPY analogue **14** in complex **20**, as a result of the homoleptic nature of the Zn(II) metallatecton. These chains are linked by weak interactions between the Ag(I) cation and the benzonitrile group of a neighboring zinc complex ($d_{\text{Ag-N}} = 3.017(3) \text{ \AA}$) leading to a double chain. Moreover, two additional silver cations having a 0.5 occupancy are coordinated to the nitrile units, either occupying the cavities of the network or its periphery. Their coordination sphere is completed by acetonitrile or DMF molecules. Within the crystal, these double-chains are separated by solvent molecules and the AsF₆[−] anions. It should be noted that, as observed for the free complex **23**, a deviation from tetrahedral environment is observed since the angle between the two dipyrinato chelates is 61.73°.

Crystals have been obtained with this metallatecton and other AgX salts and are currently under investigation.

I.7 Conclusion and perspectives

Taking advantage of the reactivity towards aldehydes, *via* a Knoevenagel type synthesis, of methyl groups at positions 1 and 9 of the bispyrrolic backbone, a new series of dipyrin ligands has been developed and characterized. At these positions, coordinating units such as benzonitrile or pyridyl groups have been introduced. Furthermore, the position 5, so called *meso*, has also been employed for further functionalization either using a solubilizing group such as mesityl or an additional binding unit like a pyridyl or phenyl-pyridyl moiety. These derivatives have been characterized in solution by standard analytical methods and, for some of them, in the crystalline state by X-Ray diffraction. Using these ligands, BODIPYs, homoleptic Zn(II) complexes have been prepared and studied in solution and in the crystalline state and subsequently employed as

metallatectons for the construction of coordination networks. In particular, the photophysical properties of the BODIPY derivatives have been investigated and emission with moderate to high quantum yields ($\phi = 0.43-0.87$) was measured in DMF solution, upon excitation at 570 nm. Assembly of these compounds with a variety of metal salts has been attempted and crystals that could successfully be analyzed by diffraction were obtained with Ag(I) salts. In particular, BODIPY **10** bearing peripheral benzonitrile groups at positions 1 and 9 was found to form, in a recurrent fashion, a [2+2] metallamacrocyclic motif showing an anion and solvent dependent organization in the crystalline state. In the solid state, these assemblies showed weak emission. Other BODIPYs seem prone to form coordination networks; unfortunately, the crystal quality has so far not been sufficient for a complete structure determination, in particular with the carboxylic acid appended derivative **13**.

Regarding the Zn(II) complexes, they also show emission in DMF solution, although the determined quantum yields are much lower than for the BODIPY analogues. An heterometallic network has been obtained and characterized by X-Ray diffraction upon combination of metallatecton **22**, bearing two pyridyl groups and four benzonitrile moieties, with AgAsF₆. In this architecture, coordination of the pyridine units seems to be the strongest interaction as observed with the BODIPY analogue **14** that yielded a mononuclear complex. This leads to one-dimensional chains that are connected *via* interaction with the nitrile groups.

This series of ligands and the aforementioned results show promises for the development of emissive heterometallic coordination polymers. In order to ease the preparation of such architectures, introduction of more solubilizing groups could be considered, since the poor solubility of the tectons has been a limiting issue in this study.

- ¹ (a) S. R. Batten, R. Robson, *Angew. Chem., Int. Ed.*, **1998**, *37*, 1460. (b) M. Eddaoudi, D. B. Moler, H. Li, B. Chen, T. M. Reineke, M. O’Keeffe, O. M. Yaghi, *Acc. Chem. Res.*, **2001**, *34*, 319. (c) S. Kitagawa, R. Kitaura, S. I. Noro, *Angew. Chem. Int. Ed.*, **2004**, *43*, 2334. (d) J. R. Long, O. M. Yaghi, *Chem. Soc. Rev.*, **2009**, *38*, 1213. (e) *Chem. Soc. Rev.*, **2009**, *38* (5), themed issue on metalorganic frameworks. (f) C. Janiak, J. K. Vieth, *New J. Chem.*, **2010**, *34*, 2366. (g) *Chem. Rev.*, **2012**, *112* (2), 2012 Metal–Organic Frameworks special issue. (h) C. Wang, W. Lin, *J. Am. Chem. Soc.*, **2013**, *135*, 13222.
- ² (a) M. D. Allendorf, C. A. Bauer, R. K. Bhakta and R. J. T. Houk, *Chem Soc Rev.*, **2009**, *38*, 1330. (b) J. Rocha, L. D. Carlos, F. A. Almeida Paz and D. Ananias, *Chem. Soc. Rev.*, **2011**, *40*, 926. (c) Y. Cui, Y. Yue, G. Qiang and B. Chen, *Chem. Rev.*, **2012**, *112*, 1126. (d) J. Heine and K. Müller-Buschbaum, *Chem. Soc. Rev.*, **2013**, *42*, 9232. (e) Z. Hu, B. J. Deibert and J. Li, *Chem Soc Rev.*, **2014**, *43*, 5815. (f) M. C. So, G. P. Wiederrecht, J. E. Mondloch, J. T. Hupp and O. K. Farha, *Chem. Commun.*, **2015**, *51*, 3501. (g) D. E. Williams and N. B. Shustova, *Chem. Eur. J.*, **2015**, *21*, 15474. (h) L. Zhang, Z. Kang, X. Xin and D. Sun, *CrystEngComm.*, **2016**, *18*, 193.
- ³ S. A. Baudron, *CrystEngComm.*, **2016**, *18*, 4671.
- ⁴ C. Y. Lee, O. K. Farha, B. J. Hong, A. A. Sarjeant, S. T. Nguyen and J. T. Hupp, *J. Am. Chem. Soc.*, **2011**, *133*, 15858.
- ⁵ M. Li, Y. Yao, J. Ding, L. Liu, J. Qin, Y. Zhao, H. Hou and Y. Fan, *Inorg. Chem.*, **2015**, *54*, 1346.
- ⁶ (a) A. Béziau, S. A. Baudron, A. Guenet and M. W. Hosseini, *Chem. Eur. J.*, **2013**, *19*, 3215. (b) A. Béziau, S. A. Baudron, A. Fluck and M. W. Hosseini, *Inorg. Chem.*, **2013**, *52*, 14439.
- ⁷ A. Béziau, S. A. Baudron, G. Rogez and M. W. Hosseini, *CrystEngComm.*, **2013**, *15*, 5980.
- ⁸ (a) K. Rurack, M. Kollmannsberger and J. Daub., *New J. Chem.*, **2001**, *25*, 289. (b) R. Ziessel, G. Ulrich, A. Harriman, M. A. H. Alamiry, B. Stewart and P. Retailleau, *Chem. Eur. J.*, **2009**, *15*, 1359 – 1369. (c) J. Bartelmess and W. W. Weare, *Dyes and Pigments.*, **2013**, *97*, 1. (d) R. Sakamoto, T. Iwashima, J. F. Kögel, S. Kusaka, M. Tsuchiya, Y. Kitagawa and H. Nishihara, *J. Am. Chem. Soc.*, **2016**, *138*, 5666.
- ⁹ T. Bura, P. Retailleau, G. Ulrich and R. Ziessel, *J. Org. Chem.*, **2011**, *76*, 1109.
- ¹⁰ M. W. Hosseini, *CrystEngComm.*, **2004**, *6*, 318.
- ¹¹ (a) E. Knoevenagel, *Ber. Dtsch. Chem. Ges.*, **1898**, *31*, 2596. (b) R. Ziessel, T. Bura, J. H. Olivier, *Synlett.*, **2010**, *15*, 2304.
- ¹² (a) H. L. Kee, C. Kirmaier, L. Yu, P. Thamyonkit, W. J. Youngblood, M. E. Calder, L. Ramos, B. C. Noll, D. F. Bocian, W. R. Scheidt, R. R. Birge, J. S. Lindsey, D. Holten, *J. Phys. Chem. B.*, **2005**, *109*, 20433. (b) V. S. Thoi, J. R. Stork, D. Magde, S. M. Cohen, *Inorg. Chem.*, **2006**, *45*, 10688. (c) J. Kobayashi, T. Kushida, T. Kawashima, *J. Am. Chem. Soc.*, **2009**, *131*, 10836. (d) C. Bronner, S. A. Baudron, M. W. Hosseini, C. A. Strassert, A. Guenet, L. De Cola, *Dalton Trans.*, **2010**, *39*, 180. (e) K. Hanson, A. Tamayo, V. V. Diev, M. T. Whited, P. I. Djurovich, M. E. Thompson, *Inorg. Chem.*, **2010**, *49*, 6077. (f) T. M. McLean, J. L. Moody, M. R. Waterland, S. G. Telfer, *Inorg. Chem.*, **2012**, *51*, 446. (g) C. Bronner, M. Veiga, A. Guenet, L. De Cola, M. W. Hosseini, C. A. Strassert, S. A. Baudron, *Chem. Eur. J.*, **2012**, *18*, 4041.
- ¹³ L. Fu, F.-L. Jiang, D. Fortin, P. D. Harvey and Y. Liu, *Chem. Commun.*, **2011**, *47*, 5503.

- ¹⁴ (a) C. Bruckner, V. Karunaratne, S. J. Rettig and D. Dolphin, *Can. J. Chem.*, **1996**, *74*, 2182.
(b) C. Bruckner, Y. J. Zhang, S. J. Rettig and D. Dolphin, *Inorg. Chim. Acta.*, **1997**, *263*, 279.
- ¹⁵ G. Ulrich, R. Ziessel and A. Harriman, *Angew. Chem. Int. Ed.*, **2008**, *47*, 1184.
- ¹⁶ C. O. Obondi, G. N. Lim, P. A. Karr, V. Nesterov and F. D'Souza, *Phys. Chem. Chem. Phys.*, **2016**, *18*, 18187.
- ¹⁷ (a) A. T. Rhys Williams and S. A. Winfield, *Analyst.*, **1983**, *108*, 1067.
- ¹⁸ D. Magde, J. H. Brannon, T. L. Cremers and J. Olmsted, *J. Phys. Chem.*, **1976**, *83*, 696.
- ¹⁹ (a) G. J. Hedley, A. Ruseckas, A. Harriman, I. D. W. Samuel, *Angew. Chem., Int. Ed.*, **2011**, *50*, 6634. (b) M. Buyuktemiz, S. Duman and Y. Dede, *J. Phys. Chem. A.*, **2013**, *117*, 1665.
- ²⁰ (a) D. Salazar-Mendoza, S. A. Baudron and M. W. Hosseini, *Chem. Commun.*, **2007**, 2252. (b) D. Salazar-Mendoza, S. A. Baudron and M.W. Hosseini, *Inorg. Chem.*, **2008**, *47*, 766. (c) D. Pogozhev, S. A. Baudron and M. W. Hosseini, *Inorg. Chem.*, **2010**, *49*, 331. (d) B. Kilduff, D. Pogozhev, S. A. Baudron and M. W. Hosseini, *Inorg. Chem.*, **2010**, *49*, 11231. (e) A. Béziau, S. A. Baudron and M. W. Hosseini, *Dalton Trans.*, **2012**, *41*, 7227.
- ²¹ F. Zhang, S. A. Baudron and M. W. Hosseini, *CrystEngComm.*, **2017**, *19*, 4393.
- ²² (a) E. A. Hall Griffith and E. L. Amma, *J. Am. Chem. Soc.*, **1974**, *96*, 743. (b) K. Shelly, D. C. Finster, Y. J. Lee, R. Scheidt and C. A. Reed, *J. Am. Chem. Soc.*, **1985**, *107*, 5955. (c) M. Munakata, L. P. Wu and G. L. Ning, *Coord. Chem. Rev.*, **2000**, *198*, 171. (d) S. V. Lindeman, R. Rathore and J. K. Kochi, *Inorg. Chem.*, **2000**, *39*, 5707. (e) A. N. Khlobystov, A. J. Blake, N. R. Champness, D. A. Lemenovskii, A. G. Majouga, N. V. Zyk and M. R. Schröder, *Coord. Chem. Rev.*, **2001**, *222*, 155. (f) T. C. W. Mak and L. Zhao, *Chem. Asian. J.*, **2007**, *2*, 456. (g) J. Burgess and P. J. Steel, *Coord. Chem. Rev.*, **2011**, *255*, 2094.
- ²³ (a) H. Ruffin, S. A. Baudron, D. Salazar-Mendoza and M. W. Hosseini, *Chem. Eur. J.*, **2014**, *20*, 2449. (e) S. A. Baudron and M. W. Hosseini, *Chem. Commun.*, **2016**, *52*, 13000. (f) A. Mazel, S. A. Baudron and M. W. Hosseini, *CrystEngComm*, **2017**, *19*, 897. (g) J. Wojaczyński, J. Maciolek and P. J. Chmielewski, *Chem. Asian J.*, **2017**, *12*, 643.
- ²⁴ G. R. Desiraju, *Chem. Commun.*, **2005**, 2995.
- ²⁵ A. L. Spek, PLATON, The University of Utrecht, Utrecht, The Netherlands, 1999.
- ²⁶ K. Škoch, F. Uhlik, I. Cisařova and P. Štěpnička, *Dalton Trans.*, **2016**, *45*, 10665.
- ²⁷ F. Grepioni, G. Cojazzi, S. M. Draper, N. Scully and D. Braga, *Organometallics*, **1998**, *17*, 296.
- ²⁸ (a) A. P. Côté, M. J. Ferguson, K. A. Khan, G. D. Enright, A. D. Kulynych, S. A. Dalrymple and G. K. H. Shimizu, *Inorg. Chem.*, **2002**, *41*, 287. (b) Y.-M. Lin, Z.-J. Guan, K.-G. Liu, Z.-G. Jiang and Q.-M. Wang, *Dalton Trans.*, **2015**, *44*, 2439.
- ²⁹ L. Zhou, Y. S. Xue, J. Zhang and H. B. Du, *CrystEngComm.*, **2013**, *15*, 7315.
- ³⁰ (a) D. Zhao, D. J. Timmons, D. Yuan, H.-C. Zhou, *Acc. Chem. Res.*, **2011**, *44*, 123. (b) W. Lu, Z. Wei, Z.-Y. Gu, T.-F. Liu, J. Park, J. Tian, M. Zhang, Q. Zhang, T. Gentle III, M. Bosch, H.-C. Zhou, *Chem. Soc. Rev.*, **2014**, *43*, 5561. (c) Y.-B. He, B. Li, M. O'Keefe and B.-L. Chen, *Chem. Soc. Rev.*, **2014**, *43*, 5618.
- ³¹ (a) D. N. Dybtsev, H. Chun, K. Kim, *Angew. Chem. Int. Ed.*, **2004**, *43*, 5033. (b) D. H. Hong, M. P. Suh, *Chem. Commun.*, **2012**, *48*, 9168.
- ³² (a) Y. Li and D. Dolphin, *Can. J. Chem.*, **2011**, *89*, 481. (b) R. Toyoda, M. Tsuchiya, R. Sakamoto, R. Matsuoka, K. -H. Wu, Y. Hattori and H. Nishihara, *Dalton Trans.*, **2015**, *44*, 15103.

³³ M. Asaoka, Y. Kitagawa, R. Teramoto, K. Miyagi, Y. Natori, R. Sakamoto, H. Nishihara, M. Nakano, *Polyhedron.*, **2017**, doi: 10.1016/j.poly.2017.01.058.

Chapter II

Chapter II: Functionalized 2,2'-bisdipyrin derivatives for the formation of complex architectures

The second part of this thesis concerns the functionalization of dipyrin ligands bearing a reactive group at their periphery for the development of a novel class of coordinating derivatives that will then be used for the preparation of discrete or infinite architectures. In this chapter, mono- or bis-dipyrins bearing an additional aldehyde, amine or carboxylic acid unit have been designed, prepared and employed for the reaction with a complementary reactive moiety providing novel functionalized ligands. Subsequently, the latter assemble with metal centers to afford either discrete macrocyclic species or complexes that can be regarded as metallatectons for the construction of heterometallic molecular networks.

II.1 Introduction

Over the past few years, helicates have been the subject of intense interest owing to their beauty and their potential properties in optics for example.¹ The term helicate has been introduced by J.-M. Lehn in 1987 to describe a metal complex in which the ligand strands wrap around metal centers in analogy with natural helices observed in the organization of polynucleic acids and DNA.^{1a} An example of such species is presented in Figure 1 showing the assembly of a tris-(2,2'-bispyridine) ligand with Ag(I) cations leading to a double stranded helicate.

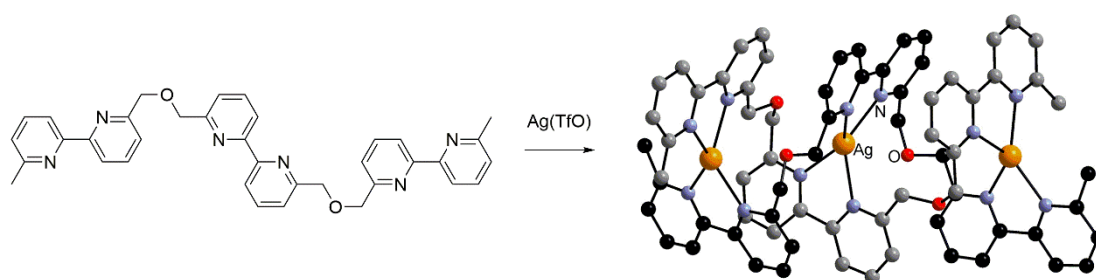


Figure 1: Example of the assembly of tris-bipyridine ligand with Ag(I) cations yielding a double-stranded helicate. Hydrogen atoms have been omitted for clarity.

¹ (a) J.-M. Lehn, A. Rigault, J. Siegel, J. Harrowfield, B. Chevrier and D. Moras, *Proc. Natl. Acad. Sci. USA.*, **1987**, *84*, 2565. (b) C. Piguet, G. Bernardinelli and G. Hopfgartner, *Chem Rev.*, **1997**, *97*, 2005. (c) A. Williams, *Chem. Eur. J.*, **1997**, *3*, 15. (d) J.-M. Lehn, *Chem. Eur. J.*, **2000**, *6*, 2097. (e) M. Albrecht, *Chem. Rev.*, **2001**, *101*, 3457. (f) H. Miyake and H. Tsukube, *Chem. Soc. Rev.*, **2012**, *41*, 6977.

Interestingly, circular analogues have also been described.² The tris-(2,2'-bipyridine) derivative presented in Figure 2 forms a pentanuclear cyclic species upon association with FeCl₂. In this reaction, the anion of the iron salt has been shown to play a key templating role, since it is tightly bound to the center of the complex by hydrogen bonding. Indeed, it has been demonstrated that with octahedral anions, a hexanuclear species was obtained instead.³

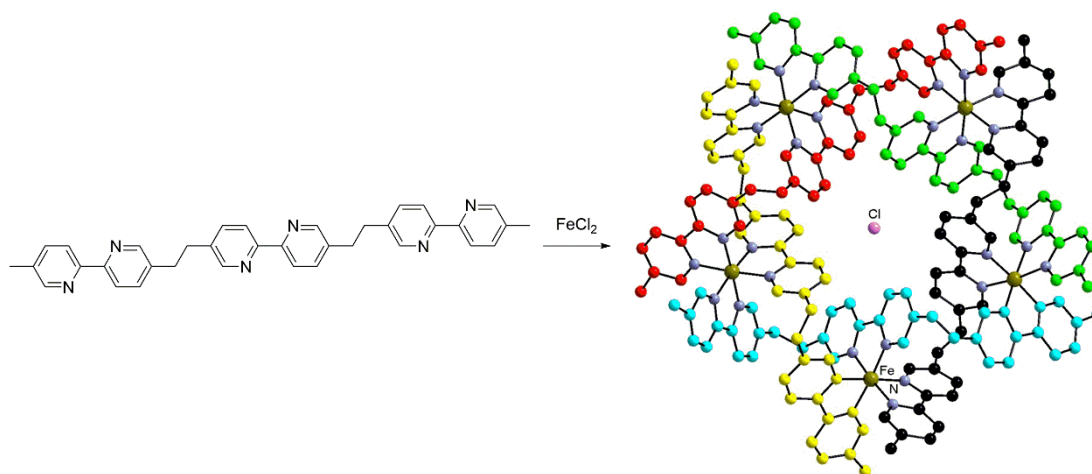


Figure 2: Formation of a pentanuclear circular helicate upon assembly of a tris-(2,2'-bispyridine) ligand with FeCl₂. Only the central anion is shown and the hydrogen atoms have been omitted for clarity.

This type of compounds has also been employed as templates for the construction of more complex architectures such as molecular knots.⁴ This approach involves the use of functionalized ligands for the construction of helicates bearing peripheral reactive groups such as alkene, aldehyde, amine or alcohol functions. The latter moieties can then be reacted to close the system. An early example of this approach has been described by J.-P. Sauvage using a linear binuclear Cu(I) helicate functionalized with phenol units.⁵ Once the helicate is formed, the complex is reacted with the diiodo derivative of hexaethyleneglycol leading to a trefoil knot as shown in

² B. Hasenknopf, J.-M. Lehn, B. O. Kneisel, G. Baum and D. Fenske, *Angew. Chem. Int. Ed.*, **1996**, 35, 1836.

³ B. Hasenknopf, J.-M. Lehn, N. Boumediene, A. Dupont-Gervais, A. Van Dorsselaer, B. Kneisel and D. Fenske, *J. Am. Chem. Soc.*, **1997**, 119, 10956.

⁴ (a) J. Bourlier, A. Jouaiti, N. Kyritsakas-Gruber, L. Allouche, J.-M. Planeix and M. W. Hosseini, *Chem. Commun.*, **2008**, 6191.

(b) J.-F. Ayme, J. E. Beves, C. J. Campbell and D. A. Leigh, *Chem. Soc. Rev.*, **2013**, 42, 1700. (c) C. J. Brunns and J. F. Stoddart, *The nature of the mechanical bond. From molecules to machines*. **2017**, John Wiley & Sons.

⁵ (a) C. O. Dietrich-Buchecker and J.-P. Sauvage, *Angew. Chem. Int. Ed. Engl.*, **1989**, 28, 189. (b) C. O. Dietrich-Buchecker, Jean Guilhem, C. Pascard and J.-P. Sauvage, *Angew. Chem. Int. Ed. Engl.*, **1990**, 29, 1154.

Figure 3.

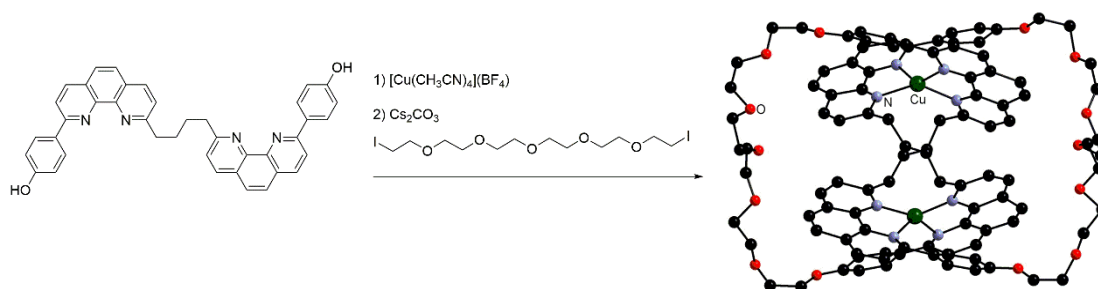


Figure 3: Templated synthesis of a trefoil knot using a binuclear linear helicite.

The group of Leigh has substituted the ligand used by Lehn and coworkers for the synthesis of the pentanuclear complex shown in Figure 2 for its analogue functionalized with aldehyde units prone to the formation of imine upon assembly with an amine derivative. The resulting compound is a pentafoil knot (Figure 4).⁶

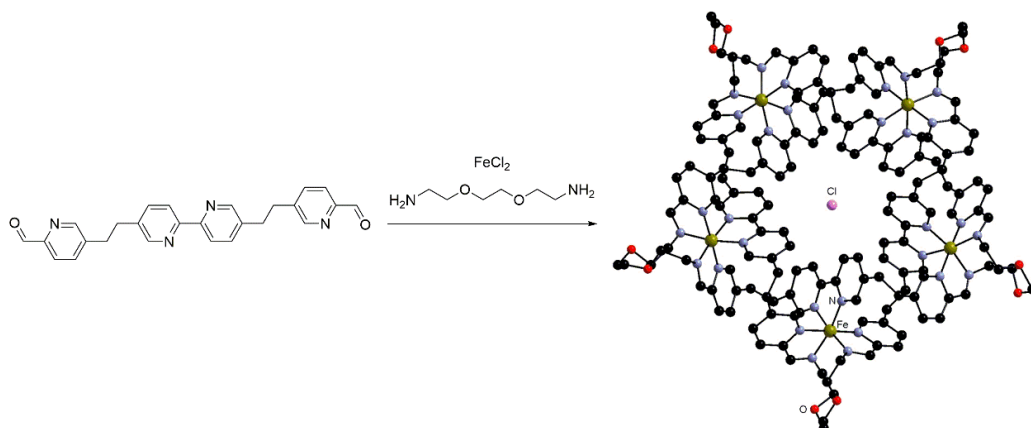


Figure 4: A pentafoil knot prepared by a template synthesis using a circular helicite.

As illustrated by these examples, polypyridine based ligands have been extensively investigated for the elaboration of helicates by self-assembly processes. Owing to the neutral nature of these ligands, these helicates are charged and need counterions for neutralization. These ions also sometimes play a role in the formation of the complex itself as presented in Figure 2 and 4. In contrast, polydipyrromethenes (polydipyrroin), comprising several dipyrroin units connected with or without a bridge can be seen as potential ligands for the coordination of various metal ions to construct neutral supramolecular architectures featuring linear and circular helicity (Figure 5).⁷ Indeed as early as 1976, Furhop and coworkers reported that octaethyl formylbiliverdinate forms

⁶ J.-F. Ayme, J. E. Beves, D. A. Leigh, R. T. McBurney, K. Rissanen and D. Schultz, *Nat. Chem.*, **2012**, 4, 15.

⁷ M. Bröring, Beyond dipyrroins: Coordination interaction and templated macrocyclizations of open-chain oligopyrroles, in *Handbook of Porphyrin Science*, **2010**, vol. 8, p. 343

a linear binuclear helicate with Zn(II) cations.⁸ More recently, the assembly of the open-chain tetrapyrrolic derivatives of the bis-dipyririn type with Zn(II) cations has been particularly studied, affording linear helical complexes as well as circular helicates (Figure 5).^{9,10,11} Our group has particularly investigated the coordination chemistry of 2,2'-bisdipyririn ligands where the two dipyririn chelates are directly connected by a single C-C bond. It has thus been shown that these ligands form a linear species as observed by the groups of Dolphin, Maeda and Bröring, but also circular species (Figure 5bottom).

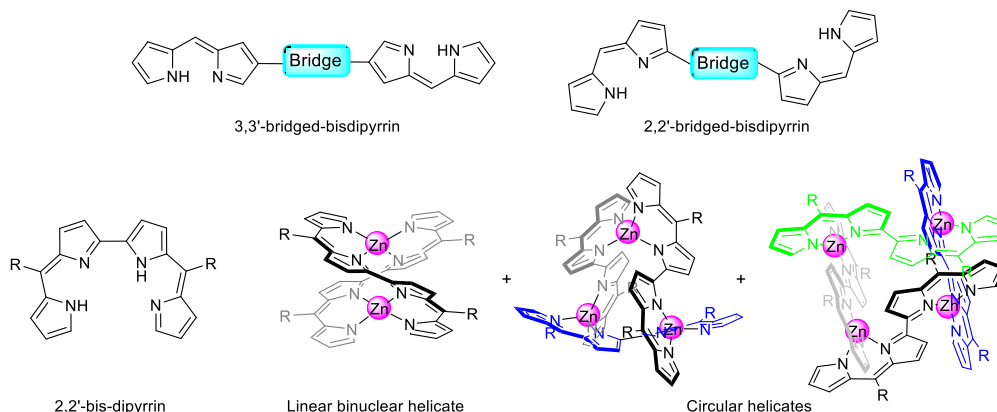


Figure 5: Schematic representations of 3,3'- and 2,2'-bisdipyririn (top) and linear as well as circular helicate complexes obtained from a 2,2'-bisdiopyririn derivative (bottom).

In analogy with the template effect considered for the formation of knots mentioned above, the coordination of bisdipyririn derivatives to the metal centers has also been envisioned as a pre-organizing event leading to a specific arrangement of the tetra-pyrrolic strands and of the peripheral units. This was taken advantage of for the formation of heterometallic coordination networks by association of linear binuclear helicates with Ag(I) cation owing to Ag- π interactions. The assembly of complex **27** bearing four peripheral coordinating benzonitrile units at the *meso* positions with Ag(I) cation allows the formation of a Ag₂Zn₂ tetranuclear motif as in the discrete compound **28**. Different Ag₂Zn₂ bimetallic positional isomers (1,4-isomer or 1,3-isomer) can be observed in these cases has exemplified in the compounds isolated with various AgX salts (X⁻ =

⁸ G. Struckmeier, U. Thewalt and J. -H. Furhop, *J. Am. Chem. Soc.*, **1976**, *98*, 278.

⁹ (a) Y. -J. Zhang, A. Thompson, S. J. Rettig and D. Dolphin, *J. Am. Chem. Soc.*, **1998**, *120*, 13537. (b) R. G. Khoury, L. Jaquinod and K. M. Smith, *Tetrahedron*, **1998**, *54*, 2339. (c) M. Bröring, S. Link, C. D. Brandt and E. Cónsul Tejero, *Eur. J. Inorg. Chem.*, **2007**, 1661. (d) T. Hashimoto, T. Nishimura, J. M. Lin, D. Khim and H. Maeda, *Chem. Eur. J.*, **2010**, *16*, 11653. (e) E. V. Antina, R. T. Kuznetsova, L. A. Antina, G. B. Guseva, N. A. Dudina, A. I. V'yugin and A. V. Solomonov, *Dyes Pigments*, **2015**, *113*, 664.

¹⁰ H. Maeda, T. Nishimura, R. Akuta, K. Takaishi, M. Uchiyamabd and A. Muranaka, *Chem. Sci.*, **2013**, *4*, 1204.

¹¹ S. A. Baudron, H. Ruffin and M. W. Hosseini, *Chem. Commun.*, **2015**, *51*, 5906.

TfO⁻, BF₄⁻, SbF₆⁻) under different solvent conditions. For example, helicate **27** afford two crystalline materials **29** and **30** in the solvent system CH₂Cl₂/AcOEt with Ag(TfO). The latter consist of the same tetranuclear helicate core as the one observed for compound **28** with similar Ag-C distances (**29**: 2.393(3) to 2.692(3); **30**: 2.420(4) to 2.688(4) Å). Whereas the 1,4-isomer of the Ag₂Zn₂ motif is observed in **29**, the 1,3-isomer one is present in **30**. In addition, the two crystallographically independent Ag(I) centers in **29** are both coordinated to a TfO⁻ anion and either a peripheral CN group of a neighboring helicate or a free TfO⁻ anion leading to 1D network. In the case of **30**, the two Ag(I) centers are both coordinated to two nitrile groups of neighboring helicates affording a 2D coordination network without coordination of the triflate anions (Figure 6).¹²

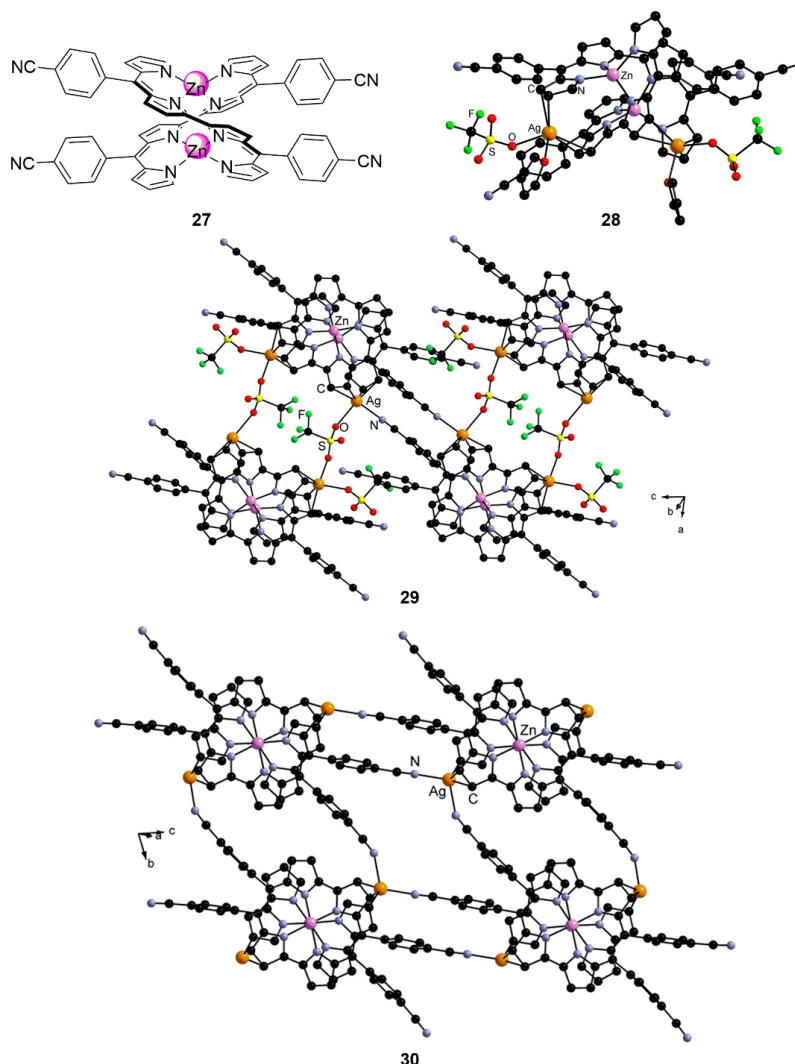


Figure 6: Chemical structure of helicate complex **27**. Crystal structures of discrete tetranuclear complex **28**, 1D coordination network **29** and 2D network **30**.

¹² H. Ruffin, S. A. Baudron, D. Salazar-Mendoza and M. W. Hosseini, *Chem. Eur. J.*, **2014**, *20*, 2449.

The formation of networks in these compounds is based on the assistance of the peripheral benzonitrile units. Using helicate complexes with aromatic units such as phenyl or anthracene, it has been demonstrated that assembly by Ag- π interactions was also operative.¹³ This strategy involves only the complexation reaction between the Ag(I) cation and the π system (either the pyrrolic or the anthracene units), and does not require the presence of additional coordinating groups. The infinite networks are here constructed with the help of the triflate anions. (Figure 7)

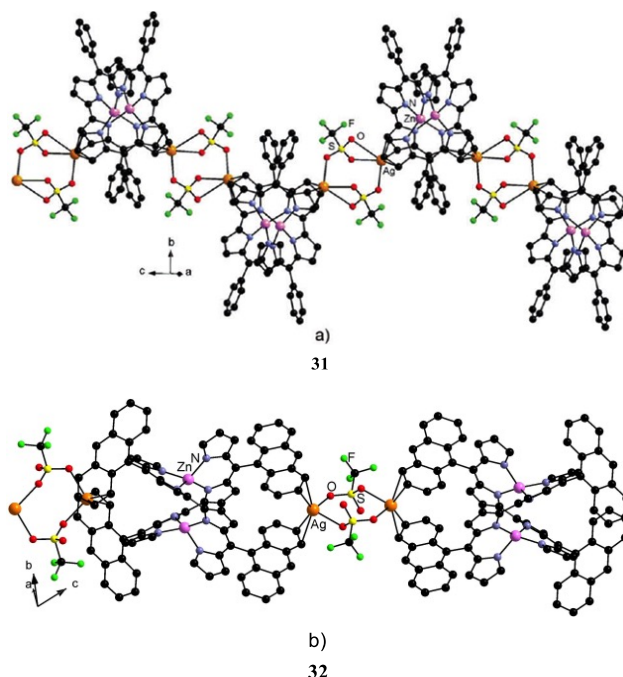


Figure 7: Portion of Crystal structures of 1D networks based on the assembly of Ag(TfO) with a Zn helicate bearing either phenyl (a) or anthracene groups (b) at the *meso* positions).

So far, most of the examples reported in the literature involve 2,2'-bisdipyrin ligands bearing either weakly or non-coordinating units. The aim of the second part of my thesis was the development of novel derivatives featuring either a reactive or a group prone to specific interactions such as a hydrogen bond donor/acceptor unit or a coordinating moiety. Using these ligands, it was envisioned to use the resulting helicates as templates for the formation of more complex architectures. A first approach consisted in the preparation of the novel 2,2'-bisdipyrin bearing peripheral *p*-benzaldehyde. The linear helicate resulting from the assembly with Zn^{2+} cations shows pre-organization of the reactive functions at the periphery. This template effect of

¹³ S. A. Baudron and M. W. Hosseini., *Chem. Commun.*, **2016**, 52, 13000.

the Zn(II) complexation has been taken advantage of for the preparation of a novel strapped helicate complex upon imine bond reaction. Secondly, the work focused on the introduction of carboxylic acid functions that were then employed for the formation of various amide type bisdipyrrens upon reaction with amines. They can assemble with the metal centers in order to provide metal complexes as well as helicates, which can be considered as metallatectons for the formation of heterometallic molecular networks *via* coordination, Ag- π interactions and/or H-bonding.

II.2 Formation of a strapped helicate based on a benzaldehyde-appended 2,2'-bis-dipyrin

It was first envisioned to use the linear helicates formed by the assembly of Zn(II) cations and 2,2'-bisdipyrin ligands functionalized with peripheral reactive groups as templates for the synthesis of metallamacrocycles. To the best of our knowledge, only one report by the group of Maeda has described a series of 2,2'-bis-dipyrin Zn(II) helicates bearing peripheral olefins leading to strapped systems upon olefin metathesis (Figure 8).¹⁰

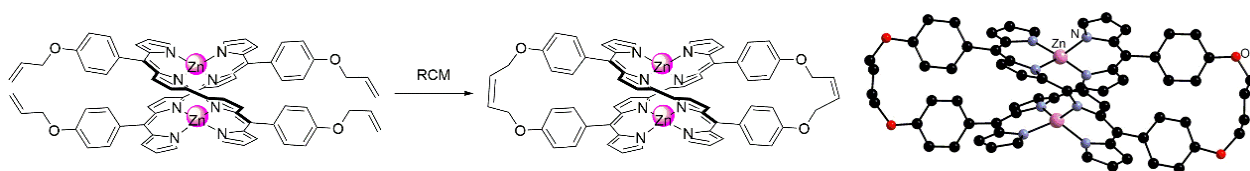
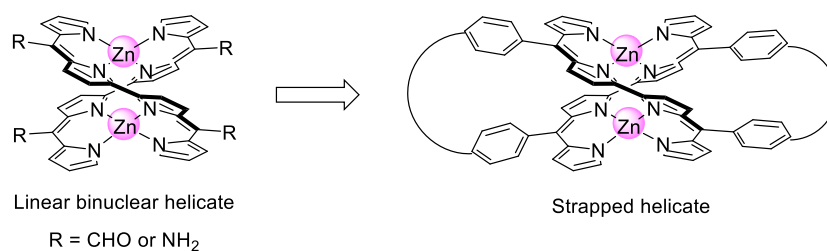


Figure 8: Strapped helicate formed by Maeda using ring-closing metathesis.

Over the past few years, the imine bond formation and its subsequent reduction have been successfully employed for the elaboration of complex supramolecular systems.¹⁴ Taking advantage of this reactivity and versatility, the approach followed here was to imagine the Zn helicate complexes bearing peripheral *p*-benzaldehyde or amine moieties as a template platform to react with an appropriately chosen amine or aldehyde respectively for the preparation of strapped

¹⁴ (a) P. T. Corbett, J. Leclaire, L. Vial, K. R. West, J.-L. Wietor, J. K. M. Sander and S. Otto, *Chem. Rev.*, **2006**, *106*, 3652. (b) J. M. Lehn, *Chem. Soc. Rev.*, **2007**, *36*, 151. (c) M. E. Belowitch and J. F. Stoddart, *Chem. Soc. Rev.*, **2012**, *41*, 2003. (d) A. M. Castilla, W. J. Ramsay and J. R. Nitschke, *Acc. Chem. Res.*, **2014**, *47*, 2063.

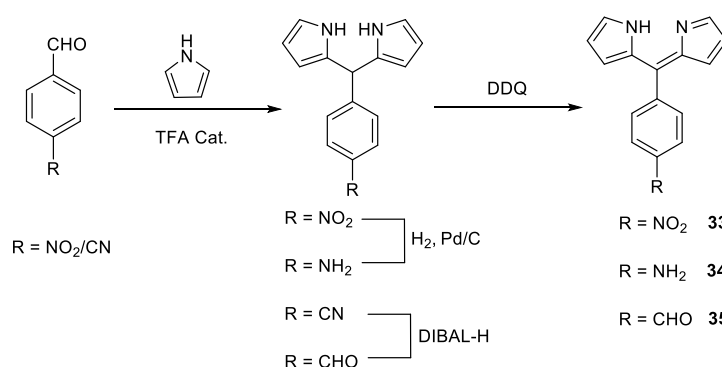
helicates (Scheme 1).



Scheme 1: Strategy for the formation of a strapped helicate type starting from linear complex bearing reactive groups.

II.2.1 Preliminary investigation for the synthesis of imine functionalized dipyrin derivatives

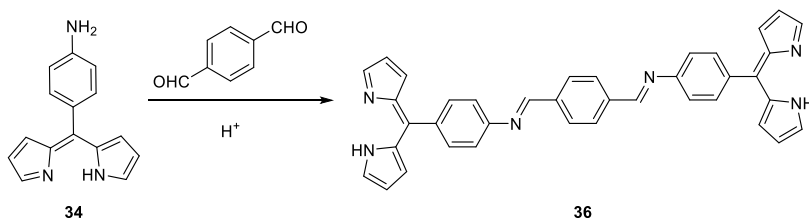
Aiming at the strategy mentioned above, a preliminary study on the reactivity towards imine bond formation of monodipyrins was first performed. Therefore, an optimized synthetic route for the preparation of two monodipyrins bearing peripheral aniline or benzaldehyde groups in the *meso* position has been established. The aniline or benzaldehyde dipyrromethanes were formed by reduction of nitrophenyl or cyanophenyl dipyrromethanes, obtained in turn by reaction of the corresponding aldehyde in pure pyrrole with a catalytic amount of trifluoroacetic acid in 85% yield. Oxidation of the corresponding dipyrromethane with DDQ gave the dipyrin derivatives **33-35** with 56% - 68% overall yields Scheme 2.¹⁵ The identity and purity of these products have been demonstrated by ¹H-NMR, ¹³C-NMR, MS/HRMS(ESI) or elemental analysis.



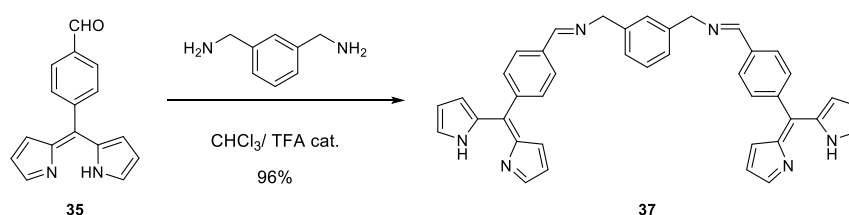
Scheme 2: Strategies for the synthesis of *meso*-substituted dipyrin derivatives **33-35**.

¹⁵ (a) C. Bruckner, Y. Zhang, S. J. Rettig, D. Dolphin, *Inorg. Chim. Acta.*, **1997**, 263, 279. (b) B. J. Littler, M. A. Miller, C. H. Hung, R. W. Wagner, D. F. O'Shea, P. D. Boyle and J. S. Lindsey, *J. Org. Chem.*, **1999**, 64, 1391. (c) P. D. Rao, S. Dhanalekshmi, B. J. Littler and J. S. Lindsey, *J. Org. Chem.*, **2000**, 65, 7323.

Theoretically, both the aniline dipyrin **34** and benzaldehyde dipyrin **35** could be employed as starting materials for the proposed synthetic approach. In fact, the locus of the nucleophile impacts the reactivity of this reaction. Due to the coexistence of the NH₂ nucleophilic group and the π -conjugated system of dipyrin moiety, electron density is withdrawn from the NH₂ unit, the aniline dipyrin is thus less reactive than an amine. In addition, the catalyst used for activation of the aldehyde group plays an important role in this case. Therefore, a series of preliminary tests has been carried out. For example, the reaction of aniline dipyrin **34** and terephthalaldehyde shown in Scheme 3 produces the corresponding di-imine bisdipyrin **36** in the presence of a Brønsted acid catalyst (acetic or trifluoroacetic acid). However, the conversion of these reactions was not satisfactory resulting from the limited activity of the NH₂ nucleophilic group, even with the help of a Dean-stark apparatus to displace water. Another difficulty in this reaction concerns the purification. The crude product was found to decompose and return to the starting species upon purification by column chromatography. In this case, the desired pure product could only be isolated by recrystallization in 30% yield.



Scheme 3: Synthesis of diimine bisdipyrin **36** based on aniline dipyrin **34**.



Scheme 4: Synthesis of diimine bisdipyrin **37** based on benzaldehyde dipyrin **35**.

Thus, another synthetic approach for the formation of dipyrin based imine bond was sought starting from the benzaldehyde appended dipyrin. The novel diimine bis-dipyrin ligand **37** was prepared with a satisfactory conversion by condensation of compound **35** and *m*-xylylenediamine in

the presence of a catalytic amount of trifluoroacetic acid (Scheme 4). The pure product **37** could be isolated by recrystallization with 96% yields.

As divergent chelating ligands, compounds **36** and **37** have the ability to coordinate with a divalent metal center to construct 1D linear or zig-zag supramolecular architectures for example (Figure 9). In our case, the method of slow liquid-liquid diffusion has been applied to obtain single crystals which could be analyzed by X-ray diffraction. However, as mentioned in the introduction of this manuscript, only very few examples of crystalline material based on such divergent bis-dipyrrins have been described.¹⁶ Indeed, these ligands are di-anionic tectons under basic conditions leading to a fast complexation of metal cations and to neutral 1D-coordination polymers that tend to aggregate randomly and amorphously; only non-crystalline powder are usually obtained. As mentioned in Chapter I, another crystallization test was performed with pyridine as a competing ligand in order to slow down the process. Under these conditions, some red crystals combining ligand **37** and Ni(OAc)₂ were obtained. Unfortunately, the quality of these crystals was not sufficient to obtain data from X-ray diffraction.

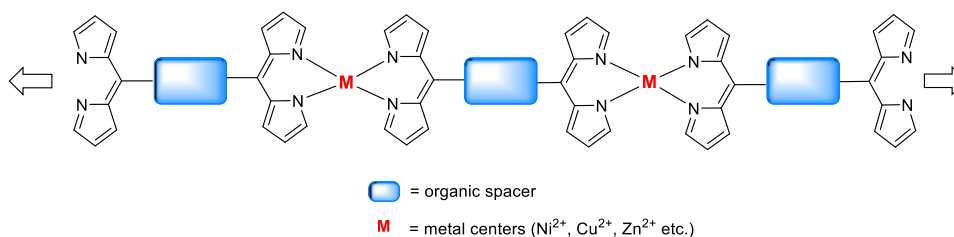


Figure 9: Schematic representation for the strategy of the formation of 1D CPs based on ligands **36** and **37**.

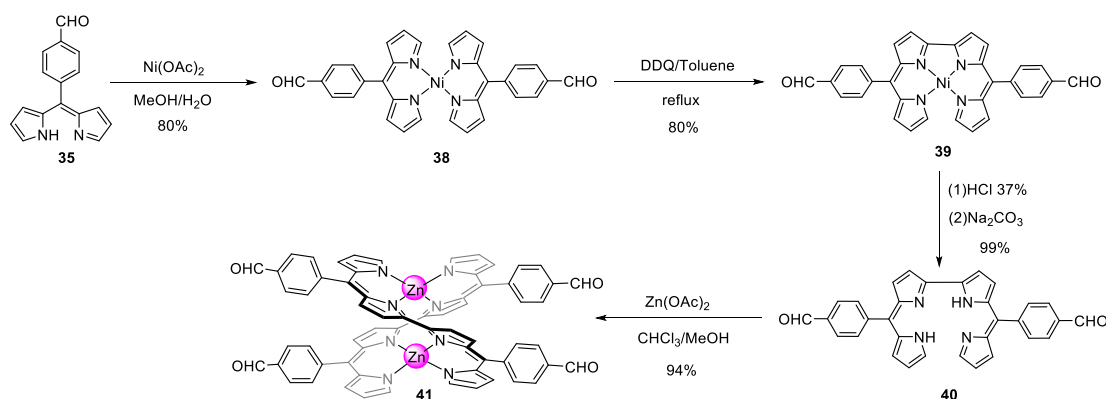
II.2.2 Synthesis of a strapped helical complex

Following the successful synthesis of **37**, the formation of a metallamacrocyclic complex by an analogous reaction with a linear Zn helicate bearing the same type of benzaldehyde groups was envisaged. The novel Zn helicate **41** has been prepared following the Ni-templated strategy developed by Scott *et al.* (Scheme 5).¹⁷ The homoleptic Ni(II) complex **38**, prepared as described

¹⁶ R. Sakamoto, K. Hoshiko, Q. Liu, T. Yagi, T. Nagayama, S. Kusaka, M. Tsuchiya, Y. Kitagawa, W.-Y. Wong and H. Nishihara, *Nat. Commun.*, **2015**, 6, 6713.

¹⁷ H. S. Gill, I. Finger, I. Božidarević, F. Szydło and M. J. Scott, *New J. Chem.*, **2005**, 29, 68.

for the Zn(II) analogue,¹⁸ has been reacted with DDQ in refluxing toluene to afford compound **39** in 80% yield. The latter was demetallated by HCl and then neutralized with NaHCO₃ saturated solution providing the free bisdipyrrin ligand **40** in 99% yield. Upon reaction of this tetrapyrrolic derivative with Zn(OAc)₂, helicate **41** was obtained in 94% yield. These compounds have been characterized in solution by ¹H- and ¹³C-NMR, UV-visible spectroscopy, mass spectrometry (see Experimental part for details).



Scheme 5: Strategy for synthesis of linear Zn helicate **41** starting from monodipyrrin **35**.

In addition to the above-mentioned characterizations, the crystal structure of these compounds has been determined by single-crystal X-Ray diffraction. As reported for other Ni(dipyrrinato)₂/Ni(2,2'-bis-dipyrrinato) systems,^{9a,11-13,17} a flattening of the coordination environment of the tetra-coordinated Ni(II) center upon formation of the pseudo-macrocyclic ligand is observed in the crystal (Figure 10). Whereas the two bipyrrrolic chelates form an angle of 60.88° in **38**, this angle decreases to 19.15° in **39**. Also, the Ni-N bond distances are in the rather narrow 1.8835(12) to 1.8930(12) Å range in the structure of **38**, while they vary from 1.8584(17) to 1.9027(18) Å for **39**, owing to the formation of the 2,2'-bis-dipyrrin backbone. For the free ligand **40**, the two bipyrrrolic chelates are oriented in a *trans* fashion and coplanar as described for the benzonitrile analogue.¹² Furthermore, an intramolecular hydrogen bond is observed within each dipyrrin moiety ($d_{N...N} = 2.753(3)$ Å; $\alpha_{N-H...N} = 122.45^\circ$). In the structure of the binuclear helicate **41**, each Zn(II) cation is in a distorted tetrahedral environment coordinated to two

¹⁸ (a) L. Yu, K. Muthukumar, I. V. Sazanovich, C. Kirmaier, E. Hindin, J. R. Diers, P. D. Boyle, D. F. Bocian, D. Holten and J. S. Lindsey, *Inorg. Chem.*, **2003**, 42, 6629. (b) K. Muthukumar, S. H. H. Zaidi, L. Yu, P. Thamyingkit, M. E. Calder, D. S. Sharada and J. S. Lindsey, *J. Porphyrins Phthalocyanines.*, **2005**, 9, 745.

dipyrrin chelates belonging to the two different strands forming an angle of 53.6°. The metal centers are separated by 3.280(8) Å, as observed for other helicates (Figure 10).

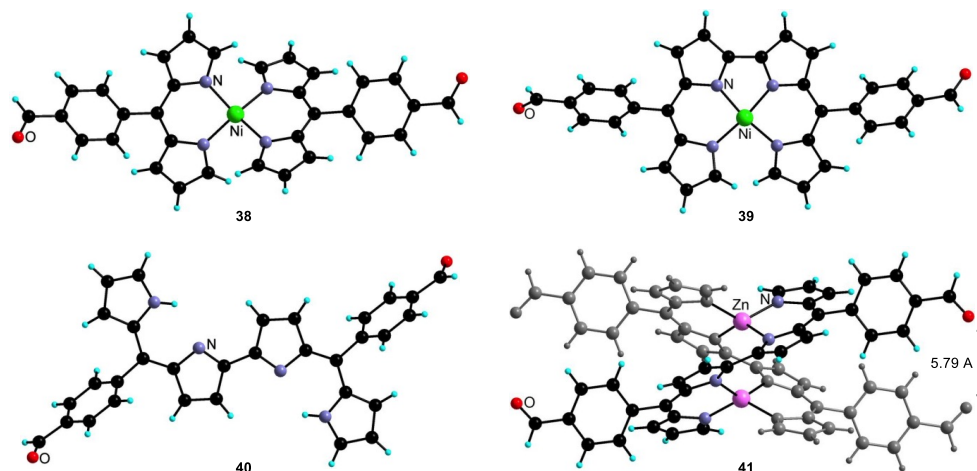


Figure 10: Crystal structures of Ni complexes **38** and **39**, of 2,2'-bis-dipyrrin ligand **40** and of Zn helicate **41**. Solvent molecules have been omitted for clarity.

To achieve the strapping of the helicate, an appropriate amine has to be chosen to react with the peripheral aldehyde groups. *m*-Xylylenediamine could be considered as the desired diamine, since the distance between the two nitrogen atoms within this compound should be compatible with the one between the carbonyl oxygen atoms, 5.797 Å, observed in the structure of **41** (Figure 10). The reaction of two equivalents of *m*-xylylenediamine with one equivalent of linear Zn helicate **41** in the presence of a catalytic amount of TFA (0.01 eq.) was thus investigated. To avoid the formation of undesired polymer and to improve the yield of the reaction shown in Figure 11top, several reaction conditions were tested. A first attempt consisting in the direct mixing of the reactants in a 1.10^{-4} mol/L CHCl_3 solution of **41** led, after three days, to the complete disappearance of the CHO signal in the ^1H -NMR spectra. However, the purity of the desired product **42** was not satisfactory and a low yield was observed given the concomitant formation of insoluble material in large amount (about 50%). The latter could not be further characterized but may correspond to non-strapped polymeric assemblies. Lowering the initial concentration to 1.10^{-5} mol/L led also to product **42**, although insoluble polymeric material was still obtained. Pure product **42** in almost quantitative yield (98%) could be isolated by the controlled slow addition of the diamine over 24 hours. Furthermore, the nature of **42** was confirmed by ^1H -/ ^{13}C -NMR and high-resolution mass spectrometry. The ^1H -NMR spectrum in CDCl_3 of the product confirms the disappearance of the

carbonyl proton along with the presence of the imine one. In particular, the appearance of two doublets assigned to the two diastereotopic protons of the methylene moiety of the *m*-xylylenediimine straps is a strong evidence for the formation of the macrocyclic helical complex **42**. (Figure 11bottom).

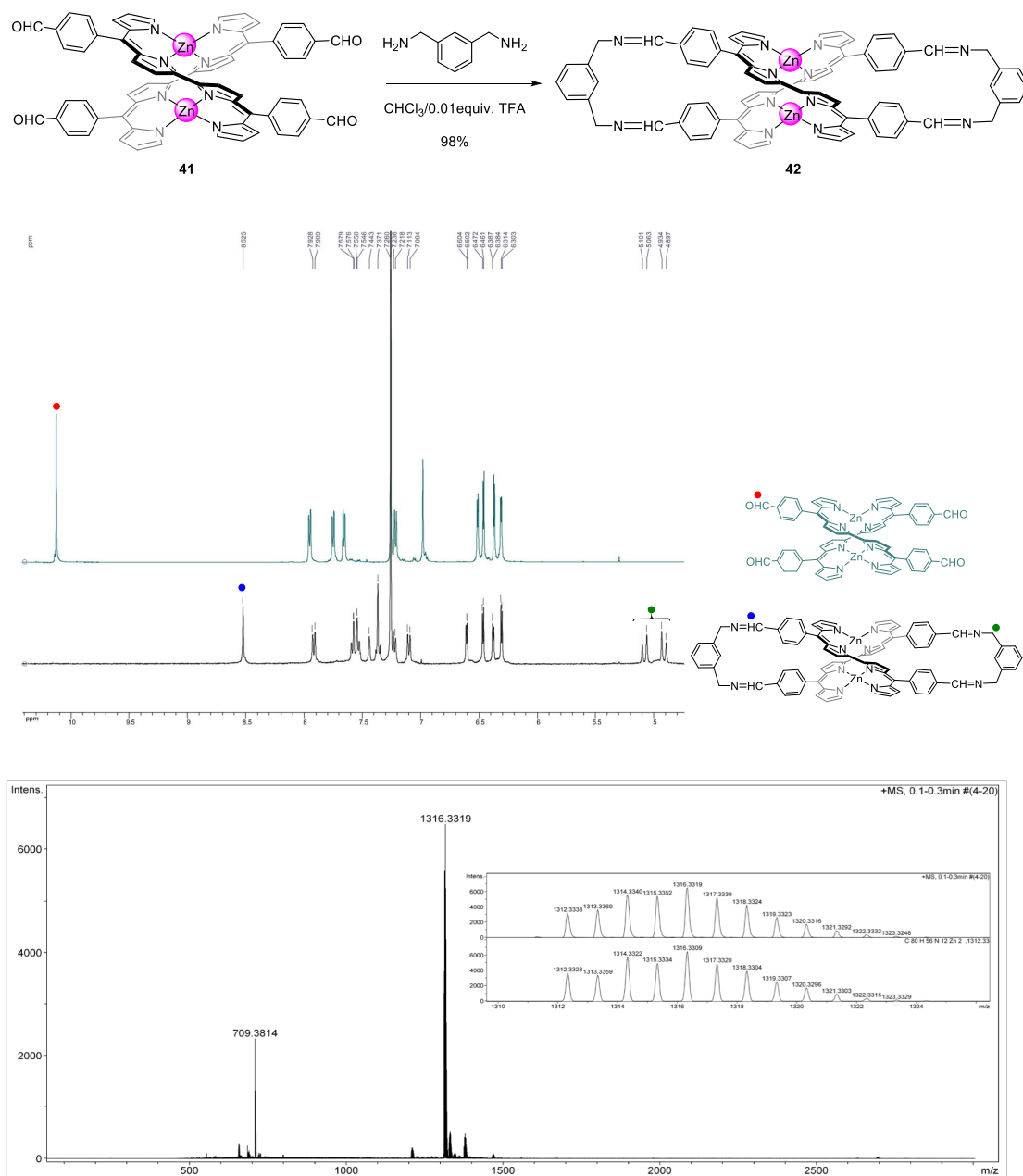


Figure 11: Synthesis (top), ¹H-NMR spectrum (middle) and high-resolution mass HRMS-ESI spectrum (bottom) of strapped tetra-imine helical complex **42**.

The stability of the macrocyclic helicate **42** was investigated. It has been observed that compound **42** was stable both in solution and in the solid state at room temperature, but it starts to degrade

upon heating in solution. Furthermore, the compound is sensitive to the presence of Lewis acids. This helicate was found to decompose to the starting material during the purification by chromatography on SiO₂.

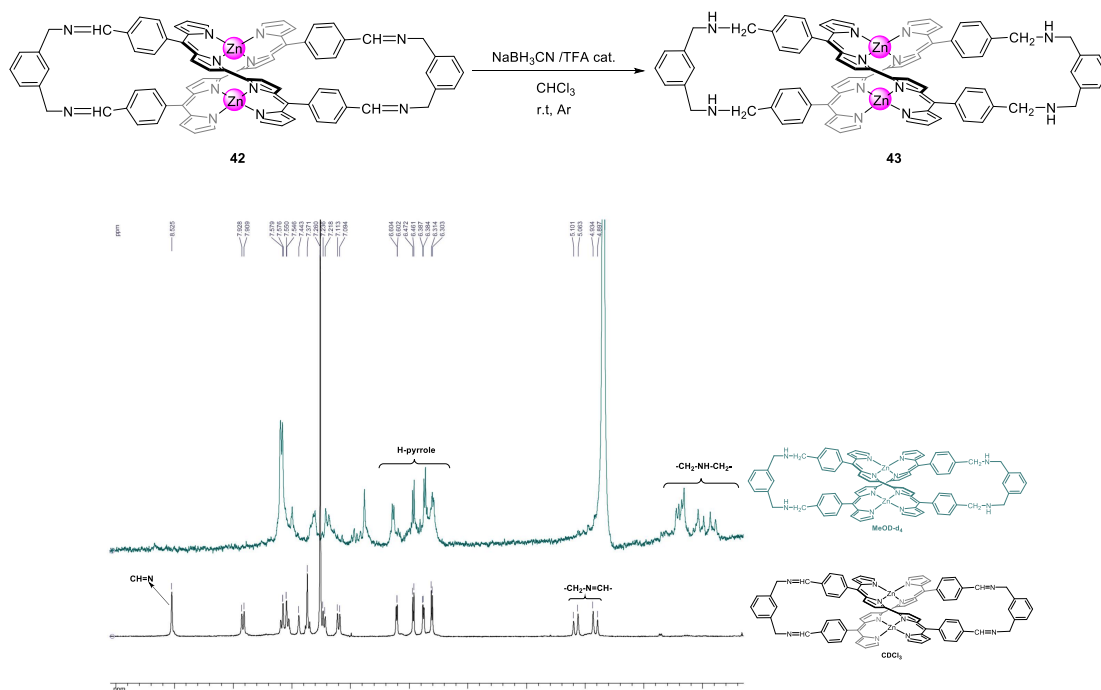


Figure 12: Synthesis (top) and the ¹H-NMR spectrum (bottom) of strapped tetra-amine helical complex **43**.

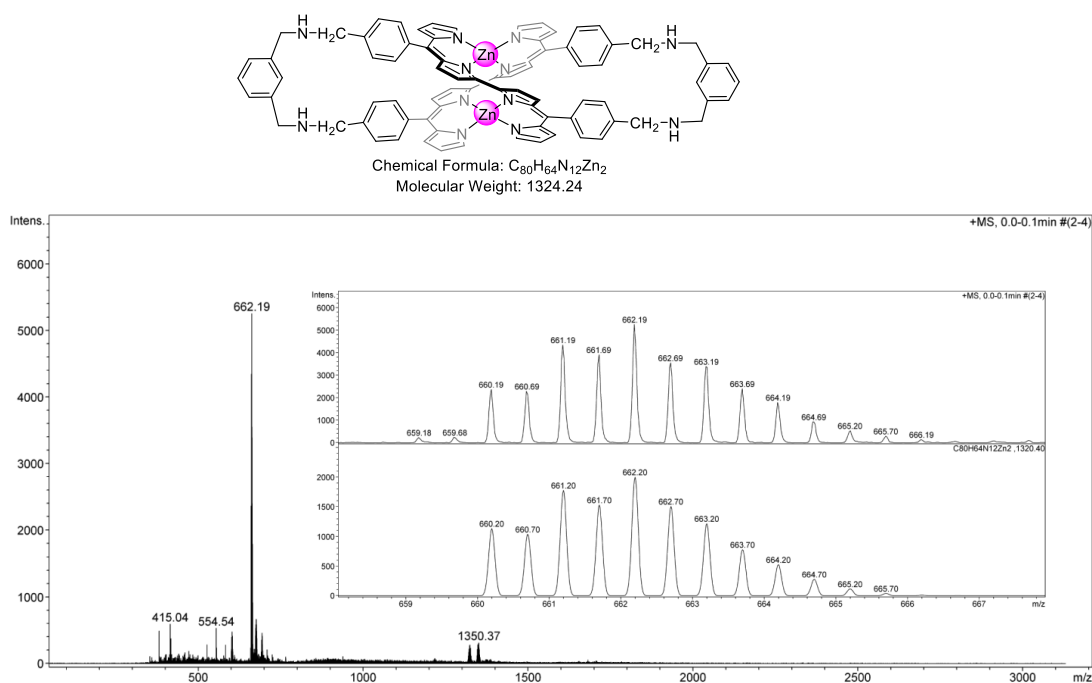


Figure 13: High-resolution mass HRMS-ESI spectrum of compound **43** with the isotope pattern as an insert.

The reduction of the tetra-imine based helicate **42** to tetra-amine helicate was also explored by reaction with the reducing agent NaBH_3CN in CHCl_3 solution (HPLC grade). The high-resolution mass spectrum supports the formation of the reduced helicate **43** with the presence of the corresponding peak as the main peak with the correct isotope pattern (Figure 13). The preliminary result by $^1\text{H-NMR}$ in MeOD-d_4 shows the disappearance of the imine proton signal as well as the new signal of the additional CH_2 belonging to the amine bridge formed upon reduction (Figure 12). The low resolution of the spectrum is caused by the poor solubility of the compound and purity. Further purification of helicate **43** is still in progress.

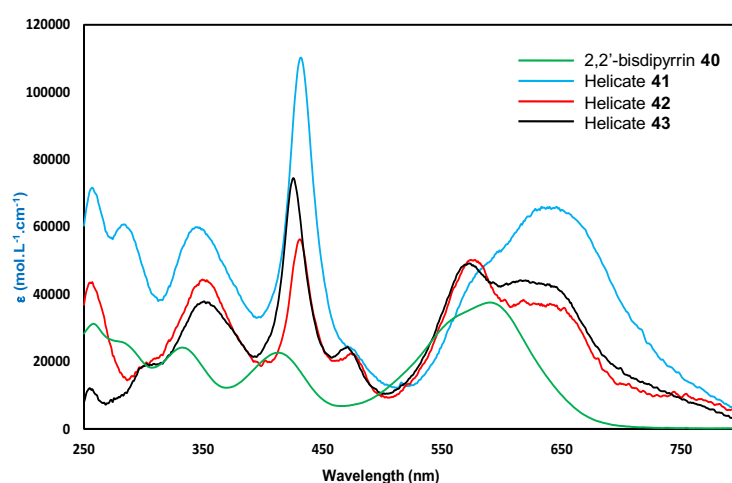


Figure 14: The absorption spectra of ligand **40** and helicates **41-43** in CH_2Cl_2 at room temperature.

Table 1: Absorption data of compound **40-43** in CH_2Cl_2 at room temperature.

Compound	$\lambda_{\text{ab}}/\text{nm}$ ($\epsilon \cdot 10^3 \text{ M}^{-1}\text{cm}^{-1}$)
40	258 (31.3), 280 (26.01), 332 (24.27), 413 (22.74), 591 (37.64)
41	257 (71.7), 284 (60.8), 345 (60), 432 (110.2), 646 (66)
42	257 (43.6), 349 (44.4), 431 (56.3), 473(22.5), 577 (50.2)
43	350 (37.8), 425 (74.4), 471 (24.3), 572 (49.1)

A photophysical study of **41-43** has been performed in CH_2Cl_2 solution (10^{-6} mol/L). The data are listed in Table 1. Figure 14 presents the UV-Visible spectra of ligand 2,2'-bisdipyrrin **40** and

helicates **41-43** in CH₂Cl₂ solution. The absorption band is red shifted for the helical complexes in comparison with the free ligand **40** as a result of the complexation of Zn(II) cations, as for other linear helicates reported in the literature.^{10,12,19} Interestingly, whereas strapped compounds **42** and **43** feature similar absorption bands between 550 nm-750 nm and molar absorptivity, it differs from the aldehyde functionalized species **41**. This may result from strapping causing a change in the Zn...Zn distance within the helicate and a modification of the relative orientation of the dipyrin chromophores within a strand and around the Zn(II) cations. Such spectral modification is in agreement with experimental and theoretical investigations reported by the group of Maeda.¹⁰

II.3 Amide functionalized 2,2'-bisdipyrin derivatives.

Up to now, efforts towards the formation of infinite architectures based on 2,2'-bisdipyrin ligands have been focusing on the use of derivatives bearing only weakly coordinating groups such as benzonitrile or phenyl and anthracenyl units prone to Ag- π interactions. Introduction of other moieties that should favor self-assembly was thus sought. In light of previous results on the benzamide functionalized mono-dipyrin presented in the introduction of this dissertation, the use of amide groups leading to hydrogen bonding based architectures was considered.²⁰ Furthermore, secondary amides represent an interesting avenue for the introduction of additional binding units such as coordinating groups. In this section, the design and preparation of novel 2,2'-bisdipyrin derivatives bearing peripheral amides were investigated, novel molecular ligands were developed for their assembly with metal centers to afford metallatectons for the construction of infinite architectures by multi-intermolecular interactions (coordination, H-bonding and/or Ag- π interaction).

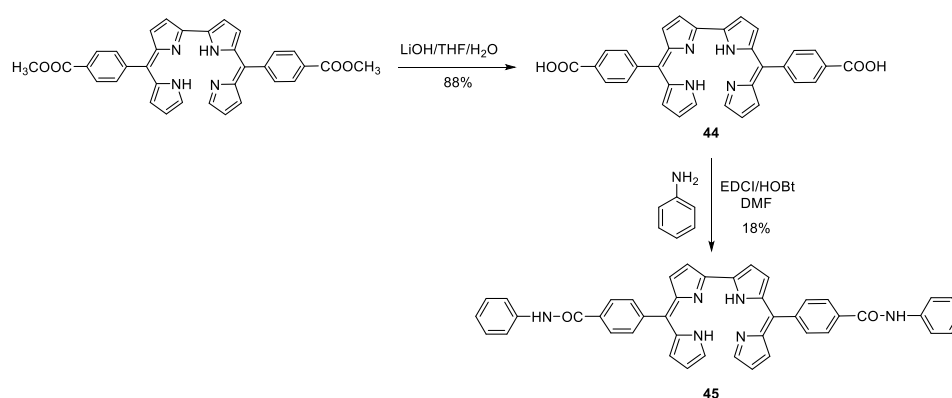
II.3.1 Symmetrical 5,5'-diamide-2,2'-bisdipyrin derivatives

The introduction of carboxylic acid groups was thus considered as a functionalizing point for the formation of various 2,2'-bisdipyrin ligands upon reaction with amines. The di-ester 2,2'-bisdipyrin was prepared following a described procedure.¹¹ Benzoic acid 2,2'-bisdipyrin

¹⁹ S. A. Baudron, *Dalton. Trans.*, **2013**, 42, 7498.

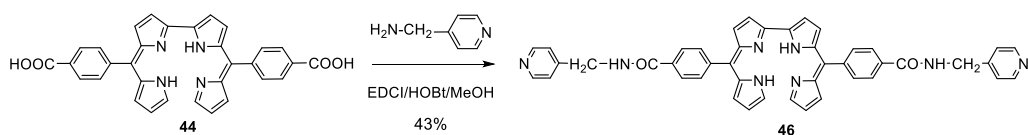
²⁰ S. A. Baudron, D. Salazar-Mendoza and M. W. Hosseini, *CrystEngComm.*, **2009**, 11, 1245.

derivative **44** was obtained by saponification of di-ester 2,2'-bisdipyrin with 10 equivalents of LiOH in a THF/H₂O mixture (1/1).²¹ At first, owing to the fact that the starting material **44** is only soluble in methanol, the reaction with aniline, EDC hydrochloride and HOBt²² was performed in dry methanol to obtain the diamide 2,2'-bisdipyrin derivative. However, it was the dissymmetric 2,2'-bisdipyrin carrying an ester and an amide functions was isolated. This results from the competition between aniline and the MeOH solvent molecule. Considering the effect of the latter and the starting reagent solubility, the formation of the novel ligand 2,2'-bisdipyrine **45** was thus carried out in dry DMF with 18% yield. (Scheme 6)



Scheme 6: Synthetic approach for the preparation of 2,2'-bisdipyrin derivative **45**.

Another new 2,2'-bisdipyrin **46** could be synthesized by combination of **44** with 4-aminomethylpyridine, EDC hydrochloride and HOBt in dry methanol in the 43% yield. In contrast with the previous case, the aminomethylpyridine was found to be more reactive than aniline as a nucleophilic reagent as expected. Therefore, this reaction could be realized in methanol. (Scheme 7)



Scheme 7: Synthesis of 2,2'-bisdipyrin derivative **46**.

²¹ (a) M. Brellier, G. Duportail and R. Baati, *Tetrahedron. Lett.*, **2010**, 51, 1269. (b) E. Rampazzo, S. Bonacchi, D. Genovese, R. Juris, M. Montalti, V. Paterlini, N. Zaccheroni, C. Dumas-Verdes, G. Clavier, R. Méallet-Renault, and L. Prodi, *J. Phys. Chem. C.*, **2014**, 118, 9261.

²² L. C. Chan and B. G. Cox, *J. Org. Chem.*, **2007**, 72, 8863.

These two new ligands **45** and **46** have been characterized (^1H - and ^{13}C -NMR, UV-visible spectroscopy, mass spectrometry) and their assembly with different metal centers is currently being explored. The preparation of the Zn binuclear helicates with ligands **45** and **46** was first investigated (Figure 15). These two helical complexes can be considered as metallatectons containing at least two different recognition sites at their periphery, therefore offering the possibility to coordinate a second metal center towards infinite architectures. These two new complexes were synthesized by liquid-liquid diffusion targeting the isolation of single crystals of two new species. Until now, helicates **47** and **48** were isolated with *ca* 91% yield and characterized by ^1H - and ^{13}C -NMR, UV-visible spectroscopy, mass spectrometry (see Experimental section for details). It is worth noting that the ^{13}C -NMR data of helicate **48** could not be obtained because of its low solubility.

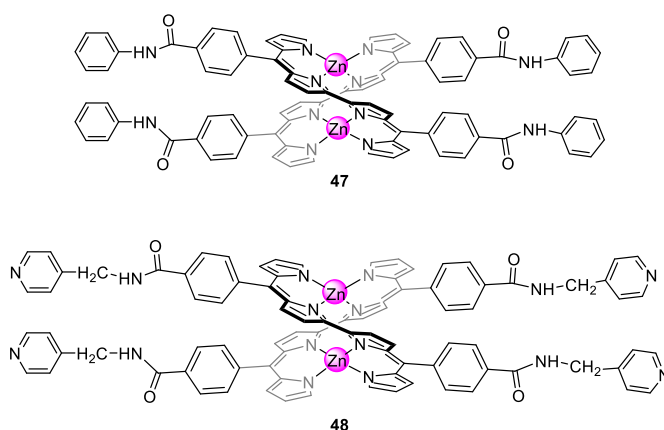


Figure 15: Chemical structures of Zn helicates **47** and **48**.

The coordination chemistry of new ligands **45** and **46** with other metal centers such as Ni^{2+} , Cu^{2+} , Cd^{2+} was also explored. In particular, the assembly of ligand **46** with $\text{Ni}(\text{II})$. Indeed, as mentioned in the introductory chapter, $\text{Ni}(\text{dpm})_2$ complexes bearing peripheral pyridyl units have been shown to have a tendency to self-assemble into coordination networks.²³ This has actually prevented, in our laboratory, the development of 2,2'-bisdipyrin ligands with directly bound pyridyl groups since the synthesis optimized by Scott goes through the Ni complex as an intermediate. In this case, these intermediates were not soluble preventing further investigations. Thus, the introduction of the pyridyl unit *via* the amide function developed in this work appeared

²³ A. Béziau, S. A. Baudron, G. Rogez and M. W. Hosseini, *CrystEngComm.*, **2013**, *15*, 5980.

as a good alternative to circumvent this synthetic issue. Upon vapour diffusion of Et₂O into a CHCl₃/MeOH mixture of **46** and Ni(OAc)₂ (H₂O)₄, single crystals of **49** were obtained. This complex (monoclinic space group *C2/c*) is a discrete species with the Ni(II) center in a distorted square planar environment bound to the four nitrogen atoms of the bisdipyrrin ligand, with the mean plane of the two dipyrin chelates forming an angle of 14.74°. The Ni-N distances range from 1.856(4) to 1.906(4) Å as observed for the aldehyde appended compound **39** described above. The complex self-assembles into a 2D network through hydrogen bonding between amide groups ($d_{\text{N-H}\cdots\text{O}} = 2.778(5)\text{--}2.819(5)$ Å, $\alpha_{\text{N-H}\cdots\text{O}} = 142.3\text{--}152.9^\circ$) (Figure 16).

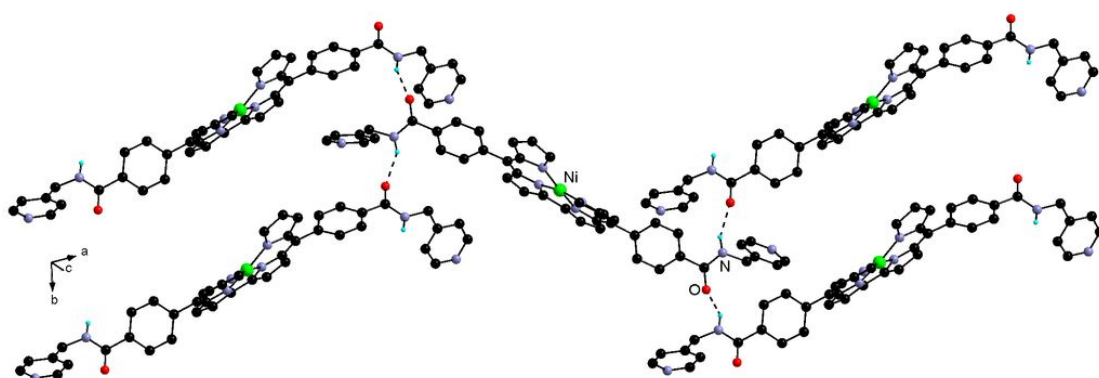


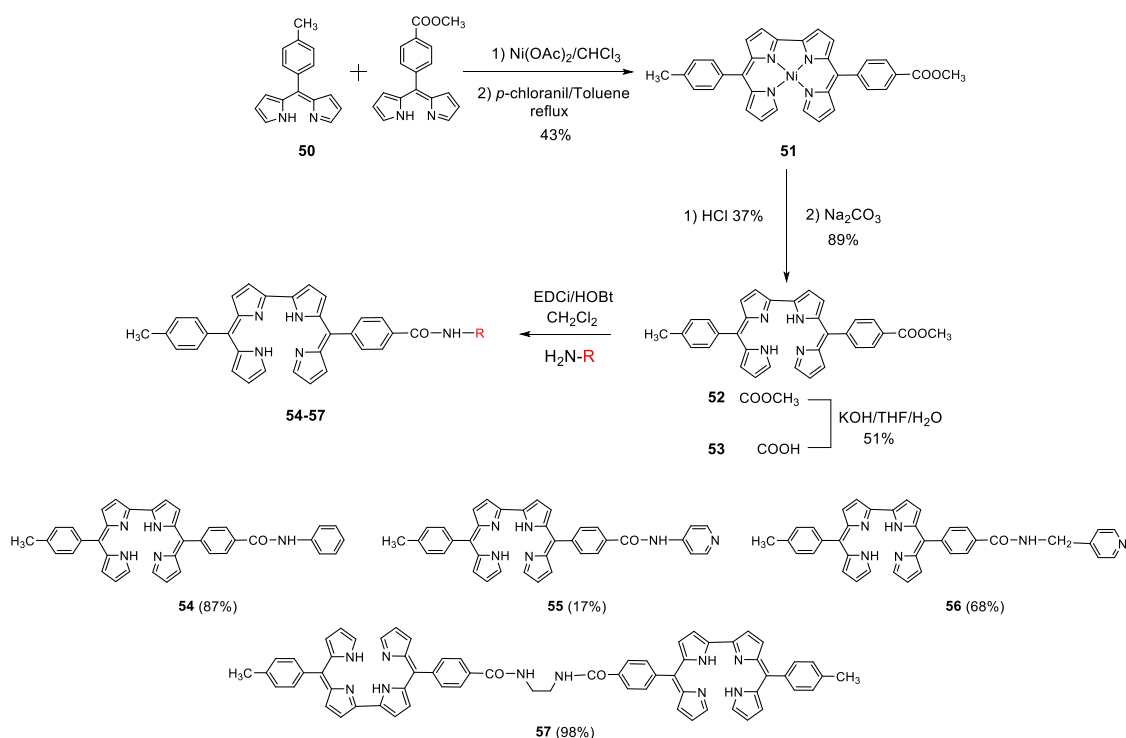
Figure 16: 2D hydrogen bonded network in the structure of Ni complex **49** based on the symmetric 2,2'-bisdipyrin derivative **46**. Only NH hydrogen atoms are shown for clarity.

In contrast with the other pyridyl appended Ni complexes described in the introduction, compound **46** forms a network without coordination of the peripheral groups. This soluble discrete complex can thus be envisioned as a potential metallatecton for the formation of heterometallic networks upon assembly with a second metal center. Investigations in this direction are currently ongoing.

II.3.2 Dissymmetrical 5-amide-2,2'-bisdipyrin derivatives

It has been observed that the solubility of new ligands **45** and **46** is limited owing to the presence of the amide group. The corresponding symmetrical helicates **47** and **48** are only soluble in THF or DMF. A strategy for increasing the solubility of such species was therefore developed. One approach that has been considered is to introduce the tolyl moiety at the periphery of the bisdipyrin backbone to improve the solubility of both ligand and complex.

Thus, new asymmetric 2,2'-bisdipyrrins ligands **54-57** were designed and prepared (Scheme 8). They are constructed from the derivative **53** comprising, on one hand, a tolyl unit, to improve the solubility of the compounds as mentioned above and, on the other hand, a benzoic acid for the formation of amide bonds. The synthetic approach for the preparation of dissymmetrical 2,2'-bisdipyrrin ligands has been developed by Maeda and coworkers on other compounds and relies on the use of the two corresponding mono-dipyrrins to form a mixture of three Ni(II) complexes followed by reaction with *p*-chloranil and purification to isolate the desired Ni(bisdpm^adpm^b)? that is subsequently demetallated.¹⁰ Following this procedure, the asymmetric complex **51** was formed from the monodipyrrin **50** and 5-phenylesterdipyrrin with 43% yield. After demetallation and saponification, the dissymmetrical bisdipyrrin **53** has been isolated. By reaction with amines in the presence of EDC hydrochloride and HOBT in dry CH₂Cl₂, the four new ligands **54-57** could be obtained with 17-98% yield. All compounds were characterized in solution by ¹H-/¹³C-NMR, high resolution mass spectroscopy HRMS(ESI) and UV-Visible spectroscopy.



Scheme 8: Synthesis of dissymmetrical 2,2'-bisdipyrrin derivatives **54-57**.

Furthermore, crystals of complex **51** and bis-dipyrrin **52** could be obtained and the structure

determined by X-Ray diffraction. Both compounds crystallize in the triclinic *P*-1 space group. The arrangement around the Ni(II) cation in **51** is analogous to what has been observed for complexes **39** and **46**, with a 18.97° angle between the two dipyrin chelates and Ni-N distances ranging from 1.841(3) to 1.888(3) Å. For ligand **52**, the two bispyrrolic fragments organize in a *cis* fashion as reported for the symmetrical diester analogue.¹¹ An intramolecular hydrogen bond is observed within each dipyrin moiety ($d_{N\cdots N} = 2.685(4)$ - $2.695(5)$ Å; $\alpha_{N-H\cdots N} = 124.07$ - 124.67°).

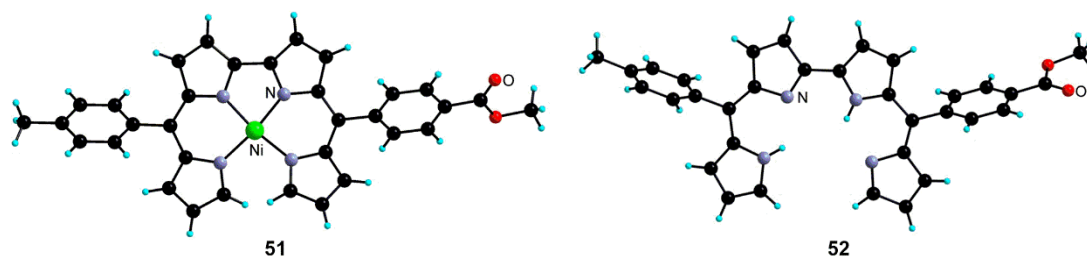
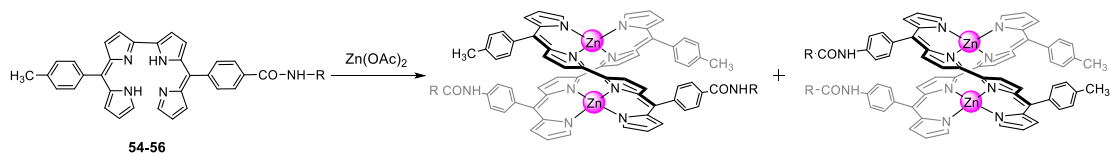


Figure 17: Crystal structure of Ni complex **51** and 2,2'-bisdipyrin **52**.

The four new amide based ligands have also been explored for the formation of linear Zn helicates (Scheme 9). The corresponding helicate complexes were characterized by $^1\text{H-NMR}$, DOSY-NMR and high resolution mass spectroscopy HRMS(ESI). Although the $^1\text{H-NMR}$ spectra of these species show the presence of two compounds, only one signal was recorded in the mass spectrum and the same diffusion coefficient was observed in DOSY-NMR spectrum. Thus, the results of $^1\text{H-NMR}$, DOSY-NMR and high-resolution mass spectroscopy demonstrate that assembly of dissymmetric ligand and Zn cation provides two linear regioisomeric helicates. The separation of the two isomers by chromatography is virtually impossible because of their similar polarity. Crystallization has been considered as an alternative separation method. However, only precipitates in most cases were obtained so far. Upon vapour diffusion of Et_2O into a $\text{CHCl}_3/\text{MeOH}$ mixture of **54** and $\text{Zn}(\text{OAc})_2$, few single crystals of helicate **58** were obtained and characterized by X-Ray diffraction. In the crystal (monoclinic *P*2/*n*), only the isomer with the amide moieties on the same side of the helicate is present. Owing to H-bonding interactions between the amide groups of neighboring helicates ($d_{\text{NH}\cdots\text{O}} = 2.022$ Å, $\alpha_{\text{NH}\cdots\text{O}} = 170.27^\circ$, Figure), a 1D network is formed. In the case of the bis-bisdipyrin ligand **57**, a single species was isolated that according to mass spectrometry is a tetranuclear bis-helicate complex. Attempts at

crystallizing this compound have so far been unsuccessful. Finally, the study of the assembly of the four novel dissymmetric 2,2'-bisdipyrin derivatives with other metal centers will be achieved in the future.



Scheme 9: Synthesis of isomers of Zn helicates with dissymmetric 2,2'-bisdipyrin derivatives **54-56**.

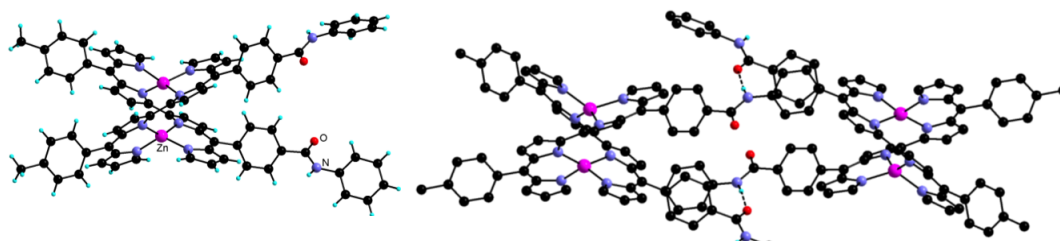


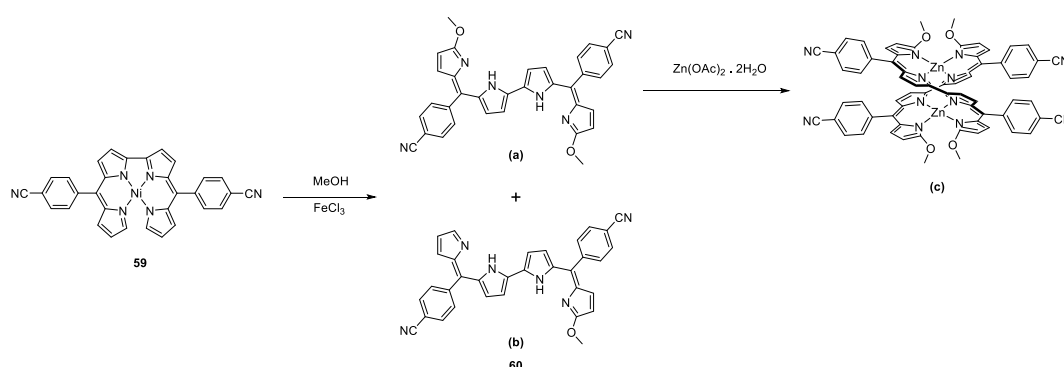
Figure 18: Structure of the Zn helicate **58** (left) and 1D network based on hydrogen bond (right).

II.4 Conclusion and perspectives

In conclusion, the first part of this chapter focused on the design and preparation of a novel 2,2'-bis-dipyrin ligand bearing peripheral *p*-benzaldehyde units. Its assembly with Zn(II) cations leads to the formation of a linear binuclear helicate, featuring the reactive aldehyde groups on each side of the complex at a relative distance of *ca* 5.8 Å according to the structure determination by single-crystal X-Ray diffraction. This pre-organization of the two groups at the periphery resulting from the template effect of the Zn(II) binding has been taken advantage of for the strapping of the helicate upon reaction with an appropriately chosen diamine, *m*-xylylenediamine. Slow addition of the latter to a dilute solution of the helicate in CHCl₃ in the presence of catalytic amount of TFA afforded quantitatively the strapped tetra-imine helicate as demonstrated by ¹H- and ¹³C-NMR spectroscopy and high-resolution mass spectrometry. Reduction by NaBH₃CN afforded the tetra-amine analogue **6**. In the future, other reactive groups such as coordinating linker for

the formation of a novel type of strapped helicates will be investigated. This should allow the formation of infinite heterometallic networks with high complexity.

The second part was centred on the introduction of the additional *p*-benzoic acid on one/both side of the 2,2'-bisdipyrrin backbone, which led to the formation of novel symmetric and dissymmetric amide-appended 2,2-bisdipyrrin derivatives. The assembly of these novel ligands and Zn cation towards binuclear linear helicates has been explored. As mentioned above, future work will focus on the use of these functionalized 2,2-bisdipyrrin ligands for the construction of other assemblies.



Scheme 10: The synthesis of α, α' -dimethoxy 2,2'-bisdipyrrin derivative and the corresponding helicate.

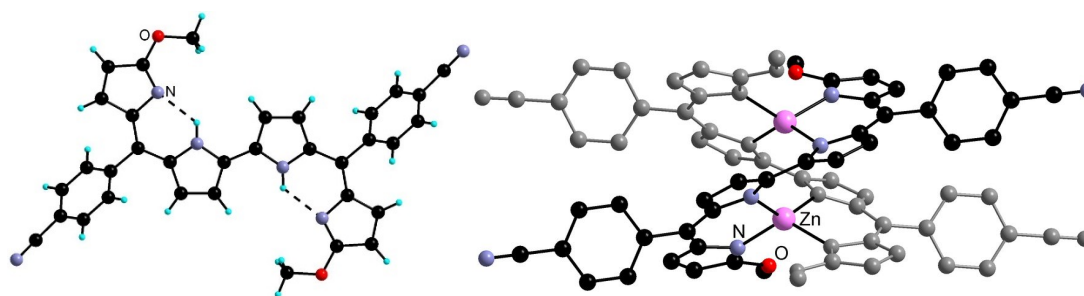


Figure 19: The crystal structures of ligand **60(a)** and helicate **60(c)**.

More recently, the Xie group reported the α -alkoxylation with methanol of the pentafluorophenyl functionalized 2,2'-bisdipyrrin ligand in the presence of iron(III) chloride.²⁴ This publication opened a new avenue for the functionalization of 2,2'-bisdipyrrin ligands at the α, α' -positions. For example, this reactivity could be exploited for the design of novel α -2,2'-bisdipyrrin derivatives by using different alcohols

²⁴ J. Kong, Q. Li, M. Li, X. Li, X. Liang, W. Zhu, H. Ågren and Y. Xie, *Dyes and Pigments.*, **2017**, 137, 430.

incorporating a reactive or a coordinating group for example. The impact of these new functionalized ligands on the arrangement of molecular networks will be studied. A preliminary investigation has been performed by Victor Koehler, master 1 student in the laboratory in the spring 2017.²⁵ The *meso*-benzonitrile-appended bisdipyrrin has been first considered for functionalization with various alcohols as illustrated for the case of MeOH in Scheme 10. The reaction conditions were optimized allowing isolation and characterization of the symmetrical ligand **60(a)** and its corresponding linear Zn(II) helicate **60(c)**. In addition, the crystal structures of these compounds were also determined by X-ray diffraction (Figure 19).

In the future, other functional alcohols will be explored such as (*S*)-2-methylbutan-1-ol possessing a stereocenter and 5-hexen-1-ol bearing a terminal double bond. Furthermore, the helical complexes can be seen as metallatectons to prepare heterometallic molecular networks in the presence of Ag(I). A study focusing on the influence of the alkoxy groups position on the Ag- π interactions within the molecular networks would be interesting.

²⁵ V. Koehler, Master 1 dissertation, University of Strasbourg, France, 2017.

- ¹ (a) J.-M. Lehn, A. Rigault, J. Siegel, J. Harrowfield, B. Chevrier and D. Moras, *Proc. Natl. Acad. Sci. USA.*, **1987**, *84*, 2565. (b) C. Piguet, G. Bernardinelli and G. Hopfgartner, *Chem. Rev.*, **1997**, *97*, 2005. (c) A. Williams, *Chem. Eur. J.*, **1997**, *3*, 15. (d) J.-M. Lehn, *Chem. Eur. J.*, **2000**, *6*, 2097. (e) M. Albrecht, *Chem. Rev.*, **2001**, *101*, 3457. (f) H. Miyake and H. Tsukube, *Chem. Soc. Rev.*, **2012**, *41*, 6977.
- ² B. Hasenknopf, J.-M. Lehn, B. O. Kneisel, G. Baum and D. Fenske, *Angew. Chem. Int. Ed.*, **1996**, *35*, 1836.
- ³ B. Hasenknopf, J.-M. Lehn, N. Boumediene, A. Dupont-Gervais, A. Van Dorsselaer, B. Kneisel and D. Fenske, *J. Am. Chem. Soc.*, **1997**, *119*, 10956.
- ⁴ (a) J. Bourlier, A. Jouaiti, N. Kyritsakas-Gruber, L. Allouche, J.-M. Planeix and M. W. Hosseini, *Chem. Commun.*, **2008**, 6191. (b) J.-F. Ayme, J. E. Beves, C. J. Campbell and D. A. Leigh, *Chem. Soc. Rev.*, **2013**, *42*, 1700. (c) C. J. Bruns and J. F. Stoddart, *The nature of the mechanical bond. From molecules to machines*. **2017**, John Wiley & Sons.
- ⁵ (a) C. O. Dietrich-Buchecker and J.-P. Sauvage, *Angew. Chem. Int. Ed. Engl.*, **1989**, *28*, 189. (b) C. O. Dietrich-Buchecker, Jean Guilhem, C. Pascard and J.-P. Sauvage, *Angew. Chem. Int. Ed. Engl.*, **1990**, *29*, 1154.
- ⁶ M. Bröring, Beyond dipyrins: Coordination interaction and templated macrocyclizations of open-chain oligopyrroles, in *Handbook of Porphyrin Science*, **2010**, vol. 8, p. 343
- ⁷ G. Struckmeier, U. Thewalt and J. -H. Furhop, *J. Am. Chem. Soc.*, **1976**, *98*, 278.
- ⁸ (a) Y. -J. Zhang, A. Thompson, S. J. Rettig and D. Dolphin, *J. Am. Chem. Soc.*, **1998**, *120*, 13537. (b) R. G. Khoury, L. Jaquinod and K. M. Smith, *Tetrahedron.*, **1998**, *54*, 2339. (c) M. Bröring, S. Link, C. D. Brandt and E. Cónsul Tejero, *Eur. J. Inorg. Chem.*, **2007**, 1661. (d) T. Hashimoto, T. Nishimura, J. M. Lin, D. Khim and H. Maeda, *Chem. Eur. J.*, **2010**, *16*, 11653. (e) E. V. Antina, R. T. Kuznetsova, L. A. Antina, G. B. Guseva, N. A. Dudina, A. I. V'yugin and A. V. Solomonov, *Dyes Pigments*, **2015**, *113*, 664.
- ⁹ H. Maeda, T. Nishimura, R. Akuta, K. Takaishi, M. Uchiyamabd and A. Muranaka, *Chem. Sci.*, **2013**, *4*, 1204.
- ¹⁰ S. A. Baudron, H. Ruffin and M. W. Hosseini, *Chem. Commun.*, **2015**, *51*, 5906.
- ¹¹ H. Ruffin, S. A. Baudron, D. Salazar-Mendoza and M. W. Hosseini, *Chem. Eur. J.*, **2014**, *20*, 2449.
- ¹² S. A. Baudron and M. W. Hosseini, *Chem. Commun.*, **2016**, *52*, 13000.
- ¹³ (a) P. T. Corbett, J. Leclaire, L. Vial, K. R. West, J.-L. Wietor, J. K. M. Sander and S. Otto, *Chem. Rev.*, **2006**, *106*, 3652. (b) J. M. Lehn, *Chem. Soc. Rev.*, **2007**, *36*, 151. (c) M. E. Belowitch and J. F. Stoddart, *Chem. Soc. Rev.*, **2012**, *41*, 2003. (d) A. M. Castilla, W. J. Ramsay and J. R. Nitschke, *Acc. Chem. Res.*, **2014**, *47*, 2063.
- ¹⁴ (a) C. Bruckner, Y. Zhang, S. J. Rettig, D. Dolphin, *Inorg. Chim. Acta.*, **1997**, *263*, 279. (b) B. J. Littler, M. A. Miller, C. H. Hung, R. W. Wagner, D. F. O'Shea, P. D. Boyle and J. S. Lindsey, *J. Org. Chem.*, **1999**, *64*, 1391. (c) P. D. Rao, S. Dhanalekshmi, B. J. Littler and J. S. Lindsey, *J. Org. Chem.*, **2000**, *65*, 7323.
- ¹⁵ R. Sakamoto, K. Hoshiko, Q. Liu, T. Yagi, T. Nagayama, S. Kusaka, M. Tsuchiya, Y. Kitagawa, W.-Y. Wong and H. Nishihara, *Nat. Commun.*, **2015**, *6*, 6713.
- ¹⁶ H. S. Gill, I. Finger, I. Božidarević, F. Szydlo and M. J. Scott, *New J. Chem.*, **2005**, *29*, 68.
- ¹⁷ (a) L. Yu, K. Muthukumaran, I. V. Sazanovich, C. Kirmaier, E. Hindin, J. R. Diers, P. D. Boyle, D. F. Bocian, D. Holten and J. S. Lindsey, *Inorg. Chem.*, **2003**, *42*, 6629. (b) K. Muthukumaran, S. H. H. Zaidi, L. Yu, P. Tham Yongkit, M. E. Calder, D. S. Sharada and J. S. Lindsey, *J. Porphyrins Phthalocyanines.*, **2005**, *9*, 745.
- ¹⁸ S. A. Baudron, *Dalton. Trans.*, **2013**, *42*, 7498.
- ¹⁹ S. A. Baudron, D. Salazar-Mendoza and M. W. Hosseini, *CrystEngComm.*, **2009**, *11*, 1245.
- ²⁰ (a) M. Brellier, G. Duportail and R. Baati, *Tetrahedron. Lett.*, **2010**, *51*, 1269. (b) E. Rampazzo,

S. Bonacchi, D. Genovese, R. Juris, M. Montalti, V. Paterlini, N. Zaccheroni, C. Dumas-Verdes, G. Clavier, R. Méallet-Renault, and L. Prodi, *J. Phys. Chem. C.*, **2014**, *118*, 9261.

²¹ L. C. Chan and B. G. Cox, *J. Org. Chem.*, **2007**, *72*, 8863.

²² A. Béziau, S. A. Baudron, G. Rogez and M. W. Hosseini, *CrystEngComm.*, **2013**, *15*, 5980.

²³ J. Kong, Q. Li, M. Li, X. Li, X. Liang, W. Zhu, H. Ågren and Y. Xie, *Dyes and Pigments.*, **2017**, *137*, 430.

²⁴ V. Koehler, Master 1 dissertation, University of Strasbourg, France, **2017**.

Conclusion and Perspectives

Conclusion and Perspectives

1. Conclusion

This PhD. work focused on the development of new approaches for the functionalization of mono- and bis-dipyrrin derivatives at positions 1, 5, 9. These novel synthesized dipyrrin derivatives can be used as ligands with various metal centers leading to the construction of discrete entities and/or infinite periodic molecular networks.

In Chapter I, taking advantage of the reactivity towards aldehydes *via* a Knoevenagel reaction, the functionalization by coordinating groups in positions 1 and 9 as well as the introduction of another coordinating or solubilizing unit in position 5 have been explored leading to a series of new 1,9-divinyldipyrrin derivatives. These compounds have been characterized in solution by standard analytical methods and, for some of them, in the crystalline state by X-Ray diffraction. Using these ligands, BODIPYs and homoleptic Zn(II) complexes have been prepared and studied in solution and in the solid state. The photophysical properties of the B(III) and Zn(II) based species have been investigated and their emission was measured in DMF solution. In addition, some of these luminescent complexes have been successfully used as tectons for the construction of coordination polymers in the solid state. In particular, BODIPY **10** bearing peripheral benzonitrile groups at positions 1 and 9 was found to form a [2+2] metallamacrocyclic motif showing an anion and solvent dependent organization in the crystalline state. In the solid state, these assemblies showed weak emission.

In Chapter II, the research focused on the synthesis of novel species *via* a post-functionalization of 2,2'-bisdipyrrin derivatives featuring reactive groups at their periphery such as an aldehyde, amine or carboxylic acid moiety. Such tetrapyrrolic open chain ligands are of interest owing to their reported ability to form helicates upon assembly with Zn(II) cations. The novel 2,2'-bisdipyrrin derivative bearing benzaldehyde units at the *meso* position was first developed and the template effect of the Zn(II) complexation leading to a predefined organization of the reactive carbonyls on each strand was exploited for the formation of a strapped helicate based on imine bond upon reaction with an appropriately chosen diamine, *m*-xylylenediamine. A second investigation centred on the introduction of *p*-benzoic acid on one/both side of the 2,2'-bisdipyrrin backbone was also carried out. This led to the formation of novel symmetric and dissymmetric

amide-bearing-2,2'-bisdipyrrin derivatives. The assembly of these novel ligands with Zn(II) and Ni(II) cations has been particularly explored. Mono- and bi-nuclear complexes that can be regarded as potential metallatectons have been thus prepared and characterized.

2. Perspectives

Future work should focus on the preparation of X-Ray quality single crystals of the molecular networks mentioned above in chapter I and II for the study of their arrangement in the solid state. Use of these synthetic functionalized mono- or bis-dipyrrin derivatives for the preparation of other assemblies with other different metal centers and of periodic molecular networks could also be investigated. One can imagine that the effect of anion, solvent molecule and the nature of metal centers and tectons may lead to molecular networks differing in their arrangement, dimensionality and properties.

In the approach developed in this thesis, prior to complexation of metal centers, both structural and binding propensity of the organic tecton are coded through its synthesis using non-reversible bond formation processes. In the future, this feature could be overcome by investigating the possibility of combining reversible bond formation and crystallization processes. This, in principle, should allow to explore a larger landscape by forming libraries of organic- and/or metallatectons and their combinations with different metal centers in order to generate coordination polymers of the CMOF type, *i.e.* crystalline architectures constructed by self-assembly of metal centers or complexes *via* the formation of reversible covalent bonds instead of purely coordination bond. This concept has been only recently employed for the formation of such architectures.¹ Based on the research explored during this thesis, in particular the strapped helicate, it seems interesting to propose to combine purely organic- or metalla-tectons based on the dipyrin backbone bearing peripheral reactive groups such as aldehyde, amine or salicaldehyde etc. for the preparation of CMOFs and CM'MOFs (Figure 1). However, a rather fine tuning of the reversible organic condensation kinetics and that of the crystallization event should be

¹ (a) A. Dutta, K. Koh, A. G. Wong-Foy and A. J. Matzger, *Angew. Chem. Int. Ed.*, **2015**, *54*, 3983. (b) Y. Liu, Y. Ma, Y. Zhao, X. Sun, F. Gandara, H. Furukawa, Z. Liu, H. Zhu, C. Zhu, K. Suenaga, P. Oleynikov, A. S. Alshammari, X. Zhang, O. Terasaki and O. M. Yaghi, *Science*, **2016**, *351*, 365. (c) H. L. Nguyen, F. Gandara, H. Furukawa, T. L. H. Doan, K. E. Cordova and O. M. Yaghi, *J. Am. Chem. Soc.*, **2016**, *138*, 4330.

required to realize this approach. Although this is very difficult to achieve, one may find proper experimental conditions such as temperature, concentration of components, presence of small amounts of acids and water content to tune the kinetics of the two processes.

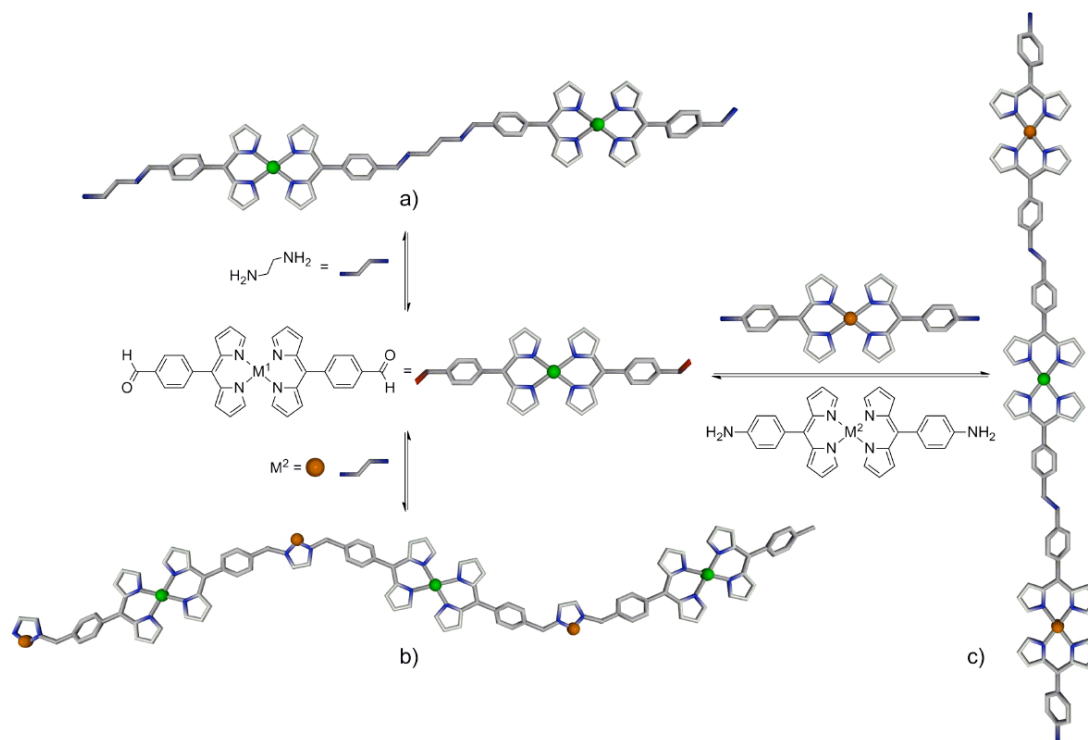


Figure 1: Example of the use of an aldehyde appended metal complex for the construction of CMOF by combination with a diamine (a), of CM'MOF upon assembly with a diamine and a metal center (b) or with an amine-appended metallatecton (c).

Some of the work developed in this PhD. work has already laid the foundation for exploring this strategy. Indeed, the optimized synthesis of 5-aminophenyl and 5-benzaldehydedipyrin has been established. Under basic conditions, these two ligands were converted into their conjugate base, which were used for the preparation of various complexes. The crystal structures of the latter were determined by X-Ray diffraction (Figure 2). Preliminary studies towards the formation of CMOFs based on these compounds has so far led to non-crystalline materials, clearly indicating that further work is needed to develop such architectures.

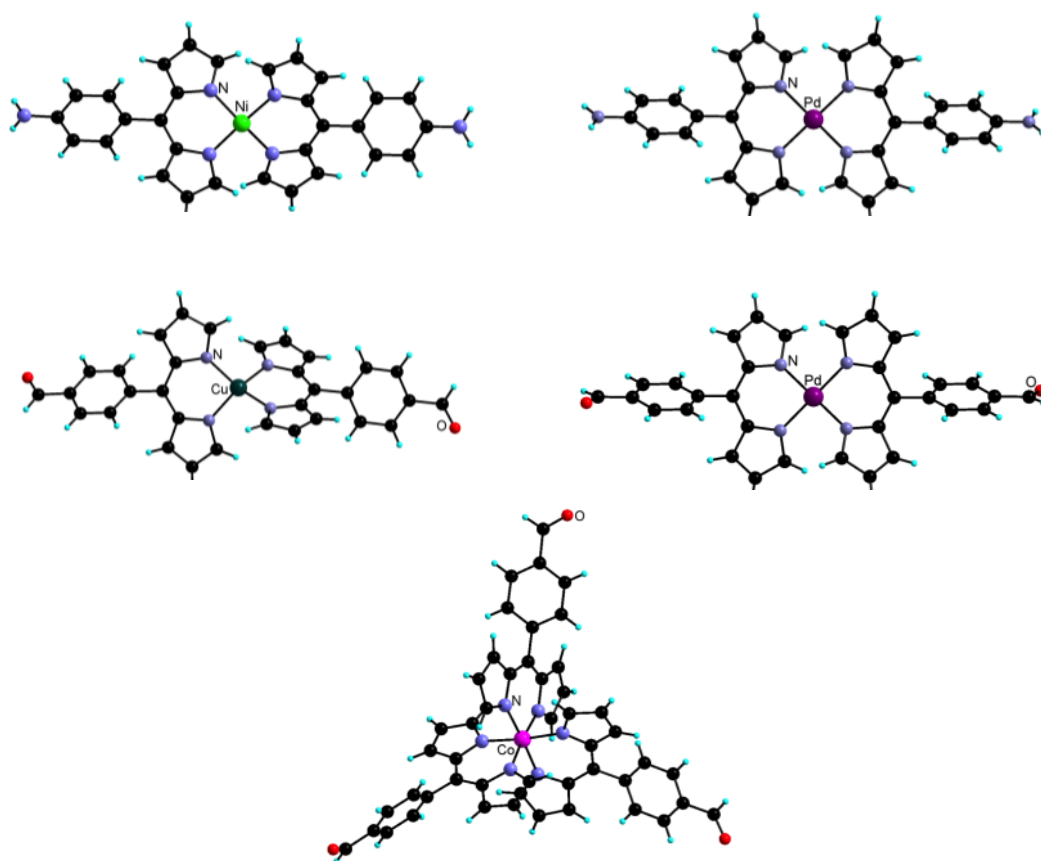


Figure 2: Crystal structures of already prepared aldehyde- or amino-appended dipyrinato complexes that can be considered for the preparation of CMOFs.

¹ (a) A. Dutta, K. Koh, A. G. Wong-Foy and A. J. Matzger, *Angew. Chem. Int. Ed.*, **2015**, 54, 3983. (b) Y. Liu, Y. Ma, Y. Zhao, X. Sun, F. Gandara, H. Furukawa, Z. Liu, H. Zhu, C. Zhu, K. Suenaga, P. Oleynikov, A. S. Alshammari, X. Zhang, O. Terasaki and O. M. Yaghi, *Science*, **2016**, 351, 365. (c) H. L. Nguyen, F. Gandara, H. Furukawa, T. L. H. Doan, K. E. Cordova and O. M. Yaghi, *J. Am. Chem. Soc.*, **2016**, 138, 4330.

Experimental section

Experimental section

V.1 Solvents and Products

Anhydrous dichloromethane, toluene, diethyl ether and THF obtained from commercial sources were purified by Dry Solvent Station GT s100. NEt_3 was distilled over KOH. Ethylenediamine was purified by distillation under argon. Pyrrole was purified by filtration on alumina. All other solvents (analytical grade or HPLC grade) and available chemical products were purchased from commercial sources and used without further purification.

V.2 Analysis and Characterization

V.2.1 Nuclear magnetic resonance (NMR)

^1H -NMR and ^{13}C -NMR spectra were recorded at 25 °C on Bruker Advance AV 300 (300 MHz), 400 (400 MHz) or 500 (500 MHz) spectrometers with the deuterated solvent and residual solvent as internal reference (CDCl_3 : 7.26 ppm for ^1H , 77.16 ppm for ^{13}C ; CD_2Cl_2 : 5.32 ppm for ^1H , 53.84 ppm for ^{13}C ; DMSO: 2.50 ppm for ^1H , 39.52 ppm for ^{13}C ; MeOD-d_4 : 3.31 ppm for ^1H , 49.00 ppm for ^{13}C , Acetone- d_6 : 2.05 ppm for ^1H , 29.84 ppm for ^{13}C , THF- d_8 : 3.58 ppm for ^1H , 67.21 ppm for ^{13}C). All chemical shifts are given in ppm and coupling constant (J) in Hz. The abbreviations of spin multiplicities are given as follows: s = singlet, d = doublet, dd = doublet of doublet, m = multiplet, br = broad.

V.2.2 Mass spectrometry

Mass spectrometry was performed at Service de Spectrométrie de Masse-Université de Strasbourg. ESI-MS standard or ESI-HRMS was recorded on Thermoquest AQA Navigator® with time of flight detector (TOF).

V.2.3 Elemental analyses

Elemental analyses were performed on a Thermo Scientific Flash 2000 by the Service de Microanalyse de l'Université de Strasbourg.

V.2.4 Photophysical analyses

UV-Visible spectra in solution and in the solid state were measured on a Perkin Elmer UV/Vis spectrometer lambda 650S. Wavelengths (λ) are given in nm and molar absorption coefficients (ϵ) are given in $\text{mol}^{-1} \cdot \text{L} \cdot \text{cm}^{-1}$.

Luminescence spectra in solution were recorded on a Perkin Elmer LS 55 spectrometer. Emission and excitation spectra were corrected for source intensity (lamp and grating) and emission spectral response (detector and grating) by standard correction curves. All solvents used were of spectrometric grade.

V.2.5 FT-IR

FT-IR spectra were obtained on a Perkin Elmer FT-IR Spectrometer Spectrum equipped with a UATR (diamond).

V.2.6 X-ray diffraction

X-ray crystallography data were collected by Dr. Stéphane Baudron on a Bruker APEX8 CCD diffractometer equipped with an Oxford Cryosystem liquid N_2 device at 173(2) K and Mo-K_α ($\lambda = 0.71073 \text{ \AA}$) radiation operating at 50 kV and 600 mA. The structures were solved using SHELXS-97 and refined by full matrix least-squares on F^2 using SHELXL-2014 with anisotropic thermal parameters for all non-hydrogen atoms. The hydrogen atoms were introduced at calculated positions and were not refined (riding model).

V.2.7 Powder X-ray diffraction

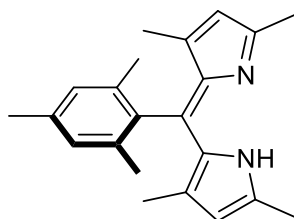
The powder X-ray diffraction (PXRD) patterns were carried out on a Bruker D8 AV diffractometer using Cu-K_α radiation ($\lambda = 1.5406 \text{ \AA}$) operating at 40 KV and 40 mA with a scanning rate between 3.8 and 70° by a scan step size of 2°/min.

V.3 Synthesis

All air and/or moisture sensitive reaction were performed under argon using distilled solvents. For light sensitive reactions, aluminum foil was used for protection. Column

chromatography was performed using either silica gel (MERCK, type 60) or aluminum oxide (MERCK, type 90). Thin-layer chromatography (TLC) was carried out on either silica plates of type 60F₂₅₄ provided by Merck Millipore or aluminum oxide plates of Polygram Alox G/UV₂₅₄ type provided by Macherey-Nagel. The Dean-Stark instrument was used to remove water in all Knoevenagel type reactions.

Compound 1:



Chemical Formula: C₂₂H₂₆N₂
Molecular Weight: 318.46

Mesitaldehyde (1.5 mL; 10.2 mmol) and 2,4-dimethylpyrrole (2.1 mL; 20.4 mmol) were dissolved in dichloromethane (75 mL) under an argon atmosphere. Trifluoroacetic acid TFA (2 drops) was added and the mixture was stirred at room temperature overnight. The reaction was monitored by TLC. The resulting mixture was evaporated under reduced pressure and the residue was dissolved in THF (40 mL). Then, a solution of DDQ (2.1 g; 9.25 mmol) in THF (40 mL) was added dropwise. The mixture was stirred at room temperature overnight. After evaporation under reduced pressure, the residue was purified by column chromatography (SiO₂, CH₂Cl₂/Et₃N: 99/1) affording **1** as a yellow solid (1.8 g, 56%).

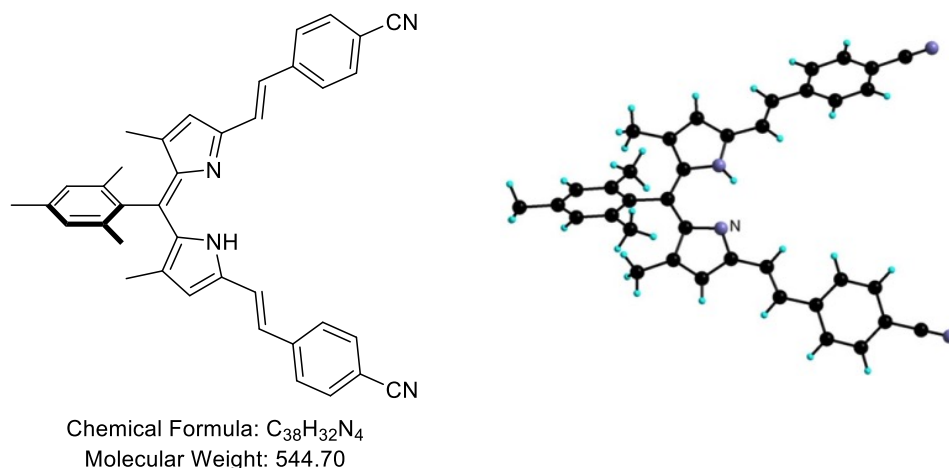
¹H-NMR (500 MHz, CDCl₃, 25 °C): δ = 6.89 (s, 2H, PhH), 5.85 (s, 2H, pyrroleH), 2.34 (s, 6H, CH₃), 2.32 (s, 3H, CH₃), 2.09 (s, 6H, CH₃), 1.29 (s, 6H, CH₃) ppm.

¹³C-NMR (125 MHz, CDCl₃, 25 °C): δ = 151.3, 139.8, 137.9, 137.7, 135.8, 135.6, 134.1, 128.7, 119.1, 21.9, 19.7, 16.3, 13.8 ppm.

MS (ESI): m/z (M+H)⁺ calcd for C₂₂H₂₇N₂: 319.22, Found 319.22.

Elem. Anal. Calcd for C₂₂H₂₆N₂: C 82.97; H 8.23; N 8.80. Found C 82.34; H 8.23; N 8.63

Compound 2:



Mesityldipyrrin **1** (0.5 g; 1.57 mmol), 4-cyanobenzaldehyde (1.15 g; 8.77 mmol), piperidine (1.5 mL) and *p*-TSA (cat.) were dissolved in distilled toluene (50 mL) under an argon atmosphere. The mixture was stirred under refluxing conditions for 24 hours. The resulting mixture was evaporated under reduced pressure and the residue was purified by column chromatography (SiO₂, CH₂Cl₂/Et₃N: 99/1) affording **2** as a purple solid (0.5 g, 58%). Single crystals were obtained by slow evaporation of a solution of the ligand in toluene.

¹H NMR (500 MHz, CD₂Cl₂, 25 °C): δ = 7.68 (d, *J* = 8.4 Hz, 4H, PhH), 7.64 (d, *J* = 8.4 Hz, 4H, PhH), 7.27 (d, *J* = 16.4 Hz, 2H, C=CH), 7.15 (d, *J* = 16.4 Hz, 2H, C=CH), 6.98 (s, 2H, PhH), 6.46 (s, 2H, pyrroleH), 2.35 (s, 3H, CH₃), 2.10 (s, 6H, CH₃), 1.38 (s, 6H, CH₃) ppm.

¹³C NMR (125 MHz, CD₂Cl₂, 25 °C): δ = 150.4, 141.5, 141.0, 139.5, 138.6, 138.4, 135.6, 133.3, 132.7, 129.7, 128.9, 127.1, 124.4, 119.1, 119.0, 110.9, 21.0, 19.5, 13.6 ppm.

HRMS (ESI): *m/z* (M+H)⁺ calcd for C₃₈H₃₃N₄: 545.2700, Found 545.2686.

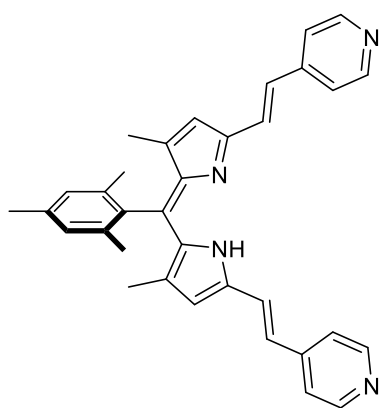
λ_{max} (CH₂Cl₂)/nm (ε/mol⁻¹ L cm⁻¹): 350 (78600), 575 (49700).

IR (ATR): 2220 cm⁻¹ (CN)

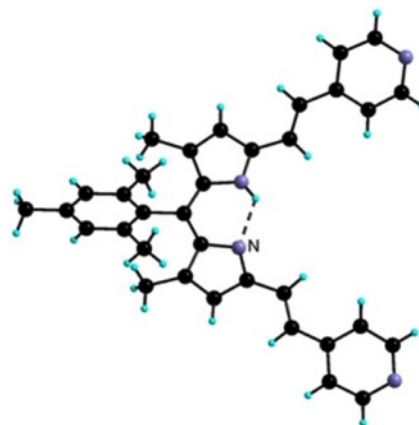
Crystallographic data for compound 2

Formula	C ₃₈ H ₃₂ N ₄
Formula weight	544.67
Temperature	173(2) K
Wavelength	0.71073 Å
Crystal system	Monoclinic
Space group	<i>P</i> 2 ₁ / <i>n</i>
Unit cell dimensions	<i>a</i> = 9.9301(8) Å <i>α</i> = 90°. <i>b</i> = 23.0445(19) Å <i>β</i> = 99.355(5)°. <i>c</i> = 13.4889(11) Å <i>γ</i> = 90 °.
Volume	3045.7(4) Å ³
<i>Z</i>	4
Density (calculated)	1.188 Mg/m ³
Absorption coefficient	0.070 mm ⁻¹
<i>F</i> (000)	1152
Crystal size	0.120 x 0.050 x 0.050 mm ³
Theta range for data collection	2.259 to 30.224°
Index ranges	-14 ≤ <i>h</i> ≤ 14, -32 ≤ <i>k</i> ≤ 32, -18 ≤ <i>l</i> ≤ 19
Reflections collected	81015
Independent reflections	8377 [<i>R</i> (int) = 0.1358]
Completeness to theta = 25.242°	97.2 %
Absorption correction	Semi-empirical from equivalents
Max. and min. transmission	0.995 and 0.991
Refinement method	Full-matrix least-squares on <i>F</i> ²
Data / restraints / parameters	8377 / 0 / 384
Goodness-of-fit on <i>F</i> ²	0.999
Final <i>R</i> indices [<i>I</i> > 2σ(<i>I</i>)]	<i>R</i> ₁ = 0.0657, <i>wR</i> ₂ = 0.1454
<i>R</i> indices (all data)	<i>R</i> ₁ = 0.1698, <i>wR</i> ₂ = 0.1871
Largest diff. peak and hole	0.267 and -0.245 e.Å ⁻³

Compound 3:



Chemical Formula: $C_{34}H_{32}N_4$
Molecular Weight: 496.66



Mesityldipyrin **1** (0.5 g; 1.57 mmol), 4-pyridinecarboxaldehyde (0.42 g; 3.93 mmol), piperidine (1.5 mL) and *p*-TSA (cat.) were dissolved in distilled toluene (50 mL) under argon. The mixture was stirred at reflux for 3 days. After evaporation under reduced pressure, the residue was purified by column chromatography (SiO_2 , CH_2Cl_2/Et_3N : 99/1) affording **3** as a purple solid (0.39 g, 50%).

1H NMR (500 MHz, $CDCl_3$, 25 °C): δ = 8.55 (d, J = 4.9 Hz, 4H, pyH), 7.37 (d, J = 4.9 Hz, 4H, pyH), 7.30 (d, J = 16.2 Hz, 2H, C=CH), 7.04 (d, J = 16.2 Hz, 2H, C=CH), 6.95 (s, 2H, PhH), 6.43 (s, 2H, pyrroleH), 2.35 (s, 3H, CH_3), 2.12 (s, 6H, CH_3), 1.39 (s, 6H, CH_3) ppm.

^{13}C NMR (125 MHz, $CDCl_3$, 25 °C): δ = 150.5, 150.2, 144.3, 141.2, 139.5, 139.2, 138.4, 135.7, 133.3, 129.0, 129.0, 125.4, 121.0, 119.4, 21.4, 19.8, 14.0 ppm.

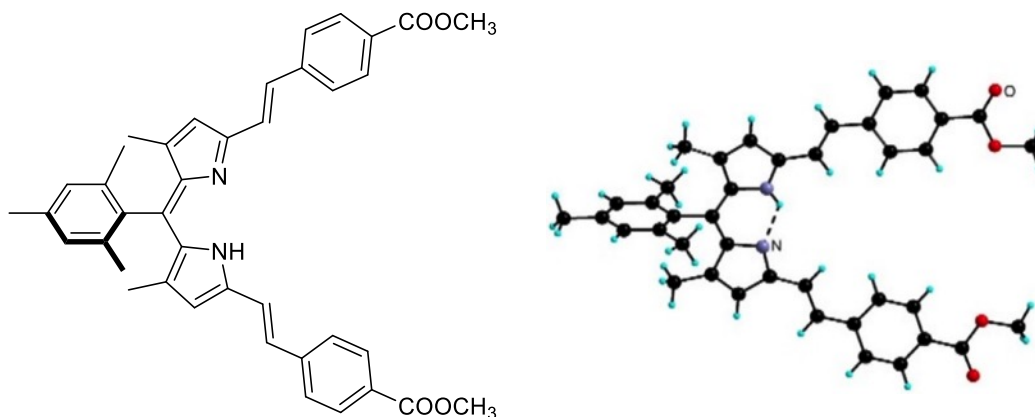
HRMS (ESI): m/z ($M+H$)⁺ calcd for $C_{34}H_{33}N_4$: 497.2700, Found 497.2730.

λ_{max} (CH_2Cl_2)/nm ($\epsilon/mol^{-1} L cm^{-1}$): 336 (47900), 560 (29700).

Crystallographic data for compound 3

Formula	C ₃₄ H ₃₂ N ₄
Formula weight	496.63
Temperature	180(2) K
Wavelength	0.71073 Å
Crystal system	Orthorhombic
Space group	<i>Pbcn</i>
Unit cell dimensions	$a = 11.1980(5) \text{ Å}$ $\alpha = 90^\circ$. $b = 12.4554(5) \text{ Å}$ $\beta = 90^\circ$. $c = 19.3724(8) \text{ Å}$ $\gamma = 90^\circ$.
Volume	2702.0(2) Å ³
Z	4
Density (calculated)	1.221 Mg/m ³
Absorption coefficient	0.072 mm ⁻¹
F(000)	1056
Crystal size	0.100 x 0.070 x 0.030 mm ³
Theta range for data collection	2.103 to 30.147 °
Index ranges	-15 ≤ h ≤ 15, -17 ≤ k ≤ 16, -27 ≤ l ≤ 26
Reflections collected	62415
Independent reflections	3995 [R(int) = 0.0545]
Completeness to theta = 25.242°	100.0 %
Absorption correction	Semi-empirical from equivalents
Refinement method	Full-matrix least-squares on F ²
Data / restraints / parameters	3995 / 0 / 177
Goodness-of-fit on F ²	1.120
Final R indices [I > 2σ(I)]	$R_1 = 0.0611$, $wR_2 = 0.1424$
R indices (all data)	$R_1 = 0.1110$, $wR_2 = 0.1769$
Largest diff. peak and hole	0.334 and -0.282 e.Å ⁻³

Compound 4:



Chemical Formula: $C_{40}H_{38}N_2O_4$
Molecular Weight: 610.75

Mesityldipyrin **1** (0.5 g; 1.57 mmol), methyl 4-formylbenzoate (1.2 g; 7.07 mmol), piperidine (1.5 mL) and *p*-TSA (cat.) were dissolved in distilled toluene (50 mL) under argon. The mixture was stirred under refluxing conditions for 2 days. The resulting mixture was evaporated under reduced pressure and the residue was washed with Et_2O to remove the remaining excess aldehyde. The crude product was purified by column chromatography (SiO_2 , CH_2Cl_2 /Cyclohexane/ Et_3N : 97/2/1) affording **4** as a purple solid (0.6 g, 63%).

1H NMR (500 MHz, CD_2Cl_2 , 25 °C): δ = 8.05 (d, J = 8.1 Hz, 4H, PhH), 7.64 (d, J = 8.1 Hz, 4H, PhH), 7.28 (d, J = 16.3 Hz, 2H, C=CH), 7.21 (d, J = 16.3 Hz, 2H, C=CH), 6.98 (s, 2H, PhH), 6.45 (s, 2H, pyrroleH), 3.92 (s, 6H, $COOCH_3$), 2.35 (s, 3H, CH_3), 2.12 (s, 6H, CH_3), 1.39 (s, 6H, CH_3) ppm.

^{13}C NMR (125 MHz, CD_2Cl_2 , 25 °C): δ = 166.9, 150.9, 141.9, 141.1, 139.6, 138.7, 138.5, 136.0, 130.9, 130.4, 129.8, 129.2, 126.9, 123.8, 119.3, 52.4, 21.3, 19.8, 13.9 ppm.

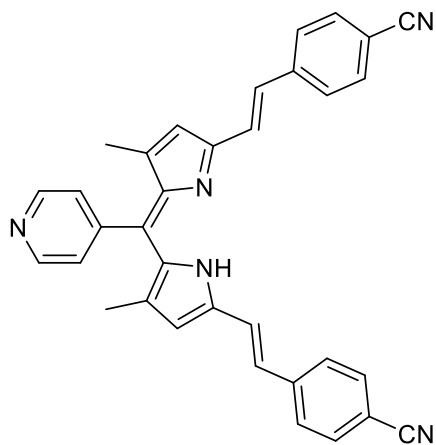
HRMS (ESI): m/z ($M+H$)⁺ calcd for $C_{40}H_{39}N_2O_4$: 611.2904, Found 611.2940.

λ_{max} (CH_2Cl_2)/nm ($\epsilon/mol^{-1} L cm^{-1}$): 350 (86400), 574 (49700).

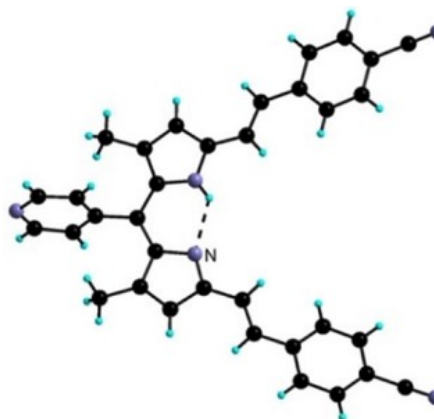
Crystallographic data for compound 4

Formula	$C_{40}H_{38}N_2O_4$
Formula weight	610.72
Temperature	173(2) K
Wavelength	0.71073 Å
Crystal system	Monoclinic
Space group	<i>Pc</i>
Unit cell dimensions	$a = 8.4576(4) \text{ Å}$ $\alpha = 90^\circ$. $b = 24.5157(10) \text{ Å}$ $\beta = 104.099(2)^\circ$. $c = 8.0013(3) \text{ Å}$ $\gamma = 90^\circ$.
Volume	1609.05(12) Å ³
Z	2
Density (calculated)	1.261 Mg/m ³
Absorption coefficient	0.081 mm ⁻¹
F(000)	648
Crystal size	0.100 x 0.070 x 0.030 mm ³
Theta range for data collection	1.661 to 30.211°
Index ranges	-11 ≤ h ≤ 11, -34 ≤ k ≤ 33, -9 ≤ l ≤ 11
Reflections collected	36806
Independent reflections	8658 [R(int) = 0.0345]
Completeness to theta = 25.242°	99.7 %
Absorption correction	Semi-empirical from equivalents
Max. and min. transmission	0.997 and 0.991
Refinement method	Full-matrix least-squares on F ²
Data / restraints / parameters	8658 / 2 / 422
Goodness-of-fit on F ²	1.048
Final R indices [I > 2σ(I)]	$R_I = 0.0500$, $wR_2 = 0.1235$
R indices (all data)	$R_I = 0.0723$, $wR_2 = 0.1360$
Largest diff. peak and hole	0.320 and -0.220 e.Å ⁻³

Compound 7:



Chemical Formula: $C_{34}H_{25}N_5$
Molecular Weight: 503.61



Compound **5** (0.28 g; 1 mmol), methyl 4-formylbenzoate (0.78 g; 6 mmol), piperidine (1.5 mL) and *p*-TSA (cat.) were dissolved in distilled toluene (25 mL) under an argon atmosphere. The mixture was stirred at reflux for 48 hours and was then evaporated under reduced pressure. The residue was washed with Et₂O to remove the remaining excess aldehyde. The crude product was purified by column chromatography (SiO₂, CH₂Cl₂/Cyclohexane/Et₃N: 97/2/1) affording dipyrrole **7** as a purple solid (0.26 g, 52%).

¹H NMR (500 MHz, CD₂Cl₂, 25 °C): δ = 8.74 (d, J = 5.8 Hz, 2H, pyH), 7.69 (d, J = 8.4 Hz, 4H, PhH), 7.65 (d, J = 8.4 Hz, 4H, PhH), 7.36 (d, J = 5.8 Hz, 2H, pyH), 7.27 (d, J = 16.3 Hz, 2H, C=CH), 7.16 (d, J = 16.3 Hz, 2H, C=CH), 6.51 (s, 2H, pyrroleH), 1.43 (s, 6H) ppm.

¹³C NMR (125 MHz, CD₂Cl₂, 25 °C): δ = 151.5, 150.8, 141.6, 141.5, 139.5, 133.1, 133.0, 130.9, 127.5, 127.5, 124.8, 124.5, 120.0, 119.2, 111.5, 15.2 ppm.

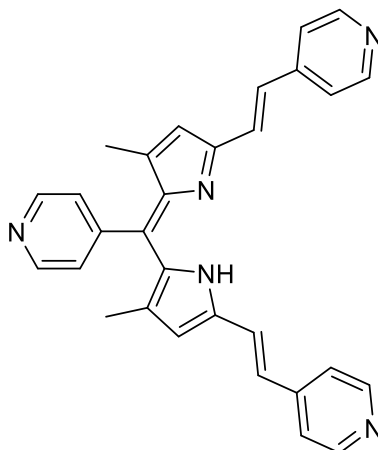
MS (ESI): m/z (M+H)⁺ calcd for C₃₄H₂₆N₅ : 504.22, Found 504.22.

λ_{max} (CH₂Cl₂)/nm ($\epsilon/\text{mol}^{-1} \text{ L cm}^{-1}$): 353 (51600), 580 (28000).

IR (ATR): 2222 cm⁻¹ (CN)

Crystallographic data for compound (7)₂(CHCl₃)

Formula	C ₆₉ H ₅₁ Cl ₃ N ₁₀
Formula weight	1126.54
Temperature	180(2) K
Wavelength	0.71073 Å
Crystal system	Triclinic
Space group	<i>P</i> -1
Unit cell dimensions	<i>a</i> = 8.7464(5) Å <i>α</i> = 68.647(2)°. <i>b</i> = 17.5398(12) Å <i>β</i> = 86.370(2)°. <i>c</i> = 20.3017(13) Å <i>γ</i> = 77.819(2)°.
Volume	2835.1(3) Å ³
<i>Z</i>	2
Density (calculated)	1.320 Mg/m ³
Absorption coefficient	0.216 mm ⁻¹
<i>F</i> (000)	1172
Crystal size	0.100 x 0.100 x 0.020 mm ³
Theta range for data collection	1.941 to 30.263°
Index ranges	-9 ≤ <i>h</i> ≤ 12, -24 ≤ <i>k</i> ≤ 24, -28 ≤ <i>l</i> ≤ 28
Reflections collected	48199
Independent reflections	15276 [<i>R</i> (int) = 0.0570]
Completeness to theta = 25.242°	95.7 %
Absorption correction	Semi-empirical from equivalents
Max. and min. transmission	0.997 and 0.991
Refinement method	Full-matrix least-squares on <i>F</i> ²
Data / restraints / parameters	15276 / 0 / 743
Goodness-of-fit on <i>F</i> ²	1.028
Final <i>R</i> indices [<i>I</i> > 2σ(<i>I</i>)]	<i>R</i> ₁ = 0.0907, <i>wR</i> ₂ = 0.2452
<i>R</i> indices (all data)	<i>R</i> ₁ = 0.1679, <i>wR</i> ₂ = 0.2957
Largest diff. peak and hole	1.287 and -1.121 e.Å ⁻³

Compound 8:

Chemical Formula: $C_{30}H_{25}N_5$

Molecular Weight: 455.57

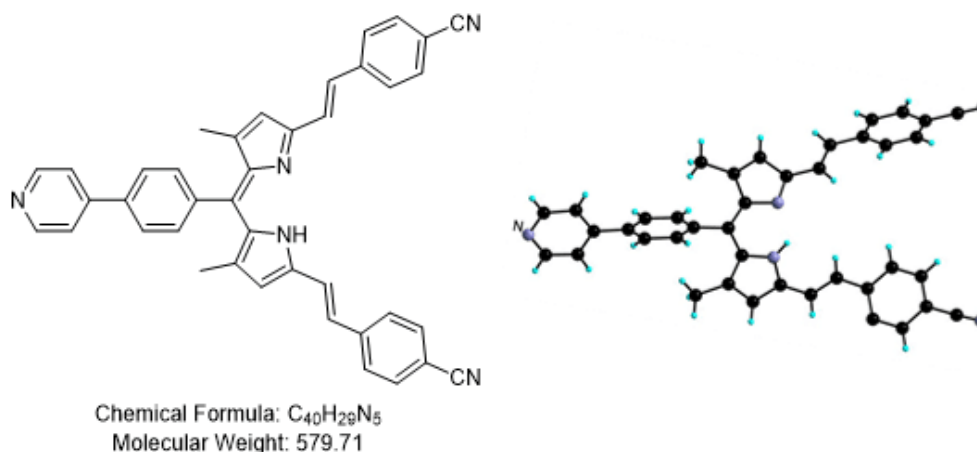
Compound **5** (0.46 g; 1.66 mmol), 4-pyridinecarboxaldehyde (0.80 g; 7.46 mmol), piperidine (1.5 mL) and *p*-TSA (cat.) were dissolved in distilled toluene (25 mL) under an argon atmosphere. The mixture was stirred at reflux for 48 hours. The resulting mixture was evaporated under reduced pressure and the residue was washed with Et₂O to remove the remaining excess aldehyde. The crude product was purified by column chromatography (SiO₂, CH₂Cl₂/Cyclohexane/Et₃N: 96/3/1) affording compound **8** as a purple solid (0.46 g, 62%).

¹H NMR (500 MHz, CD₂Cl₂, 25 °C): δ = 8.74 (d, J = 5.9 Hz, 2H, pyH), 8.6 (d, J = 6.2 Hz, 4H, pyH), 7.41 (d, J = 6.2 Hz, 4H, pyH), 7.36 (d, J = 5.9 Hz, 2H, pyH), 7.36 (d, J = 16.1 Hz, 2H, C=CH), 7.09 (d, J = 16.1 Hz, 2H, C=CH), 6.51 (s, 2H, pyrroleH), 1.43 (s, 6H, CH₃) ppm.

¹³C NMR (125 MHz, CD₂Cl₂, 25 °C): δ = 151.3, 150.7, 145.8, 144.2, 141.5, 139.4, 136.1, 130.2, 125.2, 124.8, 121.2, 120.1, 15.2 ppm.

MS (ESI): m/z (M+H)⁺ calcd for C₃₀H₂₆N₅ : 456.22, Found 456.22.

λ_{\max} (CH₂Cl₂)/nm (ε/mol⁻¹ L cm⁻¹): 353(55100), 562 (33100).

Compound 9:

Compound **6** (0.53 g; 1.5 mmol), 4-cyanobenzaldehyde (0.49 g; 3.75 mmol), piperidine (1.5 mL) and *p*-TSA (cat.) were dissolved in distilled toluene (50 mL) under argon atmosphere. The mixture was stirred under reflux conditions for 3 days. It was then evaporated under reduced pressure and the residue was purified by column chromatography (SiO₂, CH₂Cl₂/MeOH/Et₃N: 97/2/1) affording **9** as a purple solid (0.70 g, 81%). Single crystals were obtained by *n*-pentane vapor diffusion into a solution of the dipyrrole in THF.

¹H NMR (500 MHz, CD₂Cl₂, 25 °C): δ = 8.68 (dd, J = 4.7 Hz, J = 1.6 Hz, 2H, pyH), 7.83 (d, J = 8.5 Hz, 2H, PhH), 7.69 (d, J = 8.7 Hz, 4H, PhH), 7.65 (d, J = 8.7 Hz, 4H, PhH), 7.63 (dd, J = 4.7 Hz, J = 1.6 Hz, 2H, pyH), 7.50 (d, J = 8.5 Hz, 2H, PhH), 7.29 (d, J = 16.6 Hz, 2H, C=CH), 7.16 (d, J = 16.6 Hz, 2H, C=CH), 6.51 (s, 2H, pyrroleH), 1.45 (s, 6H, CH₃) ppm.

¹³C NMR (125 MHz, CD₂Cl₂, 25 °C): δ = 150.8, 150.5, 141.5, 141.3, 140.0, 138.4, 138.4, 138.2, 132.6, 130.1, 130.1, 127.4, 127.1, 124.3, 121.4, 119.4, 118.9, 111.0, 14.8 ppm.

HRMS (ESI): m/z (M+H)⁺ calcd for C₄₀H₃₀N₅: 580.2496, Found 580.2481.

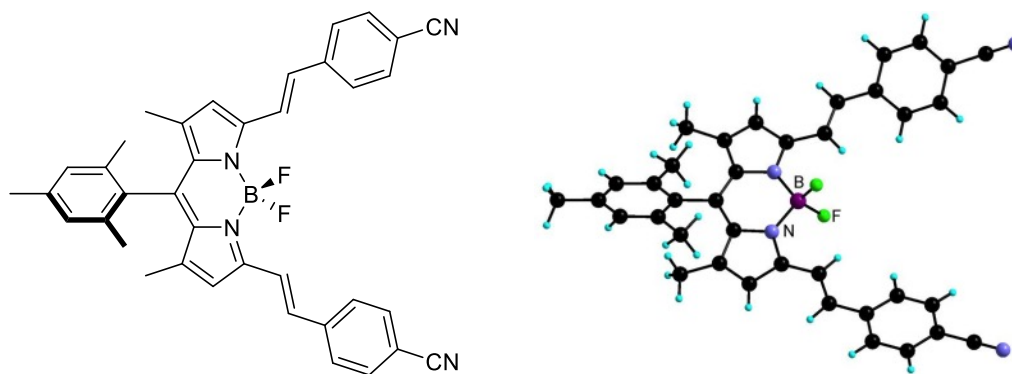
λ_{max} (CH₂Cl₂)/nm (ϵ /mol⁻¹ L cm⁻¹): 266 (31700), 355 (61800), 574 (32300).

IR (ATR): 2218 cm⁻¹ (CN)

Crystallographic data for compound (9)(H₂O)

Formula	C ₄₀ H ₃₁ N ₅ O	
Formula weight	597.70	
Temperature	173(2) K	
Wavelength	0.71073 Å	
Crystal system	Triclinic	
Space group	<i>P</i> -1	
Unit cell dimensions	<i>a</i> = 9.3286(4) Å	<i>α</i> = 88.789(2)°.
	<i>b</i> = 11.4879(5) Å	<i>β</i> = 85.395(2)°.
	<i>c</i> = 14.3862(6) Å	<i>γ</i> = 87.817(2)°.
Volume	1535.37(11) Å ³	
Z	2	
Density (calculated)	1.293 Mg/m ³	
Absorption coefficient	0.079 mm ⁻¹	
F(000)	628	
Crystal size	0.100 x 0.070 x 0.040 mm ³	
Theta range for data collection	1.774 to 30.113°	
Index ranges	-13 ≤ <i>h</i> ≤ 12, -15 ≤ <i>k</i> ≤ 16, -20 ≤ <i>l</i> ≤ 20	
Reflections collected	37270	
Independent reflections	8290 [R(int) = 0.0294]	
Completeness to theta = 25.242°	96.0 %	
Absorption correction	Semi-empirical from equivalents	
Max. and min. transmission	0.997 and 0.993	
Refinement method	Full-matrix least-squares on F ²	
Data / restraints / parameters	8290 / 0 / 417	
Goodness-of-fit on F ²	1.030	
Final R indices [I > 2σ(I)]	<i>R</i> ₁ = 0.0641, <i>wR</i> ₂ = 0.1732	
R indices (all data)	<i>R</i> ₁ = 0.0875, <i>wR</i> ₂ = 0.1914	
Largest diff. peak and hole	0.548 and -0.578 e. Å ⁻³	

Compound 10:



Chemical Formula: $C_{38}H_{31}BF_2N_4$

Molecular Weight: 592.50

Compound **2** (0.06 g; 0.11 mmol) and triethylamine (0.8 mL; 5.51 mmol) were dissolved in distilled toluene (60 mL) under argon. Then, $BF_3 \cdot Et_2O$ (1.56 g; 10 mmol) was added dropwise. The mixture was stirred at reflux under argon for 4 hours. The reaction was quenched by addition of cold ethanol (100 mL). The resulting mixture was evaporated under reduced pressure and the residue was washed with MeOH affording **10** as a dark solid (60 mg, 92%). Single crystals were obtained by Et_2O vapor diffusion into a solution of the BODIPY in $CHCl_3$.

1H NMR (500 MHz, $CDCl_3$, 25 °C): δ = 7.79 (d, J = 16.5 Hz, 2H, C=CH), 7.67 (s, 8H, PhH), 7.2 (d, J = 16.5 Hz, 2H, C=CH), 6.97 (s, 2H, PhH), 6.66 (s, 2H, pyrroleH), 2.34 (s, 3H, CH_3), 2.10 (s, 6H, CH_3), 1.46 (s, 6H, CH_3) ppm.

^{13}C NMR (125 MHz, $CDCl_3$, 25 °C): δ = 151.7, 142.4, 140.9, 140.8, 139.2, 135.1, 133.8, 133.4, 132.6, 130.7, 129.2, 127.8, 122.5, 118.9, 111.7, 21.3, 19.7, 13.8 ppm.

^{19}F NMR (282 MHz, $CDCl_3$, 25 °C): δ = -136.6 (q, J = 32.7 Hz) ppm.

HRMS (ESI): m/z $[M]^+$ calcd for $C_{38}H_{31}BF_2N_4$: 591.2641, Found 591.2557.

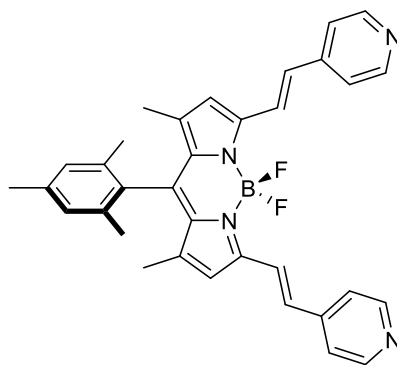
λ_{max} (DMF)/nm ($\epsilon/mol^{-1} L cm^{-1}$): 358(99700), 585(44400), 635 (123600).

IR (ATR): 2222 cm^{-1} (CN)

Crystallographic data for compound 10

Formula	$\text{C}_{38}\text{H}_{31}\text{BF}_2\text{N}_4$	
Formula weight	592.48	
Temperature	173(2) K	
Wavelength	0.71073 Å	
Crystal system	Monoclinic	
Space group	$P2_1/m$	
Unit cell dimensions	$a = 8.0763(4)$ Å	$\alpha = 90^\circ$.
	$b = 18.6613(11)$ Å	$\beta = 91.980(2)^\circ$.
	$c = 10.3428(5)$ Å	$\gamma = 90^\circ$.
Volume	1557.88(14) Å ³	
Z	2	
Density (calculated)	1.263 Mg/m ³	
Absorption coefficient	0.083 mm ⁻¹	
F(000)	620	
Crystal size	0.100 x 0.100 x 0.030 mm ³	
Theta range for data collection	1.970 to 30.214°	
Index ranges	-11 ≤ h ≤ 11, -26 ≤ k ≤ 26, -13 ≤ l ≤ 14	
Reflections collected	32037	
Independent reflections	4407 [R(int) = 0.0510]	
Completeness to theta = 25.242°	97.9 %	
Absorption correction	Semi-empirical from equivalents	
Max. and min. transmission	0.997 and 0.991	
Refinement method	Full-matrix least-squares on F ²	
Data / restraints / parameters	4407 / 0 / 245	
Goodness-of-fit on F ²	1.109	
Final R indices [I > 2σ(I)]	$R_1 = 0.0645$, $wR_2 = 0.1318$	
R indices (all data)	$R_1 = 0.1091$, $wR_2 = 0.1531$	
Largest diff. peak and hole	0.286 and -0.326 e.Å ⁻³	

Compound 11:



Chemical Formula: $C_{34}H_{31}BF_2N_4$
Molecular Weight: 544.46

Dipyrin **3** (0.05 g; 0.101 mmol) and triethylamine (0.7 mL; 5 mmol) were dissolved in distilled toluene (60 mL) under argon. Then, $BF_3 \cdot Et_2O$ (1.42 g; 10 mmol) was added dropwise. Under argon atmosphere, the mixture was stirred at reflux and for 4 hours. The reaction was quenched by addition of cold ethanol (100 mL). The resulting mixture was evaporated under reduced pressure and the residue was washed with EtOAc affording **11** as a dark solid (30 mg, 55%).

1H NMR (400 MHz, MeOD- d_4 , 25 °C): δ = 8.85 (d, J = 6.7 Hz, 4H, pyH), 8.27 (d, J = 16.0 Hz, 2H, C=CH), 8.25 (d, J = 6.7 Hz, 4H, pyH), 7.75 (d, J = 16.0 Hz, 2H, C=CH), 7.23 (s, 2H, PhH), 7.17 (s, 2H, pyrroleH), 2.48 (s, 3H, CH_3), 2.23 (s, 6H, CH_3), 1.65 (s, 6H, CH_3) ppm.

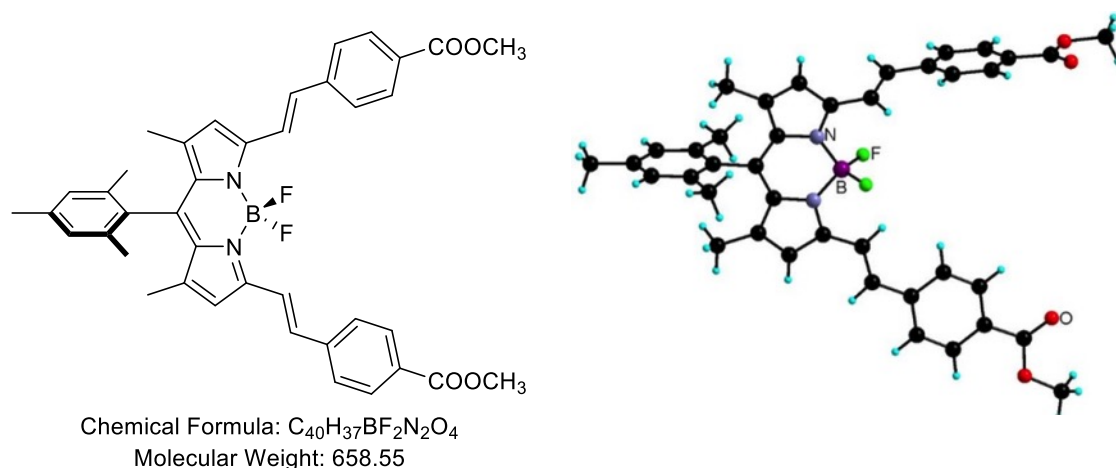
^{13}C NMR (125 MHz, MeOD- d_4 , 25 °C): δ = 152.7, 151.4, 146.2, 144.8, 143.8, 141.2, 136.1, 135.6, 132.8, 131.7, 130.6, 127.9, 124.2, 120.8, 21.3, 19.7, 13.9 ppm.

^{19}F NMR (282 MHz, MeOD- d_4 , 25 °C): δ = -155.70 (q, J = 33.3 Hz) ppm.

HRMS (ESI): m/z $[M+H]^+$ calcd. for $C_{34}H_{32}BF_2N_4$: 544.2719, Found 544.2696.

λ_{max} (DMF)/nm ($\epsilon/mol^{-1} L cm^{-1}$): 340 (38600), 568 (23100), 616 (70300)

Compound 12:



Dipyrin **4** (0.27 g; 0.44 mmol) and triethylamine (3.1 mL; 22 mmol) were dissolved in distilled toluene (150 mL) under argon atmosphere. Then, $BF_3 \cdot Et_2O$ (6.27 g; 44 mmol) was added dropwise. The mixture was stirred under reflux and argon for 4 hours. The reaction was quenched by addition of cold ethanol (300 mL). The resulting mixture was evaporated under reduced pressure and the residue was washed with MeOH affording compound **12** as a dark solid (0.28 g, 96%). Single crystals were obtained by *n*-pentane vapor diffusion into a solution of the BODIPY in $CHCl_3$.

1H NMR (500 MHz, CD_2Cl_2 , 25 °C): δ = 8.06 (d, J = 8.3 Hz, 4H, PhH), 7.8 (d, J = 16.4 Hz, 2H, C=CH), 7.71 (d, J = 8.3 Hz, 4H, PhH), 7.33 (d, J = 16.4 Hz, 2H, C=CH), 7.02 (s, 2H, PhH), 6.72 (s, 2H, pyrroleH), 3.92 (s, 6H, $COOCH_3$), 2.36 (s, 3H, CH_3), 2.12 (s, 6H, CH_3), 1.49 (s, 6H, CH_3) ppm.

^{13}C NMR (125 MHz, CD_2Cl_2 , 25 °C): δ = 166.8, 152.3, 142.8, 141.2, 140.6, 139.5, 135.4, 135.1, 133.5, 131.2, 130.5, 130.3, 129.5, 127.6, 121.5, 118.2, 52.4, 21.3, 19.7, 13.8 ppm.

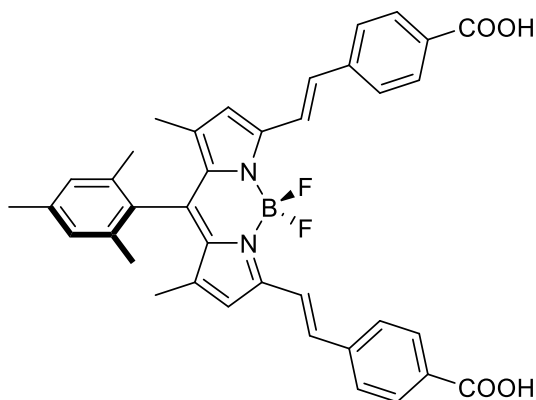
^{19}F NMR (282 MHz, CD_2Cl_2 , 25 °C): δ = -138.8 (q, J = 33.1 Hz) ppm.

HRMS (ESI): m/z $[M]^+$ calcd for $C_{40}H_{37}BF_2N_2O_4$: 657.2845, Found 657.2898.

$\lambda_{max}(CH_2Cl_2)/nm$ ($\epsilon/mol^{-1} L cm^{-1}$): 359(87000), 586(38200), 635 (118300).

Crystallographic data for compound 12

Formula	$\text{C}_{40}\text{H}_{37}\text{BF}_2\text{N}_2\text{O}_4$	
Formula weight	658.52	
Temperature	173(2) K	
Wavelength	0.71073 Å	
Crystal system	Monoclinic	
Space group	$P2_1/n$	
Unit cell dimensions	$a = 11.0795(8)$ Å	$\alpha = 90^\circ$.
	$b = 12.8631(9)$ Å	$\beta = 95.628(2)^\circ$.
	$c = 23.4751(17)$ Å	$\gamma = 90^\circ$.
Volume	3329.5(4) Å ³	
Z	4	
Density (calculated)	1.314 Mg/m ³	
Absorption coefficient	0.092 mm ⁻¹	
F(000)	1384	
Crystal size	0.080 x 0.060 x 0.030 mm ³	
Theta range for data collection	2.118 to 30.202°	
Index ranges	-15 ≤ h ≤ 15, -18 ≤ k ≤ 18, -32 ≤ l ≤ 33	
Reflections collected	39967	
Independent reflections	9790 [R(int) = 0.0621]	
Completeness to theta = 25.242°	99.9 %	
Absorption correction	Semi-empirical from equivalents	
Max. and min. transmission	0.996 and 0.992	
Refinement method	Full-matrix least-squares on F ²	
Data / restraints / parameters	9790 / 0 / 449	
Goodness-of-fit on F ²	1.016	
Final R indices [I > 2σ(I)]	$R_1 = 0.0609$, $wR_2 = 0.1350$	
R indices (all data)	$R_1 = 0.1151$, $wR_2 = 0.1623$	
Largest diff. peak and hole	0.332 and -0.228 e.Å ⁻³	

Compound 13:

Chemical Formula: $C_{38}H_{33}BF_2N_2O_4$
Molecular Weight: 630.50

To a THF (15 mL) solution of compound **12** (0.1 g; 0.15 mmol), a H_2O (15 mL) solution of LiOH (0.073 g; 3 mmol) was added. The mixture was stirred at 40 °C for 2 days before it was evaporated under reduced pressure. The residue was acidified by 37% HCl to pH = 2, and extracted by AcOEt and water (3 × 50 mL). The organic layers were combined, dried over Na_2SO_4 , filtered and evaporated under reduced pressure. The residue was recrystallized in a AcOEt/Cyclohexane mixture affording a dark solid (0.08 g, 84%).

1H NMR (500 MHz, DMSO- d_6 , 25 °C): δ = 13.03 (s, 2H, COOH), 8.02 (d, J = 8.4 Hz, 4H, PhH), 7.74 (d, J = 8.4 Hz, 4H, PhH), 7.68 (d, J = 16.5 Hz, 2H, C=CH), 7.63 (d, J = 16.5 Hz, 2H, C=CH), 7.11 (s, 2H, PhH), 7.05 (s, 2H, pyrroleH), 2.34 (s, 3H, CH_3), 2.08 (s, 6H, CH_3), 1.44 (s, 6H, CH_3) ppm.

^{13}C NMR (125 MHz, DMSO- d_6 , 25 °C): δ = 166.9, 151.8, 141.7, 140.2, 139.3, 138.7, 136.0, 134.6, 132.4, 130.9, 130.1, 129.5, 129.0, 127.2, 120.1, 118.8, 20.8, 19.1, 13.3 ppm.

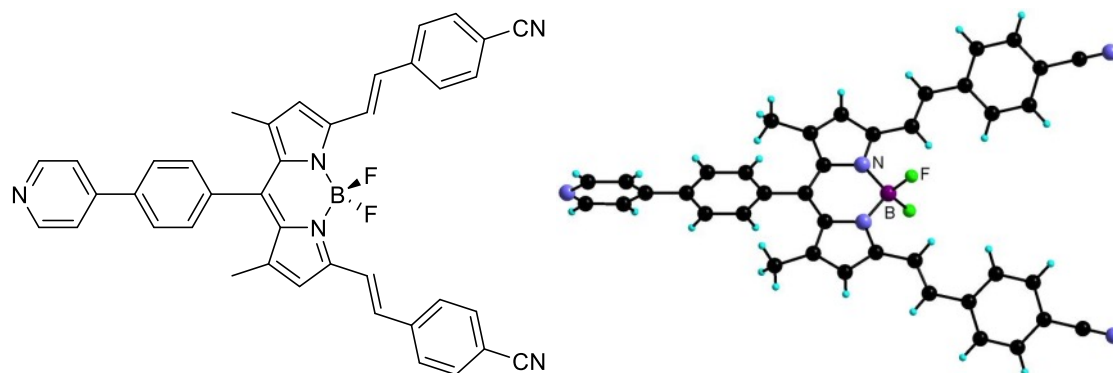
^{19}F NMR (282 MHz, DMSO- d_6 , 25 °C): δ = -136.6 (q, J = 29.4 Hz) ppm.

HRMS (ESI): m/z $[M]^+$ calcd for $C_{38}H_{33}BFN_2O_4$: 629.2532, Found 629.2498.

λ_{max} (DMF)/nm (ϵ / $mol^{-1} L cm^{-1}$): 359(67900), 585(32800), 628(64200).

IR (ATR): 2922 cm^{-1} (OH), 1682 cm^{-1} (CO)

Compound 14:



Chemical Formula: $C_{40}H_{28}BF_2N_5$

Molecular Weight: 627.51

Dipyrin **9** (0.1 g; 0.17 mmol) and triethylamine (1.2 mL; 8.63 mmol) were dissolved in distilled toluene (65 mL) under argon. Then, $BF_3 \cdot Et_2O$ (2.45 g; 17 mmol) was added dropwise. The mixture was refluxed under argon for 4 hours. The reaction was then quenched by addition of cold ethanol (100 mL). The resulting mixture was evaporated under reduced pressure and the solid was washed with MeOH affording **14** as a dark solid (100 mg, 92%). Single crystals were obtained by Et_2O vapor diffusion into a solution of the BODIPY in DMF

1H NMR (500 MHz, DMSO- d_6 , 25 °C): δ = 8.7 (d, J = 5.5 Hz, 2H, pyH), 8.09 (d, J = 8.1 Hz, 2H, PhH), 7.93 (d, J = 8.2 Hz, 4H, PhH), 7.87 (d, J = 5.5 Hz, 2H, pyH), 7.8 (d, J = 8.2 Hz, 4H, PhH), 7.72 (d, J = 16.4 Hz, 2H, C=CH), 7.65 (d, J = 16.4 Hz, 2H, C=CH), 7.65 (d, J = 8.2 Hz, 2H, PhH), 7.09 (s, 2H, pyrroleH), 1.51 (s, 6H, CH_3) ppm.

^{13}C NMR (125 MHz, DMSO- d_6 , 25 °C): δ = 162.3, 151.9, 143.9, 142.6, 140.4, 139.2, 136.9, 135.7, 133.2, 133.2, 133.1, 129.7, 128.8, 127.9, 123.6, 121.0, 119.5, 118.9, 111.1, 14.6 ppm.

^{19}F NMR (282 MHz, DMSO- d_6 , 25 °C): δ = -136.12 (q, J = 29.9 Hz) ppm.

HRMS (ESI): m/z $[M+H]^+$ calcd for $C_{40}H_{29}BF_2N_5$: 628.2485, Found 628.2405.

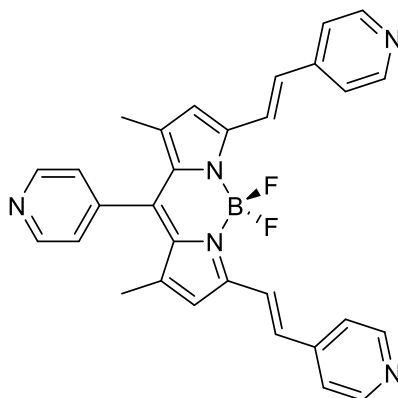
λ_{max} (DMF)/nm (ϵ / $mol^{-1} L cm^{-1}$): 361(94400), 586(41600), 636(112800).

IR (ATR): 2216 cm^{-1} (CN)

Crystallographic data for compound 14

Formula	$\text{C}_{40}\text{H}_{28}\text{BF}_2\text{N}_5$	
Formula weight	627.48	
Temperature	180(2) K	
Wavelength	0.71073 Å	
Crystal system	Monoclinic	
Space group	$C2/c$	
Unit cell dimensions	$a = 8.6255(5)$ Å	$\alpha = 90^\circ$.
	$b = 28.0408(17)$ Å	$\beta = 105.3130(10)^\circ$.
	$c = 13.8261(7)$ Å	$\gamma = 90^\circ$.
Volume	3225.3(3) Å ³	
Z	4	
Density (calculated)	1.292 Mg/m ³	
Absorption coefficient	0.085 mm ⁻¹	
F(000)	1304	
Crystal size	0.100 x 0.100 x 0.080 mm ³	
Theta range for data collection	2.108 to 30.072°	
Index ranges	-12 ≤ h ≤ 12, -39 ≤ k ≤ 39, -19 ≤ l ≤ 19	
Reflections collected	28446	
Independent reflections	4734 [R(int) = 0.0455]	
Completeness to theta = 25.242°	99.8 %	
Absorption correction	Semi-empirical from equivalents	
Refinement method	Full-matrix least-squares on F ²	
Data / restraints / parameters	4734 / 0 / 221	
Goodness-of-fit on F ²	1.015	
Final R indices [I > 2σ(I)]	$R_1 = 0.0541$, $wR_2 = 0.1369$	
R indices (all data)	$R_1 = 0.0938$, $wR_2 = 0.1615$	
Largest diff. peak and hole	0.269 and -0.199 e.Å ⁻³	

Compound 15:



Chemical Formula: $C_{30}H_{24}BF_2N_5$
Molecular Weight: 503.36

Compound **8** (0.1 g; 0.22 mmol) and triethylamine (1.5 mL; 11 mmol) were dissolved in distilled toluene (65 mL) under argon atmosphere. Then, $BF_3 \cdot Et_2O$ (3.12 g; 22 mmol) was added dropwise. The mixture was refluxed under argon for 4 hours. The reaction was quenched by the addition of cold ethanol (100 mL). The resulting mixture was evaporated under reduced pressure and the solid was washed with MeOH affording BODIPY **15** as a dark solid (100 mg, 92%).

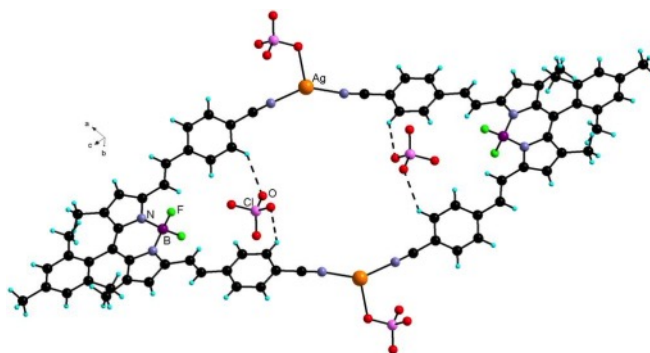
1H NMR (400MHz, Acetone- d_6 , 25°C): δ = 9.13 (d, J = 6.4 Hz, 2H, pyH), δ = 9.06 (d, J = 6.8 Hz, 4H, pyH), 8.38 (d, J = 6.8 Hz, 4H, pyH), 8.19 (d, J = 16.1 Hz, 2H, C=CH), 8.1 (d, J = 6.4 Hz, 2H, pyH), 7.92 (d, J = 16.1 Hz, 2H, C=CH), 7.21 (s, 2H, pyrroleH), 1.62 (s, 6H, CH_3) ppm.

HRMS (ESI): m/z $[M+H]^+$ calcd for $C_{30}H_{25}BF_2N_5$: 504.2171, Found 504.2207.

λ_{max} (DMF)/nm (ϵ / $mol^{-1} L cm^{-1}$): 341(51700), 572(22100), 620(69200).

General procedure for the synthesis of compounds **16–18**: a CHCl_3 solution (1 mL) of compound **10** (5 mg, 0.0084 mmol) was first layered with a 1/1 $\text{CHCl}_3/\text{AcOEt}$ (1 mL) mixture and then with an AcOEt solution (1 mL) of the silver salt (0.084 mmol). After a few days, crystals suitable for X-ray analysis were obtained.

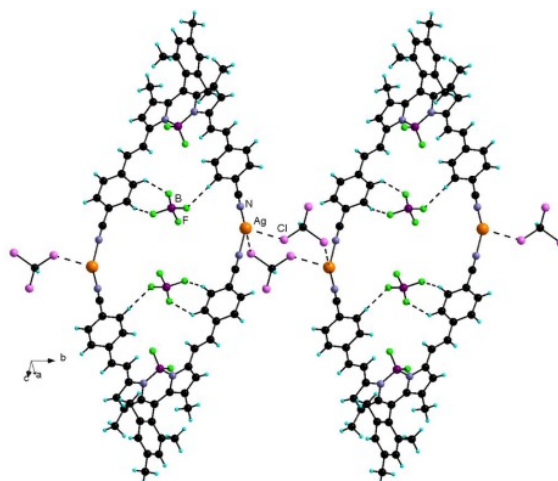
Compound 16:



Yield: 6 mg

IR (ATR): 2251 cm^{-1} (CN)

Compound 17:

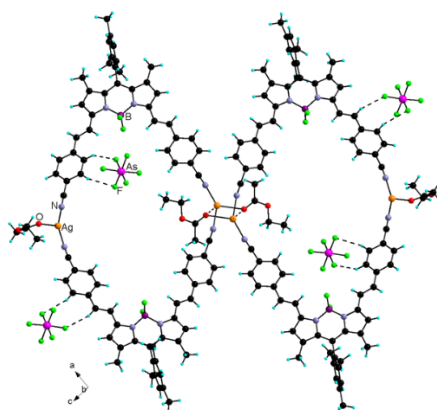


Yield: 5 mg (65%)

Anal. calcd. for $\text{C}_{39}\text{H}_{32}\text{AgB}_2\text{Cl}_3\text{F}_6\text{N}_4$: C, 51.67%; H, 3.56%; N, 6.18%; Found: C, 54.17%; H, 4.02%; N, 6.58%.

IR (ATR): 2259 cm^{-1} (CN)

Compound 18:



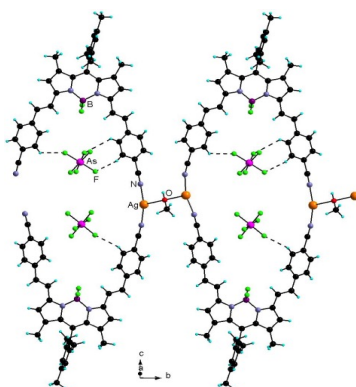
Yield: 5 mg (57%)

Anal. calcd. for $(C_{38}H_{31}BF_2N_4AgAsF_6)_4(CHCl_3)_2$: C, 48.73%; H, 3.35%; N, 5.90%; Found: C, 48.12%; H, 3.57%; N, 6.11%.

IR (ATR): 2260 cm^{-1} (CN)

Compound 19:

A $CHCl_3$ solution (1 mL) of BODIPY **10** (6 mg, 0.02 mmol) was layered with a 1/1 $CHCl_3$ /MeOH (1 mL) mixture and then with a MeOH solution (1 mL) of $AgAsF_6$ (0.04 mmol). After one week, no crystalline material had formed. The vial was set for Et_2O (6–8 mL) vapour diffusion. Crystals suitable for X-ray analysis were obtained after a few days.



Yield: 5 mg (52%)

Anal. calcd. for $(C_{38}H_{31}BF_2N_4AgAsF_6)_2(CH_4O)$: C, 51.08%; H, 3.67%; N, 6.19%; Found: C, 49.22%; H, 3.97%; N, 5.86%.

IR (ATR): 2239 cm^{-1} (CN)

Crystallographic data for compound 16

Formula	$\text{C}_{78}\text{H}_{64}\text{Ag}_2\text{B}_2\text{Cl}_8\text{F}_4\text{N}_8\text{O}_8$	
Formula weight	1838.33	
Temperature	173(2) K	
Wavelength	0.71073 Å	
Crystal system	Triclinic	
Space group	$P\bar{1}$	
Unit cell dimensions	$a = 10.2626(5)$ Å	$\alpha = 112.493(2)^\circ$.
	$b = 19.2729(10)$ Å	$\beta = 91.099(2)^\circ$.
	$c = 21.5355(11)$ Å	$\gamma = 92.320(2)^\circ$.
Volume	$3929.5(3)$ Å ³	
Z	2	
Density (calculated)	1.554 Mg/m ³	
Absorption coefficient	0.841 mm ⁻¹	
F(000)	1856	
Crystal size	0.080 x 0.040 x 0.030 mm ³	
Theta range for data collection	1.806 to 30.267°	
Index ranges	-13 ≤ h ≤ 14, -25 ≤ k ≤ 27, -30 ≤ l ≤ 30	
Reflections collected	116798	
Independent reflections	21506 [R(int) = 0.0774]	
Completeness to theta = 25.242°	96.6 %	
Absorption correction	Semi-empirical from equivalents	
Refinement method	Full-matrix least-squares on F ²	
Data / restraints / parameters	21506 / 1 / 1036	
Goodness-of-fit on F ²	1.055	
Final R indices [I > 2σ(I)]	$R_1 = 0.0631$, $wR_2 = 0.1677$	
R indices (all data)	$R_1 = 0.1646$, $wR_2 = 0.2037$	
Largest diff. peak and hole	2.151 and -1.012 e.Å ⁻³	

Crystallographic data for compound 17

Formula	$C_{39}H_3Ag_2B_2Cl_3F_6N_4$	
Formula weight	906.55	
Temperature	173(2) K	
Wavelength	0.71073 Å	
Crystal system	Monoclinic	
Space group	$P2_1/n$	
Unit cell dimensions	$a = 18.9253(8)$ Å	$\alpha = 90^\circ$.
	$b = 8.4818(4)$ Å	$\beta = 101.466(2)^\circ$.
	$c = 24.5491(11)$ Å	$\gamma = 90^\circ$.
Volume	3862.0(3) Å ³	
Z	4	
Density (calculated)	1.559 Mg/m ³	
Absorption coefficient	0.794 mm ⁻¹	
F(000)	1824	
Crystal size	0.040 x 0.040 x 0.020 mm ³	
Theta range for data collection	2.492 to 30.137°	
Index ranges	-26 ≤ h ≤ 21, -11 ≤ k ≤ 11, -34 ≤ l ≤ 34	
Reflections collected	96266	
Independent reflections	10592 [R(int) = 0.0596]	
Completeness to theta = 25.242°	97.3 %	
Absorption correction	Semi-empirical from equivalents	
Refinement method	Full-matrix least-squares on F ²	
Data / restraints / parameters	10592 / 4 / 478	
Goodness-of-fit on F ²	1.025	
Final R indices [I > 2σ(I)]	$R_1 = 0.1248$, $wR_2 = 0.3275$	
R indices (all data)	$R_1 = 0.1842$, $wR_2 = 0.3709$	
Largest diff. peak and hole	2.436 and -1.933 e.Å ⁻³	

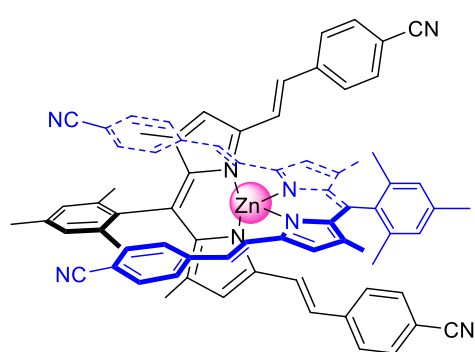
Crystallographic data for compound 18

Formula	$\text{C}_{170}\text{H}_{158}\text{Ag}_4\text{As}_4\text{B}_4\text{Cl}_6\text{F}_{32}\text{N}_{16}\text{O}_8$	
Formula weight	4148.21	
Temperature	173(2) K	
Wavelength	0.71073 Å	
Crystal system	Triclinic	
Space group	$P\bar{1}$	
Unit cell dimensions	$a = 12.7233(5)$ Å	$\alpha = 90.384(2)^\circ$
	$b = 14.9725(6)$ Å	$\beta = 91.008(2)^\circ$
	$c = 23.8231(10)$ Å	$\gamma = 103.876(2)^\circ$
Volume	4404.9(3) Å ³	
Z	1	
Density (calculated)	1.564 Mg/m ³	
Absorption coefficient	1.369 mm ⁻¹	
F(000)	2084	
Crystal size	0.060 x 0.060 x 0.040 mm ³	
Theta range for data collection	1.633 to 30.186°	
Index ranges	-17 ≤ h ≤ 17, -19 ≤ k ≤ 21, -33 ≤ l ≤ 33	
Reflections collected	99759	
Independent reflections	23829 [R(int) = 0.0608]	
Completeness to theta = 25.242°	96.2 %	
Absorption correction	Semi-empirical from equivalents	
Refinement method	Full-matrix least-squares on F ²	
Data / restraints / parameters	23829 / 0 / 1113	
Goodness-of-fit on F ²	1.037	
Final R indices [I > 2σ(I)]	$R_1 = 0.0862$, $wR_2 = 0.2291$	
R indices (all data)	$R_1 = 0.1700$, $wR_2 = 0.2786$	
Largest diff. peak and hole	3.227 and -1.348 e.Å ⁻³	

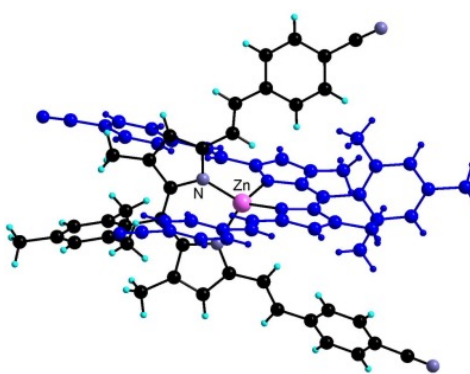
Crystallographic data for compound 19

Formula	$C_{81}H_{76}Ag_2As_2B_2F_{16}N_8O_2$	
Formula weight	1884.69	
Temperature	180(2) K	
Wavelength	0.71073 Å	
Crystal system	Monoclinic	
Space group	$P2_1$	
Unit cell dimensions	$a = 15.0721(8)$ Å	$\alpha = 90^\circ$.
	$b = 15.6298(9)$ Å	$\beta = 92.792(2)^\circ$.
	$c = 17.0390(10)$ Å	$\gamma = 90^\circ$.
Volume	4009.2(4) Å ³	
Z	2	
Density (calculated)	1.561 Mg/m ³	
Absorption coefficient	1.397 mm ⁻¹	
F(000)	1896	
Crystal size	0.120 x 0.100 x 0.040 mm ³	
Theta range for data collection	1.196 to 30.152°.	
Index ranges	-21 ≤ h ≤ 19, -22 ≤ k ≤ 21, -24 ≤ l ≤ 24	
Reflections collected	68702	
Independent reflections	22917 [R(int) = 0.0595]	
Completeness to theta = 25.242°	100.0 %	
Absorption correction	Semi-empirical from equivalents	
Refinement method	Full-matrix least-squares on F ²	
Data / restraints / parameters	22917 / 1 / 1020	
Goodness-of-fit on F ²	1.024	
Final R indices [I > 2σ(I)]	$R_I = 0.0442$, $wR_2 = 0.0916$	
R indices (all data)	$R_I = 0.0742$, $wR_2 = 0.1037$	
Absolute structure parameter	0.115(5)	
Largest diff. peak and hole	0.818 and -0.655 e.Å ⁻³	

Compound 21:



Chemical Formula: C₇₆H₆₂N₈Zn
Molecular Weight: 1152.77



To a CHCl₃ (20 mL) solution of dipyrrole **2** (120 mg; 0.22 mmol), a MeOH (20 mL) solution of Zn(OAc)₂ (H₂O)₂ (70 mg; 0.33 mmol) was added. The mixture was stirred at room temperature for 2 days. It was then evaporated under reduced pressure and the residue was recrystallized from a CHCl₃/toluene mixture affording a dark solid (100 mg, 90%). Single crystals were obtained by *n*-pentane vapor diffusion into a solution of the complex in THF.

¹H NMR (500 MHz, CDCl₃, 25 °C): δ = 7.43 (d, *J* = 8.1 Hz, 8H, PhH), 7.15 (d, *J* = 8.1 Hz, 8H, PhH), 6.96 (d, *J* = 16.3 Hz, 4H, C=CH), 6.92 (s, 4H, PhH), 6.84 (d, *J* = 16.3 Hz, 4H, C=CH), 6.68 (s, 4H, pyrroleH), 2.38 (s, 6H, CH₃), 1.84 (s, 12H, CH₃), 1.43 (s, 12H, CH₃) ppm.

¹³C NMR (125 MHz, CDCl₃, 25 °C): δ = 155.7, 144.9, 144.5, 141.5, 139.0, 135.3, 134.8, 132.3, 131.1, 129.4, 127.3, 125.0, 119.1, 119.1, 110.5, 21.3, 19.6, 15.5 ppm.

HRMS (ESI): *m/z* [M+H]⁺ calcd. for C₇₆H₆₃N₈Zn: 1151.4462, Found 1151.4443.

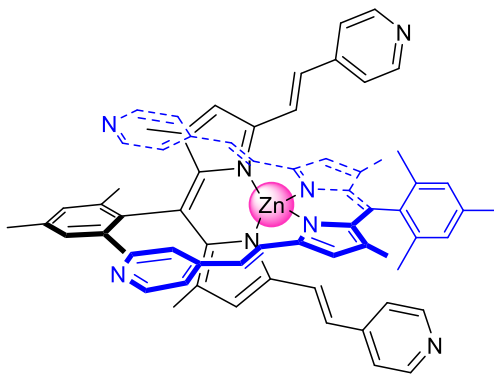
λ_{max} (DMF)/nm (ε/mol⁻¹ L cm⁻¹): 355 (68600), 580 (74100), 623 (109600).

IR (ATR): 2158 cm⁻¹ (CN)

Crystallographic data for compound (21)(THF)_{2.25}

Formula	C ₈₅ H ₈₀ N ₈ O _{2.25} Zn	
Formula weight	1314.94	
Temperature	180(2) K	
Wavelength	0.71073 Å	
Crystal system	Triclinic	
Space group	<i>P</i> -1	
Unit cell dimensions	<i>a</i> = 12.3686(4) Å	<i>α</i> = 76.9540(10)°.
	<i>b</i> = 13.7569(4) Å	<i>β</i> = 86.2620(10)°.
	<i>c</i> = 23.2357(8) Å	<i>γ</i> = 70.0080(10)°.
Volume	3619.2(2) Å ³	
<i>Z</i>	2	
Density (calculated)	1.207 Mg/m ³	
Absorption coefficient	0.393 mm ⁻¹	
<i>F</i> (000)	1388	
Crystal size	0.140 x 0.140 x 0.140 mm ³	
Theta range for data collection	1.614 to 30.097°.	
Index ranges	-17 ≤ <i>h</i> ≤ 16, -19 ≤ <i>k</i> ≤ 16, -32 ≤ <i>l</i> ≤ 32	
Reflections collected	70458	
Independent reflections	19415 [<i>R</i> (int) = 0.0359]	
Completeness to theta = 25.242°	95.9 %	
Absorption correction	Semi-empirical from equivalents	
Refinement method	Full-matrix least-squares on <i>F</i> ²	
Data / restraints / parameters	19415 / 9 / 886	
Goodness-of-fit on <i>F</i> ²	1.060	
Final <i>R</i> indices [<i>I</i> > 2σ(<i>I</i>)]	<i>R</i> _{<i>I</i>} = 0.0582, <i>wR</i> ₂ = 0.1704	
<i>R</i> indices (all data)	<i>R</i> _{<i>I</i>} = 0.0922, <i>wR</i> ₂ = 0.1887	
Largest diff. peak and hole	0.996 and -0.505 e.Å ⁻³	

Compound 22:



Chemical Formula: $C_{68}H_{62}N_8Zn$

Molecular Weight: 1056.68

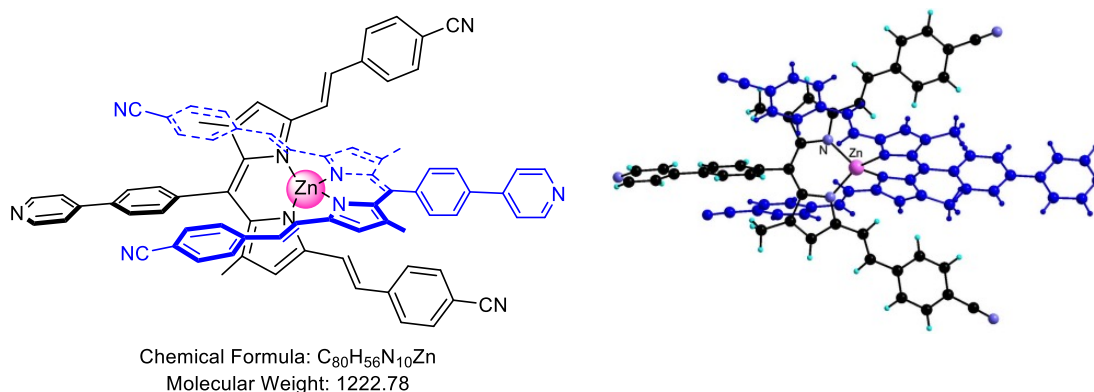
To a $CHCl_3$ (10 mL) solution of dipyrin **3** (20 mg; 0.04 mmol), a MeOH (10 mL) solution of $Zn(OAc)_2 \cdot (H_2O)_2$ (13 mg; 0.06 mmol) was added. The mixture was stirred at room temperature for 2 days. After evaporation under reduced pressure, the residue was recrystallized from $CHCl_3$ /toluene affording the complex as a dark solid (18 mg, 85%).

1H NMR (300 MHz, DMSO- d_6 , 25 °C): δ = 8.41 (d, J = 5.9 Hz, 8H, pyH), 7.03 (d, J = 5.9 Hz, 8H, pyH), 6.99 (d, J = 16.2 Hz, 4H, C=CH), 6.99 (s, 4H, pyrroleH), 6.86 (d, J = 16.2 Hz, 4H, C=CH), 2.30 (s, 6H, CH_3), 1.80 (s, 12H, CH_3), 1.42 (s, 12H, CH_3).

HRMS (ESI): m/z $[M+H]^+$ calcd. for $C_{68}H_{63}N_8Zn$: 1055.4462, Found 1055.4433.

λ_{max} (DMF)/nm ($\epsilon/mol^{-1} L cm^{-1}$): 359(32600), 560 (40600), 606 (58100).

Compound 23:



To a $CHCl_3$ (50 mL) solution of compound **9** (300 mg, 0.52 mmol), a MeOH (50 mL) solution of $Zn(OAc)_2(H_2O)_2$ (170 mg, 0.78 mmol) was added. The mixture was stirred at room temperature for 2 days. The resulting mixture was evaporated under reduced pressure and the residue was recrystallized from a $CHCl_3$ /toluene mixture affording complex **23** as a dark solid (250 mg, 79%).

In a test tube, a $CHCl_3$ (1 mL) solution of dipyrin **9** (0.005 mmol) was layered with a $CHCl_3$ /MeOH (1/1, 2mL) buffer before a solution of $Zn(OAc)_2$ (0.005 mmol) in MeOH (1 mL) was added. After few weeks, single crystals of **23** were obtained.

1H NMR (500 MHz, $CDCl_3$, 25 °C): δ = 8.78 (d, J = 5.1 Hz, 4H, pyH), 7.95 (d, J = 7.9 Hz, 4H, PhH), 7.77 (d, J = 5.1 Hz, 4H, pyH), 7.49 (d, J = 8.1 Hz, 8H, PhH), 7.41 (d, J = 7.9 Hz, 4H, PhH), 7.21 (d, J = 8.1 Hz, 8H, PhH), 6.91 (d, J = 16.3 Hz, 4H, C=CH), 6.84 (d, J = 16.3 Hz, 4H, C=CH), 6.61 (s, 4H, pyrroleH), 1.45 (s, 12H, CH_3) ppm.

^{13}C NMR (125 MHz, $CDCl_3$, 25 °C): δ = 156.1, 150.7, 145.3, 143.9, 141.7, 140.3, 139.4, 139.3, 132.5, 131.2, 130.7, 128.0, 127.3, 125.3, 122.1, 120.0, 119.1, 111.0, 16.4 ppm.

HRMS (ESI): m/z $[M+H]^+$ calcd. for $C_{80}H_{57}N_{10}Zn$: 1221.4054, Found 1221.4016.

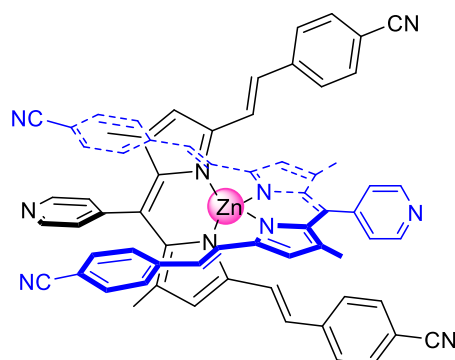
λ_{max} (DMF)/nm ($\epsilon/mol^{-1} L cm^{-1}$): 358(81300), 579(68900), 626(92300).

IR (ATR): 2221 cm^{-1} (CN)

Crystallographic data for compound 23

Formula	$\text{C}_{82}\text{H}_{58}\text{Cl}_6\text{N}_{10}\text{Zn}$	
Formula weight	1461.45	
Temperature	173(2) K	
Wavelength	0.71073 Å	
Crystal system	Triclinic	
Space group	$P\bar{1}$	
Unit cell dimensions	$a = 13.8475(6)$ Å	$\alpha = 75.296(2)^\circ$.
	$b = 13.9105(5)$ Å	$\beta = 83.923(2)^\circ$.
	$c = 20.9147(9)$ Å	$\gamma = 65.307(2)^\circ$.
Volume	3540.4(3) Å ³	
Z	2	
Density (calculated)	1.371 Mg/m ³	
Absorption coefficient	0.627 mm ⁻¹	
F(000)	1504	
Crystal size	0.100 x 0.100 x 0.080 mm ³	
Theta range for data collection	1.906 to 30.088°.	
Index ranges	-19 ≤ h ≤ 19, -18 ≤ k ≤ 19, -29 ≤ l ≤ 29	
Reflections collected	69477	
Independent reflections	19124 [R(int) = 0.0925]	
Completeness to theta = 25.242°	96.7 %	
Absorption correction	Semi-empirical from equivalents	
Max. and min. transmission	0.951 and 0.939	
Refinement method	Full-matrix least-squares on F ²	
Data / restraints / parameters	19124 / 1 / 937	
Goodness-of-fit on F ²	0.991	
Final R indices [I > 2σ(I)]	$R_I = 0.0700$, $wR_2 = 0.1686$	
R indices (all data)	$R_I = 0.2050$, $wR_2 = 0.2141$	
Largest diff. peak and hole	1.154 and -0.686 e.Å ⁻³	

Compound 24:



Chemical Formula: $C_{68}H_{48}N_{10}Zn$
Molecular Weight: 1070.58

To a $CHCl_3$ (10 mL) solution of compound **7** (50 mg, 0.099 mmol), a MeOH (10 mL) solution of $Zn(OAc)_2 \cdot (H_2O)_2$ (33 mg, 0.15 mmol) was added. The mixture was stirred at room temperature overnight. The resulting mixture was evaporated under reduced pressure and the residue was recrystallized from $CHCl_3$ /toluene affording the complex as a dark solid (30 mg, 62%).

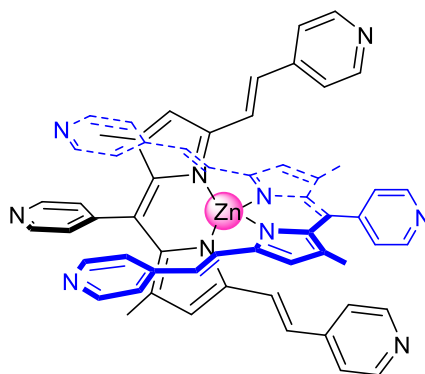
1H NMR (500 MHz, $DMSO-d_6$, 25 °C): δ = 8.89 (d, J = 5.9 Hz, 4H, pyH), 7.54 (d, J = 8.0 Hz, 8H, PhH), 7.27 (d, J = 5.9 Hz, 4H, pyH), 7.24 (d, J = 8.0 Hz, 8H, PhH), 6.99 (d, J = 16.3 Hz, 4H, C=CH), 6.87 (d, J = 16.3 Hz, 4H, C=CH), 6.60 (s, 4H, pyrroleH), 1.45 (s, 12H, CH_3) ppm.

HRMS (ESI): m/z $[M+H]^+$ calcd. for $C_{68}H_{49}N_{10}Zn$: 1069.3428, Found 1069.3401.

λ_{max} (DMF)/nm ($\epsilon/mol^{-1} L cm^{-1}$): 353 (47100), 581 (37700), 622 (47100).

IR (ATR): 2224 cm^{-1} (CN)

Compound 25:



Chemical Formula: $C_{60}H_{48}N_{10}Zn$
Molecular Weight: 974.49

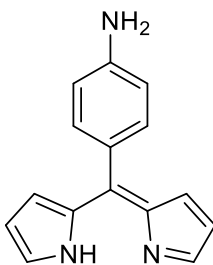
To a $CHCl_3$ (10 mL) solution of compound **8** (50 mg, 0.011 mmol), a MeOH (10 mL) solution of $Zn(OAc)_2 \cdot (H_2O)_2$ (36 mg, 0.17 mmol) was added. The mixture was stirred at room temperature overnight. The resulting mixture was evaporated under reduced pressure and the residue was washed with MeOH affording complex **25** as a dark solid (40 mg, 79%).

1H NMR (500 MHz, DMSO- d_6 , 25 °C): δ = 8.64 (d, J = 4.2 Hz, 8H, pyH), 8.52 (d, J = 5.9 Hz, 4H, pyH), 7.8 (d, J = 4.2 Hz, 8H, pyH), 7.19 (d, J = 16.2 Hz, 4H, CH=C), 7.12 (d, J = 5.9 Hz, 4H, pyH), 6.93 (d, J = 16.2 Hz, 4H, CH=C), 6.86 (s, 4H, pyrroleH), 1.42 (s, 12H, CH_3) ppm.

HRMS (ESI): m/z $[M+H]^+$ calcd. for $C_{68}H_{49}N_{10}Zn$: 973.3428, Found 973.3418.

λ_{max} (DMF)/nm ($\epsilon/mol^{-1} L cm^{-1}$): 329 (33500), 557 (26100), 607 (35500).

Compound 34:



Chemical Formula: C₁₅H₁₃N₃

Molecular Weight: 235.29

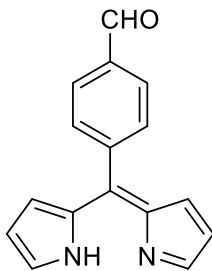
To a THF (100 mL) solution of 5-(4-aminophenyl)dipyrromethene, prepared according to a reported procedure¹ (0.8 g; 2.93 mmol), a THF (100 mL) solution of DDQ (0.73 g; 3.22 mmol) was added dropwise and stirred at room temperature overnight. The resulting mixture was evaporated under reduced pressure and the residue was purified by column chromatography (SiO₂, CH₂Cl₂/MeOH/Et₃N: 98/1/1) affording **34** (0.55 g, 80%).

¹H NMR (500 MHz, CDCl₃, 25 °C): δ = 7.63 (s, 2H, pyrroleH), 7.34 (d, J = 8.3 Hz, 2H, PhH), 6.74 (d, J = 4.4 Hz, 2H, pyrroleH), 6.72 (d, J = 8.3 Hz, 2H, PhH), 6.42 (d, J = 4.4 Hz, 2H, pyrroleH) ppm.

¹³C NMR (125 MHz, CDCl₃, 25 °C): δ = 147.8, 143.1, 143.0, 140.9, 132.9, 128.9, 127.4, 117.3, 114.0 ppm.

MS (ESI): m/z (M+H)⁺ calcd for C₁₅H₁₄N₃: 236.12, Found 236.12.

¹ R. W. Boyle *et al. Inter. J. Oncol.*, **2006**, 28,1561-1569.

Compound 35:Chemical Formula: C₁₆H₁₂N₂O

Molecular Weight: 248.29

To a dry CH₂Cl₂ (70 mL) solution of 5-(4-cyanophenyl)dipyrromethane² (2.0 g; 8.09 mmol), a dry CH₂Cl₂ (70 mL) solution of DIBAL-H (1.0 M; 10.5 mL) was added dropwise at 0 °C under argon atmosphere. The mixture was stirred at room temperature for 6 hours. The reaction was quenched by addition of a saturated NH₄Cl solution (40 mL), the resulting mixture was stirred for 4 hours at room temperature. It was then extracted by CHCl₃ and 1.0 M NaOH solution (3× 30 mL). The organic layers were combined, dried with Na₂SO₄, filtered and evaporated under reduced pressure. The crude compound was dissolved in THF (100 mL) and a THF (50 mL) solution of DDQ (2.5 g; 11.0 mmol) was added dropwise. The mixture was stirred at room temperature overnight. After evaporation under reduced pressure, the residue was purified by column chromatography (SiO₂, CH₂Cl₂/MeOH/Et₃N: 98/1/1) affording **35** as a brown oil (1.3 g, 65%).

¹H NMR (500 MHz, CDCl₃, 25 °C): δ = 10.12 (s, 1H, CHO), 7.97 (d, *J* = 7.5 Hz, 2H, PhH), 7.67 (m, 2H, pyrroleH), 7.67 (m, 2H, PhH), 6.52 (d, *J* = 4.3 Hz, 2H, pyrroleH), 6.41 (d, *J* = 4.3 Hz, 2H, pyrroleH) ppm.

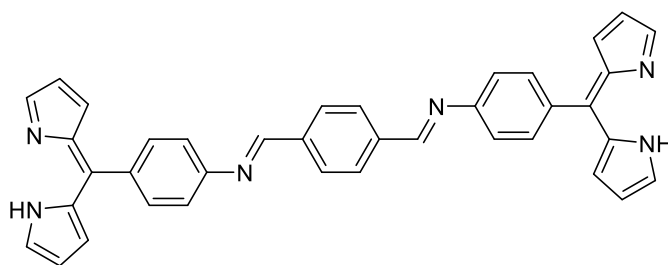
¹³C NMR (125 MHz, CDCl₃, 25 °C): δ = 191.8, 144.3, 143.4, 140.5, 139.9, 136.5, 131.4, 129.0, 128.4, 118.2 ppm.

MS (ESI): *m/z* (M+H)⁺ calcd for C₁₆H₁₃N₂O: 249.10, Found 249.10.

Elem. Anal. Calcd for C₁₆H₁₂N₂O: C 77.40; H 4.87; N 11.28, Found C 77.15; H 5.15; N 10.78.

² P. D. Rao, S. Dhanalekshmi, B. J. Littler and J. S. Lindsey, *J. Org. Chem.*, **2000**, 65, 7323-7344.

Compound 36:



Chemical Formula: C₃₈H₂₈N₆
Molecular Weight: 568.68

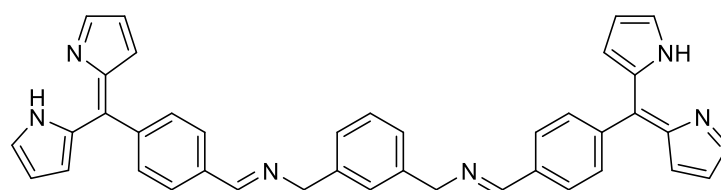
5-(4-aminophenyl)dipyrin **34** (0.3 g; 1.28 mmol), terephthalaldehyde (0.08 g; 0.58 mmol), distilled toluene (25 mL) and acetic acid (2 drops) were introduced under argon in a 50 mL two-neck flask equipped with a Dean-stark apparatus. The mixture was refluxed and the progress of the reaction was monitored by ¹H-NMR. The mixture was evaporated under reduced pressure and the crude product was recrystallized from CH₂Cl₂/cyclohexane mixture to afford **36** as a solid (0.11 g, 30%).

¹H NMR (500 MHz, CD₂Cl₂, 25 °C): δ = 8.65 (s, 2H, CH=N), 8.10 (s, 4H, PhH), 7.66 (s, 4H, pyrroleH), 7.57 (d, *J* = 8.4 Hz, 4H, PhH), 7.35 (d, *J* = 8.4 Hz, 4H, PhH), 6.68 (d, *J* = 4.2 Hz, 4H, pyrroleH), 6.44 (d, *J* = 4.2 Hz, 4H, pyrroleH) ppm.

¹³C NMR (125 MHz, CD₂Cl₂, 25 °C): δ = 160.4, 152.8, 144.0, 141.8, 141.3, 135.6, 132.4, 130.3, 129.6, 128.9, 120.6, 118.0 ppm.

HRMS (ESI): *m/z* (M+H)⁺ calcd for C₃₈H₂₉N₆: 569.2417, Found 569.2415.

Compound 37:



Chemical Formula: C₄₀H₃₂N₆

Molecular Weight: 596.74

Compound **35** (0.2 g; 0.81 mmol) was dissolved in dry CHCl₃ (40 mL) under argon atmosphere. Then, *m*-xylylenediamine (80 μ L; 0.604 mmol) and TFA (1 drop) were added. The mixture was stirred at room temperature and the reaction was followed by ¹H-NMR. The resulting mixture was evaporated under reduced pressure and the crude product was recrystallized from a CHCl₃/cyclohexane mixture to afford **37** as a solid (0.27 g, 96%).

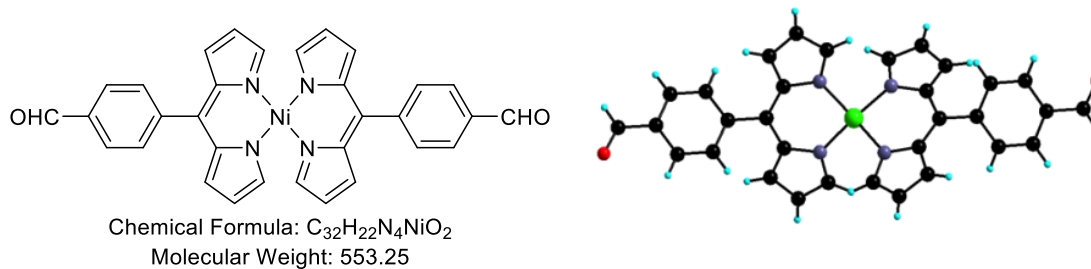
¹H NMR (500 MHz, CD₂Cl₂, 25 °C): δ = 8.52 (s, 2H, CH=N), 7.87 (d, *J* = 8.1 Hz, 4H, PhH), 7.64 (s, 4H, pyrroleH), 7.55 (d, *J* = 8.1 Hz, 4H, PhH), 7.40-7.35 (m, 2H, PhH), 7.29 (d, *J* = 7.8 Hz, 2H, PhH), 6.58 (d, *J* = 4.2 Hz, 4H, pyrroleH), 6.4 (d, *J* = 4.2 Hz, 4H, pyrroleH) ppm.

¹³C NMR (125 MHz, CD₂Cl₂, 25 °C): δ = 161.5, 144.2, 141.4, 141.1, 140.2, 139.9, 137.3, 131.5, 129.0, 128.8, 128.1, 127.8, 127.1, 118.1, 65.5 ppm.

HRMS (ESI): *m/z* (M+H)⁺ calcd for C₄₀H₃₃N₆: 597.2761, Found 597.2764.

λ_{max} (CH₂Cl₂)/nm ($\epsilon/\text{mol}^{-1} \text{ L cm}^{-1}$): 314 (22260), 434 (33540).

Compound 38:



To a $CHCl_3$ (50 mL) solution of 5-(4-formylphenyl)dipyririn **35** (0.83 g; 3.34 mmol), a MeOH (50 mL) solution of $Ni(OAc)_2 \cdot 4H_2O$ (0.42 g; 1.67 mmol) was added. The mixture was stirred at room temperature overnight. It was then evaporated under reduced pressure and the residue was washed with MeOH affording the complex as a dark red solid (0.76 g, 82%).

1H NMR (300 MHz, $CDCl_3$, 25 °C): δ = 10.38 (s, 4H, pyrroleH), 10.10 (s, 2H, CHO), 8.20 (s, 4H, pyrroleH), 7.92 (d, 4H, J = 7.9 Hz, PhH), 7.53 (d, 4H, J = 7.9 Hz, PhH), 6.70 (s, 4H, pyrroleH) ppm.

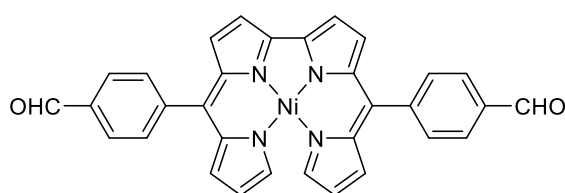
^{13}C NMR (125 MHz, $CDCl_3$, 25 °C): δ = 191.9, 177.2, 150.4, 142.8, 141.6, 139.8, 138.1, 136.7, 131.3, 128.9 ppm.

HRMS (ESI): m/z (L+H)⁺ calcd for $C_{16}H_{13}N_2O$: 249.10, Found 249.10.

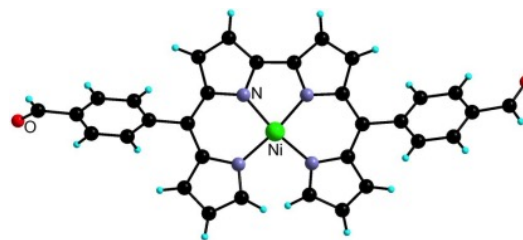
Crystallographic data for compound 38

Formula	C ₃₂ H ₂₂ N ₄ NiO ₂
Formula weight	553.24
Temperature	173(2) K
Wavelength	0.71073 Å
Crystal system	Triclinic
Space group	<i>P</i> -1
Unit cell dimensions	$a = 9.7819(2)$ Å $\alpha = 110.8970(10)^\circ$. $b = 11.6608(3)$ Å $\beta = 98.8930(10)^\circ$. $c = 12.9613(3)$ Å $\gamma = 111.0520(10)^\circ$.
Volume	1219.34(5) Å ³
<i>Z</i>	2
Density (calculated)	1.507 Mg/m ³
Absorption coefficient	0.836 mm ⁻¹
<i>F</i> (000)	572
Crystal size	0.150 x 0.100 x 0.070 mm ³
Theta range for data collection	1.778 to 30.160°.
Index ranges	-13 ≤ <i>h</i> ≤ 13, -16 ≤ <i>k</i> ≤ 16, -16 ≤ <i>l</i> ≤ 18
Reflections collected	24117
Independent reflections	6572 [<i>R</i> (int) = 0.0251]
Completeness to theta = 25.242°	95.8 %
Absorption correction	Semi-empirical from equivalents
Max. and min. transmission	0.943 and 0.884
Refinement method	Full-matrix least-squares on <i>F</i> ²
Data / restraints / parameters	6572 / 0 / 352
Goodness-of-fit on <i>F</i> ²	1.053
Final <i>R</i> indices [<i>I</i> > 2σ(<i>I</i>)]	<i>R</i> _{<i>I</i>} = 0.0326, <i>wR</i> ₂ = 0.0768
<i>R</i> indices (all data)	<i>R</i> _{<i>I</i>} = 0.0396, <i>wR</i> ₂ = 0.0800
Largest diff. peak and hole	0.414 and -0.370 e.Å ⁻³

Compound 39:



Chemical Formula: $C_{32}H_{20}N_4NiO_2$
Molecular Weight: 551.23



A toluene (150 mL) solution of DDQ (0.34 g; 1.49 mmol) was added dropwise to a toluene (200 mL) solution of complex **38** (0.75 g; 1.36 mmol). The color of the mixture turned from red to brown, upon heating at reflux for 24 hours. After evaporation under reduced pressure, the residue was purified by column chromatography (SiO_2 , CH_2Cl_2 /Cyclohexane: 9/1) affording the desired compound as a red solid (0.6 g, 80%).

1H NMR (500 MHz, $CDCl_3$, 25 °C): δ = 10.14 (s, 2H, CHO), 8.00 (d, 4H, J = 8.2 Hz, PhH), 7.73 (d, 4H, J = 8.2 Hz, PhH), 6.73 (d, 2H, J = 4.7 Hz, pyrroleH), 6.68 (d, 2H, J = 4.4 Hz, pyrroleH), 6.65 (d, 2H, J = 4.4 Hz, pyrroleH), 6.46 (d, 2H, J = 4.7 Hz, pyrroleH), 5.94 (s, 2H, pyrroleH) ppm.

^{13}C NMR (125 MHz, $CDCl_3$, 25 °C): δ = 191.9, 161.9, 154.1, 142.9, 141.7, 138.6, 136.7, 135.5, 134.7, 131.6, 130.0, 129.1, 117.8, 116.0 ppm

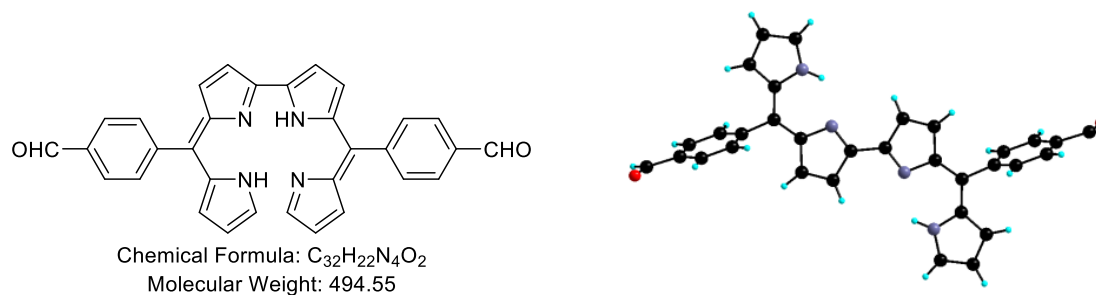
HRMS (ESI): m/z (M)⁺ calcd. for $C_{32}H_{20}N_4NiO_2$: 550.0934, Found 550.0947.

λ_{max} (CH_2Cl_2)/nm (ϵ / mol^{-1} L cm^{-1}): 302 (22750), 355 (24200), 418 (35410), 573 (12930), 775 (5570).

Crystallographic data for compound 39

Formula	C ₃₂ H ₂₀ N ₄ NiO ₂
Formula weight	551.23
Temperature	173(2) K
Wavelength	0.71073 Å
Crystal system	Triclinic
Space group	<i>P</i> -1
Unit cell dimensions	<i>a</i> = 9.8321(3) Å <i>α</i> = 103.1690(10)°. <i>b</i> = 10.7832(3) Å <i>β</i> = 102.6240(10)°. <i>c</i> = 13.3416(3) Å <i>γ</i> = 111.8220(10)°.
Volume	1204.51(6) Å ³
<i>Z</i>	2
Density (calculated)	1.520 Mg/m ³
Absorption coefficient	0.846 mm ⁻¹
<i>F</i> (000)	568
Crystal size	0.080 x 0.060 x 0.030 mm ³
Theta range for data collection	2.164 to 30.170°.
Index ranges	-13 ≤ <i>h</i> ≤ 13, -15 ≤ <i>k</i> ≤ 15, -18 ≤ <i>l</i> ≤ 17
Reflections collected	23901
Independent reflections	6497 [<i>R</i> (int) = 0.0408]
Completeness to theta = 25.242°	95.7 %
Absorption correction	Semi-empirical from equivalents
Max. and min. transmission	0.974 and 0.934
Refinement method	Full-matrix least-squares on <i>F</i> ²
Data / restraints / parameters	6497 / 0 / 352
Goodness-of-fit on <i>F</i> ²	1.030
Final <i>R</i> indices [<i>I</i> > 2σ(<i>I</i>)]	<i>R</i> _{<i>I</i>} = 0.0416, <i>wR</i> ₂ = 0.0946
<i>R</i> indices (all data)	<i>R</i> _{<i>I</i>} = 0.0628, <i>wR</i> ₂ = 0.1051
Largest diff. peak and hole	0.638 and -0.390 e.Å ⁻³

Compound 40:



A 12 M solution of HCl (20 mL) was added to a $CHCl_3$ (80 mL) solution of complex **39** (0.56 g; 1.02 mmol) and the mixture stirred at room temperature overnight. Upon addition of a saturated Na_2CO_3 solution, the organic layer turned from green to dark blue. The mixture was extracted with $CHCl_3$ (3×100 mL) and the combined organic layers were dried over Na_2SO_4 , filtered and evaporated affording the 2,2'-bisdipyrrole as a dark blue solid (0.5 g, 99%). Single crystals were obtained by slow evaporation of a solution of the complex in $CHCl_3$.

1H NMR (500 MHz, $CDCl_3$, 25 °C): δ = 10.14 (s, 2H, CHO), 8.01(d, J = 8.2 Hz, 4H, PhH), 7.72 (d, J = 8.2 Hz, 4H, PhH), 7.64 (s, 2H, pyrroleH), 7.02(d, J = 4.4 Hz, 2H, pyrroleH), 6.68 (d, J = 4.4 Hz, 2H, pyrroleH), 6.52 (d, J = 4.1 Hz, 2H, pyrroleH), 6.44 (d, J = 4.1 Hz, 2H, pyrroleH) ppm.

^{13}C NMR (125 MHz, $CDCl_3$, 25 °C): δ = 191.9, 153.1, 145.2, 143.5, 139.6, 139.0, 138.8, 136.6, 131.8, 131.7, 129.2, 126.5, 120.8, 116.7 ppm.

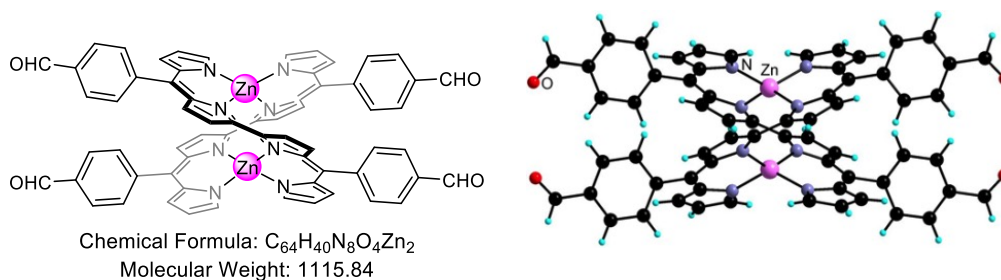
HRMS (ESI): m/z ($M+H$)⁺ calcd. for $C_{32}H_{23}N_4O_2$: 495.1816, Found 495.1775.

$\lambda_{max}(CH_2Cl_2)/nm$ ($\epsilon/mol^{-1} L cm^{-1}$): 258 (31300), 280 (26010), 332 (24270), 413 (22740), 591 (37640).

Crystallographic data for compound (40)(CHCl₃)

Formula	C ₃₃ H ₂₃ Cl ₃ N ₄ O ₂	
Formula weight	613.90	
Temperature	173(2) K	
Wavelength	0.71073 Å	
Crystal system	Monoclinic	
Space group	<i>P</i> 2 ₁ / <i>n</i>	
Unit cell dimensions	<i>a</i> = 11.4063(4) Å	<i>α</i> = 90°.
	<i>b</i> = 9.7778(3) Å	<i>β</i> = 94.7850(10)°.
	<i>c</i> = 13.4576(4) Å	<i>γ</i> = 90°.
Volume	1495.67(8) Å ³	
<i>Z</i>	2	
Density (calculated)	1.363 Mg/m ³	
Absorption coefficient	0.344 mm ⁻¹	
<i>F</i> (000)	632	
Crystal size	0.080 x 0.080 x 0.080 mm ³	
Theta range for data collection	2.748 to 30.082°.	
Index ranges	-16 ≤ <i>h</i> ≤ 16, -13 ≤ <i>k</i> ≤ 13, -18 ≤ <i>l</i> ≤ 14	
Reflections collected	28945	
Independent reflections	4084 [<i>R</i> (int) = 0.0233]	
Completeness to theta = 25.242°	96.9 %	
Absorption correction	Semi-empirical from equivalents	
Max. and min. transmission	0.972 and 0.972	
Refinement method	Full-matrix least-squares on <i>F</i> ²	
Data / restraints / parameters	4084 / 1 / 208	
Goodness-of-fit on <i>F</i> ²	1.039	
Final <i>R</i> indices [<i>I</i> > 2σ(<i>I</i>)]	<i>R</i> ₁ = 0.0701, <i>wR</i> ₂ = 0.1929	
<i>R</i> indices (all data)	<i>R</i> ₁ = 0.0802, <i>wR</i> ₂ = 0.2026	
Largest diff. peak and hole	0.756 and -0.735 e.Å ⁻³	

Compound 41:



A MeOH (60 mL) solution of $Zn(OAc)_2 \cdot 2H_2O$ (78 mg; 0.36 mmol) was added to a $CHCl_3$ (60 mL) solution of ligand **40** (0.16 g; 0.32 mmol). Upon stirring for 24 hours at room temperature, the solution turned from dark blue to dark green. After evaporation under reduced pressure, the residue was washed with MeOH (3×50 mL) affording helicate **41** (0.17 g, 94%).

1H NMR (500 MHz, $CDCl_3$, 25 °C): δ = 10.13 (s, 4H, CHO), 7.95 (d, 4H, J = 7.8 Hz, PhH), 7.75 (d, 4H, J = 7.8 Hz, PhH), 7.66 (d, 4H, J = 7.8 Hz, PhH), 7.22 (d, 4H, J = 7.8 Hz, PhH), 6.98 (s, 4H, pyrroleH), 6.51 (d, J = 4.3 Hz, 4H, pyrroleH), 6.44 (d, J = 4.1 Hz, 4H, pyrroleH), 6.35 (d, J = 4.1 Hz, 4H, pyrroleH), 6.31 (d, J = 4.3 Hz, 4H, pyrroleH) ppm.

^{13}C NMR (125 MHz, $CDCl_3$, 25 °C): δ = 191.9, 154.9, 150.4, 145.4, 144.8, 141.6, 140.9, 136.5, 132.9, 132.2, 132.2, 131.7, 128.7, 128.4, 118.4, 117.3 ppm.

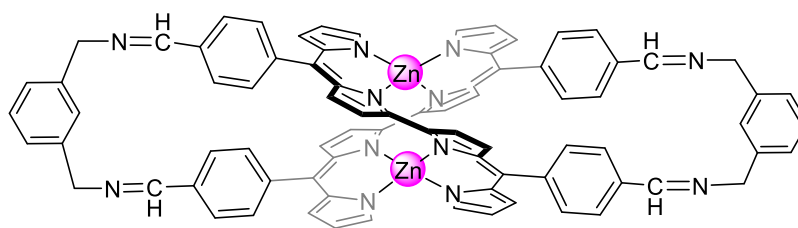
HRMS (ESI): m/z (M)⁺ calcd. for $C_{64}H_{40}N_8O_4Zn_2$: 1112.1750, Found 1112.1804.

$\lambda_{max}(CH_2Cl_2)/nm$ ($\epsilon/mol^{-1} L cm^{-1}$): 257 (71700), 284 (60800), 345 (60000), 432 (110200), 646 (66000).

Crystallographic data for compound 41

Formula	$C_{64}H_{40}N_8O_4Zn_2$	
Formula weight	1115.78	
Temperature	173(2) K	
Wavelength	0.71073 Å	
Crystal system	Tetragonal	
Space group	$P-4n2$	
Unit cell dimensions	$a = 11.9527(3)$ Å	$\alpha = 90^\circ$.
	$b = 11.9527(3)$ Å	$\beta = 90^\circ$.
	$c = 17.7035(7)$ Å	$\gamma = 90^\circ$.
Volume	2529.25(16) Å ³	
Z	2	
Density (calculated)	1.465 Mg/m ³	
Absorption coefficient	1.010 mm ⁻¹	
F(000)	1144	
Crystal size	0.100 x 0.080 x 0.030 mm ³	
Theta range for data collection	2.056 to 30.193°.	
Index ranges	-16 ≤ h ≤ 16, -14 ≤ k ≤ 16, -24 ≤ l ≤ 25	
Reflections collected	40519	
Independent reflections	3750 [R(int) = 0.0574]	
Completeness to theta = 25.242°	99.9 %	
Absorption correction	Semi-empirical from equivalents	
Max. and min. transmission	0.969 and 0.905	
Refinement method	Full-matrix least-squares on F ²	
Data / restraints / parameters	3750 / 0 / 177	
Goodness-of-fit on F ²	1.050	
Final R indices [I > 2σ(I)]	$R_I = 0.0532$, $wR_2 = 0.1285$	
R indices (all data)	$R_I = 0.0809$, $wR_2 = 0.1443$	
Absolute structure parameter	0.011(8)	
Largest diff. peak and hole	0.625 and -0.615 e.Å ⁻³	

Compound 42:



Chemical Formula: $C_{80}H_{56}N_{12}Zn_2$

Molecular Weight: 1316.17

To a dry $CHCl_3$ (250 mL) solution of the zinc helicate **41** (5.0 mg; 4.48×10^{-2} mmol), a dry $CHCl_3$ (250 mL) solution of *m*-xylylenediamine (12.4 μ L; 9.41×10^{-2} mmol) and TFA (0.01 equiv) were added under argon. The mixture was stirred at room temperature for 24 hours. It was then evaporated under reduced pressure affording **42** as a solid (5.8 mg, 98%).

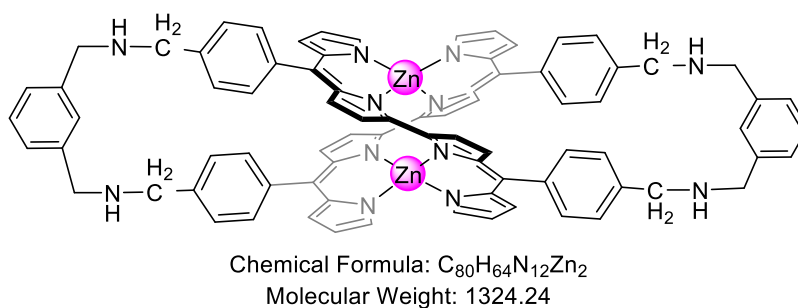
1H NMR (400 MHz, $CDCl_3$, 25 °C): δ = 8.53 (s, 4H, CH=N), 7.92 (d, J = 7.5 Hz, 4H, PhH), 7.59 (d, J = 7.5 Hz, 4H, PhH), 7.54 (d, J = 7.5 Hz, 4H, PhH), 7.44 (s, 2H, PhH), 7.39-7.35 (m, 6H, PhH/pyrroleH), 7.23 (d, J = 7.5 Hz, 4H, PhH), 7.1 (d, J = 7.5 Hz, 4H, PhH), 6.61 (d, J = 4.3 Hz, 4H, pyrroleH), 6.47 (d, J = 4.3 Hz, 4H, pyrroleH), 6.38 (d, J = 4.3 Hz, 4H, pyrroleH), 6.31 (d, J = 4.3 Hz, 4H, pyrroleH), 5.08 (d, J = 15.2 Hz, 4H, CH_2), 4.92 (d, J = 15.2 Hz, 4H, CH_2) ppm.

^{13}C NMR (125 MHz, $CDCl_3$, 25 °C): δ = 162.1, 155.4, 150.0, 146.3, 142.0, 141.7, 140.9, 140.5, 136.7, 133.8, 132.9, 132.4, 131.1, 129.1, 128.2, 125.2, 124.7, 117.7, 117.3, 63.6 ppm.

HRMS (ESI): m/z (M)⁺ calcd. for $C_{80}H_{56}N_{12}Zn_2$: 1312.3328, Found 1312.3338.

λ_{max} (CH_2Cl_2)/nm ($\epsilon/mol^{-1} L cm^{-1}$): 257 (43600), 349 (44400), 431 (56300), 473 (22500), 577 (50200).

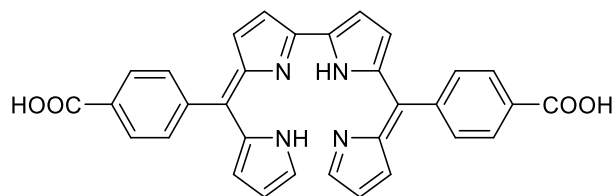
Compound 43:



To a dry CHCl₃ (15 mL) solution of the zinc helicate **42** (22 mg; 1.67×10⁻² mmol), a dry MeOH (4 mL) solution of NaBH₃CN (4.7 mg; 7.52×10⁻² mmol) and TFA (0.01 equiv) were added under argon. The mixture was stirred at room temperature under Ar. The reaction was monitored by ¹H-NMR. The mixture was washed with distilled H₂O (3 × 20 mL) and extracted with CHCl₃ (3 × 20 mL), the combined organic layers were dried over Na₂SO₄ and then filtered. After evaporation under reduced pressure, the residue was purified by column chromatography (SiO₂, CH₂Cl₂/MeOH/Et₃N: 92/7/1) affording the desired compound as a solid (15 mg).

MS (ESI): m/z (M)²⁺ calcd. for C₈₀H₅₆N₁₂Zn₂: 660.20, Found 660.19.

λ_{max}(CH₂Cl₂)/nm (ε/mol⁻¹ L cm⁻¹): 350 (37800), 425 (74400), 471 (24300), 572 (49100).

Compound 44:

Chemical Formula: C₃₂H₂₂N₄O₄
Molecular Weight: 526.55

A LiOH solution (0.16 g, 30 mL H₂O) was added to a THF (30 mL) solution of diester-2,2'-bisdipyrin³ (0.36 g; 0.65 mmol). The mixture was stirred at room temperature for 2 days and then evaporated under reduced pressure. The residue was acidified with 37% HCl down to pH = 2. A saturated NaHCO₃ solution was added until neutralization. The precipitate was isolated, then re-dissolved in MeOH. The solution was dried over Na₂SO₄, filtered and evaporated under reduced pressure. The crude product was washed by a Et₂O/MeOH (9/1) mixture, affording the compound **44** as a dark blue solid (0.3 g, 88%).

¹H NMR (500 MHz, DMSO-d₆/20% MeOD-d₄, 25 °C): δ = 7.97 (d, J = 8.0 Hz, 4H, PhH), 7.68 (s, 2H, pyrroleH), 7.46 (d, J = 4.3 Hz, 2H, pyrroleH), 7.42 (d, J = 8.0 Hz, 4H, PhH), 6.78 (d, J = 4.3 Hz, 2H, pyrroleH), 6.43 (d, J = 4.1 Hz, 2H, pyrroleH), 6.38 (d, J = 4.1 Hz, 2H, pyrroleH) ppm.

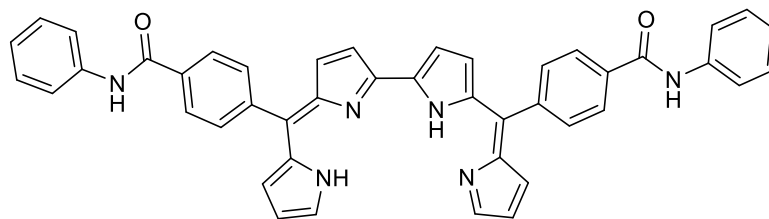
¹³C NMR (125 MHz, DMSO-d₆/20% MeOD-d₄, 25 °C): δ = 169.0, 157.6, 156.7, 147.3, 141.7, 141.1, 137.0, 135.2, 133.4, 129.8, 128.4, 124.7, 122.7, 113.9 ppm.

HRMS (ESI): m/z (M+H)⁺ calcd. for C₃₂H₂₃N₄O₄ 527.1714, Found 527.1739.

λ_{max} (MeOH)/nm ($\epsilon/\text{mol}^{-1} \text{ L cm}^{-1}$): 254 (17600), 337 (17570), 408 (19090), 583 (27270).

³ S. A. Baudron, H. Ruffin and M. W. Hosseini, *Chem. Commun.*, **2015**, 51, 5906.

Compound 45:



Chemical Formula: C₄₄H₃₂N₆O₂

Molecular Weight: 676.78

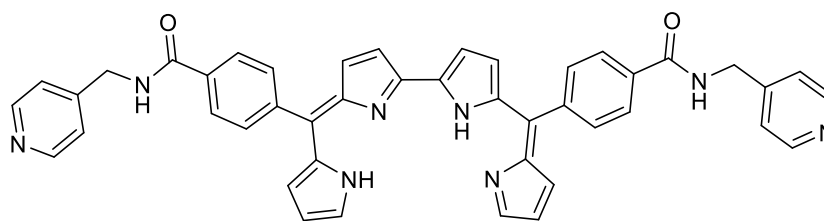
Bisdipyrrole-COOH **44** (0.4 g; 0.76 mmol) was dissolved in DMF (100 mL) under argon. Then, EDCi·HCl (0.36 g; 1.9 mmol), HOBt (0.26 g; 1.9 mmol) and Aniline (0.15 mL, 1.67 mmol) were added. The resulting mixture was refluxed and stirred under argon overnight. Upon removal of DMF, the residue was extracted with CHCl₃ and a NaHCO₃ saturated solution (100 mL), and the combined organic layers were dried over Na₂SO₄, filtered and evaporated under reduced pressure. The residue was purified by column chromatography (SiO₂, CH₂Cl₂/Et₃N: 99/1) affording the compound **45** (0.09 g, 18%).

¹H NMR (500 MHz, CDCl₃, 25 °C): δ = 8.0 (d, *J* = 8.6 Hz, 4H, PhH), 7.71-7.66 (m, 10H, PhH), 7.43-7.40 (m, 4H, PhH/pyrroleH), 7.2 (t, *J* = 7.9 Hz, 2H, PhH), 7.09 (d, *J* = 4.6 Hz, 2H, pyrroleH), 6.78 (d, *J* = 4.6 Hz, 2H, pyrroleH), 6.57 (d, *J* = 4.6 Hz, 2H, pyrroleH), 6.45 (d, *J* = 4.6 Hz, 2H, pyrroleH) ppm.

¹³C NMR (125 MHz, CDCl₃, 25 °C): δ = 165.4, 153.9, 146.0, 141.1, 139.5, 139.1, 138.5, 135.9, 132.2, 131.7, 129.4, 126.9, 126.5, 126.4, 125.0, 121.0, 120.6, 116.4 ppm.

HRMS (ESI): *m/z* (M+H)⁺ calcd. for C₄₄H₃₃N₆O₂: 677.2660, Found 677.2624.

λ_{max}(CH₂Cl₂)/nm (ε/mol⁻¹ L cm⁻¹): 265 (42100), 332 (32100), 412 (30780), 589 (46500).

Compound 46:

Chemical Formula: C₄₄H₃₄N₈O₂
Molecular Weight: 706.81

Bisdipyrrole-COOH **44** (0.32 g; 0.61 mmol) was dissolved in MeOH (50 mL) under argon atmosphere. Then, EDCi·HCl (0.29 g; 1.52 mmol), HOBt (0.21 g; 1.52 mmol) and 4-(aminomethyl)pyridine (0.14 mL, 1.34 mmol) were added and stirred at room temperature under argon for 2 days. After removing the solvent, the residue was extracted with CHCl₃ and saturated NaHCO₃ solution (100 mL), and the combined organic layers were dried over Na₂SO₄, filtered and evaporated. The crude product was purified by column chromatography (SiO₂, CH₂Cl₂/MeOH/Et₃N: 94/5/1). The resulting product was recrystallized from a MeOH/Et₂O: 2/20 mixture affording the compound **46** (0.2 g, 43%).

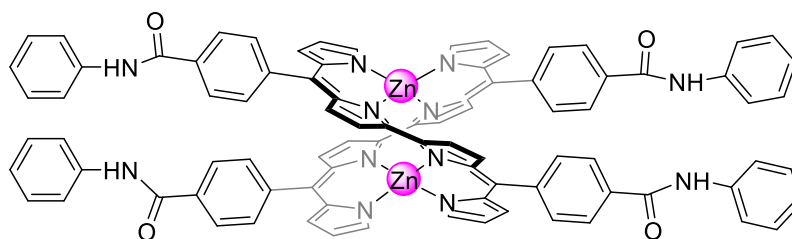
¹H NMR (500 MHz, CDCl₃, 25 °C): δ = 8.61 (d, *J* = 6.0 Hz, 4H, pyH), 7.93 (d, *J* = 8.1 Hz, 4H, PhH), 7.65-7.63 (m, 6H, PhH/ pyrroleH), 7.31 (d, *J* = 6.0 Hz, 4H, pyH), 7.0 (d, *J* = 4.5 Hz, 2H, pyrroleH), 6.70-6.68 (m, 4H, pyrroleH), 6.52 (d, *J* = 4.5 Hz, 2H, pyrroleH), 6.43 (d, *J* = 4.5 Hz, 2H, pyrroleH), 4.73 (d, *J* = 6.0 Hz, 4H, CH₂) ppm.

¹³C NMR (125 MHz, CDCl₃, 25 °C): δ = 167.3, 153.0, 150.4, 147.3, 145.3, 141.1, 139.4, 139.1, 139.1, 134.4, 131.7, 131.4, 126.6, 122.5, 120.7, 116.5, 43.1 ppm.

HRMS (ESI): *m/z* (M+H)⁺ calcd. for C₄₄H₃₅N₈O₂: 707.2877, Found 707.2867.

λ_{max}(CH₂Cl₂)/nm (ε/ mol⁻¹ L cm⁻¹): 331 (23760), 410 (27160), 587 (37780).

Compound 47:



Chemical Formula: $C_{88}H_{60}N_{12}O_4Zn_2$
Molecular Weight: 1480.29

A $CHCl_3$ solution (1 mL) of compound **44** (5 mg, 0.0074 mmol) was first layered with a 1/1 $CHCl_3$ /MeOH (1 mL) mixture and then with a MeOH solution (1 mL) of $Zn(OAc)_2 \cdot 2H_2O$ (0.0081 mmol). After a few days, a precipitate appeared which was isolated by filtration. (5 mg, 91%)

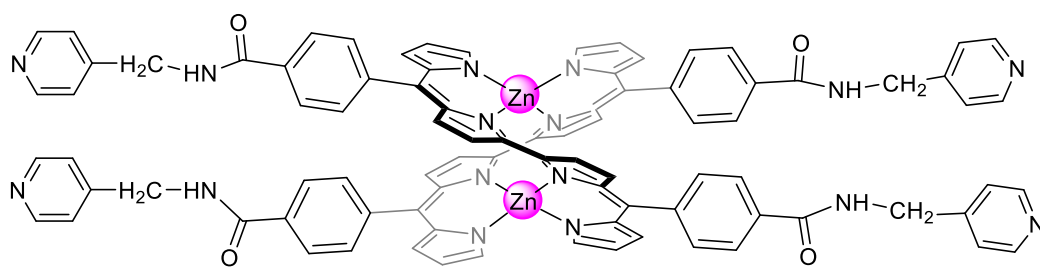
1H NMR (300 MHz, THF- d_8 , 25 °C): δ = 6.59 (d, J = 8.2 Hz, 4H, PhH), 6.44-6.38 (m, 12H, PhH/pyrroleH), 6.1(d, J = 8.2 Hz, 4H, PhH), 5.82 (d, J = 7.4 Hz, 4H, PhH), 5.79 (d, J = 7.4 Hz, 4H, PhH), 5.70 (s, 4H, PhH), 5.65 (d, J = 8.2 Hz, 4H, PhH), 5.59 (t, J = 7.4 Hz, 4H, PhH), 5.09 (d, J = 4.2 Hz, 4H, pyrroleH), 4.89 (d, J = 4.2 Hz, 4H, pyrroleH), 4.86 (d, J = 4.2 Hz, 4H, pyrroleH), 4.81 (d, J = 4.2 Hz, 4H, pyrroleH) ppm.

^{13}C NMR (125 MHz, THF- d_8 , 25 °C): δ = 165.9, 155.9, 150.4, 146.5, 142.9, 142.6, 141.5, 140.1, 140.0, 136.4, 134.0, 132.4, 132.1, 131.6, 129.1, 127.4, 127.1, 124.4, 121.3, 121.2, 118.2, 117.5 ppm.

HRMS (ESI): m/z ($M+Na$)⁺ calcd. for $C_{88}H_{60}N_{12}NaO_4Zn_2$: 1499.3336, Found 1499.3316.

λ_{max} (THF)/nm ($\epsilon/mol^{-1} L cm^{-1}$): 269 (66600), 339 (41490), 428 (49830), 573 (62410), 645 (41580).

Compound 48:



Chemical Formula: $C_{88}H_{64}N_{16}O_4Zn_2$

Molecular Weight: 1540.35

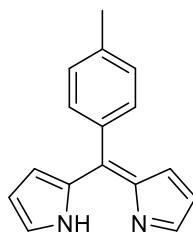
A $CHCl_3$ solution (1 mL) of compound **46** (5 mg, 0.0071 mmol) was first layered with a 1/1 $CHCl_3$ /MeOH (1 mL) mixture and then with a MeOH solution (1 mL) of $Zn(OAc)_2 \cdot 2H_2O$ (0.011 mmol). After a few days, the precipitate formed was isolated by filtration. (5 mg, 92%)

1H NMR (300 MHz, $DMSO-d_6$, 25 °C): δ = 9.2 (d, J = 4.1 Hz, 4H, pyrroleH), 8.52 (d, J = 5.4 Hz, 8H, pyH), 8.01 (d, J = 8.1 Hz, 4H, PhH), 7.88 (d, J = 8.1 Hz, 4H, PhH), 7.59 (d, J = 8.1 Hz, 4H, PhH), 7.53 (d, J = 5.4 Hz, 8H, pyH), 7.09 (d, J = 8.1 Hz, 4H, PhH), 6.83 (s, 4H, pyrroleH), 6.58 (d, J = 4.1 Hz, 4H, pyrroleH), 6.49 (d, J = 4.1 Hz, 4H, pyrroleH), 6.36 (d, J = 4.1 Hz, 4H, pyrroleH), 4.54 (d, J = 5.9 Hz, 8H, CH_2) ppm.

MS (ESI): m/z ($M+2H$) $^{2+}$ calcd. for $C_{88}H_{64}N_{16}O_4Zn_2H_2$: 769.20, Found 769.21.

λ_{max} (DMF)/nm ($\epsilon/mol^{-1} L cm^{-1}$): 338 (34890), 421 (46200), 571 (58670), 631 (32560).

Compound 50:



Chemical Formula: C₁₆H₁₄N₂

Molecular Weight: 234.30

To a THF (300 mL) solution of 5-(4-methylphenyl)dipyrromethane⁴ (3.16 g; 13 mmol), a THF (300 mL) solution of DDQ (3.37 g; 15 mmol) was added dropwise. The resulting mixture was stirred at room temperature overnight and then evaporated under reduced pressure. The residue was purified by column chromatography (SiO₂, CH₂Cl₂/Et₃N: 99/1) affording **50** (0.85 g, 28%).

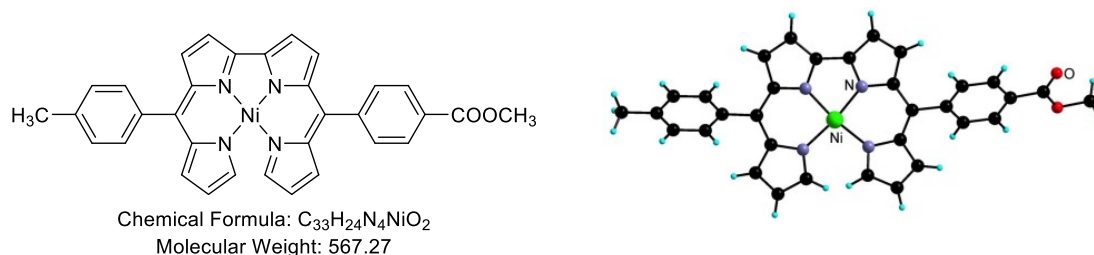
¹H NMR (500 MHz, CD₂Cl₂, 25 °C): δ = 7.63 (s, 2H, pyrroleH), 7.38 (d, J = 8.2 Hz, 2H, PhH), 7.27 (d, J = 8.2 Hz, 2H, PhH), 6.61 (d, J = 4.2 Hz, 2H, pyrroleH), 6.4 (d, J = 4.2 Hz, 2H, pyrroleH), 2.45 (s, 3H, CH₃) ppm.

¹³C NMR (125 MHz, CD₂Cl₂, 25 °C): δ = 143.7, 142.5, 141.4, 139.6, 134.6, 131.2, 129.0, 128.7, 117.8, 21.5 ppm.

MS (ESI): m/z (M+H)⁺ calcd for C₁₆H₁₅N₂: 235.12, Found 235.12.

⁴ B. J. Littler, M. A. Miller, C.-H. Hung, R. W. Wagner, D. F. O'Shea, P. D. Boyle and J. S. Lindsey, *J. Org. Chem.*, **1999**, *64*, 1391.

Compound 51:



5-(4-methylphenyl)dipyrin **50** (0.54 g; 2.3 mmol), 5-(4-methoxycarbonylphenyl)dipyrin⁵ (0.64 g; 2.3 mmol) and Ni(OAc)₂·4H₂O (5.72 g; 23 mmol) was dissolved in chloroform (150 mL). The mixture was stirred at room temperature for 24h and then evaporated under reduced pressure. The residue and *p*-chloranil (5.66 g; 23 mmol) were dissolved in toluene (150 mL). The mixture was refluxed for 2 days. The mixture was then filtered and the filtrate was evaporated under reduced pressure. The residue was re-dissolved in CHCl₃, filtered to remove remaining *p*-chloranil and evaporated under reduced pressure. The crude product was purified by column chromatography (SiO₂, CH₂Cl₂/EtOAc: 9/1) affording **51** as a black solid (0.56 g, 43%).

¹H NMR (400 MHz, CDCl₃, 25 °C): δ = 8.15 (d, *J* = 8.4 Hz, 2H, PhH), 7.64 (d, *J* = 8.4 Hz, 2H, PhH), 7.46 (d, *J* = 7.8 Hz, 2H, PhH), 7.28 (d, *J* = 7.8 Hz, 2H, PhH), 6.82 (d, *J* = 4.6 Hz, 1H, pyrroleH), 6.77 (d, *J* = 4.2 Hz, 1H, pyrroleH), 6.72 (d, *J* = 4.6 Hz, 1H, pyrroleH), 6.67 (d, *J* = 4.2 Hz, 1H, pyrroleH), 6.62 (d, *J* = 4.2 Hz, 2H, pyrroleH), 6.45-6.43 (m, 2H, pyrroleH), 5.98 (s, 1H, pyrroleH), 5.96 (s, 1H, pyrroleH), 3.99 (s, 3H, COOCH₃), 2.47 (s, 3H, CH₃) ppm.

¹³C NMR (125 MHz, CDCl₃, 25 °C): δ = 169.7, 166.9, 161.1, 154.3, 153.1, 144.3, 142.0, 141.5, 140.9, 139.5, 139.2, 138.6, 136.2, 135.4, 135.3, 134.4, 134.0, 131.2, 131.1, 130.7, 130.1, 129.0, 128.6, 117.3, 117.3, 115.6, 115.4, 29.9, 21.6 ppm.

HRMS (ESI): *m/z* (M+H)⁺ calcd. for C₃₃H₂₅N₄NiO₂: 567.1326, Found 567.1365.

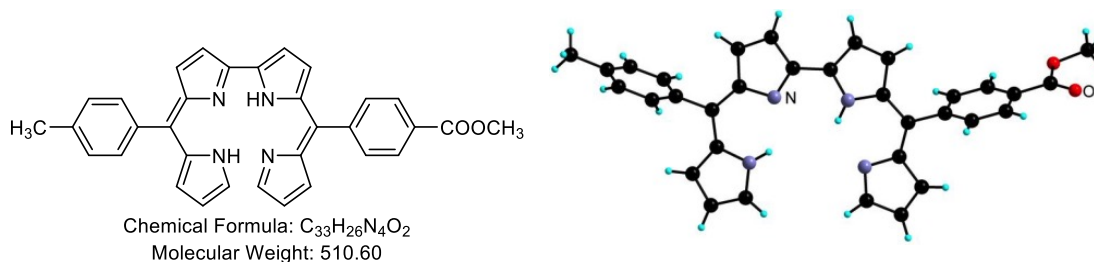
λ_{max} (CH₂Cl₂)/nm (ε/mol⁻¹ L cm⁻¹): 292 (32090), 359 (13670), 413 (20990), 562 (6910).

⁵ D. Dolphin *et al.* *Can. J. Chem.*, **1996**, 74, 2182-2193.

Crystallographic data for compound 51

Formula	$\text{C}_{33}\text{H}_{24}\text{N}_4\text{NiO}_2$	
Formula weight	567.27	
Temperature	173(2) K	
Wavelength	0.71073 Å	
Crystal system	Triclinic	
Space group	$P\bar{1}$	
Unit cell dimensions	$a = 10.4334(4)$ Å	$\alpha = 64.165(2)^\circ$.
	$b = 11.4214(4)$ Å	$\beta = 78.961(2)^\circ$.
	$c = 12.7442(5)$ Å	$\gamma = 71.119(2)^\circ$.
Volume	1291.05(9) Å ³	
Z	2	
Density (calculated)	1.459 Mg/m ³	
Absorption coefficient	0.791 mm ⁻¹	
F(000)	588	
Crystal size	0.040 x 0.040 x 0.020 mm ³	
Theta range for data collection	2.059 to 30.264°.	
Index ranges	-14 ≤ h ≤ 14, -15 ≤ k ≤ 16, -17 ≤ l ≤ 17	
Reflections collected	17194	
Independent reflections	6986 [R(int) = 0.0508]	
Completeness to theta = 25.242°	96.2 %	
Absorption correction	Semi-empirical from equivalents	
Max. and min. transmission	0.983 and 0.968	
Refinement method	Full-matrix least-squares on F ²	
Data / restraints / parameters	6986 / 0 / 363	
Goodness-of-fit on F ²	1.027	
Final R indices [I > 2σ(I)]	$R_I = 0.0697$, $wR_2 = 0.1725$	
R indices (all data)	$R_I = 0.1298$, $wR_2 = 0.2015$	
Largest diff. peak and hole	1.512 and -0.466 e.Å ⁻³	

Compound 52:



A 12 M solution of HCl (8 mL) was added to a $CHCl_3$ (40 mL) solution of complex **51** (1.0 g; 1.76 mmol) and the mixture stirred at room temperature for 4 hours. Upon addition of a saturated Na_2CO_3 solution, the organic layer turned from green to dark blue. The mixture was extracted with $CHCl_3$ (3×100 mL) and the combined organic layers were dried over Na_2SO_4 , filtered and evaporated affording **52** as a dark blue solid (0.8 g, 89%).

1H NMR (500 MHz, $CDCl_3$, 25 °C): δ = 8.15 (d, J = 8.0 Hz, 2H, PhH), 7.63-8.15 (m, 4H, Ph/pyrroleH), 7.44 (d, J = 8.0 Hz, 2H, PhH), 7.28 (d, J = 8.0 Hz, 2H, PhH), 7.0 (t, J = 4.6 Hz, 2H, pyrroleH), 6.79 (d, J = 4.3 Hz, 1H, pyrroleH), 6.71 (d, J = 4.6 Hz, 1H, pyrroleH), 6.64 (d, J = 4.3 Hz, 1H, pyrroleH), 6.5 (d, J = 4.3 Hz, 1H, pyrroleH), 6.42 (d, J = 4.3 Hz, 1H, pyrroleH), 6.41 (d, J = 4.3 Hz, 1H, pyrroleH), 3.98 (s, 3H, $COOCH_3$), 2.47 (s, 3H, CH_3) ppm.

^{13}C NMR (125 MHz, $CDCl_3$, 25 °C): δ = 166.9, 154.1, 151.9, 145.7, 145.3, 142.1, 141.3, 139.9, 139.7, 139.3, 139.0, 138.5, 138.2, 134.4, 132.1, 131.8, 131.1, 131.1, 130.6, 129.1, 128.6, 127.3, 125.9, 120.8, 119.8, 116.4, 115.9, 52.5, 21.6 ppm.

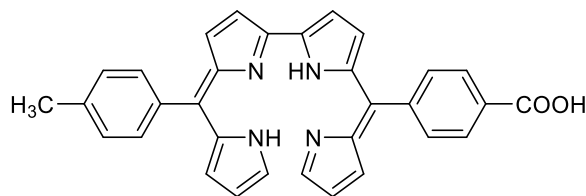
HRMS (ESI): m/z ($M+H$)⁺ calcd. for $C_{33}H_{27}N_4O_2$: 511.2129, Found 511.2104.

$\lambda_{max}(CH_2Cl_2)/nm$ ($\epsilon/mol^{-1} L cm^{-1}$): 292 (32850), 336 (16500), 408 (21080), 587 (32280).

Crystallographic data for compound 52

Formula	$C_{33}H_{26}N_4O_2$	
Formula weight	510.58	
Temperature	180(2) K	
Wavelength	0.71073 Å	
Crystal system	Triclinic	
Space group	$P -1$	
Unit cell dimensions	$a = 7.4764(5)$ Å	$\alpha = 94.177(3)^\circ$.
	$b = 9.8577(7)$ Å	$\beta = 90.378(3)^\circ$.
	$c = 18.0856(12)$ Å	$\gamma = 98.712(3)^\circ$.
Volume	1313.82(16) Å ³	
Z	2	
Density (calculated)	1.291 Mg/m ³	
Absorption coefficient	0.082 mm ⁻¹	
F(000)	536	
Crystal size	0.100 x 0.070 x 0.040 mm ³	
Theta range for data collection	2.096 to 30.111°.	
Index ranges	-10 ≤ h ≤ 10, -13 ≤ k ≤ 13, -25 ≤ l ≤ 25	
Reflections collected	34406	
Independent reflections	7028 [R(int) = 0.0506]	
Completeness to theta = 25.242°	95.7 %	
Absorption correction	Semi-empirical from equivalents	
Refinement method	Full-matrix least-squares on F ²	
Data / restraints / parameters	7028 / 0 / 354	
Goodness-of-fit on F ²	1.086	
Final R indices [I > 2σ(I)]	$R_I = 0.1060$, $wR_2 = 0.3160$	
R indices (all data)	$R_I = 0.1348$, $wR_2 = 0.3376$	
Largest diff. peak and hole	0.783 and -0.337 e.Å ⁻³	

Compound 53:



Chemical Formula: C₃₂H₂₄N₄O₂
Molecular Weight: 496.57

1M KOH solution (20 mL) was added to a THF (30 mL) solution of 2,2'-bisdipyrin **52** (0.2 g; 0.39 mmol). The mixture was refluxed overnight and then evaporated under reduced pressure. The residue was acidified with 37% HCl down to pH = 2. A saturated NaHCO₃ solution was added until neutralization. After extraction with CHCl₃ and H₂O (3 × 30 mL), the combined organic layers were dried over Na₂SO₄, filtered and evaporated under reduced pressure, affording the compound **53** as a dark blue solid (0.1 g, 51%).

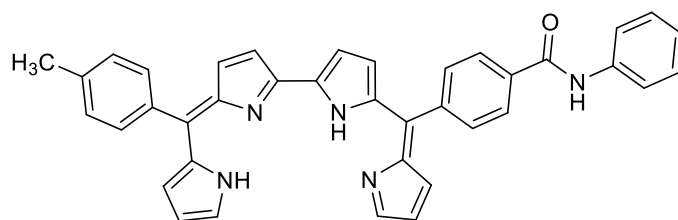
¹H NMR (300 MHz, Acetone-d₆, 25 °C): δ = 8.2 (d, *J* = 8.2 Hz, 2H, PhH), 7.72 (s, 2H, pyrroleH), 7.68 (d, *J* = 8.2 Hz, 2H, PhH), 7.44 (d, *J* = 8.1 Hz, 2H, PhH), 7.36 (d, *J* = 8.1 Hz, 2H, PhH), 7.27 (t, *J* = 4.1 Hz, 2H, pyrroleH), 6.78 (t, *J* = 4.6 Hz, 2H, pyrroleH), 6.54 (d, *J* = 4.1 Hz, 1H, pyrroleH), 6.48 (d, *J* = 4.6 Hz, 2H, pyrroleH), 6.42-6.39 (m, 2H, pyrroleH), 2.46 (s, 3H, CH₃) ppm.

¹³C NMR (125 MHz, Acetone-d₆, 25 °C): δ = 167.3, 157.7, 156.1, 147.8, 147.6, 142.7, 142.0, 140.1, 140.0, 138.5, 138.0, 137.5, 137.3, 135.3, 133.5, 133.3, 131.9, 131.7, 131.7, 130.0, 129.4, 126.5, 125.7, 122.9, 122.1, 115.7, 115.5, 21.4 ppm.

HRMS (ESI): *m/z* (M+H)⁺ calcd. for C₃₂H₂₄N₄O₂: 497.1972, Found 497.1935.

λ_{max}(CH₂Cl₂)/nm (ε/mol⁻¹ L cm⁻¹): 267 (19590), 338 (13140), 410 (17240), 581 (18810).

Compound 54:



Chemical Formula: C₃₈H₂₉N₅O

Molecular Weight: 571.68

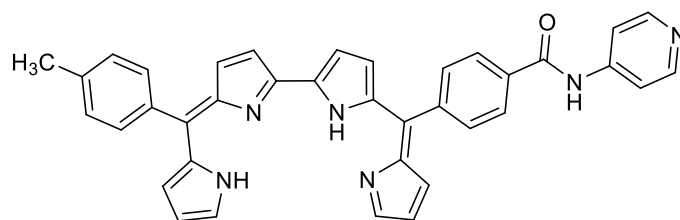
Bisdipyrin **53** (0.05 g; 0.1 mmol) was dissolved in distilled CH₂Cl₂ (10 mL) under argon atmosphere. Then, EDCiHCl (0.023 g; 0.12 mmol), HOBT (0.016 g; 0.12 mmol) and Aniline (11 μ L; 0.12 mmol) were added and the mixture was stirred at room temperature under argon for 2 days. The reaction was quenched by addition of H₂O (20 mL). After addition of a saturated NaHCO₃ solution (20 mL), the mixture was extracted with CHCl₃ (100 mL). The combined organic layers were dried over Na₂SO₄, filtered and evaporated reduced pressure. The residue was purified by column chromatography (SiO₂, CH₂Cl₂/MeOH/Et₃N: 94/5/1) affording **54** (0.05 g, 87%).

¹H NMR (500 MHz, CDCl₃, 25 °C): δ = 7.98 (d, J = 8.1 Hz, 2H, PhH), 7.9 (s, 1H, CONH), 7.7 (d, J = 7.5 Hz, 2H, PhH), 7.68 (d, J = 8.1 Hz, 2H, PhH), 7.64 (s, 1H, pyrroleH), 7.6 (s, 1H, pyrroleH), 7.44 (d, J = 8.1 Hz, 2H, PhH), 7.41 (d, J = 8.1 Hz, 2H, PhH), 7.28 (d, J = 7.5 Hz, 2H, PhH), 7.2 (t, J = 7.4 Hz, 1H, PhH), 7.03 (d, J = 4.3 Hz, 1H, pyrroleH), 7.01 (d, J = 4.3 Hz, 1H, pyrroleH), 6.8 (d, J = 4.3 Hz, 1H, pyrroleH), 6.74 (d, J = 4.3 Hz, 1H, pyrroleH), 6.64 (d, J = 4.3 Hz, 1H, pyrroleH), 6.52 (d, J = 4.3 Hz, 1H, pyrroleH), 6.43-6.41 (m, 2H, pyrrole), 2.47 (s, 3H, CH₃) ppm.

¹³C NMR (125 MHz, CDCl₃, 25 °C): δ = 165.4, 154.2, 151.9, 145.8, 145.3, 141.4, 141.1, 139.9, 139.7, 139.3, 138.7, 138.4, 138.0, 137.9, 135.5, 134.4, 132.2, 131.8, 131.5, 131.1, 129.4, 128.6, 127.4, 126.6, 125.8, 124.9, 120.9, 120.3, 119.8, 116.4, 115.9, 21.6 ppm.

HRMS (ESI): m/z (M+H)⁺ calcd. for C₃₈H₃₀N₅O: 572.2445, Found 572.2440.

λ_{max} (CH₂Cl₂)/nm (ϵ /mol⁻¹ L cm⁻¹): 261 (28700), 335 (24630), 410 (25840), 588 (40080).

Compound 55:Chemical Formula: C₃₇H₂₈N₆O

Molecular Weight: 572.67

Bisdipyrin **53** (0.05 g; 0.1 mmol) was dissolved in distilled CH₂Cl₂ (10 mL) under argon. Then, EDCi·HCl (0.048 g; 0.25 mmol), HOBt (0.034 g; 0.25 mmol) and 4-aminopyridine (0.024 g; 0.25 mmol) were added and the mixture was stirred at room temperature for 2 days. The reaction was quenched by addition of H₂O (20 mL). After addition of saturated NaHCO₃ solution (20 mL), the mixture was extracted with CHCl₃ (100 mL). The combined organic layers were dried over Na₂SO₄, filtered and evaporated under reduced pressure. The residue was purified by column chromatography (SiO₂, CH₂Cl₂/MeOH/Et₃N: 97/2/1) affording **55** (0.01 g, 17%).

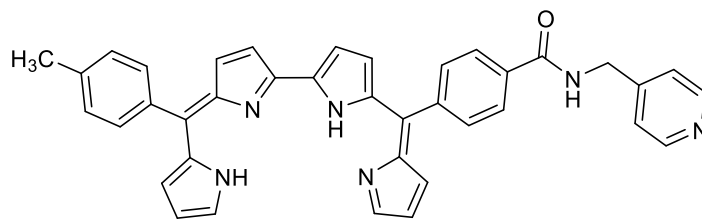
¹H NMR (500 MHz, CDCl₃, 25 °C): δ = 8.57 (d, *J* = 5.0 Hz, 2H, pyH), 7.99 (d, *J* = 7.7 Hz, 2H, PhH), 7.69-7.66 (m, 5H, PhH/pyH/pyrroleH), 7.61 (s, 1H, pyrroleH), 7.43 (d, *J* = 7.7 Hz, 2H, PhH), 7.28 (d, *J* = 7.7 Hz, 2H, PhH), 7.01-6.99 (m, 2H, pyrroleH), 6.79 (s, 1H, pyrroleH), 6.69 (s, 1H, pyrroleH), 6.65 (s, 1H, pyrroleH), 6.48 (s, 1H, pyrroleH), 6.44 (s, 1H, pyrroleH), 6.42 (s, 1H, pyrroleH), 2.47 (s, 3H, CH₃) ppm.

¹³C NMR (125 MHz, CDCl₃, 25 °C): δ = 165.8, 154.3, 151.5, 150.9, 145.8, 145.2, 141.7, 140.1, 139.5, 138.0, 134.5, 134.4, 132.3, 131.9, 131.6, 131.2, 128.6, 127.9, 126.8, 125.8, 121.2, 119.8, 116.6, 115.9, 114.1, 21.6 ppm.

HRMS (ESI): *m/z* (M+H)⁺ calcd. for C₃₇H₂₉N₆O: 573.2397, Found 573.2414.

λ_{max}(CH₂Cl₂)/nm (ε/mol⁻¹ L cm⁻¹): 258 (25500), 332 (18020), 408 (18520), 585 (24250).

Compound 56:



Chemical Formula: C₃₈H₃₀N₆O

Molecular Weight: 586.70

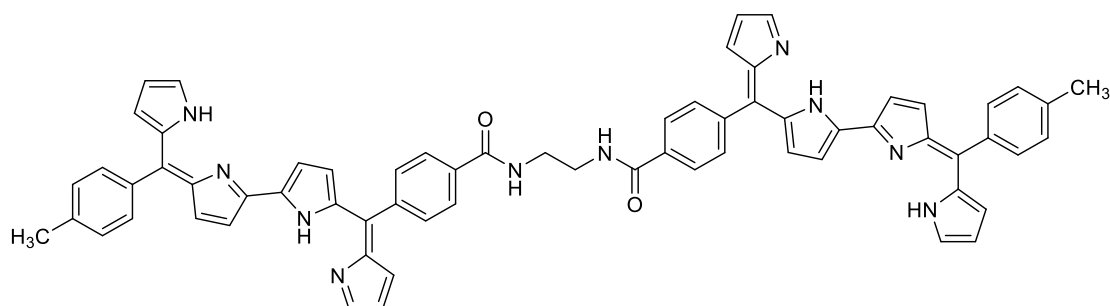
Bisdipyrin **53** (0.1 g; 0.2 mmol) was dissolved in distilled CH₂Cl₂ (25 mL) under argon. Then, EDCi·HCl (0.046 g; 0.24 mmol), HOBT (0.033 g; 0.24 mmol) and 4-(aminomethyl)pyridine (0.024 g, 0.22 mmol) were added and the mixture was stirred at room temperature under argon for 2 days. The reaction was quenched by addition of pure H₂O (20 mL). After addition of a saturated NaHCO₃ solution (20 mL), the mixture was extracted with CHCl₃ (100 mL). The combined organic layers were dried over Na₂SO₄, filtered and evaporated under reduced pressure. The residue was purified by column chromatography (SiO₂, CH₂Cl₂/MeOH/Et₃N: 95/4/1) affording **56** (0.08 g, 68%).

¹H NMR (500 MHz, CD₂Cl₂, 25 °C): δ = 8.56 (d, *J* = 5.5 Hz, 2H, pyH), 7.93 (d, *J* = 8.2 Hz, 2H, PhH), 7.65 (d, *J* = 8.2 Hz, 2H, PhH), 7.63 (s, 1H, pyrroleH), 7.61 (s, 1H, pyrroleH), 7.44 (d, *J* = 8.2 Hz, 2H, PhH), 7.31-7.30 (m, 4H, PhH/pyH), 7.07-7.05 (m, 2H, pyrroleH), 6.81 (d, *J* = 4.3 Hz, 1H, pyrroleH), 6.76 (d, *J* = 4.3 Hz, 1H), 6.62 (d, *J* = 4.3 Hz, 1H, pyrroleH), 6.52 (d, *J* = 4.3 Hz, 1H, pyrroleH), 6.44-6.42 (m, 2H, pyrroleH), 4.7 (d, *J* = 6.3 Hz, 2H, CH₂), 2.47 (s, 3H, CH₃) ppm.

¹³C NMR (125 MHz, CD₂Cl₂, 25 °C): δ = 167.3, 154.8, 152.8, 150.4, 147.8, 146.3, 145.9, 141.6, 141.1, 139.8, 139.7, 139.3, 139.2, 138.5, 138.0, 134.8, 134.6, 132.5, 132.2, 131.6, 131.3, 128.8, 127.1, 126.8, 125.9, 122.6, 121.2, 120.3, 116.3, 115.9, 43.2, 21.5 ppm.

HRMS (ESI): *m/z* (M+H)⁺ calcd. for C₃₈H₃₁N₆O: 587.2554, Found 587.2598.

λ_{max}(CH₂Cl₂)/nm (ε/mol⁻¹ L cm⁻¹): 257 (27480), 335 (21750), 408 (26890), 586 (37690).

Compound 57:

Chemical Formula: $C_{66}H_{52}N_{10}O_2$
Molecular Weight: 1017.21

Under argon, bisdipyrin **53** (0.1 g; 0.2 mmol) was dissolved in dry CH_2Cl_2 (25 mL). Then, EDCiHCl (0.046 g; 0.24 mmol), HOBt (0.033 g; 0.24 mmol) and distilled ethylenediamine (6.7 μ L; 0.1 mmol) were added. The mixture was stirred at room temperature under argon atmosphere for 2 days. The reaction was quenched by addition of H_2O (20 mL). After addition of a saturated $NaHCO_3$ solution (20 mL), the mixture was extracted with $CHCl_3$ (100 mL). The combined organic layers were dried over Na_2SO_4 , filtered and evaporated. The residue was purified by column chromatography (SiO_2 , $CH_2Cl_2/MeOH/Et_3N$: 97/2/1) affording **57** (0.1 g, 98%).

1H NMR (500 MHz, $CDCl_3$, 25 $^{\circ}C$): δ = 7.95 (d, J = 8.3 Hz, 4H, PhH), 7.64 (d, J = 8.0 Hz, 4H, PhH), 7.62 (s, 2H, pyrroleH), 7.59 (s, 2H, pyrroleH), 7.43 (d, J = 8.0 Hz, 4H, PhH), 7.31 (s, 2H, CONH), 7.28 (d, J = 8.3 Hz, 4H, PhH), 7.0 (d, J = 4.5 Hz, 2H, pyrroleH), 6.99 (d, J = 4.5 Hz, 2H, pyrroleH), 6.79 (d, J = 4.5 Hz, 2H, pyrroleH), 6.71 (d, J = 4.5 Hz, 2H, pyrroleH), 6.63 (d, J = 4.2 Hz, 2H, pyrroleH), 6.5 (d, J = 4.2 Hz, 2H, pyrroleH), 4.62-6.39 (m, 4H, pyrroleH), 3.84 (s, 4H, CH_2), 2.47 (s, 6H, CH_3) ppm.

^{13}C NMR (125 MHz, $CDCl_3$, 25 $^{\circ}C$): δ = 168.6, 154.0, 151.9, 145.7, 145.3, 141.3, 141.0, 139.9, 139.6, 139.3, 138.9, 138.6, 138.2, 134.5, 134.3, 132.1, 131.8, 131.4, 131.1, 128.6, 127.3, 126.6, 125.9, 120.8, 119.8, 116.4, 115.9, 41.5, 21.6 ppm.

HRMS (ESI): m/z ($M+H$)⁺ calcd. for $C_{66}H_{53}N_{10}O_2$: 1017.4347, Found 1017.4326.

λ_{max} (CH_2Cl_2)/nm ($\epsilon/mol^{-1} L cm^{-1}$): 253 (43380), 336 (43760), 409 (52910), 588 (83670).

Molecular tectonics: Functionalized dipyrrens for the construction of metallo-organic architectures**Résumé**

L'objectif de ce travail a été de développer de nouvelles approches pour la fonctionnalisation des dérivés pyrroliques mono- et bis-dipyrrens en positions 1, 5, 9, qui peuvent être utilisés comme tectons pour l'auto-assemblage avec des centres métalliques menant à la construction d'entités discrètes et / ou de réseaux moléculaires périodiques infinis.

Dans une première partie, une série de nouveaux dérivés dipyrrens fonctionnalisés par des groupes de coordinants dans les positions 1 et 9 *via* une réaction de Knoevenagel ainsi que par une autre unité coordinante ou de solubilisation en position 5 a été préparée. La coordination de ces ligands aux cations B(III) et Zn(II) mène à la formation de dérivés luminescents du type BODIPY et de complexes homoleptiques, qui ont été utilisés comme metallatectons pour la construction de polymères de coordination hétérométalliques émissifs à l'état cristallin.

Dans une deuxième partie, une stratégie de synthèse de nouvelles espèces *via* une post-fonctionnalisation de dérivés de 2,2'-bisdipyrrene grâce à un groupement réactif à leur périphérie, telle qu'une fonction aldéhyde, amine ou acide carboxylique, a été mise au point. D'une part, un ligand tétrapyrrolique à chaîne ouverte portant des motifs benzaldéhyde en positions *méso* a été utilisé pour la formation d'un hélicate fermé par des liaisons imines. D'autre part, l'introduction d'un acide *p*-benzoïque sur l'un ou les deux côtés du squelette 2,2'-bisdipyrrene a été utilisée pour la formation de nouveaux dérivés symétriques et dissymétriques. L'assemblage de ces nouveaux ligands avec les cations Zn(II) et Ni(II) a été particulièrement exploré.

Mots-clés : auto-assemblage, tectonique moléculaire, réseaux de coordination, hélicate, dipyrrene.

Abstract:

The aim of this work was to develop new approaches for the functionalization of mono- and bis-dipyrren derivatives at positions 1, 5, 9, which can be used as tectons for self-assembly with various metal centers for the construction of discrete entities and/or infinite periodic molecular networks.

In the first part, a series of new 1,9-divinyldipyrren derivatives functionalized by coordinating groups in positions 1 and 9 *via* a Knoevenagel reaction and bearing another coordinating or solubilizing unit in position 5 has been explored. The assembly of these ligands with B(III) or Zn(II) centers provide luminescent complexes, which can be used as metallatectons for the construction of heterometallic coordination polymers emissive in the solid state.

In the second part, the synthetic strategy for novel species *via* a post-functionalization of 2,2'-bisdipyrren derivatives featuring reactive groups at their periphery such as an aldehyde, amine or carboxylic acid moiety has been explored. On one hand, a tetrapyrrolic open-chain ligand bearing benzaldehyde units at the *meso* position was exploited for the preparation of a strapped helicate based on imine bond formation. On the other hand, the introduction of a *p*-benzoic acid on one/both side of the 2,2'-bisdipyrren backbone has been employed for the formation of novel symmetric and dissymmetric amide-bearing derivatives. The assembly of these novel ligands with Zn(II) and Ni(II) cations has been particularly explored.

Keywords: self-assembly, molecular tectonics, coordination network, helicate, dipyrren.